THE UNIVERSITY
of EDINBURGH

Investigating the genetic requirements for the PCNA interacting motifs in Pif1 family helicases in *Saccharomyces cerevisiae*

Oleksii Kotenko

Thesis presented for the degree of Doctor of Philosophy

Institute of Cell Biology

The University of Edinburgh

August 2019

Declaration

I declare that this thesis has been composed by myself and the work presented herein is my own, unless stated otherwise. This work has not been submitted for any other degree or professional qualification.

Oleksii Kotenko

August 2019

Acknowledgements

I would like to express gratitude to my supervisor Dr Sveta Makovets for allowing me to do PhD in her lab. Thank you for being a great mentor, teaching and supporting me during my PhD.

I would also like to thank my thesis committee members Dr Sara Buonomo and Prof David Leach for the critical reading of my reports and for their help and advice with my project.

I am very grateful to the University of Edinburgh for their financial support which allowed me to live and study in Edinburgh.

Finally, I would like to say thank you to my friends and colleagues Tadas Andriuskevicius, Benura Azeroglu, Dima Degtev, Anton Dubenko, John Hutchinson, Lisa Iurchenko, Sebastian Jaramillo-Riveri, Caroline Millet, Viktoria Stancheva, Andrei Sukhareuski and Yuilia Vasianovich for sharing their experience, having friendly conversations, participating in the lab meeting and discussing the scientific ideas.

Abstract

Stable maintenance and transmission of the genetic material requires tight coordination between DNA replication and DNA repair. One of the factors that couples DNA replication and DNA repair is proliferative cell nuclear antigen (PCNA). PCNA is a homotrimeric complex that encircles DNA and plays a structural role interacting with different enzymes, tethering them to DNA and promoting their catalytic activity. PCNA is heavily post-translationally regulated, which was shown to change its affinity to the interacting partners and therefore to confer differential recruitment of the required proteins to the DNA substrates.

Pif1 family of DNA helicases in *Saccharomyces cerevisiae* is composed of the two paralogues Pif1 and Rrm3. In addition to the overlapping functions during DNA replication, Pif1 and Rrm3 have certain distinct roles. Rrm3 is required for DNA replication through the “hard-to-replicate” regions, such as *rDNA* repeats, telomeres and origins of replication. The unique functions of Pif1 involve telomerase inhibition at telomeres and at DNA double-strand breaks (DSBs) and promotion of break induced replication (BIR). The underlying mechanism that defines functional specialisation of Pif1 family helicases is not understood.

Both Pif1 and Rrm3 were shown earlier to physically interact with PCNA. The experiment presented here shows that, in addition to the previously reported C-terminal PCNA interacting peptides (PIP1 and PIP2), the N-terminus of Pif1 contains putative PCNA interacting motifs (PIP3 and SIM). The Pif1 roles in DNA replication, BIR and telomerase inhibition require different PCNA-interacting motifs. In addition, Pif1 recruitment to stalled forks and DSBs was PCNA-dependent.

Despite the fact that the Pif1-PCNA complex was shown to be required for Pol δ-mediated DNA synthesis during BIR, it is still not clear if other stages of this DNA repair pathway are Pif1-dependent. This study shows that the broken strand invasion and the initiation of DNA synthesis during BIR occur independently of Pif1, however both the long-range DNA synthesis and re-synthesis of the resected strand require Pif1 and its previously reported Rad53/Dun1-dependent phosphorylation.

Based on the published data, the interaction between Rrm3 and PCNA occurs via the N-terminally located PCNA interacting motif (PIP1 in Rrm3). The experiment presented here shows that PIP1 in Rrm3 was not required for DNA replication through the sites that require Rrm3 helicase. In contrast, replication associated function of Rrm3 required the C-terminally located putative PCNA interacting motif (PIP2 in Rrm3), homologous to the previously reported C-terminal PCNA interacting motif in Pif1 (PIP2 in Pif1).

Overall, this work provides a systematic characterisation of the newly identified and previously reported *pif1* and *rrm3* alleles and shows that different functions of Pif1 can be distinguished by the genetic requirements for its PCNA-interacting elements. Based on the obtained data, I would like to hypothesise that differential recruitment of Pif1 helicases via interaction with PCNA could be the reason of the functional specialisation of Pif1 and Rrm3.

Lay summary

Double-stranded DNA encodes the genetic information necessary for progeny development and is maintained in the form of linear chromosomes in the nuclei of the eukaryotic cells. On the cellular level, reproduction involves accurate duplication of chromosomes and is executed by the DNA replication proteins.

DNA damage that occurs spontaneously during cell metabolism threatens genome stability and cell survival. To overcome this, cells evolved a defensive mechanism, called DNA repair, which involves specialised proteins.

One of the most dangerous types of DNA damage are DNA double-strand breaks (DSBs). DSBs create the new ends of chromosomes which have to be distinguished from the natural ends to prevent aberrant DNA repair that could lead to chromosome fusions. This is achieved by telomeres that cap natural chromosome ends and protect them from DNA repair proteins. Telomeres shorten with every DNA replication round and therefore they have to be extended by a specialised enzyme called telomerase.

On the other hand, telomerase can add new telomeres to DSBs, which could lead to the loss of a chromosome arm with all genetic information in it. Therefore, the DNA repair factors inhibit telomerase at the DSBs.

The Pif1 family helicases are multifunctional enzymes implicated in DNA replication, DNA repair and telomere maintenance. In the budding yeast, there are two Pif1 family helicases – Pif1 and Rrm3 that are very similar and yet have different non-overlapping functions. Rrm3 is mostly involved in DNA replication, while Pif1 regulates telomere length, inhibits telomerase at DSBs and promotes break induced replication, DNA repair pathway which is used to repair the one-ended DSBs.

Both Rrm3 and Pif1 were shown to interact with PCNA, an important structural protein involved in the recruitment of different enzymes to DNA. The interaction between Pif1 and PCNA occurs via different PCNA interacting motifs in Pif1. However, the role of the interaction between the Pif1 family helicases and PCNA was not considered in the context of their various functions.

This work addresses the requirements for the different PCNA interacting motifs in the Pif1 family helicases for their functions in DNA replication, telomerase inhibition and BIR. Based on the results presented here, I would like to formulate a hypothesis that differential PCNA-dependent recruitment of Pif1 and Rrm3 to their substrates could be the reason of the different functions of these enzymes.

Abbreviations

ALT	alternative lengthening of telomeres
APS	ammonium persulfate
ATP	adenosine triphosphate
BIR	break-induced replication
bp	base pair(s)
CDK	cyclin-dependent kinase
CMG	Cdc45-GINS-Mcm2-7 complex
ChIP	chromatin immunoprecipitation
DDK	Dbf4-dependent kinase
DDR	DNA damage response
DNA	deoxyribonucleic acid
dNTP	deoxyribonucleotide triphosphate
D-loop	displacement loop
DNTA	*de novo* telomere addition
DSB	double-strand break
dsDNA	double-stranded DNA
FEN1	flap endonuclease 1
Gal	galactose
h	hour(s)
HR	homologous recombination
IDCL	inter-domain connecting loop
IP	immunoprecipitation
kb	kilobase(s)
kDa	kilodalton(s)
min	minute(s)
MMS	methyl methanesulfonate
nt	nucleotide(s)
OD_{600}	optical density at 600 nm
OF	Okazaki fragments
o/n	overnight

ORF	open reading frame
PCR	polymerase chain reaction
qPCR	quantitative PCR
PCNA	proliferating cell nuclear antigen
PEG	polyethylene glycol
PIP	PCNA-interacting peptide box
PVDF	polyvinylidene difluoride
Raf	raffinose
RNA	ribonucleic acid
rpm	revolutions per minute
sec	second (s)
SDS	sodium dodecyl sulphate
SDS-PAGE	SDS polyacrylamide gel electrophoresis
SIM	SUMO-interacting motif
SSA	single-strand annealing
SSC	saline sodium citrate
ssDNA	single-stranded DNA
STR	Sgs1-Top3-Rmi1 complex
TEMED	N,N,N',N'-tetramethylethylenediamine
TBE	Tris-borate-EDTA
TBST	Tris-buffered saline with Tween
TCA	trichloroacetic acid
TE	Tris-EDTA
T_m	temperature of melting
v/v	volume per volume
w/v	weight per volume

Contents

List of Figures

List of Tables

Chapter I. General introduction

The ability to reproduce is one of the defining features of the living organisms. At the cellular level, it involves accurate duplication of chromosomes and their faithful segregation during cell division. Additional challenges for genome maintenance include repair of DNA damage, such as DNA double-stranded breaks (DSBs).

DSBs occur spontaneously during normal cell metabolism as a result of oxidative damage or replication errors (Friedberg et al. 2006; Murnane 2012). DSBs can also be induced by ionizing radiation or exogenous chemicals (Degrassi, Fiore, and Palitti 2004; Ward 1998). Inappropriate repair of DSBs may cause chromosomal abnormalities, genome instability and tumorigenesis (Murnane 2012; Sandell and Zakian 1993; Weinert and Hartwell 1988) and a single unrepairable DSB can lead to cell death (Resnick and Martin 1976).

DSBs have to be distinguished from the natural ends of linear eukaryotic to prevent chromosome fusions and genomic rearrangements (Longhese 2008; McClintock 1939; Muller 1938; Sandell and Zakian 1993). This is achieved by forming telomeres that require special maintenance after each replication cycle (Szostak and Blackburn 1982).

Genome maintenance relies on a complex machinery consisting of a number of different enzymes. Pif1 helicases are multifunctional enzymes implicated in DNA replication, DNA repair and telomere maintenance. This chapter gives a brief overview of the crucial events and players involved in DNA replication, telomere maintenance and DNA repair, and current understanding of the role of Pif1 helicases in these processes.

1.1. Semiconservative DNA replication

DNA duplication occurs in a similar fashion in all living organisms, in a manner first proposed by Watson and Crick (Watson and Crick 1953). Semiconservative DNA replication involves unwinding of the double helix of the parental dsDNA molecule and synthesis of the two new strands: one continuously (leading strand)

and the other one discontinuously (lagging strand), in a way that generates two dsDNA molecules, each consisting of a parental and a nascent DNA strands.

The synthesis of the leading and the lagging DNA strands are synchronised and coordinated by the multitude of proteins that form a replisome. This section describes the molecular mechanisms of replication initiation and DNA synthesis.

1.1.1. Replication initiation

Replication of the large eukaryotic chromosomes initiates at multiple places which are called origins of replication, or autonomously replicating sequences (ARS) in the budding yeast (Brewer and Fangman 1987; Huberman et al. 1987; Huberman et al. 1988). Although these sequences often have species-specific consensus motifs, other factors are involved into defining an active replication origin, for example, the epigenetic state of the surrounding region involving histone modifications and transcription (Hoggard et al. 2013; Leonard and Mechali 2013). Replication initiation must be tightly regulated to occur only once in the given S phase to avoid potentially dangerous chromosome “over-replication”. This is achieved by the temporal separation of origin recognition, replicative helicase recruitment and activation (Figure 1.1).

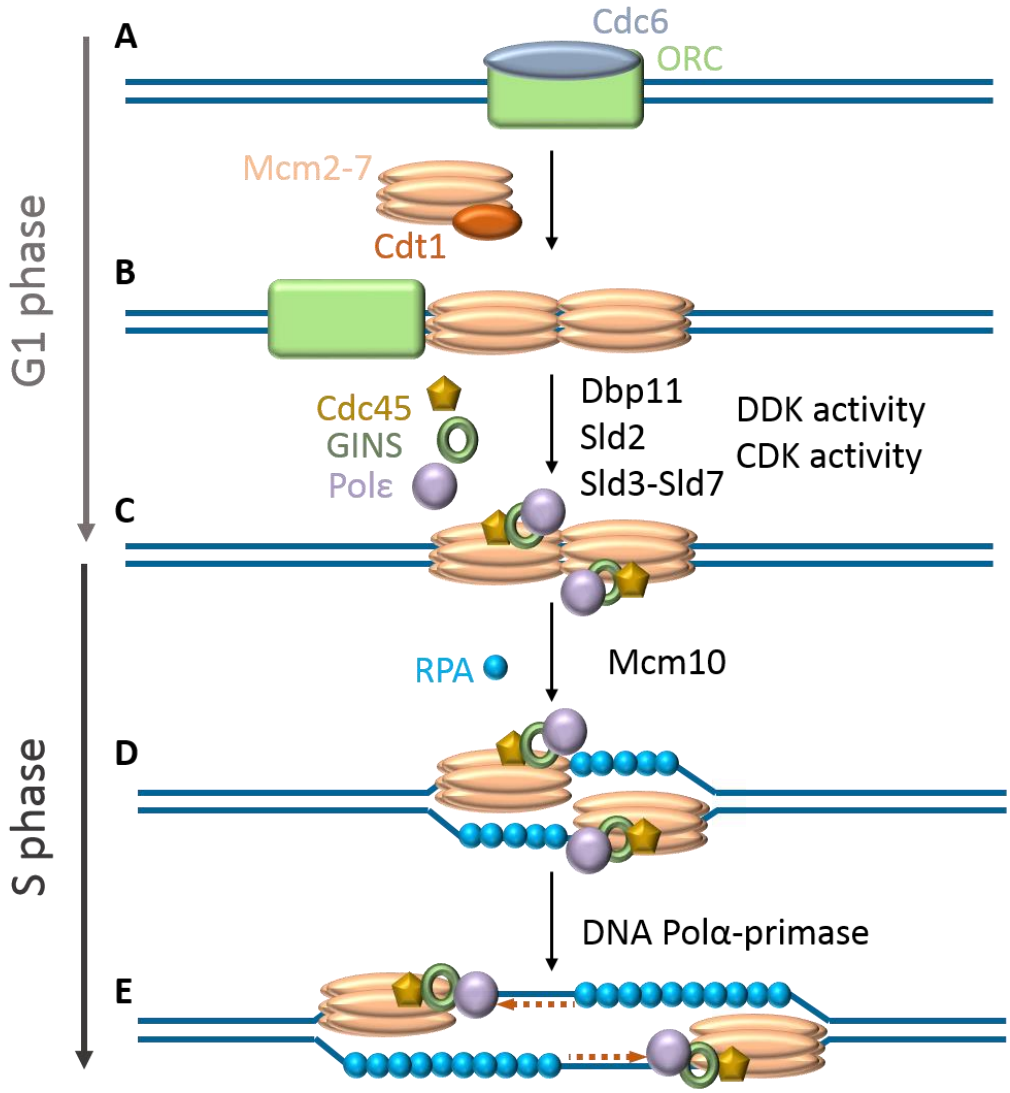

Figure 1.1. Initiation of DNA replication. Adapted from (Burgers and Kunkel 2017)

Initiation of DNA replication involves origin recognition (**A**), Mcm2-7 double hexamer loading (**B**), assembly and activation of the Cdc45-GINS-Mcm2-7 (CMG) complex (**C**), DNA melting (**D**) and initiation of the leading strand synthesis (**E**). See the main text for a detailed description.

The origin recognition complex composed of six AAA+ superfamily proteins (Orc1-6) and Cdc6 binds the double-stranded origin sequences in early G1 (Figure 1.1 A) (Bell and Stillman 1992; Bell, Kobayashi, and Stillman 1993; Sun et al. 2013). This step is crucial for the origin recognition since the fusion between either the ORC proteins or Cdc6 and Gal4 DNA binding domain was sufficient to initiate replication of a plasmid containing a tandem array of Gal4 binding sites (Takeda et al. 2005).

After the ORC-Cdc6 complex binds to the origin, it recruits two MCM hexamers (MCM2-7) in a complex with Ctd1 and positions them onto the DNA symmetrically in the inverted orientation, thereby forming a pre-replication complex (Figure 1.1. B) (Speck et al. 2005; Sun et al. 2013).

The next stage involves recruitment of the additional factors to form a pre-initiation complex (Figure 1.1 C) and is regulated by a combined action of DDK (Cdc7/Dbf4 kinase) and CDK (cyclin-dependent kinase). DDK binds MCM via the interactions with Mcm4 and Mcm2 and facilitates Sld3 and Sld7-dependent recruitment of Cdc45 to the double MCM hexamer (Ramer et al. 2013; Sheu and Stillman 2006, 2010; Masai et al. 2006; Tanaka et al. 2011; Yabuuchi et al. 2006). CDK was shown to phosphorylate Cdc45, Sld2, Sld3, and Sld7 (Heller et al. 2011; Masumoto et al. 2002; Muramatsu et al. 2010; Tanaka et al. 2007; Yeeles et al. 2015; Zegerman and Diffley 2007). Additionally, CDK associates with Dpb11 to recruit the GINS complex (Sld5, Psf1, Psf2 and Psf3), Sld2 and DNA polymerase ε (Pol ε) (Araki et al. 1995; Kamimura et al. 1998; Kamimura et al. 2001; Muramatsu et al. 2010; Takayama et al. 2003; Tanaka et al. 2013). The complex formed by Cdc45, Mcm2-7 and GINS (CMG complex) on the double-stranded DNA (dsDNA) constitutes the inactive replicative helicase.

The next stage, activation of the CMG, is currently not well understood. It involves DNA unwinding within the origin and separation of the MCM double hexamers into the two ssDNA binding single rings (Figure 1.1 D). This reaction is catalysed by Mcm10 and the ssDNA binding protein complex RPA (replication protein A) (Heller et al. 2011; Kanke et al. 2012; van Deursen et al. 2012; Quan et al. 2015; Perez-Arnaiz, Bruck, and Kaplan 2016). MCM10 was shown to interact with the CMG complex and stabilise the replisome (Gregan et al. 2003; Ricke and Bielinsky 2004). The dsDNA melting during the activation of the replicative helicase generates single stranded DNA (ssDNA) which is bound by RPA. The DNA polymerase α (Pol α) complex is bridged to the replicative helicase by CTF4 (Simon et al. 2014; Villa et al. 2016) and uses RPA-coated ssDNA as a substrate to prime the leading strand synthesis (Figure 1.1 E).

1.1.2. Leading strand DNA replication

The leading strand replication is executed by a combined action of the replicative helicase and Pol ε. CMG utilises the energy released by ATP hydrolysis to unwind the parental DNA duplex while moving in the 5'-3' directionality.

Pol ε is a multiprotein complex composed of Pol2 and the Dpb2-4 components. Pol2 is the DNA polymerase catalytic subunit which has the N-terminal domain capable of DNA polymerisation and 3'-5'-exonucleolytic degradation, and the catalytically inactive C-terminus which interacts with other replisome components and is required for checkpoint activation (Kesti et al. 1999; Dua, Levy, and Campbell 1999; Feng and D'Urso 2001; Ohya et al. 2002; Pavlov, Shcherbakova, and Kunkel 2001; Navas, Zhou, and Elledge 1995; Lou et al. 2008). The catalytic domain of Pol ε encircles the nascent dsDNA which may contribute to its relatively high processivity (in comparison with the lagging strand polymerase Pol δ) (Hogg et al. 2014). The non-catalytic component of Pol ε Dbp2 is essential, while Dbp3 and Dbp4 are not (Hogg and Johansson 2012). However, Dpb3 and Dpb4 further promote Pol ε processivity by bridging it to the replication clamp (PCNA) (Chilkova et al. 2007). The essential function of Dpb2 is bridging Pol ε to the Psf1 subunit of GINS (Sengupta et al. 2013). Additionally, Dpb2 interacts with Mcm5 via its C-terminal domain (Sun, Shi, et al. 2015).

Overall, the leading strand replisome is a very stable and processive complex, which could result from multiple physical interactions between its components and stable association with the DNA template (Sun, Shi, et al. 2015).

1.1.3. Lagging strand replication

Due to the discontinuous nature of the lagging strand DNA synthesis, DNA replication requires a cyclic action of the lagging strand replisome components to synthesise Okazaki fragments (OF) that eventually copy the whole lagging strand. Each cycle consists of priming, elongation and processing of a new OF.

Priming is executed by the Pol α/primase complex, which consists of a primase (Pri1), a DNA polymerase (Pol1) and two regulatory subunits (Pri2 and Pol12). First, Pri1 synthesises a short RNA primer (∼ 10 nt). Increasing steric

clashes are predicted to occur as the primer grows in length, which may facilitate the switch between the primase and the DNA polymerase (Baranovskiy et al. 2016). The DNA synthesis performed by Pol1 is normally limited to ∼ 20-30 nt. There are two hypotheses that explain how the switch between Pol1 and Pol δ occurs. One assumes that the Pol α-mediated DNA synthesis is terminated by the loading of PCNA by the replication clamp loader replication factor C (RFC) (Tsurimoto and Stillman 1991; Yuzhakov, Kelman, and O'Donnell 1999). The other hypothesis postulates that the transition from the A helix conformation of the RNA-DNA duplex formed upon the primer synthesis to the B helix as the DNA extension of the primer is added decreases the affinity of Pol α to the DNA substrate and leads to its dissociation (Perera et al. 2013).

Elongation of OFs is catalysed by Pol δ (Figure 1.2 A) which consists of an essential catalytic subunit in Pol3, an essential non-catalytic subunit in Pol31 and a non-essential non-catalytic subunit in Pol32 (Huang, Mat-Arip, and Guo 1997; Gerik et al. 1998). Pol δ is a much less processive enzyme *in vitro* than Pol ε, however the activity of Pol δ is greatly stimulated by PCNA, making the reactions catalysed by both polymerases almost as efficient in the presence of the replication clamp (Chilkova et al. 2007).

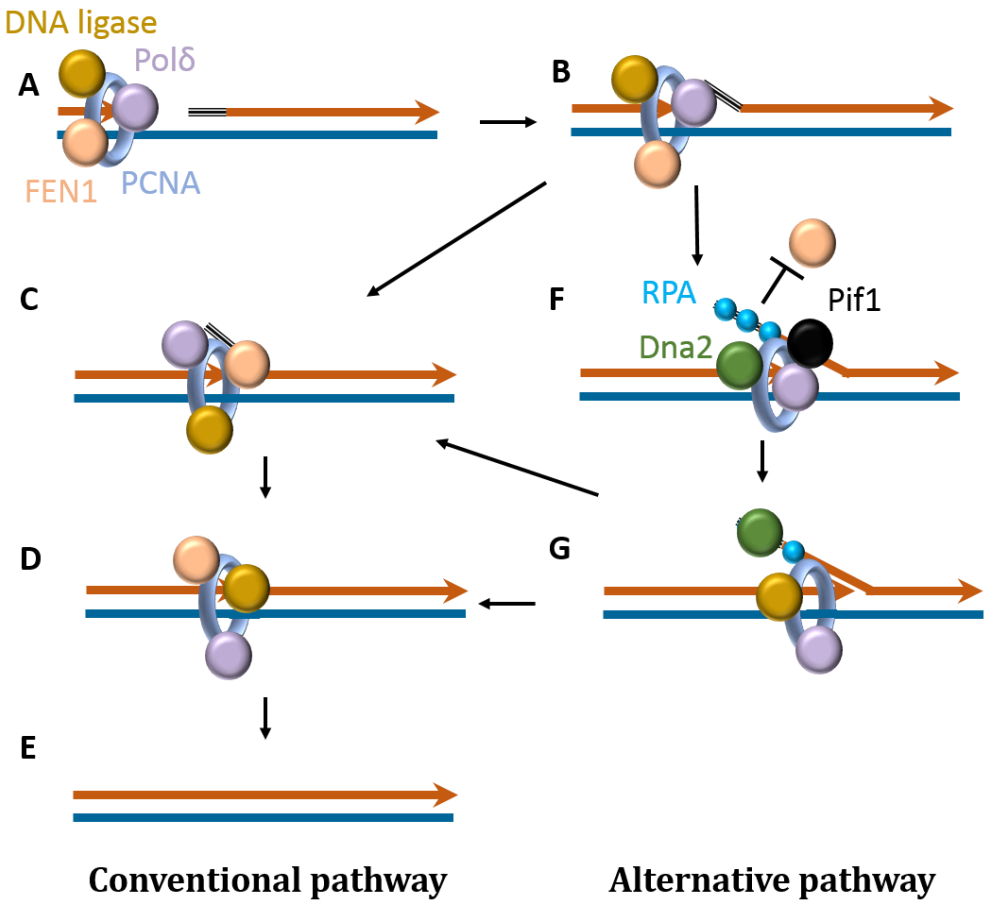

Figure 1.2. Okazaki fragment processing. Adapted from (Dovrat et al. 2014)**.**

During the lagging strand synthesis Pol δ approaches the RNA primer of the preceding OF (**A**) and initiates the strand displacement DNA synthesis creating a short 5' flap (**B**). The short flaps are recognised and removed by FEN1 creating a nick (**C)** that can be ligated by DNA ligase I (**D**) to create a continuous dsDNA strand (**E**). Pif1 creates long 5' flaps bound by RPA which inhibit FEN1 cleavage (**F**). Long flaps are removed by Dna2 (**G**) generating a nick which can be ligated by Lig1, or a short flap that can be processed by FEN1.

The next step of the lagging strand synthesis is the OF maturation, which involves the removal of the RNA primer and joining the fragments of the newly synthesised DNA strand to generate continuous dsDNA. When Pol δ reaches the 5' end of the previous Okazaki fragment, it uses its strand displacement activity to generate a small 5' flap required for the subsequent step of flap processing (Figure 1.2 B). RNA primers have to be removed for the efficient ligation of the OFs by DNA ligase I. The flap removal is normally achieved by the structure-specific endonuclease FEN1 (Rad27 in the budding yeast). FEN1 recognises and removes the small 5'-flaps generated during the strand displacement DNA

synthesis by Pol δ, thereby generating a nick which can be ligated by DNA ligase I (Figure 1.2, C) (Jin et al. 2001; Jin et al. 2003).

In spite of the importance of the OF ligation, cells lacking *RAD27* are viable, suggesting that there are alternative mechanisms of the RNA primer removal (Qiu et al. 1999). In addition, FEN1 activity is inhibited by RPA *in vitro* suggesting that the longer 5' flaps bound by RPA are processed by a different enzyme (Bae et al. 2001). Dna2 helicase-nuclease can remove the long 5' flaps and its catalytic activity is stimulated by RPA (Bae et al. 2001; Budd and Campbell 2000; Hu et al. 2012; Levikova and Cejka 2015). Overexpression of Dna2 compensates for the catalytic defects of the mutant forms of FEN1 (Budd and Campbell 2000).

Recent studies using electron microscopy have shown that long flaps are generated on the lagging strand during DNA replication in both *S. pombe* and *S. cerevisiae* (Liu et al. 2017; Rossi, Foiani, and Giannattasio 2018). The abundance of the long flaps and the corresponding RPA foci is greatly elevated in the cells lacking either FEN1 or Dna2 and is even higher in the cells missing both enzymes, suggesting that they act in the parallel pathways (Liu et al. 2017). Deletion of *DNA2* gene does not produce a viable progeny unless the cells are additionally missing *PIF1*, *POL32* or *RAD9* (Budd et al. 2006; Budd et al. 2011). By using conditional Dna2 depletion, Giannattasio and colleagues have demonstrated that the cells lacking this enzyme arrest in the first cell cycle with a near 2N amount of DNA and an active DNA damage checkpoint. Upon Dna2 depletion, the cells accumulate replication intermediates containing long, up to several kb, flapped ssDNA tails, which can be averted by removing Pif1 (Rossi, Foiani, and Giannattasio 2018). Pif1 is a 5'-3' helicase which has a high specificity for the RNA-DNA hybrids (Lahaye, Leterme, and Foury 1993; Ramanagoudr-Bhojappa et al. 2013; Zhou et al. 2014; Boule and Zakian 2007). Thus, a hypothesis has been proposed that Pif1 generates long flaps during the lagging strand replication (Figure 1.2, F) that require Dna2 to be processed (Figure 1.2, G). This pathway was named the alternative OF processing (Pike et al. 2009). An additional, albeit smaller roles in RNA primer removal was also assigned to Exo1 and RNAse H2 (Liu et al. 2017) .

1.1.4. PCNA is a universal DNA metabolism scaffold

The coordinated action of the OF processing factors relies on the interactions between the relevant enzymes and PCNA (Figure 1.2). PCNA is one of the most well-studied structural proteins in the nucleus. It forms a homotrimeric complex that upon the RFC-dependent loading onto a ds/ss DNA junction encircles the double helix and provides a landing platform for different enzymes involved in DNA metabolism. PCNA not only recruits different enzymes to the DNA but also enhances their catalytic activity (e.g. Pol ε and Pol δ, see sections 1.1.2 and 1.1.3). Additionally, the interactions between certain proteins and PCNA may lead to their post translational modifications and proteasome-dependent degradation (e.g. CDT1, p21 and SET8) (Havens and Walter 2011) . Apart from its role in DNA replication, PCNA is a structural component of different protein complexes involved in, recombination, DNA repair, chromatin assembly and many other processes (Choe and Moldovan 2017; Moldovan, Pfander, and Jentsch 2007; Slade 2018).

An assembled PCNA trimer has the inner surface, which faces the DNA and the outer surface, which is involved in the interactions with other proteins. The inner surface has the basic residues, which form a polar interaction with the phosphates of the DNA sugar-phosphate backbone and allow PCNA to slide along the double helix (De March et al. 2017). PCNA monomers consist of the N and C-terminal domains joined by the inter-domain connecting loop (IDCL). The IDCL is a shared protein interacting surface on the outer PCNA surface, which faces in the direction of DNA synthesis (Choe and Moldovan 2017; Mailand, Gibbs-Seymour, and Bekker-Jensen 2013; Boehm and Washington 2016).

The interaction between PCNA and most of the DNA metabolism enzymes occurs via a PCNA-interacting protein motif (a PIP box, referred to as PIP in this work). The consensus motif for the PIP is $Q_1\ x_2\ x_3\ \psi_4\ x_5\ x_6\ \varphi_7\ \varphi_8$, where x is any amino acid, ψ is a hydrophobic amino acid and φ is an aromatic amino acid (Figure 1.3). The amino acids 4-8 from the PIP peptide usually form a short α-helical structure where ψ_4 , φ_7 and φ_8 bind a hydrophobic pocket in the IDCL, whereas Q in the position 1 binds a “Q pocket” formed by the C-terminal domain of PCNA.

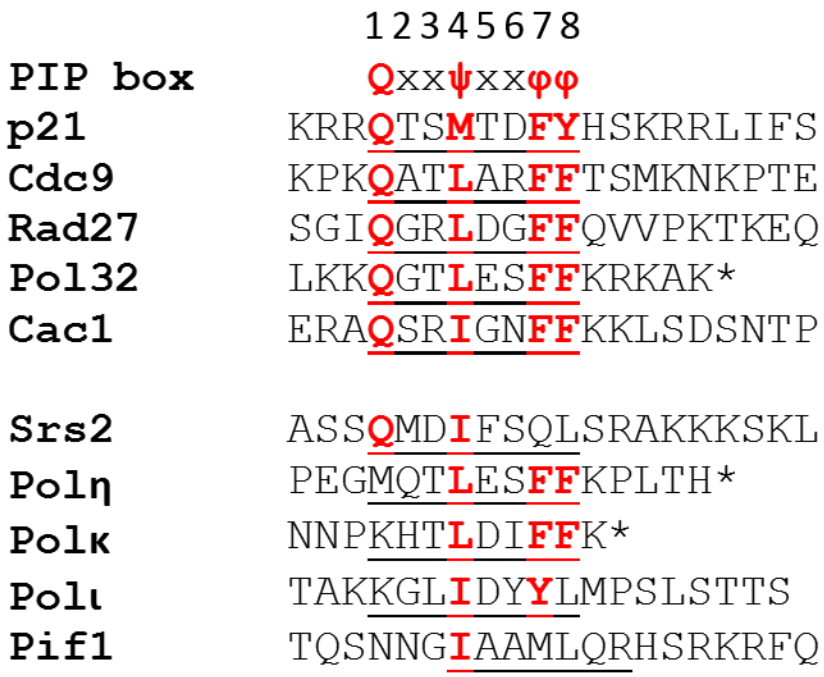

Figure 1.3. Alignment of some known PCNA interacting motifs.

The alignment shows the PIP box consensus (at the top) and the peptides from human and the budding yeast PCNA interacting proteins. The top group of the proteins contains canonical PIPs (the sequences fit the consensus shown in red). The bottom group contains non-canonical PIPs where one or more amino acids do not match the PIP box consensus. The underlined sequences are implicated in the key interactions with PCNA (See the text for details).

However, a subset of PCNA-interacting proteins possess non-canonical PIPs lacking the Q at the position 1 (like Pol η, κ, τ) and/or the aromatic amino acids in the position 7 or 8 (like Srs2 and Pif1) (Armstrong, Mohideen, and Lima 2012; Hishiki et al. 2009; Buzovetsky et al. 2017). Interestingly, the key interactions with PCNA still occur through the binding of the hydrophobic pocket in the IDCL by the amino acids at the positions 4, 7 and 8. Additionally, several works suggest that the sequences surrounding both canonical and non-canonical PIPs have a great impact on the strength of interactions with PCNA (Bruning and Shamoo 2004; Prestel et al. 2019).

The interactions between PCNA and its partners are regulated by various posttranslational modifications of PCNA. Rad6-Rad18-dependent monoubiquitination of K164 in PCNA occurs in response to the accumulation of

the ssDNA when the DNA polymerase stalls and disengages from the replicative helicase (Hoege et al. 2002). Instead of the stalled replicative polymerase, the monoubiquitinated PCNA interacts with a specialised translesion polymerase that contains a PIP and a ubiquitin binding domain (UBD) (Kannouche, Wing, and Lehmann 2004).

Polyubiquitination of K164 on PCNA, which occurs in an MMS2-UBC13-HLTF-dependent manner (Mms2-Ubc13-Rad5 in the budding yeast), promotes error-free DNA damage bypass through template switching (fork regression or strand invasion). This is achieved by recruiting the translocase/structure specific nuclease ZRANB3, which has been reported to promote fork reversal and mediate DNA repair (Ciccia et al. 2012; Weston, Peeters, and Ahel 2012; Vujanovic et al. 2017).

SUMOylation of K164 on PCNA occurs as an alternative to the ubiquitination on this residue and prevents recombination at stalled forks. This is achieved by the activity of helicase Srs2, which dismantles Rad51 filaments (Pfander et al. 2005; Papouli et al. 2005). Localisation of Srs2 to the stalled replication forks relies on its interaction with the SUMOylated PCNA via the C-terminal PIP and a SUMO-interacting motif (SIM) (Armstrong, Mohideen, and Lima 2012).

Additional posttranslational modifications of PCNA include acetylation of lysine residues on the inner surface (Billon et al. 2017; Cazzalini et al. 2014), K248 methylation (Takawa et al. 2012), multiple tyrosine methylations (Waraky et al. 2017; Ortega et al. 2015; Wang et al. 2006); they were also shown to affect the interactions between PCNA and certain proteins.

To conclude, accumulating evidence suggest that PCNA and its posttranslational modifications are important for the timely recruitment and assembly of the relevant enzymes during normal DNA metabolism and in response to DNA damage.

1.2. Break induced replication (BIR)

DNA damage is a dangerous attribute of DNA replication. The probability of generating DSB during DNA replication in the budding yeast was estimated around 10-12 % (Coic et al. 2008; Claussin et al. 2017), while the mammalian cells, which have much bigger genomes, are expected to generate up to 50 DSBs per cell per cell cycle (Vilenchik and Knudson 2003). For example, replication through the nicked DNA can generate a one-ended DSB. In this situation, the broken DNA fragment (recipient chromosome) can use the unbroken sister chromatid (donor chromosome) to initiate the DNA repair pathway called break induced replication (BIR).

BIR is a potentially deleterious DNA repair pathway as it is highly mutagenic, may lead to loss of heterozygosity and DNA translocations if the broken chromosome shares homology to an ectopic sequence (Bosco and Haber 1998; Deem et al. 2011; Hastings, Ira, and Lupski 2009; Sakofsky et al. 2014; Smith, Llorente, and Symington 2007).

BIR shares the initial steps with other homology-based DSB repair pathways, but also has its unique genetic requirements since it involves a long-range DNA synthesis. DNA synthesis during BIR is different from conventional DNA replication because it occurs in a conservative manner (Donnianni and Symington 2013; Saini et al. 2013). The current insights into the molecular mechanisms of BIR as well as its unique genetic requirements are reviewed in this section.

1.2.1. Broken end processing, DNA damage checkpoint activation and D-loop formation

The first critical step during BIR is nucleolytic processing of broken DNA end (Figure 1.4 A) to expose the homology to the donor chromosome and form a recombination proficient Rad51 filament. This is achieved by the combined action of short- and long-range resection machinery. First, the MRX complex, composed of the Mre11, Rad50 and Xsr2 proteins, with the aid of Sae2 endonucleolitically removes a stretch of the 5’-end of the broken end and generates a short (~ 270 nt) 3’-overhang (Neale, Pan, and Keeney 2005; Zakharyevich et al. 2010; Garcia

et al. 2011; Mimitou and Symington 2009). More extensive resection required for exposing longer stretches of homology (Figure 1.4 B), is executed by the two redundant pathways. The first pathway relies on the exonucleolytic activity of Exo1 (Llorente and Symington 2004), which is promoted by RPA and PCNA (Chen et al. 2013; Myler et al. 2016). The second pathway involves the Dna2 and Sgs1 complex, where Sgs1 unwinds the DNA duplex and the Dna2 endonuclease degrades the 5' strand (Cejka et al. 2010; Nimonkar et al. 2011; Niu et al. 2010). The Sgs1 interacting partners Top3 and Rmi1 (STR complex) are essential for the Dna2-dependent resection *in vivo* and were shown to promote Sgs1 localisation to the DNA ends *in vitro* (Cejka et al. 2010; Niu et al. 2010; Zhu et al. 2008).

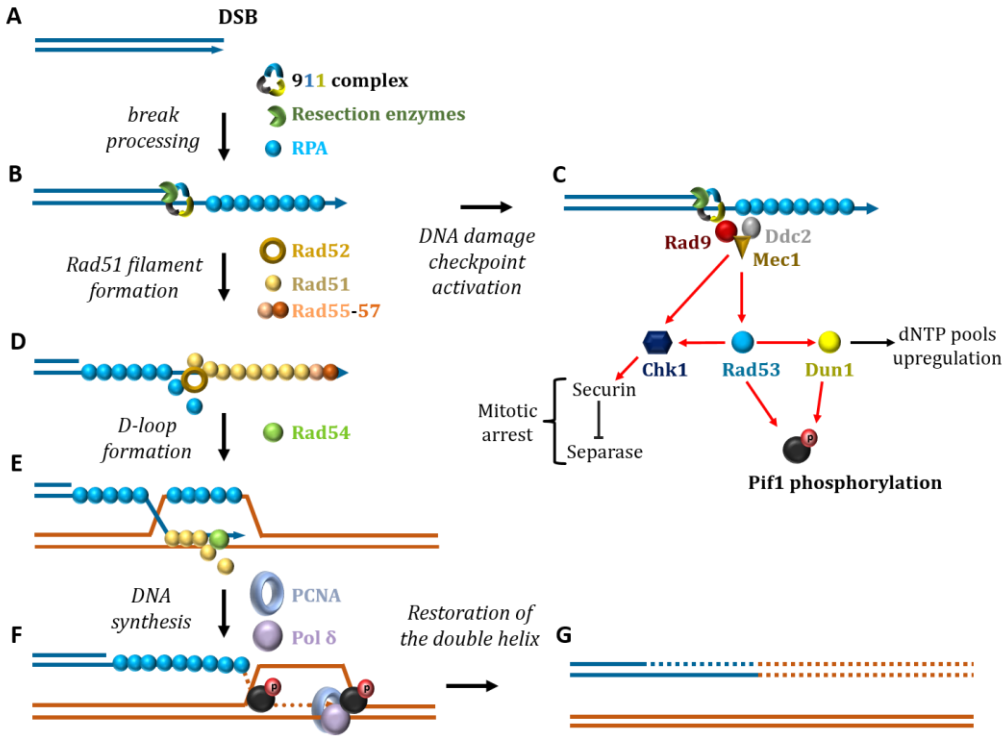

Figure 1.4 Break induced DNA replication.

A simplified schematic describing the main events during BIR. A one ended DSB (**A**) is resected to form RPA-coated ssDNA (**B**), which activates the DNA damage checkpoint (**C**). Rad52 catalyses the formation of a Rad51 filament by replacing RPA with Rad51 (**D**). Rad51 executes the homology search and strand invasion into the donor sequence, which leads to the formation of a D-loop (**E**). Rad54 removes Rad51 from the dsDNA formed after the invasion. The replication components, including PCNA, Pol δ and Pif1 are recruited to the D-loop to initiate conservative DNA synthesis (**F**). The second strand of the recipient chromosome is synthesised to complete the repair (**G**). See the main text for more details. The red arrows in **C** illustrate phosphorylation.

Another important attribute of the cellular response to a DSB is activation of the DNA damage checkpoint (Figure 1.4 C). The early events of the DNA damage checkpoint involve recruitment of Tel1 to the DSB by the MRX complex and Mec1 by the PCNA-like complex 9-1-1 (Ddc1/Mec3/Rad17) with Dpb11 (Ciccia and Elledge 2010; Pfander and Diffley 2011). Subsequently, Mec1 and Tel1 phosphorylate H2A generating γ-H2A. Once the resection has started, the RPA-coated ssDNA recruits Mec1-Ddc2 (Zou and Elledge 2003). Mec1 initiates the phosphorylation cascade that activates the downstream kinases Chk1, Rad53 and Dun1 and phosphorylates Sae2, Dna2 and RPA (Baroni et al. 2004; Brush et al. 1996; Chen et al. 2011; Ciccia and Elledge 2010; Gobbini et al. 2013).

The checkpoint activation is important for several reasons. The Rad53 and Dun1 activation leads to upregulation of the dNTP pool, which is required for the post-replicative DNA repair (Chabes et al. 2003; Sabouri et al. 2008) and for phosphorylation of a number of repair proteins, one of which is Pif1 helicase (Makovets and Blackburn 2009). Phosphorylation of Chk1 leads to the cell cycle arrest and prevents cell division until the repair is complete and the checkpoint is shut down (Sanchez et al. 1999; Wang et al. 2001). γ-H2A recruits the checkpoint proteins to the resected DNA, one of which is Rad9 that negatively regulates both Exo1 and Dna2-STR branches of the long range resection (Chen et al. 2012; Lazzaro et al. 2008; Ngo and Lydall 2015). The 9-1-1 complex regulates DNA resection by promoting recruitment of the resection enzymes and Rad9 (Ngo and Lydall 2015).

The homology search is catalysed by Rad51 that binds to the single-stranded 3’ overhang of the broken chromosome by replacing RPA and forming a recombination-proficient Rad51-filament (Figure 1.4 D). Rad51 nucleation is promoted by Rad52 *in vitro* and *in vivo* (Sung 1997; Song and Sung 2000; Shinohara and Ogawa 1998; New et al. 1998; Gibb et al. 2014). This activity involves physical interactions of Rad52 with both RPA and Rad51 (Stauffer and Chazin 2004; New and Kowalczykowski 2002).

The stability of the Rad51 filament is increased by Rad51 paralogues Rad55 and Rad57, which form heterodimers. The Rad55/57 complex interacts with

Rad51 and incorporates into the growing Rad51 filament (Lim and Hasty 1996; Sugawara, Wang, and Haber 2003; Hays, Firmenich, and Berg 1995).

The strand annealing activity of Rad51 is achieved via the binding of the two DNA molecules through its primary and secondary DNA binding sites (Prasad, Yeykal, and Greene 2006; Zhang et al. 2009; Matsuo et al. 2006). Rad54 has been reported to stabilise the Rad51 filament before the invasion (Mazin et al, 2003) and remove Rad51 from the dsDNA post-invasion in order to promote the recruitment of the replication machinery and initiation of DNA synthesis (Li and Heyer 2009; Andriuskevicius, Kotenko, and Makovets 2018).

The invasion of the broken chromosome end leads to the displacement of the corresponding strand of the donor chromosome (D-loop formation, Figure 1.4 E). The defining distinction of break-induced replication from the conventional homology-mediated DNA repair is that only one end of the broken chromosome is involved in the repair. Several groups have reported that the start of the DNA synthesis during BIR is delayed in comparison with other homology-based repair pathways (Donnianni and Symington 2013; Malkova et al. 2005). Presumably, this delay is caused by the recombination execution checkpoint that prevents DNA synthesis initiation until the second end is captured (Jain et al. 2009). The precise molecular mechanism of this checkpoint is not known, but genetically it requires Sgs1 and Mph1 helicases (Jain et al. 2009; Jain et al. 2016). A deletion of either *SGS1* or *MPH1* gene increases the frequency of BIR and the ***sgs1Δ mph1Δ*** double mutants do not delay the start of DNA synthesis during BIR (Jain et al. 2016).

1.2.2. DNA synthesis during BIR

After a D-loop is formed, the 3'-end of the recipient chromosome can recruit replication factors and initiate DNA synthesis (Figure 1.4 F).

Experiments on BIR initiation in G2 arrested cells demonstrated the requirement of all the components of the CMG complex, and the proteins involved in the replicative helicase loading and replication initiation at the origins (Ctd1, Sld3, Dbp11, Mcm10 and Cdc7), but not the ORC-Cdc6 complex (Lydeard, Lipkin-

Moore, Sheu, et al. 2010). BIR also requires Rad18-mediated ubiquitination and Siz1-mediated SUMOylation of PCNA (Lydeard, Lipkin-Moore, Sheu, et al. 2010).

Interestingly, Pol ε may not be required for BIR, as the cells with the temperature sensitive *pol2-11* allele did not have a defect in BIR-associated DNA synthesis at the non-permissive temperature, in contrast to the cells with the temperature sensitive Pol δ allele *pol3-14* (Lydeard et al. 2007).

The DNA synthesis during BIR occurs in a conservative manner (Donnianni and Symington 2013; Saini et al. 2013). The hypothesis suggesting the asynchronous leading and lagging strand synthesis during BIR was suggested based on the substantial amount of ssDNA detected in the repair intermediates during BIR (Saini et al. 2013). The leading strand is thought to be synthesised first and ejected from the donor chromosome as the D-loop migrates toward the telomere, which generates long stretches of ssDNA covered by RPA. It is still not understood when the complementary strand synthesis is initiated and if it occurs continuously or via multiple priming events.

The recipient strand ejection/re-invasion events were detected after the initiation of DNA synthesis (Smith, Llorente, and Symington 2007). This can lead to template switching if the ejected strand shares homology with multiple loci in the genome. Surprisingly, the template switching only occurs within the first 10 kb from the invasion site, suggesting that there may be an event that stabilises the BIR DNA synthesis. Such stabilisation could be due to the Mms4/Mus81 structure-specific endonuclease that can terminate the conservative mode of DNA synthesis by resolving the D-loops and converting them into conventional replication forks (Mayle et al. 2015).

Pol32, a non-essential component of Pol δ, is strongly required for the DNA synthesis during BIR. A possible reason for this is the Pol32-dependent stimulation of the Pol δ processivity (Gerik et al. 1998). Pol32 can also increase the stability of the complex between Pol δ and PCNA, as it provides an additional PIP (Johansson, Garg, and Burgers 2004; Chilkova et al. 2007).

Pif1 helicase is another factor which is required for BIR (Chung et al. 2010). The cells missing nuclear Pif1 have a severe reduction in the frequency of BIR

and a decrease in the BIR-associated DNA synthesis (Chung et al. 2010; Saini et al. 2013; Wilson et al. 2013). Additional requirements for BIR involve the Rad53/Dun1-dependent phosphorylation of Pif1 on the TLSSAES motif in its C-terminus (Vasianovich, Harrington, and Makovets 2014) and the interaction of Pif1 with PCNA via its C-terminal PIP (Buzovetsky et al. 2017).

Pif1 promotes the strand displacement activity of Pol δ *in vitro*, which has led to a suggestion that the function of Pif1 in BIR is to promote D-loop migration by unwinding the donor DNA (Wilson et al. 2013). This suggestion is conflicted by the previously published requirement of the replicative helicase for BIR (Lydeard, Lipkin-Moore, Sheu, et al. 2010). Perhaps, Pif1 is required for the D-loop progression through certain replication barriers, similar to its role in DNA replication (see section 1.4.3). Alternatively, the establishment of the long-range BIR DNA synthesis may involve a switch between the CMG complex and Pif1. Another possible function of Pif1 in BIR could be ejection of the newly synthesised DNA strand from the D-loop, which is required for the conservative DNA synthesis (Wilson et al. 2013). The involvement of Pif1 in other aspects of BIR pathway, such as the D-loop formation, initiation of the DNA synthesis and the restoration of the double helix (Figure 1.4, G) have not been conclusively addressed.

1.3. Telomere maintenance

The linear nature of eukaryotic chromosomes creates two issues that threaten the genome stability. Firstly, the replication machinery is unable to completely replicate the lagging strand due to the priming of the OF (discussed the section 1.1.3). Thus, the progressive shortening of the chromosome ends must be overcome by a specialised mechanism (Olovnikov 1971; Watson 1972). The second problem is that chromosomal termini must be distinguished from the DSBs. Otherwise, aberrant repair may lead to chromosome fusions and breakage during mitosis (Longhese 2008; McClintock 1939; Muller 1938; Sandell and Zakian 1993). For instance, mammalian chromosome ends are threatened by at least seven distinct DNA damage response pathways (de Lange 2018).

The ends of chromosomes are marked by the distinct species specific nucleotide sequences called telomeres. Telomeres recruit specialised proteins that protect the DNA ends from nucleolytic degradation and checkpoint activation.

In most eukaryotes, the replication-associated telomere shortening is overcome by employing a specialised enzyme called telomerase, which extends telomeres. The telomere length must be maintained within certain species-specific boundaries as short telomeres do not allow binding of the sufficient amount of telomere-protecting proteins while excessively long telomeres are prone to illegitimate recombination. Thus, telomerase has to be tightly regulated. This section provides an overview of the telomere structure and maintenance in budding yeast, as well as the mechanisms that control telomerase activity.

1.3.1. *S. cerevisiae* telomeres and subtelomeric regions

The telomeres in the budding yeast S. cerevisiae consist of ~ 350 bp of dsDNA sequence, composed of T(G_{1-3}) repeats on the 5'-3' strand (Szostak and Blackburn 1982; Shampay, Szostak, and Blackburn 1984; McEachern and Blackburn 1994) and a short (12-15 bases) 3'-extention called a G-tail generated by a controlled degradation of the 5' C-strand (Larrivee, LeBel, and Wellinger 2004). The chromosomal regions preceding the telomeres contain subtelomeric repeats of the two families – X and Y' elements. Most chromosomes have X

elements, which may slightly vary in size and sequence. About half of the subtelomeric regions contain one to four copies of the Y' elements, which could be either 5.2 or 6.2 kb long and are always located between the X elements and telomeres. Telomeric repeats can often be found between the X and Y' elements and between the tandem copies of the Y'-elements (Walmsley et al. 1984). Additionally, origins of replication are located within the Y' elements (Chan and Tye 1983).

The double-stranded regions of the telomeric repeats are bound by Rap1 protein (Figure 1.5). Rap1 has a C-terminal domain, which provides interaction with other telomeric proteins – Rif1/Rif2 and Sir3/Sir4 (Kyrion, Boakye, and Lustig 1992; Wotton and Shore 1997; Graham et al. 1999). Rap1 prevents telomere-telomere fusions (Pardo and Marcand 2005; Marcand et al. 2008), promotes telomere localisation to the nuclear periphery (Gotta and Gasser 1996; Laroche et al. 1998), transcriptional silencing (Hardy, Sussel, and Shore 1992; Hardy, Balderes, and Shore 1992; Kyrion et al. 1993; Palladino et al. 1993) and protects chromosomal ends from nucleases (Negrini et al. 2007; Vodenicharov, Laterreur, and Wellinger 2010).

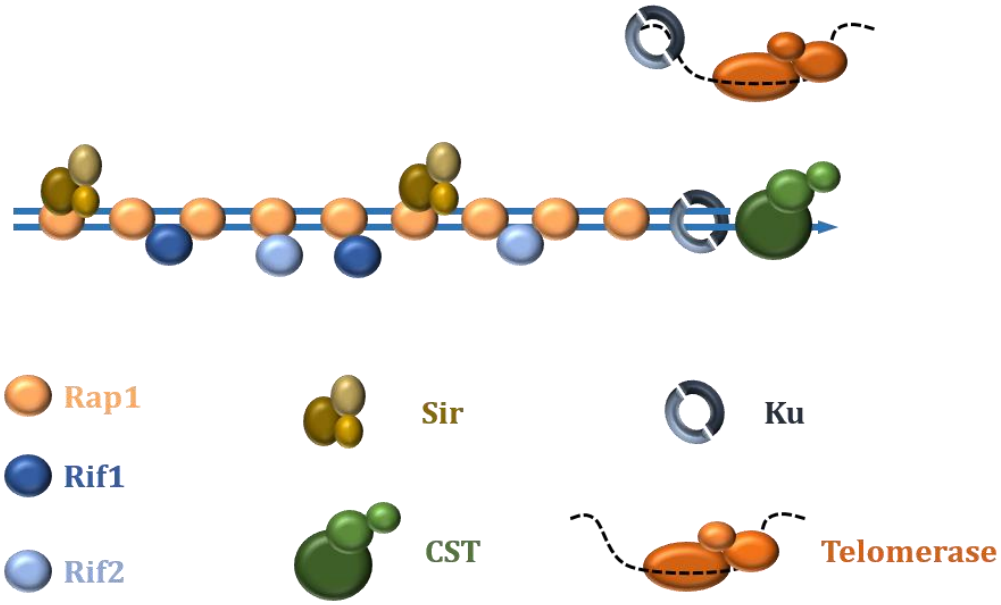

Figure 1.5. Telomere-interacting proteins

The schematic represents the double-stranded and the single-stranded regions of a telomere and the proteins normally associated with these regions. See text for details.

Rif1 and Rif2 proteins bind the C-terminus of Rap1 and form a higher order structure interconnecting different Rap1 units (Figure 1.5) (Shi et al. 2013). *rif1* and *rif2* mutants have longer telomeres, but the double *rif1 rif2* mutant has even longer telomeres indicating that Rif1 and Rif2 act in parallel pathways to regulate telomere length. Rif2 also prevents the association of the Tel1/MRX complex with the telomeres (Hirano, Fukunaga, and Sugimoto 2009; Chapman et al. 2013). In the absence of the G-tail protection, Rif1, but not Rif2, is important for the cell viability (Addinall et al. 2011; Anbalagan et al. 2011; Di Virgilio et al. 2013).

The SIR complex, consisting of the Sir2, Sir3 and Sir4 proteins localises to the telomeres via the interaction with the Rap1 C-terminus (Figure 1.5) and plays a role in the transcriptional silencing of the subtelomeric genes (Cubizolles et al. 2006) and tethers telomeres to the nuclear envelope (Bupp et al. 2007).

Yku70 and Yku80 proteins form a Ku complex that plays an important role in telomere maintenance (Figure 1.5) (Porter et al. 1996). The Ku complex participates in the nuclear import of telomerase RNA (TLC1) (Rathmell and Chu 1994), in anchoring the telomeres to the nuclear periphery (Laroche et al. 1998)

and protecting telomeres as well as broken chromosomes from the nucleases (Bonetti, Clerici, Anbalagan, et al. 2010; Bonetti, Clerici, Manfrini, et al. 2010; Mimitou and Symington 2010). The Ku complex was initially hypothesised to recruit telomerase to telomeres through a simultaneous interaction with TLC1 and a telomeric DNA end (Bertuch and Lundblad 2003; Peterson et al. 2001). However, the later experiments showed that the Ku complex interacts with TLC1 and DNA in a mutually exclusive manner (Pfingsten et al. 2012). It is still possible that the Ku complex helps recruiting telomerase via bridging Est1 to Sir4 (Hass and Zappulla 2015; Chen et al. 2018).

The telomeric G-tail is bound by the CST complex consisting of Cdc13, Stn1 and Ten1 proteins (Figure 1.5). CST is structurally similar to the RPA complex and outcompetes it in binding to the telomeric ssDNA for most of the cell cycle (Schramke et al. 2004; Luciano et al. 2012; Grandin and Charbonneau 2013). Cdc13 is thought to recruit telomerase via its interaction with the Est1 subunit of telomerase (Evans and Lundblad 1999; Qi and Zakian 2000; Pennock, Buckley, and Lundblad 2001; Bianchi, Negrini, and Shore 2004). Additionally, Cdc13 protects telomeres from the Exo1-dependent resection and checkpoint activation (Garvik, Carson, and Hartwell 1995; Maringele and Lydall 2004b, 2004a; Vodenicharov and Wellinger 2006). Cdc13 and Stn1 are implicated in the recruitment of Pol α/Primase to initiate the synthesis of the C-strand after the G-strand has been elongated by telomerase (Chandra et al. 2001; Grossi et al. 2004; Qi and Zakian 2000; Lue et al. 2014). Additionally, Stn1 could limit telomere elongation by competing with Est1 for the interaction with Cdc13 (Chandra et al. 2001; Puglisi et al. 2008).

Thus, both double-stranded and single stranded parts of telomeres are tightly bound by the telomere associated proteins, which are required for telomere protection and telomerase dependent telomere maintenance.

1.3.2. Telomerase-dependent telomere maintenance

Telomerase in S. cerevisiae consist of the three proteins - Est1, Est2 and Est3, and the RNA component - TLC1.

Est2 is a catalytic subunit of telomerase – a reverse-transcriptase (Lingner et al. 1997). Apart from the catalytic domain, Est2 has a long basic N-terminal (TEN) domain which is involved in the interaction with TLC1 (Friedman and Cech 1999) and Est3 (Friedman et al. 2003; Talley et al. 2011). Est2 has a low abundance, < 40 molecules/cell (Tuzon et al. 2011) and its levels are reduced in the absence of TLC1 (Taggart, Teng, and Zakian 2002).

Est1 plays two major roles in telomere lengthening. Firstly, it recruits telomerase to the chromosome end by interacting with TLC1 and Cdc13 (Seto et al. 2002; Wu and Zakian 2011). Secondly, it recruits the Est3 subunit, which is required for activating telomerase (Tuzon et al. 2011). Additionally, Est1 is the only component of the telomerase holoenzyme which is regulated in a cell cycle dependent manner via proteasome-dependent proteolysis (Taggart, Teng, and Zakian 2002; Wu and Zakian 2011; Osterhage, Talley, and Friedman 2006). This is important for the temporal regulation of the telomerase activity.

Est3 is a small protein which associates with telomerase via interacting with both Est1 and Est2 (Osterhage, Talley, and Friedman 2006; Tuzon et al. 2011). Although Est1 and Est3 are not required for the telomerase catalytic activity *in vitro*, both are required for the telomerase-dependent telomere elongation *in vivo* (Lendvay et al. 1996; Lingner et al. 1997).

TLC1 is an RNA component of telomerase present at about 30 molecules per cell (Mozdy and Cech 2006). It is folded into a complex secondary structure which is important for its interactions with the other telomerase components as well as telomere elongation. The conserved pseudoknot domain contains the templating region (Lin et al. 2004) and interacts with Est2 (Livengood, Zaug, and Cech 2002; Dandjinou et al. 2004; Zappulla and Cech 2004; Qiao and Cech 2008). Additionally, TLC1 includes the Est1-binding arm, which is essential for the telomerase activity *in vivo* (Seto et al. 2002)and the Yku80-binding arm, which is required for TLC1 nuclear localisation and promotes Est2 recruitment to the

telomeres in G1 (Stellwagen et al. 2003; Fisher, Taggart, and Zakian 2004; Vega et al. 2007; Gallardo et al. 2008).

Telomerase recruitment to telomeres is regulated through posttranslational modifications of Cdc13. Cdc13 SUMOylation in early/mid-S negatively regulates telomerase recruitment by strengthening the Cdc13-Stn1 interaction (Hang et al. 2011). In contrast, the Cdk1 (Cdc28)-dependent phosphorylation of Cdc13 in late S/G2 phase switches the its partner preference toward the Cdc13-Est1 interaction (Li et al. 2009). Additionally, Mec1/Tel1-dependent phosphorylation of Cdc13 promotes telomerase recruitment (Goudsouzian, Tuzon, and Zakian 2006; Tseng, Lin, and Teng 2006).

Pif1 helicase is another important regulator of telomerase, which inhibits telomerase at telomeres (Schulz and Zakian 1994; Boule, Vega, and Zakian 2005). Cells lacking nuclear Pif1 (*pif1-m2*, see section 1.4.1) have a long telomere phenotype, which depends on functional telomerase. In contrast, *PIF1* overexpression leads to telomere shortening (Schulz and Zakian 1994; Zhou et al. 2000). Pif1 has been reported to localise preferentially to the long telomeres (Phillips et al. 2015). RNA-DNA hybrids are preferred substrates of Pif1 *in vitro*, which led to the suggestion that Pif1 inhibits telomerase by striping TLC1 from the G-tail (Boule, Vega, and Zakian 2005).

To summarise, telomerase activity is used to elongate the telomeric G-strands, counteracting replication-mediated telomere shortening. However, telomerase has to be tightly regulated to keep the length of telomeres within the normal range.

1.3.3. Alternative telomere lengthening

In the cells missing any of the essential telomerase components, telomeres shorten progressively with each cell division until they reach the critically short length and trigger a terminal cell cycle arrest through the DNA damage checkpoint activation. Due to the inability to repair the critically short telomeres, in most cells the arrest leads to cell death (Singer and Gottschling 1994; Lundblad and Szostak 1989; Lendvay et al. 1996; Enomoto, Glowczewski, and Berman 2002; AS and

Greider 2003). However, two types of survivors may emerge from the dying population of telomerase-deficient cells (Le et al. 1999; Teng and Zakian 1999; Lundblad and Blackburn 1993).

The first type of telomerase-deficient survivors (Type I) maintain their chromosome ends by amplifying Y'-repeats. In these cells, the telomeric TG_{1-3} repeats are kept very short but stable (Lundblad and Blackburn 1993; Larrivee and Wellinger 2006). The Type I survivors often have extrachromosomal DNA circles containing Y' repeats, which may help acquisition and amplification of Y's at the chromosomal ends (Larrivee and Wellinger 2006). This pathway requires the classical homologous recombination machinery - Rad52, 51, 55, 57 and Rad54 (Le et al. 1999; Lundblad and Blackburn 1993; Teng and Zakian 1999).

The second type of telomerase-deficient survivors (Type II) is characterised by a highly variable length of TG_{1-3} repeats (from very short to 12 kb in length) (Teng and Zakian 1999; Teng et al. 2000) and the extrachromosomal DNA circles that contain telomeric repeats (t-circles) (Lin et al. 2005; Larrivee and Wellinger 2006). This pathway is Rad51-independent, but requires Rad52, the MRX complex, Sgs1 and Rad59 (Cohen and Sinclair 2001; Huang et al. 2001; Lundblad and Blackburn 1993; McEachern and Blackburn 1994; Teng et al. 2000; Teng and Zakian 1999).

Both Type I and Type II survivors require Pol32, arguing that the telomerase-independent telomere maintenance occurs via BIR (McEachern and Haber 2006; Lydeard et al. 2007). In contrast, Pif1 was only shown to be required for generation of Type I survivors (Hu et al. 2013).

A similar mechanism of telomerase-independent telomere lengthening exists in human cells. Alternative lengthening of telomeres (ALT) is a molecular pathway that helps to overcome replicative senescence in a considerable fraction of human cancers (10-15%) (Dilley and Greenberg 2015; Heaphy et al. 2011; Reddel 2014). ALT in most human cell lines is Rad51 independent and resembles the budding yeast Type II survivors, since it produces various tracks of telomeric repeats (TTAGGG) (Cesare and Reddel 2010; Pickett and Reddel 2015; Verma and Greenberg 2016; Costantino et al. 2014). ALT^+ cells harbour extrachromosomal partially or completely single-stranded DNA circles containing telomeric repeats

(C-circles) the amount of which correlates with efficiency of telomere DNA synthesis (O'Sullivan et al. 2014; Sobinoff et al. 2017; Yu et al. 2015) . Another hallmark of ALT$^+$ cells is the ALT-associated PML bodies (APL) which co-localise with telomeres and the DNA repair machinery (RPA, RAD51, RAD52, BLM) and promote telomeric recombination (Acharya et al. 2014; Lillard-Wetherell et al. 2004; Nabetani, Yokoyama, and Ishikawa 2004; O'Sullivan et al. 2014; Potts and Yu 2007; Stavropoulos et al. 2002; Wu, Lee, and Chen 2000; Yeager et al. 1999).

Telomeric DNA amplification in ALT$^+$ cells involves conservative DNA synthesis and requires POLD3 (human Pol32) and POLD4 components of Pol δ (Dilley et al. 2016; Roumelioti et al. 2016). In contrast with the budding yeast BIR, the D-loop migration during ALT is promoted by the BLM helicase in a complex with TOP3A-RMI (homologues of the STR complex in *S. cerevisiae*) and is repressed in the SLX4-SLX1-ERCC4-dependent manner (Sobinoff et al. 2017). The telomere lengthening in ALT$^+$ cells requires RAD52 (Bhowmick, Minocherhomji, and Hickson 2016; Min, Wright, and Shay 2017; Ozer et al. 2018; Sotiriou et al. 2016; Zhang et al. 2019). In the absence of RAD52, the telomeres shorten progressively, although the C-circle formation is not affected. After a few generations, the telomere associated DNA synthesis recovers, suggesting that there may be a less efficient RAD52-independent ALT pathway (Zhang et al. 2019).

A more detailed understanding of the ALT mechanisms in human cancer cells may be very important for developing the strategies for therapeutic targeting of telomerase-negative tumours.

1.3.4. Telomere addition to DSBs

Apart from elongating telomeric DNA, telomerase can add new telomeres to DSBs in a process called *de novo* telomere addition (DNTA) (Biessmann et al. 1990; Kramer and Haber 1993; Fouladi et al. 2000). DNTA is a potentially deleterious repair pathway, as it leads to a loss of the acentromeric arm of a broken chromosome (Kramer and Haber 1993; Schulz and Zakian 1994).

The molecular mechanism of telomere extension implies annealing of the template region of TLC1 to the terminal telomeric repeats. The sites were DNTA events occur often contain sequences with partial similarity to the telomeric repeats (Putnam, Pennaneach, and Kolodner 2004). In line with this, inducing DSBs in different loci yields different probability of DNTA. For example, DSBs induced at the *NRG2* locus are predominantly repaired by DNTA (Stellwagen et al. 2003). Further analysis revealed that this locus contains the sequence readily bound by Cdc13 after the break induction and resection, which leads to telomerase recruitment (Obodo et al. 2016). Another work concluded that DNTA is greatly promoted by Cdc13 binding to DSBs and requires Cdc13 dimerization, its DNA binding and telomerase recruitment abilities (Strecker et al. 2017).

An important part of the DNTA is re-synthesis of the resected 5'-end after the telomere addition. Recent work by Makovets and colleagues showed that the Srs2 helicase is required for this process (Vasianovich et al. 2017). Rad51 binding to the ssDNA interferes with the PCNA loading and re-synthesis of the resected strand by the replicative polymerases. Srs2 dismantles Rad51 filaments allowing a successful completion of the repair.

Pif1 helicase serves as one of the main negative regulators of telomerase at DSBs (Schulz and Zakian 1994). The frequency of gross chromosomal rearrangements (GCR) that lead to terminal deletions increases 200-1,000 times in cells lacking the Pif1 helicase (Mangahas et al. 2001; Myung, Chen, and Kolodner 2001; Schulz and Zakian 1994). This phenotype is telomerase-dependent since deletion of any of the telomerase components suppresses the frequency of the GCRs back to the wild type levels (Myung, Chen, and Kolodner 2001).

Pif1 is phosphorylated by Rad53/Dun1 at the C-terminal TLSSAES motif in response to DNA damage (Figure 1.4). This phosphorylation is required for telomerase inhibition at DSBs but not at telomeres, suggesting that the two mechanisms of telomerase inhibition may differ (Makovets and Blackburn 2009). The phosphorylation-deficient Pif1-4A protein did not have a reduced enrichment at DSBs in comparison to the phosphorylation-proficient Pif1, suggesting that the posttranslational modifications are required after the Pif1 localisation to DSBs.

Interestingly, the Pif1-dependent protection of the DSB ends from DNTA can be bypassed by placing a short TG_{1-3} sequence (≥ 34 bp) which is sufficient for a Cdc13 dimer to bind *in vitro* (Mitchell et al. 2010).

The Mec1-dependent phosphorylation of Cdc13 guards DSBs against the CST complex recruitment (Zhang and Durocher 2010). Another possible mechanism of negative regulation of DNTA is the cell cycle dependent spatial segregation of TLC1 from the sites of DNA damage (Ouenzar et al. 2017). The bulk of the TLC1 foci were co-localised with the nucleolus markers in G2/M in a manner dependent on Pif1 and Rad52. However, the molecular mechanism of this process is yet to be determined.

The long-range resection of DSBs also inhibits DNTA, as *exo1Δ* and *sgs1Δ* mutations that inactivate the pathways of DNA resection substantially increase the frequency of DNTA events at the breaks and the *exo1Δ sgs1Δ* double mutants acquire telomeres at 70% of the breaks and independently of the status of *PIF1* (Chung et al. 2010; Lydeard, Lipkin-Moore, Jain, et al. 2010).

To sum up, further investigation is required to understand the molecular mechanism of telomerase inhibition at DSB, particularly the role of Pif1 and its DNA damage-dependent phosphorylation. Considering that Pif1 is a multifunctional helicase involved in many aspects of DNA metabolism, it may be important to consider its mechanism of action in a broader context. The next section provides an overview of the reported functions of Pif1 and the highly related Rrm3, which together constitute the Pif1 family of helicases.

1.4. The Pif1 family of helicases

The Pif1 family of helicases contains enzymes which are presented in most eukaryotes and are implicated in many aspects of DNA metabolism.

The Pif1 family members belong to the super family 1B of DNA helicases, which are mostly monomeric and have a 5'-3' directionality (Bochman, Sabouri, and Zakian 2010). They all consist of the helicase core, which contains seven highly-conserved SF1 motifs (I, IIa, II, III, IV, V and VI), as well as the N- and C-terminal domains that differ in size and sequence. An additional attribute of the Pif1 helicases is the Pif1-signature motif located between the helicase motifs II and III (Bochman, Sabouri, and Zakian 2010; Mohammad, Wallgren, and Sabouri 2018; Geronimo et al. 2018). The Pif1-signature motif is required for the ATPase activity *in vitro* and for all the tested Pif1 functions *in vivo* (Mohammad, Wallgren, and Sabouri 2018; Geronimo et al. 2018).

The helicase activity of Pif1 *in vitro* shows a clear preference for the forked DNA substrates with 3'-ssDNA overhangs and the substrates containing RNA-DNA hybrids (Lahaye, Leterme, and Foury 1993; Ramanagoudr-Bhojappa et al. 2013; Zhou et al. 2014; Boule and Zakian 2007). Pif1 has also been shown to be a potent unwinder of G-quadruplex (G4) DNA structures *in vitro* and a suppressor of G4-mediated replication barriers *in vivo* (Ribeyre et al. 2009; Zhou et al. 2014; Duan et al. 2015; Paeschke, Capra, and Zakian 2011; Paeschke et al. 2013; Byrd and Raney 2015; Mendoza et al. 2015).

The Pif1 helicases were found in most eukaryotes and some prokaryotes (Bochman, Sabouri, and Zakian 2010; Bochman, Judge, and Zakian 2011). Most of the eukaryotes have a single Pif1 helicase. The exceptions include *S. cerevisiae* that have a second Pif1-like helicase Rrm3. Rrm3 shares 60% similarity to Pif1 but has distinct functions in promoting DNA replication through certain replication barriers (described in 1.4.2).

Trypanosomes express eight Pif1-like helicases with distinct functions (Liu, Wang, Yildirir, et al. 2009; Liu, Wang, Yaffe, et al. 2009; Wang, Englund, and Jensen 2012), six of which are mitochondrial, one cytoplasmic and one nuclear.

Six out of the eight Pif1-like helicases in *Trypanosomes* are essential (Liu et al. 2010).

Schizosaccharomyces pombe have a single Pif1 helicase, called Pfh1 (Zhou et al. 2000). Like the *S. cerevisiae PIF1* gene, *pfh1* produces a common transcript for the nuclear and mitochondrial helicases, which are translated from the two alternative translation start sites. Both nuclear and mitochondrial Pfh1 are essential (Pinter, Aubert, and Zakian 2008). The nuclear functions of Pfh1 are similar to those of Rrm3 since Pfh1 promotes replication through the replication fork impediments (McDonald et al. 2014; Sabouri et al. 2012; Steinacher et al. 2012). Unlike Pif1, Pfh1 does not inhibit telomerase at telomeres (Zhou et al. 2002) but similarly to Pif1, Pfh1 is involved in OF maturation (Tanaka et al. 2002; Ryu et al. 2004).

Human PIF1 has been found in both nuclei and mitochondria (Mateyak and Zakian 2006; Futami, Shimamoto, and Furuichi 2007) and is believed to promote DNA replication through RNA-DNA hybrids and G-C rich loci (Gu, Masuda, and Kamiya 2008; George et al. 2009; Sanders 2010). In recent work, human PIF1 was shown to interact with BRCA1 and promote DNA resection and therefore homologous recombination (Jimeno et al. 2018). Both human and murine PIF1 have been reported to physically interact with telomerase (Mateyak and Zakian 2006; Snow et al. 2007), but the involvement of PIF1 in telomere length regulation is still debatable (Zhang et al. 2006; Mateyak and Zakian 2006; Futami, Shimamoto, and Furuichi 2007). The abundance of Pif1 in both budding yeast and human cells is regulated in a cell cycle dependent manner by the APC/C mediated proteasomal degradation (Mateyak and Zakian 2006; Vega et al. 2007). The Pif1 levels peak at G2/M and are minimal during G1, which somewhat reflects telomerase activity.

This section describes the reported functions of the *S. cerevisiae* Pif1 helicases, with the focus on the functional divergence between Pif1 and Rrm3.

1.4.1. *S. cerevisiae* Pif1 is a multifunctional helicase involved in DNA replication and DNA repair

Pif1 was originally described as a helicase required for mitochondrial DNA maintenance (Pif1 loss results in the ρ^0 phenotype – loss of mitochondrial DNA and the ability to respirate) (Foury and Kolodynski 1983; Lahaye et al. 1991), and later it was re-discovered as a factor that counteracts telomerase-dependent telomere lengthening (Schulz and Zakian 1994). The mitochondrial and nuclear isoforms of Pif1 are translated from the alternative translation start sites – M_1 and M_{40}. Mutating M_1 (*pif1-m1*) produces cells with only the nuclear enzyme, whereas yeast with the M_{40} mutation (*pif1-m2*) have only the mitochondrial enzyme (Schulz and Zakian 1994).

Nuclear Pif1 is involved in many aspects of DNA metabolism – DNA replication (see sections 1.1.3 and 1.4.3), promotion of the template switching pathway of DNA damage bypass by expanding daughter strand gaps after replication (Garcia-Rodriguez, Wong, and Ulrich 2018), suppression of recombination at the *rDNA* genes (described in 1.4.3), regulation of telomere length (section 1.3.2), inhibition of telomerase at DSBs (section 1.3.4) and DNA repair via BIR (section 1.2.2.). Despite this, absence of the nuclear Pif1 does not lead to noticeable changes in viability, gene conversion or chromosome loss (Schulz and Zakian 1994, Rossi et al. 2015).

The Rad53/Dun1-dependent phosphorylation of the C-terminal TLSSAES motif in Pif1 is required for the functions in response to DSBs – inhibition of telomerase at the breaks and BIR stimulation (Makovets and Blackburn 2009; Vasianovich, Harrington, and Makovets 2014). The mechanistic role of this phosphorylation is not clear yet. The strains expressing the phosphorylation-deficient allele *pif1-4A* (ALAAAEA) have normal telomere length, but high frequency of DNTA (see section 1.2.3.), while the cells expressing the phospho-mimic *pif1-4D* (DLDDAED) efficiently inhibit telomerase at DSBs (Makovets and Blackburn 2009), but are deficient in BIR (Vasianovich, Harrington, and Makovets 2014). This could be explained by only a partial resemblance of the aspartic acid to the phosphorylated serine/threonine, particularly if the phosphosite acts as a part of a protein-interacting surface. Alternatively, due to the complex nature of

BIR, both non-phosphorylated and phosphorylated isoforms of Pif1 may be required during the repair.

In addition to the phosphosite in the C-terminus of Pif1, the N-termini of both Pif1 and Rrm3 contain the sites that are phosphorylated by Rad53 in response to the replication stress caused by hydroxyurea (Rossi et al. 2015). Pif1 SUMOylation was also reported earlier (Hang et al. 2011). However, the functions of these posttranslational modifications still remain unknown.

Unravelling the details of the posttranslational regulation of Pif1 may help understanding the difference in the regulation of telomerase at DSBs and at telomeres, provide molecular insights into the mechanisms of BIR and understand the functional divergence between the Pif1 helicases.

1.4.2. Rrm3 is associated with the replisome and promotes replication fork progression through protein-DNA complexes

While Pif1 is recruited to its sites of action mostly post-replication, Rrm3 associates and moves with the replisome during DNA replication and has a direct interaction with Pol2 (Azvolinsky et al. 2006; Paeschke, Capra, and Zakian 2011). Deletion of *RRM3* affects replication of all the chromosomes, leads to increased replication fork pausing and breakage at many hard-to-replicate sites resulting in constitutive activation of the DNA damage response (Azvolinsky et al. 2006; Ivessa et al. 2003; Torres, Schnakenberg, and Zakian 2004; Schmidt and Kolodner 2006). Rrm3 localises to the replication origins in early S phase (Azvolinsky et al. 2006) and interacts with Orc5, a component of the origin recognition complex, via its N-terminal motif (Matsuda et al. 2007; Syed et al. 2016).

Apart from the general effect on DNA replication, Rrm3 promotes replication fork progression through the certain “hard-to-replicate” regions.

rDNA on chromosome XII was the first described Rrm3-sensitive replication locus (Ivessa, Zhou, and Zakian 2000). *rDNA* is a repetitive region, which consists of multiple *RDN1* repeats (on average 150 repeats per haploid genome). Each

RDN1 unit contains the genes encoding the 35S rRNA precursor and the 5S rRNA, a replication origin (only 15% of the replication origins in *RDN1* repeats are active in a given S phase) and a replication fork barrier (RFB) – a polar block to replication fork progression (Brewer and Fangman 1988; Linskens and Huberman 1988). The RFB leads to a programmed replication block, which stalls the leftward moving replication fork to prevent a possible replication-transcription collision at the highly transcribed 35S rRNA gene.

The programmed replication block is achieved by Fob1, which tightly binds the RFB and changes the DNA conformation of this region (Kobayashi 2003). The Rrm3 helicase is able to eject Fob1 and allow replication fork progression by the rightward moving forks. In the absence of Rrm3, the Fob1-mediated barrier becomes bi-directional and the frequency of the stalled forks increases, which in turn promotes *rDNA* recombination and the formation of the extrachromosomal *rDNA* circles (Ivessa, Zhou, and Zakian 2000). The activity of Rrm3 at RFBs is opposed by Tof1-Csm3 complex which is recruited to *RDN1* to enforce the programmed replication barrier (Mohanty, Bairwa, and Bastia 2006; Hodgson, Calzada, and Labib 2007; Bairwa et al. 2010).

Interestingly Pif1 has an opposing effect on the replication through *rDNA*. In the absence of Pif1, the leftward moving fork pausing at RFBs and *rDNA* circle generation are decreased, suggesting that Pif1 enforces the RFB and promotes *rDNA* recombination (Ivessa, Zhou, and Zakian 2000). The detailed mechanism of this process is not well understood.

Rrm3 has been shown to promote DNA replication through the telomeric repeats, inactive replication origins, tRNA genes, centromeres, and the silenced *HML* and *HMR* loci (Ivessa et al. 2002; Ivessa et al. 2003; Makovets, Herskowitz, and Blackburn 2004). The common feature of the Rrm3 sensitive replication barriers are non-histone protein-DNA complexes (Ivessa et al. 2003; Torres, Schnakenberg, and Zakian 2004). At the centromeres, the fork pausing correlates with the higher order chromatin structures and is relieved by the mutations that interfere with the chromatin state (Greenfeder and Newlon 1992). At the tRNA genes, the pausing depends on the presence of an assembled transcription initiation complex (Ivessa et al. 2003). At the telomeres and internal telomeric

repeats, the replication fork pausing is caused by Rap1 binding (Makovets, Herskowitz, and Blackburn 2004).

Thus, despite significant sequence similarity, Rrm3 has a greater influence on DNA replication than Pif1. Further investigation is required to explain the nature of the functional divergence between Pif1 and Rrm3.

1.4.3. Pif1 helicases have overlapping functions in DNA replication

In *rrm3Δ* cells, replication of several Rrm3-sensitive loci depends on Pif1. The growth of *rrm3Δ* and *pif1-m2* cells is similar to the growth in wild type cells, but the double *rrm3Δ pif1-m2* mutants grow significantly slower and accumulate cells in S phase indicating replication problems (Chen et al. 2019). This can be explained by the redundant role of the Pif1 helicases in promoting DNA replication through the replication fork impediments.

Replication forks pause at the tRNA genes, which are transcribed by RNA Polymerase III (Deshpande and Newlon 1996). The tRNA genes are highly transcribed and act as polar replication barriers affecting only replication that opposes transcription (head-on orientation). Transcription at the tRNA genes could interfere with replication either due to the transcription initiators that tightly bind DNA, or due to the generation of R-loops. A mutation that affect the assembly of the transcription initiation complex relieves the replication barrier at the tRNA genes (Deshpande and Newlon 1996), while mutations in the transcription terminator, that lead to extended transcripts, do not increase the pausing regions, pointing toward the protein-DNA complexes being the primary cause for the replication pausing (Ivessa et al. 2003).

In *rrm3Δ* cells, replication pausing at the tRNA genes is significantly increased in comparison with the wild type cells (Ivessa et al. 2003). Although *pif1Δ* replicate tRNA genes similarly to the wild type cells, *rrm3Δ pif1Δ* have greater replication fork pausing than the *rrm3Δ* cells (Osmundson et al. 2017; Tran et al. 2017). This results suggest that Pif1 acts as a back-up helicase promoting replication through this region, mainly in the absence of Rrm3. The activity of the Pif1 helicases

prevents DNA damage and gross chromosomal rearrangements at the tRNA genes (Tran et al. 2017). Interestingly, overexpression of the ribonuclease H gene partially suppresses recombination at tDNA in the *rrm3Δ pif1Δ* suggesting that the R-loops may be the cause of the DNA damage in the absence of the Pif1 helicases (Tran et al. 2017).

The centromeres in *S. cerevisiae* contain a ∼ 125 bp sequence consisting of the three elements – CDEI, CDEII and CDEIII. Several protein complexes bind centromeric elements – Cbf1 binds CDEI (Mellor et al. 1990); CDEII is bound by a nucleosome, which also contains Cse4 (centromere-specific variant of H3, like CENPA in humans); CDEIII is bound by Cbf3, which is required for kinetochore protein association with centromeres (Biggins 2013).

Transient replication pausing at the centromeres has been observed in the wild type cells (Greenfeder and Newlon 1992). In line with the proposed role of Rrm3 in removing protein-DNA complexes, the replication fork pausing at the centromeres increases up to threefold in the *rrm3Δ* cells (Ivessa et al. 2003). Like at the *rDNA* locus, Tof1 has been shown to stabilise the replication forks at the centromeres and counteract the Rrm3 activity (Mohanty, Bairwa, and Bastia 2006; Hodgson, Calzada, and Labib 2007).

Both Pif1 family helicases have been shown to localise to active centromeres, although with a different timing within a cell cycle. Rrm3 localises in early/mid-S, supposedly during the centromere replication, while Pif1 localises later in S (Chen et al. 2019). Interestingly, removal of either of the Pif1 helicases affects the recruitment pattern of the other helicase. Although Pif1 is not required for the centromere replication in *RRM3* cells, *rrm3Δ pif1-m2* cells have a synergistic increase in the replication fork pausing at centromeres (Chen et al. 2019). A Similar synthetic effect has been reported for the frequency of the loss of a centromere containing plasmid (Chen et al. 2019).

High G-C content DNA in the *S. cerevisiae* mostly A-T rich genome is concentrated mainly at telomeres and *rDNA*. However, the rest of the genome contains more than 500 G-rich sequences prone to forming G4 secondary structures (G4 motifs), which are predicted to impede replication fork progression (Capra et al. 2010; Hershman et al. 2008). Recombinant human and budding

yeast Pif1 bind and unwind G4 structures *in vitro* (Sanders 2010; Ribeyre et al. 2009). In the budding yeast, Pif1 has been shown to localise to the G4 motifs after replication (Paeschke, Capra, and Zakian 2011). In *pif1* mutants, the replication forks passing through the G4 motifs slow down and break with a higher frequency than in the wild type cells, which may lead to GCR (Paeschke, Capra, and Zakian 2011; Lopes et al. 2011). One of the two recently identified C-terminal PIP motifs in Pif1 was suggested to be required for promoting replication fork progression through the G4 motifs (Dahan et al. 2018). Deletion of *RRM3* gene does not lead to an increased fork instability at the G4 motifs (Paeschke et al. 2013). However, in the absence of Pif1, Rrm3 localises to the G4 motifs. *pif1-m2 rrm3* cells have higher G4-induced GCR rate than *pif1-m2* mutants, indicating that Rrm3 acts as a backup helicase promoting replication through the G4 motifs.

Apart from the promoting replication fork progression through the replication barriers, the Pif1 helicases have been recently shown to be involved in the resolution of the converging replication forks and replication termination (Deegan et al. 2019). Either Pif1 or Rrm3 were required for replication termination in the reconstituted system (Deegan et al. 2019). The *rrm3Δ pif1-m2* but not the single mutants accumulated replication intermediates during plasmid replication that migrated as double-Y structures on 2D-gels, suggesting that the Pif1 family helicases act redundantly to promote replication termination *in vivo* (Deegan et al. 2019).

1.5. Introduction summary and the aims of the study.

Pif1 helicases are important factors that are required for normal DNA metabolism in many eukaryotes. The functions of *S. cerevisiae* Pif1 helicases involve DNA replication, telomere maintenance and DNA repair. However, it is not known how the functional specificity of Pif1 helicases is defined molecularly.

Recent studies show that both Pif1 and Rrm3 physically interact with PCNA (Wilson et al. 2013; Buzovetsky et al. 2017; Dahan et al. 2018; Schmidt, Derry, and Kolodner 2002). The two C-terminal PIP motifs in Pif1 (PIP1 and PIP2) were suggested to be required for BIR and DNA replication through G4 motifs

respectively (Buzovetsky et al. 2017; Dahan et al. 2018). The function of the N-terminally located PIP in Rrm3 was not addressed. Apart from the published PCNA-interacting motifs, Pif1 has putative PIP and SIM motifs in the N-terminus and the C-terminus of Rrm3 has a sequence homologous to the PIP2 motif in Pif1, which could also serve as a PCNA-interacting motif (S. Makovets, personal observation).

Notably, the reported PCNA-interacting motifs in both Pif1 and Rrm3 are located in the regions that are least conserved between the two proteins, suggesting that the interaction with PCNA via different motifs in the Pif1 helicases may be connected with their diverged functions. This work is aimed to address the genetic requirements for the PCNA-interacting elements in Pif1 and Rrm3 for their unique and overlapping functions.

Chapter II Materials and Methods

2.1. Yeast strains

The yeast strains used in this study are presented in Table 1.

2.2. Growth media

The growth media used in this study are listed in Table 2. The concentration of the ingredients is shown in weight/volume (w/v). The rich medium was prepared by mixing a solution of filter-sterilized carbon source (glucose, galactose, raffinose or glycerol) and supplements (adenine, uracil and tryptophan) with autoclaved yeast extract, peptone and agar dissolved in water. Synthetic defined (SD) medium, depleted from certain components, was made by mixing a solution of filter-sterilised carbon source, a drop-out mixture (Complete Supplement Mixture recipe, Formedium) and supplements with autoclaved yeast nitrogen base (Formedium) and agar.

2.3. Plasmids

The plasmids used in this study are listed in Table 3.

2.4. Primers

The list of oligonucleotides used in this study is presented in Table 4. The SerialCloner 1.3-11 software was used to design primers which were subsequently manufactured by Integrated DNA Technologies (IDT). 100 µM stock solutions of the primers were prepared by dissolving lyophilised oligonucleotides in Milli-Q H2O and stored at room temperature (or at -20oC for long term).

2.5. Restriction enzymes

The restriction enzymes used in this study were purchased from New England Biolabs (NEB), stored and used in accordance with the manufacturer recommendations.

2.6. Antibodies

The list of antibodies used in this study is presented in Table 5. All antibodies were aliquoted upon delivery and stored at -80ºC. The antibody dilutions used in the experiments was defined experimentally for each antibody.

Table 1. Yeast strains used in the study

Strain	Relevant genotype	Source/construction notes
	Saccharomyces cerevisiae A364a	
NK1	*MATa bar1::LEU2 trp1-289 ura3-5 leu2-3,112*	(Makovets, Herskowitz, and Blackburn 2004)
NK828	*MATa bar1::LEU2 trp1-289 ura3-5 leu2-3,112 pif1-m2*	(Makovets and Blackburn 2009)
NK1324	*MATa-inc trp1-289 ura3::NAT leu2::LEU2-Pgal-HO HEM13::HOsite-URA3 pif1-m2*	
NK1325	*MATa-inc trp1-289 ura3::NAT leu2::LEU2-Pgal-HO HEM13::HOsite-URA3 pif1-m2-TRP1-pif1-m1*	
NK1335	*MATa-inc trp1-289 ura3::NAT leu2::LEU2-Pgal-HO HEM13::HOsite-URA3 pif1-m2-TRP1-pif1-m1-4myc*	
NK3725	*MATa-inc trp1-289 ura3::NAT leu2::LEU2-Pgal-HO MNT2::kan::HOsite-URA3-STAR-TEL HIS7::kan*	(Vasianovich, Harrington, and Makovets 2014)
NK3726	*MATa-inc trp1-289 ura3::NAT leu2::LEU2-Pgal-HO MNT2::kan::HOsite-URA3-STAR-TEL HIS7::kan*	
NK3728	*MATa-inc trp1-289 ura3::NAT leu2::LEU2-Pgal-HO MNT2::kan::HOsite-URA3-STAR-TEL HIS7::kan pif1-m2*	
NK3729		
NK3731	*MATa-inc trp1-289 ura3::NAT leu2::LEU2-Pgal-HO MNT2::kan::HOsite-URA3-STAR-TEL HIS7::kan pif1-m2-TRP1-pif1-m1-4A*	
NK4070	*MATa-inc ura3::NAT leu2::LEU2-Pgal-HO MNT2::KAN-(ARO4-SPO23)::HOsite-URA3-STAR-TEL HIS7::kan*	(Vasianovich et al. 2017)
NK4072	*MATa-inc ura3::NAT leu2::LEU2-Pgal-HO MNT2::KAN-(ARO4-SPO23)::HOsite-URA3-STAR-TEL HIS7::kan pif1-m2*	Multiple steps
NK4079	*MATa-inc ura3::NAT leu2::LEU2-Pgal-HO MNT2::KAN-(ARO4-SPO23)::HOsite-URA3-STAR-TEL HIS7::kan*	(Vasianovich et al. 2017)
NK4080	*MATa-inc ura3::NAT leu2::LEU2-Pgal-HO MNT2::KAN-(ARO4-SPO23)::HOsite-URA3-STAR-TEL HIS7::kan pif1-m2*	Multiple steps
NK4232	*MATa-inc ura3::NAT leu2::LEU2-Pgal-HO trp1::HYG MNT2::HOsite-URA3-STAR-TEL pif1-m2:: pif1-m1-TRP1*	(Vasianovich et al. 2017)
NK4626	*MATa-inc trp1-289 ura3::NAT leu2::LEU2-Pgal-HO MNT2::kan::HOsite-URA3-STAR-TEL PDR18::kan::HYG pif1-m2*	Multiple steps
NK4627		
NK4628	*MATa-inc trp1-289 ura3::NAT leu2::LEU2-Pgal-HO MNT2::kan::HOsite-URA3-STAR-TEL PDR18::kan::HYG*	
NK4629		
NK5474		4072::pYT147/*Bgl*II

NK5475	*MATa-inc ura3::NAT leu2::LEU2-Pgal-HO MNT2::KAN-(ARO4-SPO23)::HOsite-URA3-STAR-TEL HIS7::kan pif1-m2-TRP1-pif1-m1*	
NK5476		4080::pYT147/*Bgl*II
NK5477		
NK5478	*MATa-inc ura3::NAT leu2::LEU2-Pgal-HO MNT2::KAN-(ARO4-SPO23)::HOsite-URA3-STAR-TEL HIS7::kan pif1-m2-TRP1-pif1-m1-4A*	4072::pYT148/*Bgl*II
NK5479		
NK5480		4080::pYT148/*Bgl*II
NK5481		
NK6025	*MATa-inc trp1-289 ura3::NAT leu2::LEU2-Pgal-HO MNT2::KAN-(5 kb homology to chrII)-HOsite-URA3-STAR-TEL HIS7::kan rad51::HYG*	NK4070 + PCR(OSM145 + OSM146)
NK6026	*MATa-inc trp1-289 ura3::NAT leu2::LEU2-Pgal-HO MNT2::KAN-(5 kb homology to chrII)-HOsite-URA3-STAR-TEL HIS7::kan pif1-m2 rad51::HYG*	NK4072 + PCR(OSM145 + OSM146)
NK6027	*MATa-inc trp1-289 ura3::NAT leu2::LEU2-Pgal-HO MNT2::KAN-(5 kb homology to chrII)-HOsite-URA3-STAR-TEL HIS7::kan rad51::HYG*	NK4079 + PCR(OSM145 + OSM146)
NK6028	*MATa-inc trp1-289 ura3::NAT leu2::LEU2-Pgal-HO MNT2::KAN-(5 kb homology to chrII)-HOsite-URA3-STAR-TEL HIS7::kan pif1-m2 rad51::HYG*	NK4080 + PCR(OSM145 + OSM146)
NK6351	*MATa-inc trp1-289 ura3::NAT leu2::LEU2-Pgal-HO MNT2::kan::HOsite-URA3-STAR-TEL HIS7::kan pif1-m2-TRP1-pif1-m1-Δ805*	NK3728::pYT525/*Bgl*II
NK6352		NK3729::pYT525/*Bgl*II
NK6355	*MATa-inc trp1-289 ura3::NAT leu2::LEU2-Pgal-HO MNT2::kan::HOsite-URA3-STAR-TEL HIS7::kan pif1-m2-TRP1-pif1-m1-Δ775*	NK3728::pYT527/*Bgl*II
NK6356		NK3729::pYT527/*Bgl*II
NK6359	*MATa-inc trp1-289 ura3::NAT leu2::LEU2-Pgal-HO MNT2::kan::HOsite-URA3-STAR-TEL HIS7::kan pif1-m2-TRP1-pif1-m1-Δ751*	NK3728::pYT529/*Bgl*II
NK6360		NK3729::pYT529/*Bgl*II
NK6974	*MATa-inc trp1-289 ura3::NAT leu2::LEU2-Pgal-HO MNT2::KAN-(5 kb homology to chrII)-HOsite-URA3-STAR-TEL HIS7::kan pol32::HYG*	NK4070 + PCR(OSM1497 + OSM1498)
NK6975		
NK6976		NK4079 + PCR(OSM1497 + OSM1498)
NK6977	*MATa-inc trp1-289 ura3::NAT leu2::LEU2-Pgal-HO MNT2::KAN-(5 kb homology to chrII)-HOsite-URA3-STAR-TEL HIS7::kan pif1-m2 pol32::HYG*	NK4072 + PCR(OSM1497 + OSM1498)
NK6978		NK4080 + PCR(OSM1497 + OSM1498)
NK6979		
NK7380	*MATa-inc trp1-289 ura3::NAT leu2::LEU2-Pgal-HO MNT2::kan::HOsite-URA3-STAR-TEL HIS7::kan pif1-m2-TRP1-pif1-m1-pip1*	NK3728::pYT540/*Bgl*II
NK7381		
NK7382		NK3729::pYT540/*Bgl*II
NK7383		
NK7448	*MATa-inc trp1-289 ura3::NAT leu2::LEU2-Pgal-HO*	NK3728::pYT147/*Bgl*II
NK7449		NK3729::pYT147/*Bgl*II
NK7450		

	MNT2::kan::HOsite-URA3-STAR-TEL HIS7::kan pif1-m2-TRP1-pif1-m1	
NK7458	*MATa-inc trp1-289 ura3::NAT leu2::LEU2-Pgal-HO MNT2::kan::HOsite-URA3-STAR-TEL HIS7::kan pif1-m2-TRP1-pif1-m1-pip2*	NK3728::pYT433/*Bgl*II
NK7459		
NK7460		NK3729::pYT433/*Bgl*II
NK7462	*MATa-inc trp1-289 ura3::NAT leu2::LEU2-Pgal-HO HEM13::HOsite-URA3 KAN pif1-m2-TRP1-pif1-m1-pip2-4myc*	NK1324::pYT437/*Bgl*II
NK7463		
NK7464		
NK7468	*MATa-inc trp1-289 ura3::NAT leu2::LEU2-Pgal-HO HEM13::HOsite-URA3 KAN pif1-m2-TRP1-pif1-m1-pip1-4myc*	NK1324::pYT541/*Bgl*II
NK7469		
NK7470		
NK7477	*MATa-inc trp1-289 ura3::NAT leu2::LEU2-Pgal-HO HEM13::HOsite-URA3 KAN pif1-m2-TRP1-pif1-m1-pip1,pip2-4myc*	NK1324::pYT615/*Bgl*II
NK7478		
NK7479		
NK7511	*MATa bar1::LEU2 trp1-289 ura3-5 leu2-3,112 rrm3::KAN pif1-m2*	NK828 + PCR (OSM70 + OSM71) on kanMX4
NK7512		
NK7513		
NK7614	*MATa bar1::LEU2 trp1-289 ura3-5 leu2-3,112 rrm3::KAN pif1-m2-TRP1-pif1-m1*	NK7511::pYT147/*Bgl*II
NK7615		
NK7616		NK7512::pYT147/*Bgl*II
NK7617	*MATa bar1::LEU2 trp1-289 ura3-5 leu2-3,112 rrm3::KAN pif1-m2-TRP1-pif1-m1-pip1*	NK7511::pYT540/*Bgl*II
NK7618		
NK7619		NK7512::pYT540/*Bgl*II
NK7620	*MATa bar1::LEU2 trp1-289 ura3-5 leu2-3,112 rrm3::KAN pif1-m2-TRP1-pif1-m1-pip2*	NK7511::pYT433/*Bgl*II
NK7621		
NK7622		NK7512::pYT433/*Bgl*II
NK7623	*MATa bar1::LEU2 trp1-289 ura3-5 leu2-3,112 rrm3::KAN pif1-m2-TRP1-pif1-m1-pip3*	NK7511::pYT635/*Bgl*II
NK7624		
NK7625		NK7512::pYT635/*Bgl*II
NK7626	*MATa bar1::LEU2 trp1-289 ura3-5 leu2-3,112 rrm3::KAN pif1-m2-TRP1-pif1-m1-sim*	NK7511::pYT636/*Bgl*II
NK7627		
NK7628		NK7512::pYT636/*Bgl*II
NK7635	*MATa-inc trp1-289 ura3::NAT leu2::LEU2-Pgal-HO MNT2::kan::HOsite-URA3-STAR-TEL HIS7::kan pif1-m2-TRP1-pif1-m1-pip3*	NK3728::pYT635/*Bgl*II
NK7636		NK3729::pYT635/*Bgl*II
NK7637		
NK7638	*MATa-inc trp1-289 ura3::NAT leu2::LEU2-Pgal-HO MNT2::kan::HOsite-URA3-STAR-TEL HIS7::kan pif1-m2-TRP1-pif1-m1-sim*	NK3728::pYT636/*Bgl*II
NK7639		
NK7640		NK3729::pYT636/*Bgl*II
NK7647	*MATa-inc trp1-289 ura3::NAT leu2::LEU2-Pgal-HO HEM13::HOsite-URA3 KAN pif1-m2-TRP1-pif1-m1-pip3-4myc*	NK1324::pYT622/*Bgl*II
NK7648		
NK7649		
NK7650	*MATa-inc trp1-289 ura3::NAT leu2::LEU2-Pgal-HO HEM13::HOsite-URA3 KAN pif1-m2-TRP1-pif1-m1-sim-4myc*	NK1324::pYT623/*Bgl*II
NK7651		
NK7652		
NK7674	*MATa bar1::LEU2 trp1-289 ura3-5 leu2-3,112 rad18::HYG*	NK1 + PCR (OSM3384+3385) on pAG32
NK7676	*MATa bar1::LEU2 trp1-289 ura3-5 leu2-3,112 rad18::NAT*	NK1 + PCR (OSM3384+3385) on pAG25
NK7680	*MATa bar1::LEU2 trp1-289 ura3-5 leu2-3,112 rad18::HYG srs2::SRS2-TRP1*	NK7674:: pYT342/*Bgl*II
NK7682	*MATa bar1::LEU2 trp1-289 ura3-5 leu2-3,112 rad18::NAT srs2::SRS2-TRP1*	NK7676::pYT342/*Bgl*II

NK7684	*MATa bar1::LEU2 trp1-289 ura3-5 leu2-3,112 rad18::HYG srs2::srs2-Δ[PIP-SIM]-TRP1*	NK7674::pYT652/*Bgl*II
NK7686	*MATa bar1::LEU2 trp1-289 ura3-5 leu2-3,112 rad18::NAT srs2::srs2-Δ[PIP-SIM]-TRP1*	NK7676::pYT652/*Bgl*II
NK7688	*MATa bar1::LEU2 trp1-289 ura3-5 leu2-3,112 rad18::HYG srs2::srs2-[PIP3-SIM]$_{PIF1}$-TRP1*	NK7674::pYT653/*Bgl*II
NK7690	*MATa bar1::LEU2 trp1-289 ura3-5 leu2-3,112 rad18::NAT srs2::srs2-[PIP3-SIM]$_{PIF1}$-TRP1*	NK7676::pYT653/*Bgl*II
NK7692	*MATa bar1::LEU2 trp1-289 ura3-5 leu2-3,112 rad18::HYG srs2::srs2-[PIP3-SIM]$_{PIF1}$-TRP1*	NK7674::pYT654/*Bgl*II
NK7694	*MATa bar1::LEU2 trp1-289 ura3-5 leu2-3,112 rad18::NAT srs2:: srs2-[PIP1-SIM]$_{RRM3}$-TRP1*	NK7676::pYT654/*Bgl*II
NK7696	*MATa bar1::LEU2 trp1-289 ura3-5 leu2-3,112 rad18::HYG srs2:: srs2-[PIP1-SIM$_{TT57/58EE}$]$_{RRM3}$-TRP1*	NK7674::pYT655/*Bgl*II
NK7698	*MATa bar1::LEU2 trp1-289 ura3-5 leu2-3,112 rad18::NAT srs2:: srs2-[PIP1-SIM$_{TT57/58EE}$]$_{RRM3}$-TRP1*	NK7676::pYT655/*Bgl*II
NK7760 NK7761	*MATa bar1::LEU2 trp1-289 ura3-5 leu2-3,112 rrm3::KAN*	NK1 + PCR (OSM3408 + OSM3409) on kanMX4
NK7894 NK7895 NK7896	*MATa-inc trp1-289 ura3::NAT leu2::LEU2-Pgal-HO HEM13::HOsite-URA3 KAN pif1-m2-TRP1-pif1-m1-pip1,pip2,pip3-4myc*	NK1324::pYT628/*Bgl*II
NK7922 NK7923 NK7924	*MATa bar1::LEU2 trp1-289 ura3-5 leu2-3,112 rrm3::RRM3-HYG*	NK7760::pYT630/*Eco*RV+*Hin*dIII
NK7925 NK7926	*MATa bar1::LEU2 trp1-289 ura3-5 leu2-3,112 rrm3::rrm3-pip1-HYG*	NK7760::pYT695/*Eco*RV+*Hin*dIII
NK7927 NK7928		NK7761::pYT695/*Eco*RV+*Hin*dIII
NK7929 NK7930 NK7931	*MATa bar1::LEU2 trp1-289 ura3-5 leu2-3,112 rrm3::rrm3-sim-HYG*	NK7760::pYT696/*Eco*RV+*Hin*dIII NK7761::pYT696/*Eco*RV+*Hin*dIII
NK7932 NK7933 NK7934	*MATa bar1::LEU2 trp1-289 ura3-5 leu2-3,112 rrm3::rrm3-pip2-HYG*	NK7760::pYT706/*Eco*RV+*Hin*dIII NK7761::pYT706/*Eco*RV+*Hin*dIII
NK8188 NK8189	*MATa-inc trp1-289 ura3::NAT leu2::LEU2-Pgal-HO HEM13::HOsite-URA3 pif1-m2-TRP1-pif1-m1-4myc pol30::pol30-KK127,164RR-HYG*	1335::pYT725/*BsiW*I+*Spe*I
NK8173 NK8174 NK8175 NK8176	*MATa bar1::LEU2 trp1-289 ura3-5 leu2-3,112 rrm3::KAN pif1-m2-TRP1-pif1-m1-pip2,pip3*	NK7511::pYT726/*Bgl*II NK7512::pYT726/*Bgl*II
NK8177 NK8178 NK8179 NK8180	*MATa bar1::LEU2 trp1-289 ura3-5 leu2-3,112 rrm3::KAN pif1-m2-TRP1-pif1-m1-pip1,pip3*	NK7511::pYT728/*Bgl*II NK7512::pYT728/*Bgl*II
NK8181 NK8182		NK7511::pYT735/*Bgl*II

NK8183	*MATa bar1::LEU2 trp1-289 ura3-5 leu2-3,112 rrm3::KAN pif1-m2-TRP1-pif1-m1-pip1,pip2*	NK7512::pYT735/*Bgl*II
NK8184		
NK8185	*MATa bar1::LEU2 trp1-289 ura3-5 leu2-3,112 rrm3::KAN pif1-m2-TRP1-pif1-m1-pip1,pip2,pip3*	NK7511::pYT736/*Bgl*II
NK8186		NK7512::pYT736/*Bgl*II
NK8187		

Table 2. Growth media

Yeast rich media	
YPD	1% bacto-yeast extract, 2% bacto-peptone, 2% bacto-agar, 2% D-glucose, 0.01% adenine sulphate, 0.01% L-tryptophan, 0.002% uracil
YPGal	1% bacto-yeast extract, 2% bacto-peptone, 2% bacto-agar, 2% D-galactose, 0.01% adenine sulphate, 0.01% L-tryptophan, 0.002% uracil
YPRaf	1% bacto-yeast extract, 2% bacto-peptone, 2% bacto-agar, 2% D-raffinose, 0.01% adenine sulphate, 0.01% L-tryptophan, 0.002% uracil
Yeast rich media with drugs	
YPD + G418	YPD Agar containing 200 µg/ml G418 disulphate (Formedium, G4185)
YPD + HYG	YPD Agar containing 300 µg/ml Hygromycin B (Toku-E, H010)
YPD + NAT	YPD Agar containing 100 µg/ml Nourseothricin (Jena Bioscience, AB-102)
Synthetic defined (SD) drop-out media	
SD –URA	0.69% yeast nitrogen base without amino acids, 2% D-glucose, 2% bacto-agar supplemented with –URA complete supplement mixture (CSM) drop-out (Formedium)
SD –TRP	0.69% yeast nitrogen base without amino acids, 2% D-glucose, 2% bacto-agar supplemented with –TRP complete supplement mixture (CSM) drop-out (Formedium)
SD –TRP–URA	0.69% yeast nitrogen base without amino acids, 2% D-glucose, 2% bacto-agar supplemented with –TRP–URA synthetic complete (Kaiser) drop-out (Formedium)
Bacterial media	
LB	1% bacto-tryptone, 0.5% bacto-yeast extract, 1% NaCl, pH adjusted to 7.0 with 1 M NaOH
LB + Amp	1% bacto-tryptone, 0.5% bacto-yeast extract, 1% NaCl, 100 µg/ml ampicillin sodium salt (Sigma, A0166), pH adjusted to 7.0 with 1 M NaOH

Table 3. Plasmids used in the study

Plasmid	Description	Source/Construction notes
kanMX4	*pFA6-kanMX4*	(Wach et al. 1994)
pAG25	*pFA6a - natMX4*	(Goldstein and McCusker 1999)
pAG32	*pFA6a - hphMX4*	
pYT58	*pRS316-RRM3*	(Makovets, Herskowitz, and Blackburn 2004)
pYT147	*pRS404-pif1-m1*	(Makovets and Blackburn 2009)
pYT148	*pRS404-pif1-m1-4A*	
pYT161	*pRS404-pif1-m1-4myc*	(Makovets and Blackburn 2009)
pYT342	*pRS404 - SRS2 (3'-end)*	Makovets lab plasmid collection
pYT433	*pRS404-pif1-m1-pip2*	This work. Recombinant PCR (OSM2577 + OSM2581) + (OSM2580 +OSM449) on pYT147, cloned replacing *Bst*EII-*Bgl*II fragment in pYT161
pYT437	*pRS404-pif1-m1-pip2-4myc*	This work. Recombinant PCR (OSM2577 + OSM2581) + (OSM2580 +OSM449) on pYT161, cloned replacing *Bst*EII-*Bgl*II fragment in pYT161
pYT525	*pRS404-pif1-m1-Δ805*	This work. PCR (OSM2577 + OSM2857) on pYT147, cloned as *Bst*EII – *Bgl*II fragment into pYT147
pYT527	*pRS404-pif1-m1-Δ775*	This work. PCR (OSM2577 + OSM2861) on pYT147, cloned as *Bst*EII – *Bgl*II fragment into pYT147
pYT529	*pRS404-pif1-m1-Δ751*	This work. PCR (OSM2577 + OSM2865) on pYT147, cloned as *Bst*EII – *Bgl*II fragment into pYT147
pYT540	*pRS404-pif1-m1-pip1*	This work. Recombinant PCR (OSM2577 + OSM2882) + (OSM2881 +OSM449) on pYT147, cloned replacing *Bst*EII-*Bgl*II fragment in pYT161
pYT541	*pRS404-pif1-m1-pip1-4myc*	This work. Recombinant PCR (OSM2577 + OSM2882) + (OSM2881 +OSM449) on pYT161, cloned replacing *Bst*EII-*Bgl*II fragment in pYT161
pYT615	*pRS404-pif1-m1-pip1,pip2-4myc*	This work. Recombinant PCR (OSM2577 + OSM2581) on pYT433 + (OSM2580 + OSM449) on pYT541, cloned

		as *Bst*EII-*Bgl*II fragment into pYT147
pYT622	*pRS404-pif1-m1-pip3-4myc*	Makovets lab plasmid collection
pYT623	*pRS404-pif1-m1-sim-4myc*	
pYT628	*pRS404-pif1-m1-pip1,pip2,pip3-4myc*	Makovets lab plasmid collection
pYT630	*pAG32-RRM3*	Makovets lab plasmid collection
pYT631	*pRS404-rrm3 (promotor 5'-ORF)*	This work. Subcloned as *Eag*I-*Sal*I fragment from pYT58 into pYT161
pYT632	*pRS404-rrm3-pip1 (promotor 5'-ORF)*	This work. Recombinant PCR (OSM3289 + OSM3290) + (OSM3291 + OSM3292) on pYT58, cloned as *Bam*HI - *Bst*EII into pYT631
pYT633	*pRS404-rrm3 (3'-ORF and 3'-utr)*	This work. PCR (OSM3304 + OSM3305) on pYT58, cloned as *Eag*I – *Spe*I fragment into pYT161
pYT634	*pRS404-rrm3-pip2 (3'-ORF and 3'-utr)*	This work. Recombinant PCR (OSM3304 + OSM3295) + (OSM3296 + OSM3305) on pYT58, cloned as *Eag*I – *Spe*I fragment into pYT161
pYT635	*pRS404-pif1-m1-pip3*	This work. SalI-PstI fragment subcloned from pYT147 into pYT622
pYT636	*pRS404-pif1-m1-sim*	This work. SalI-PstI fragment subcloned from pYT147 into pYT623
pYT652	*pRS404 - srs2-Δ[PIP-SIM] (3'-end, amino acids 1149-1174 are removed)*	Makovets lab plasmid collection Inserts were amplified using oligos OSM3376-OSM3383
pYT653	*pRS404 - srs2-[PIP3-SIM]$_{PIF1}$ (3'-end, amino acids 1149-1174 are replaced with the 48-74 from PIF1)*	
pYT654	*pRS404 - srs2-[PIP1-SIM]$_{RRM3}$ (3'-end, amino acids 1149-1174 are replaced with the 35-57 from PIF1)*	
pYT655	*pRS404 - srs2-[PIP1-SIM$_{TT57/58EE}$]$_{RRM3}$ (3'-end, same as 654 but with the indicated amino acid substitutions)*	
pYT695	*pAG32-rrm3-pip1*	This work. Subcloned as *Psi*I-*Nhe*I fragment from pYT632 into pYT630
pYT696	*pAG32-rrm3-sim*	This work. PCR (OSM3321 + OSM3422) on pYT630, cloned as *Bst*EII-*Bst*EII into pYT630
pYT706	*pAG32-rrm3-pip2*	This work. Subcloned as *Bgl*II-*Bgl*II fragment from pYT634 into pYT630
pYT725	*pAG32-pol30-KK127,164RR*	Makovets lab plasmid collection

pYT726	*pRS404-pif1-m1-pip2,pip3*	This work. SalI-PstI fragment subcloned from pYT433 into pYT622
pYT728	*pRS404-pif1-m1-pip1,pip3*	This work. SalI-PstI fragment subcloned from pYT540 into pYT622
pYT735	*pRS404-pif1-m1-pip1,pip2*	This work. Recombinant PCR (OSM2577 + OSM2581) + (OSM2580 + OSM449) on pYT540, cloned replacing *Bst*EII-*Bgl*II fragment in pYT161
pYT736	*pRS404-pif1-m1-pip1,pip2,pip3*	This work. Recombinant PCR (OSM2577 + OSM2581) + (OSM2580 + OSM449) on pYT540, cloned replacing *Bst*EII-*Bgl*II fragment in pYT622

Table 4. Primers used in the study

Primer	Sequence	Purpose
EHB15-265	CCCCGTCGACTCTCCCAGAATTGTTATACACGCCC	*RRM3* promotor direct
EHB-15-512	GCC ATT TAC AAA AAC ATA ACG	To amplify DNA fragments to probe for the *RDN1* repeats (Weitao, Budd, and Campbell 2003)
EHB-15-513	GGG CCT AGT TTA GAG AGA AGT	
EHB15-532	CCCCGGTACCGGTTTGCCTACAAGATAAAAGTAAATT	To amplify the DNA fragments for *MNT2* probe (Makovets and Blackburn 2009)
EHB15-533	CCCCGAATTCGAATTACGTGAATATTATGCATCACC	
OSM60	CCCACACTTTTCACATCTACCTCTACTCTCGCTGTCACTCCTTACCCGGC	Use with OSM106 to amplify the DNA fragments for KL1 probe (Makovets, Herskowitz, and Blackburn 2004)
OSM70 (F1)	ATCATCTCGA ACAATAAGCA GAGGAGAACA AGCTCAAAAG TCGAGAGATTGCCTCGTCCCCGCCGGGTCA	To knockout *RRM3*
OSM71 (R1)	TAGAGTATATGCATTTATTCGTTGCAAGTCATTTCAA AGTTTCTAAACGTACTGGATGGCGGCGTTAGTA	
OSM72	CCCGAATGCGCATGCATTATTCC	To screen after *RRM3* knockout (use with OSM631)
OSM106	CCCCGAATTCCGGCATTCCTGTCGATGCTGATAGGG	Use with OSM60 to amplify the KL1 probe (Makovets, Herskowitz, and Blackburn 2004)
OSM145	AAGAGCAGACGTAGTTATTT GTTAAAGGCC TACTAATTTGTTATCGTCATCGGATCCCCGGGTTAATTAA	To knockout *RAD51*
OSM146	AGAATTGAAAGTAAACCTGTGTAAATAAATAGAGAC AAGAGACCAAATACGAATTCGAGCTCGTTTAAAC	
OSM147	CGCGTCATTTCCGCTATTTCTGTCC	To screen after *RAD51* knockout (use with OSM631)
OSM205	TTAATTAACCCGGGGATCC	To screen gene knockouts (anti-F1)
OSM449	CCCCAGATCTATGTTTCACTTTTTTCTATCGAAGGAGG	*Bgl*II - *PIF1* +2780 rev
OSM631	TTAATTAACCCGGGGATCCG	To screen gene knockouts (anti-F1)
OSM801	GTTTAAACGAGCTCGAATTC	To screen gene knockouts (anti-R1)
OSM937	AGCAGGATATTCAGCGGTGT	RS2.6 probe
OSM1497	ATAATATTTCACATTAACTAACAACCAGAAATAGGCT TTAGTTAACTCAATCGGTAATTAGGATCCCCGGGTT AATTAA	To knockout *POL32*
OSM1498	CATTTGTATTATACATTACATCACAATTAGTAATGGA AAGTGTTTGGAAAAAAAAGAAGAGAATTCGAGCTCG TTTAAAC	
OSM1499	ACGAATAGGTCTATTTTCCACTAC	To screen after *POL32* knockout (use with OSM205)

OSM1500	TTACCTAGTAGCATGGCAACACTT	To screen after *POL32* knockout (use with OSM801)
OSM2332	AGGAGAAAGTATCAGTACATTGC	RS6.8 probe
OSM2333	GGAACTTTCATAGTAGATTAGCC	
OSM2336	GTTACGGTGAAAGTTATGAGAGC	BIR6 probe
OSM2337	GAAGTGATCTCTCCATCTGCTGC	
OSM2338	GATTTGCCATCGCCAGATGAAGG	BIR36 probe
OSM2339	TGTTCCAGGCTGTTGAAGTAGCC	
OSM2340	TGGTATTCCACACCAAAGCGAGG	BIR77 probe
OSM2341	AAGTCCACTGATGATATCCCACC	
OSM2344	GCATTATTTGCCTCGGCAGATGG	ARS522 probe
OSM2345	CGAAATTGAAGCTCGCGCTAACC	
OSM2347	TTATCTCTGATATTACCACCTGG	RS15.2 probe
OSM2348	GTCTATGTCAGATTATCTATTCC	
OSM2349	AGGCCGCGATTAAATTCC	To qPCR the recombinant DNA fragment created during BIR across the 500 bp homology
OSM2350	CATGAGTGACGACTGAATCC	
OSM2380	TAGAACCAGTTCAAAGTAGCAGC	RS2.6 probe
OSM2546	GGTATGGTAGGTTTGGGAGAAG	To synthesise DNA fragment for the probe to the chrII region 50 bp from the homology
OSM2547	CCTAGGTATTTCCTTCAGGTTCC	
OSM2577	CGAAGGTTACCTCTCGTGAGATTC	PIF1 at *Bst*EII site
OSM2580	GGATCAAAGCACATCAAAAGGATATCGATGCAGCTCTTACTTTATCTTCAGCC	Mutating V757D and FY760/761AA in Pif1 (creates ERV site and removes *Bsa*BI site)
OSM2581	GGCTGAAGATAAAGTAAGAGCTGCATCGATATCCTTTTGATGTGCTTTGATCC	
OSM2857	CCCCAGATCTTTATGCTGGAGAATTTGACTTTGACTTG	To make PIF1 truncations on the integration plasmids
OSM2861	CCCCAGATCTTTACTCAAGTTGCTTATAGGCACTTTC	
OSM2865	CCCCAGATCTTTAGATCCTAGTTCTGTCAAAATTTAAC	
OSM2881	AGAGCAGCGCGACGTCAAGAGCACAGTAGGAAGAGATTTCAGTTG	To make PIP1 mutation in Pif1, creates *Bsa*HI
OSM2882	CTCTTGACGTCGCGCTGCTCTACCATTATTAGATTGTGTGGTCGC	
OSM2938	CAAGCGCGCAATTAACCCTCACTAAAGG	pRS404 backbone forward
OSM3276	CAAAGAGGAGAGTAACTTTAACG	PIF1 -150 *Bse*RI
OSM3277	CCCCCGGCCGCTTGAGCAAAGTTAGCAGACCTGAAACCACG	To make PIP3 mutation in Pif1, creates *Eag*I
OSM3278	CCCCCGGCCGCTAAGCATCCTTCCATAC	
OSM3279	CTGGGTTTAAACATATCGTTCC	PIF1 *Pme*I reverse
OSM3280	CCCCCGGCCGCGTCTTCTTTTGAAAGTATGGAA	To make SIM mutation in Pif1, creates *Eag*I
OSM3281	CCCCCGGCCGCTGCTTCTGATTCGGATGATTGGGA	

OSM3289	CCCCGGATCCTAGTCTTCTTTCGTC	To introduce FF41/42AA mutation into RRM3 (N-PIP, creates NcoI site, sequence with OSM2938 and OSM3293)
OSM3290	ACCCATGGCTGCCGAAGACAACGTTTGTTGCC	
OSM3291	CTTCGGCAGCCATGGGTTGCGGCAAAAAATCTG	
OSM3292	CCCCGGTTACCTTCGTCACCGC	
OSM3293	CCTTGACTCTGCGAGAATAAGG	
OSM3294	CCCCCGGCCGTTGAGGAGAATTTTCGAAGCC	To clone the C-terminus and terminator of RRM3 and introduce the FF715/716AA (XhoI site created in LE two amino acids after Y) into C-PIP (use OSM3294+OSM265 as flanking oligos, sequence with OSM2938 and OSM265)
OSM3295	TCGAGACGTTTGGCAGCATCTTTTACTCTTTCATTG GTGCG	
OSM3296	CTGCCAAACGTCTCGAGACTTTGAAATGACTTGCAA CG	
OSM3299	TGCACTCACACCATTCACACT	To amplify the probes for 2D gel analysis of replication through tRNA genes (Tran et al. 2017)
OSM3300	ATTGGCCCAAAAGGGATCAT	
OSM3376	GAATTAGATCTATCCGATGAGGAG	To delete Srs2 PIP-SIM in pYT342 by replacing the *Bgl*II-*Cla*I fragment
OSM3377	CCCCATCGATCTAACTTGATGCAGGTTCATTCTTCA CC	
OSM3378	CCCCCTTAAGATGGAAGGATGCTTCAATTGTGCTTG AATAAAGTTATTACTTGATGCAGGTTCATTCTTC	To replace Srs2 PIP-SIM with Pif1 PIP3-SIM (use *Bgl*II-*Sal*I for cloning)
OSM3379	CCCCCTTAAGTAAAGAAGACCTAGATTTGCTCTCTG ATTCGGATGATTAGTAGCACTTTCATGCCTGAC	
OSM3380	CGAGGTCGACCATACTGCTCATTC	
OSM3381	CCCCCTGCAGCAGATTTTTTGCCGCAACCCATAAAG AACGAAGACAACGTTTGTTGACTTGATGCAGGTTCA TTCTTC	To replace Srs2 PIP-SIM with RRM3 PIP-SIM (use *Bgl*II-*Sal*I for cloning)
OSM3382	CCCCCTGCAGCTTCAAAAAACAGCACGACAATAATT GATTTGGAAAGCGGTGACGAATAGTAGCACTTTCAT GCCTGAC	
OSM3383	CCCCCTGCAGCTTCAAAAAACAGCGAAGAAATAATT GATTTGGAAAGCGGTGACGAATAGTAGCACTTTCAT GCCTGAC	Alternative to OSM3382 with EE substituting TT in SIM
OSM3384 (F1)	CCATCCGCAAGTGAGCATCACAGCTACTAAGAAAAG GCCATTTTTACTACTCCGGATCCCCGGGTTAATTAA	To knockout *RAD18*
OSM3385 (R1)	TTAACAAATGTGCACAAGCTAACAAACAGGCCTGAT TACATATACACACCGAATTCGAGCTCGTTTAAAC	
OSM3386	ATACAGTATTTAGCTGAAGTTTCC	To screen after *RAD18* knockout (use with OSM631)
OSM3387	CCGTAAACTACGCTGGCCTTC	To screen after *RAD18* knockout (use with OSM801)
OSM3395	TTCAACAACTAATGTACCTAGTAG	To genotype Srs2-PIP-SIM plasmid integrations (pYT652-655)
OSM3396	CGTAGTCAGGCATGAAAGTGCTA	
OSM3397	GCTTCAATTGTGCTTGAATAAAG	
OSM3398	AAGAACGAAGACAACGTTTGTTG	
OSM3408	GAGGAGAACAAGCTCAAAAGTCGAGAGATTTGTTCT TATAAGACATCCCGGAATTCGAGCTCGTTTAAAC	

OSM3409	AACAAGAAAAGAAAACTTCAACTAGAGTATATGCATT TATTCGTTGCAAGCGGATCCCCGGGTTAATTAA	To knockout *RRM3* with the cassettes going in the reverse orientation

Table 5. Antibodies used in the study

Antibody	Working concentration	Manufacturer
c-Myc (9E10), mouse monoclonal	1:1000 (Western blotting) 1:500 (ChIP)	Thermo Fisher Scientific (13-2500)
Rad51 (y-180) rabbit polyclonal	1:500 (ChIP)	Santa Cruz Biotechnology (sc-33626)
anti-beta Actin, mouse monoclonal	1:200000 (Western blotting)	Abcam (ab8224)

2.7. Growth and manipulation of yeast and bacteria

2.7.1. Yeast stocks

Patches of yeast strains were grown overnight (o/n) on a YPD plate (or SD -URA for the strains with an inducible break). Cells were re-suspended in 2 ml of 25% (w/v) glycerol in YPD in a 2ml Corning™ Cryogenic Vial. Stocks were stored at -80°C.

2.7.2. Yeast transformation

Materials

- 10x TE: 100 mM Tris, pH 8.0, 10 mM EDTA
- Transformation wash: 0.1 M lithium acetate pH 7.2, 1x TE
- PEG mix (freshly made): 40% (w/v) polyethylene glycol (PEG) 3.350 in 1 x TE, 0.1 M lithium acetate pH 7.2
- 10 mg/ml (w/v) carrier DNA solution (single stranded salmon or bovine ssDNA)

Cells from patches grown o/n on YPD plates were inoculated into YPD liquid medium at $OD_{600} \approx 0.1$ and grown at 30 degrees until a mid-log phase ($OD_{600} \approx 0.4$ - 0.6) with an appropriate aeration. The cells were pelleted in 50 ml conical tubes at 3,000 rpm for 3 min at room temperature using Eppendorf centrifuge 5810R. The cell pellets were re-suspended in 1 ml of Transformation wash, transferred into 1.7 ml Eppendorf microcentrifuge tubes and centrifuged at 5,000 rpm for 2 min using Eppendorf microcentrifuge 5424. Washed cells were re-suspended in (n+1) x 100 µl of Transformation wash, where n is the number of the transformation reactions intended for a given per strain. (n+1) x 10 µl of carrier DNA solution was added to the tubes. Cell suspensions were mixed by vortexing and aliquoted 110 µl each into tubes with the DNA to be transformed (PCR fragments of cassettes for gene knock outs or linearised plasmids for integrations, up to 10 µl per transformation) and without DNA (a negative control). 600 µl of PEG mix was added into each tube and the suspensions were mixed by vortexing.

Cells were incubated for 35 min at 30°C and then moved to 42°C water bath for 16-18 min for a heat-shock. After the heat-shock, cells were centrifuged at 5,000 rpm for 2 min, washed with 1 ml of YPD, re-suspended in 100 µl of YPD and plated onto the appropriate selective medium. In case drug resistance was used for the selection, cells were plated and grown o/n on YPD before replica-plating onto the plates with a corresponding drug.

2.7.3. Yeast growth, cell cycle synchronisation and DSB induction in liquid cultures

Materials

- Galactose
- α-factor peptide solution in water (WHWLQLKPGQPMY, Peptide Protein Research Ltd.), stock concentration - 5 mg/ml
- Nocadazole solution in DMSO, stock concentration - 5 mg/ml

For DSB induction (see section 2.8) in liquid cultures, cells from patches grown o/n on YPRaf plates were inoculated into YPRaf liquid medium at $OD_{600} \approx 0.1$, grown at 30 degrees until a mid-log phase ($OD_{600} \approx 0.4$ - 0.6) with an appropriate aeration and synchronized in G1 phase by addition of 5 µg/ml of α-factor for 2 hours. After the synchronization was complete (monitored by the appearance of shmoos and the absence of the cells with small buds using light microscopy) galactose powder was added to 2% final concentration (w/v) for 1 h to induce DSBs. After the induction of the DSBs, cells were pelleted in the 50 ml conical tubes, washed with warm YPGal and re-suspended in the fresh pre-warmed YPGal (two times the volume of the original YPRaf culture) with 15 µg/ml of Nocadazol to limits the cell cycle progression to a single S/G2 phase.

2.7.4. Preparation of *E. coli* competent cells

Materials

- 0.1 M $CaCl_2$
- 20% (w/v) glycerol in 0.1 M $CaCl_2$

The *recA E. coli* strain used for plasmid amplification DH5α was streaked for single colonies on an LB plate and grown at 37°C o/n. A single colony was inoculated into 10 ml of LB medium and grown o/n in 125 ml Erlenmeyer flask at 37°C with vigorous aeration. The o/n culture was diluted 100-fold in 200 ml of fresh LB in a 2 L Erlenmeyer flask and grown at 37°C with vigorous aeration until OD_{600} reached 0.4-0.5. The culture was cooled down rapidly by shaking in the ice water bath for 5 min. The cells were pelleted in four 50 ml conical tubes in an Eppendorf refrigerated centrifuge 5810R at 4,000 rpm for 10 min at 4°C. The cell pellets from each tube were re-suspended in 25 ml of cold 0.1 M $CaCl_2$ and incubated on ice for 1 hour. Following the incubation, the aliquots were combined in two 50 ml conical tubes and centrifuged again at the same conditions. Each pellet was re-suspended in 5 ml of ice-cold 20% (w/v) glycerol in 0.1 M $CaCl_2$, the mixtures were combined and mixed well. The cells were aliquoted into pre-chilled (-80°C) microcentrifuge tubes (100 µl each). The competent cells were stored at -80°C until use.

2.7.5. $CaCl_2$-mediated *E. coli* transformation

The aliquots of competent cells were thawed on ice. 0.1-10 µl of plasmid DNA was added to each aliquot, mixed and incubated for 30 min on ice. The tubes were transferred to 42°C water bath for 2 min and returned on ice for 1 min. O.9 ml of pre-warmed LB medium with 2% glucose was added to each tube and cells were incubated at 37°C with vigorous aeration for 1 h. Following the incubation, the cells were pelleted at 5,000 rpm for 1 min. 0.9 ml of the supernatant was discarded, the cells were re-suspended in the remaining 100 µl and plated onto selective plates (LB with 100 µg/ml ampicillin).

2.8. Combined break-induced replication and *de novo* telomere addition assay

Strains with the genetic construct described in Vasianovich et al. (Vasianovich et al., 2014), were used to test the efficiency of BIR and dnta in a particular genetic background. Briefly, a truncated version of the *kan* gene (3'-*kan*)

has been integrated into the *MNT2* locus on chromosome VIIL with the HO-endonuclease recognition sequence on its telomere-proximal side, followed by *URA3*, a STAR element and a telomere (Figure 2.1.). The remaining part of *kan* (5'-*kan*) with an additional 500 bp overlap homologous to 3'-*kan* has been inserted into the *HIS7* locus on chromosome IIR. The *HO* gene was placed under the control of the inducible *GAL* promotor (P_{GAL}) and all the strains had a non-cleavable *MATa* so that the DSB induced at the MNT2 locus was the only site cut by HO.

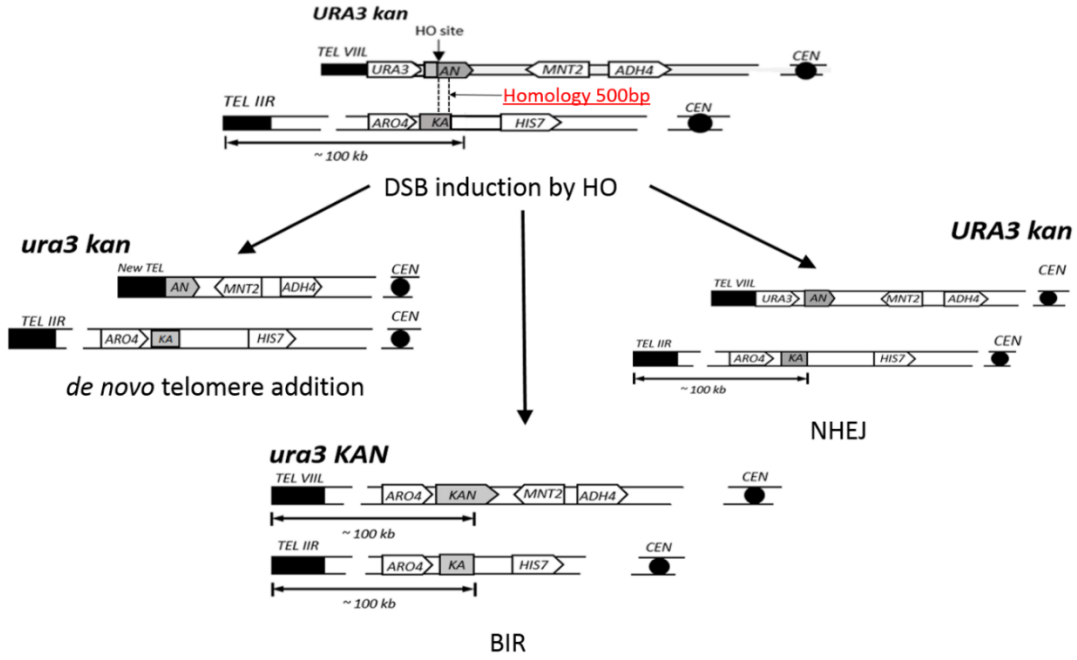

Figure 2.1 Schematic of the genetic assay used to study the repair of an inducible DSB (see the text for details, the schematic was adapted from Vasianovich, Harrington, and Makovets 2014)

The tested strains were incubated o/n on YPRaf plates to de-repress P_{GAL}. Next day, the cells were re-suspended in YP, diluted to the appropriated cell titre and plated on YPD (a no-DSB control) and YPGal plates (DSB induction).

On galactose containing plates, cells induce a DSB at the HO-recognised site in a way that only one of the broken ends shares homology to chromosome II (Figure 2.1, top). In this case, BIR is the major homology-depended repair pathway that can be used to repair such a broken chromosome. The BIR involves repair DNA synthesis on the template of a 100 kbp long arm of chromosome II,

which reconstitutes the full length *KAN* gene on chromosome VIIL but leads to the loss of the terminal chromosome VII fragment containing the *URA3* gene (Figure 2.1, bottom). As a result, the cells which use BIR can be identified as $G418^R$ Ura^- colonies by replica-plating the colonies growing on YPGal onto the corresponding selective plates.

Alternatively, the induced DSBs can be repaired via NHEJ producing $G418^S$ Ura^+ colonies (Figure 2.1, right) or as a result of telomere addition to the centromere containing fragment which results in $G418^S$ Ura^- colonies (Figure 2.1, left). A small fraction of $G418^S$ Ura^- colonies may emerge on YPGal plates due to homologous recombination with the *MAT* locus on chromosome III and therefore this assay allows only semi-quantitative comparison of the efficiency of dnta between the strains analysed.

2.9. DNA manipulation

2.9.1. Yeast colony PCR

Materials

- 20 mM NaOH
- *Taq* PCR Core Kit (Qiagen, 201225)

The cells from a single colony were re-suspended in 3 µl of 20 mM NaOH and incubated at 99°C for 10 min. The PCR-reactions were set up using Taq PCR Core Kit according to the manufacturer's recommendations with 1µM final concentration of the primers.

PCR conditions:

PCR step	temperature	time	# of cycles
Initial denaturation	94°C	2 min	1
Denaturation	94°C	30 sec	35
Annealing	49-59°C	30 sec	
Elongation	72°C	30 sec-2.5 min	
Final elongation	72°C	10 min	1

2.9.2. PCR-amplification of DNA cassettes for gene deletions, tagging, etc.

Materials

- 10x PCR buffer: 500 mM KCl, 100 mM Tris-HCl pH 9.0, 1% (v/v) Triton X-100
- 1 M Tris-HCl pH 9.0
- 25 mM $MgCl_2$
- 10 mg/ml BSA
- dNTP mix (10 mM each) from *Taq* PCR core kit (QIAGEN, 201225)
- *Taq* DNA Polymerase (NEB, M0273)
- *Vent*™ DNA polymerase (NEB, M0254)

The cassettes for gene deletion were amplified using F1 and R1 primers (Longtine et al., 1998). The cassettes containing *TRP1* selection marker were amplified from pFA6a-*TRP1* plasmid (Longtine et al., 1998), *NAT*-containing cassettes – from pAG25, *HYG*-containing cassettes – from pAG32 (Goldstein and McCusker, 1999).

Oligonucleotide design:

F1	5'-(gene-specific sequence, 50 bases)-GGATCCCCGGGTTAATTAA-3'
R1	5'-(gene-specific sequence, 50 bases)-GAATTCGAGCTCGTTTAAAC-3'

PCR mixture:

DNA template	1 µl
100 µM F1primer	0.25 µl
100 µM R1 primer	0.25 µl
10x PCR buffer	5 µl
1 M Tris pH 9.0	0.5 µl
25 mM $MgCl_2$	3 µl
dNTPs mix, 10 mM each	1 µl
10 mg/ml BSA	0.5 µl
Vent polymerase	0.5 µl
Taq polymerase	0.5 µl
Milli-Q H_2O	37.5 µl
Total volume:	50 µl

During setting up every PCR reaction the enzymes were added last to the reaction mixture.

PCR conditions:

PCR step	temperature	time	# of cycles
Initial denaturation	94°C	2 min	1
	80°C	2 min	
Denaturation	94°C	1 min	30
Annealing	55°C	45 sec	
Elongation	72°C	2.5 min	
Final elongation	72°C	10 min	1

2.9.3. Comparative DNA analysis using qPCR

qPCR reactions were performed using Brilliant II SYBR® Green QPCR Master mix, according to the manufacturer's recommendations, in MX3000P Real-Time thermocycler (Agilent Technologies).

The reaction mixture was set up as follows:

DNA (genomic DNA diluted 50-fold inputs from ChIP – diluted 10-fold IP samples - undiluted)	5 µl
2x Brilliant II SYBR Green QPCR master mix	12.5 µl
Forward primer (dilution x)	0.5 µl
Reverse primer (dilution x)	0.5 µl
ROX reference dye (diluted 1 : 500)	0.375 µl
Molecular grade H_2O	6.18 µl
Total volume:	25 µl

The primers were designed using PrimerQuest software provided by IDT (http://www.idtdna.com/primerquest/Home). The optimal working concentration for primers was chosen so that the efficiency of the reaction was as close to 100% as possible (explained below). The specificity of the primers was analysed using the conventional PCR followed by detection of the products on agarose gel as well as from analysing the melting curves during the qPCR reactions.

To detect the initiation of DNA synthesis during BIR (Chapter 3.4), primers OSM2349 and OSM2350 were used with 0.2 µM final concentration.

OSM2349 + OSM2350 (*KAN*)

PCR step	temperature	time	# of cycles
Initial denaturation	95°C	10 min	1
Denaturation	95°C	30 sec	40
Annealing	58°C	1 min	
Elongation	72°C	1 min	
Melting curve	95°C	1 min	1
	55°C	30 sec	
	95°C	30 sec	

To detect *5'-kan* for Rad51 ChIP (Chapter 3.3.), primers OSM2546 and OSM2547 were used in 0.2 µM final concentration.

OSM2546 + OSM2547 (*5'-kan*)

PCR step	temperature	time	# of cycles
Initial denaturation	95°C	10 min	1

Denaturation	95ºC	30 sec	40
Annealing	55ºC	40 sec	
Elongation	72ºC	30 sec	
Melting curve	95ºC	1 min	1
	55ºC	30 sec	
	95ºC	30 sec	

To detect the DNA fragments of *HEM13* locus in Pif1-4myc ChIP (Chapter 4.6), primers OSM559 and OSM560 were used in 0.4 µM final concentration.

OSM559 + OSM560 (*HEM13*)

PCR step	temperature	time	# of cycles
Initial denaturation	95ºC	10 min	1
Denaturation	95ºC	30 sec	40
Annealing	55ºC	1 min	
Elongation	72ºC	40 sec	
Melting curve	95ºC	1 min	1
	55ºC	30 sec	
	95ºC	30 sec	

All qPCR-based experiments included a normalisation to the reference locus (*ARO1*), using primers OSM1006 and OSM1007 at 0.2 µM final concentration.

OSM1006 + OSM1007 (*ARO1*)

PCR step	temperature	time	# of cycles
Initial denaturation	95ºC	10 min	1
Denaturation	95ºC	30 sec	40
Annealing	54ºC	40 sec	
Elongation	72ºC	30 sec	
Melting curve	95ºC	1 min	1
	55ºC	30 sec	
	95ºC	30 sec	

The relative enrichment of the crossover template, which indicates the initiation of BIR DNA synthesis at a given time-point was quantified using the following formula:

$$\boldsymbol{Crossover\ template} = \frac{\left(\mathbf{1}+\boldsymbol{E}(\boldsymbol{KAN})\right)^{\boldsymbol{\Delta Ct\ (KAN)}}}{\left(\mathbf{1}+\boldsymbol{E}(\boldsymbol{ARO1})\right)^{\boldsymbol{\Delta Ct\ (ARO1)}}}$$

where E(*KAN*): efficiency of PCR across the homology between chromosomes VII and II (OSM2349 + OSM2350)

E(*ARO1*): efficiency of PCR at *ARO1* locus (OSM1006 + OSM1007)

ΔCt = Ct(time-point X) – Ct (0h), Ct – the cycle at which the amplification curve crosses the threshold.

The protein enrichment at the given locus relative to the input and the reference locus was quantified using the next formula:

$$\boldsymbol{Relative\ enrichment} = \frac{\left(\mathbf{1}+\boldsymbol{E}(\boldsymbol{locus\ X})\right)^{\boldsymbol{\Delta Ct\ (locus\ X)}}}{\left(\mathbf{1}+\boldsymbol{E}(\boldsymbol{ARO1})\right)^{\boldsymbol{\Delta Ct\ (ARO1)}}}$$

where E(*locus X*): efficiency of PCR of the tested locus

E(*ARO1*): efficiency of PCR at *ARO1* locus (OSM1006 + OSM1007)

ΔCt = Ct(IP) – Ct (Input), Ct – the cycle at which the amplification curve crosses the threshold.

To calculate the efficiency of each PCR reaction the control DNA sample (DNA sample of the strain which have repaired the DSB using BIR – for *KAN* PCR; mixture of inputs – for other PCRs) was serially diluted (3 fold dilutions) and used in the corresponding PCR run. The Ct values were plotted against the logarithm of the DNA quantity for the corresponding dilution. The efficiency of qPCR was calculated from the linear regression of these data (slope) using the following equation:

$$\boldsymbol{E} = \mathbf{10}^{\mathbf{(-1/slope)}} - \mathbf{1}$$

2.9.4. Molecular cloning

Materials

- *Pfu* DNA Polymerase (Promega, M7741)
- QIAquick™ Gel Extraction Kit (Qiagen, 28706)
- QIAquick™ PCR Purification Kit (Qiagen, 28106)
- Restriction enzymes (NEB)
- Calf Intestinal Alkaline Phosphatase (NEB, M0290S)
- T4 DNA Ligase (NEB, M0202S)
- Wizard™ Plus SV Minipreps DNA Purification System (Promega, A1460)

DNA sequnces required for the cloning were PCR-amplified using the high fidelity *Pfu* DNA polymerase according to the manufacturer's protocol and the PCR products were purified from the reaction components and the template DNA by agarose gel electrophoresis and subsequent gel extraction using using QIAquick™ Gel extraction Kit before digesting with the appropriate restriction enzymes.

The vector was digested with the chosen restriction enzymes according to the manufacturer's recommendations. To prevent re-ligation of the vector it was treated with Calf Intestinal Phosphotase (CIP, 5 units per 20 µl) for 1 h at 37°C. The restriction fragments originated from the vector were separated by agarose gel electrophoresis and the required fragment was gel-purified. The digested inserts were column-purified with the QIAquick PCR Purification Kit and mixed with the vector fragment (for each vector a control sample without insert was added). The ligation reactions were set up in 15 µl total volume with 400 units of T4 DNA Ligase in 1x T4 Ligase buffer at room temperature for ≥ 1 h. After the ligation, up to 10 µl of the ligation mixtures were transformed into *E. coli* competent cells.

For the plasmid amplification cells from a single colony were inoculated into 5 ml LB culture with ampicillin (100 µg/ml) and grown o/n at 37°C with vigorous

aeration. Plasmid DNA was extracted using Wizard™ Plus SV Minipreps DNA Purification System according to the manufacturer's protocol. The plasmids were eluted in 100 µl of Milli-Q H_2O and stored at -20°C.

To verify the cloning results, the constructed plasmids were screened using the restriction digest and gel electrophoresis with subsequent sequencing the inserts using the GenePool Sanger sequencing facility of the University of Edinburgh (in case PCR was used for insert generation). The mixtures of plasmid and primer were submitted for the sequencing at concentrations recommended by the facility. Sequence chromatograms were analyzed using the FinchTV software.

2.9.5. Extraction of yeast genomic DNA

Materials

- SE: 1 M sorbitol, 0.1 M EDTA
- Zymolyase-100T from *Arthrobacter luteus,* 100 U/mg (MP Biomedicals, 08320932)
- EDS: 50 mM EDTA, 0.2% (w/v) SDS, 2.5 mM NaOH
- 8 M ammonium acetate
- Isopropanol
- 70% (v/v) ethanol (4°C cold
- 1x TE: 10 mM Tris, pH 8.0, 1 mM EDTA
- Ribonuclease A (RNase A) from bovine pancreas **(**Sigma, R4875)

3 – 5 OD_{600} of cells were harvested from patches or from liquid cultures, re-suspended in 150 µl of SE with zymolyase (0.1-1 mg/ml final concentration) and incubated for 10 – 20 min at 42°C to make spheroplasts. The spheroplasts were centrifuged at 5,000 rpm for 2 min at room temperature, thoroughly re-suspended in 150 µl of EDS solution and incubated at 65°C for ≥ 20 min to lyse cells and heat-inactivate nucleases. 75 µl of 8 M ammonium acetate was added

to each sample, the samples were briefly vortexted and left on ice for ≥ 30 min to precipitate proteins. The proteins and cell debris were pelleted by centrifugation at 14,000 rpm for 10 min at room temperature. The supernatants were moved to fresh tubes and the nucleic acids were precipitated with 135 µl of isopropanol. Samples were inverted several times and span down at 10,000 rpm for 10 min at room temperature. The pellets were washed with 500 µl of cold (4°C) 70% (v/v) ethanol and re-suspended in 50 µl of 1x TE with 20 µg/ml of RNAse A and incubated either for 1 h at room temperature or o/n at 4°C to make sure that the DNA is completely dissolved.

2.9.6. Agarose gel electrophoresis

Materials

- 10x TBE: 0.89 M Tris, 0.89 M boric acid, 20 mM EDTA
- 6x Gel-Loading buffer: 0.25% (w/v) bromophenol blue, 0.25% (w/v) xylene cyanol FF, 15% (w/v) Ficoll-400
- Agarose, molecular biology grade (Melford, MB1200)
- Ethidium bromide solution, 10 mg/ml (Fisher Scientific, E/P800/03)
- 100 bp and 1 kb DNA ladder, 500 µg/ml (NEB, N3231L, N3232L)

Agarose gel was prepared by melting agarose in 1x TBE buffer in a microwave oven. Ethidium bromide was added to the final concentration of 0.5 µg/ml, agarose was mixed, cast into the gel casting trays with the required combs and allowed to polymerise. After the gel was ready, 1x TBE was added and the combs were removed. DNA samples were prepared for loading on a gel by mixing with 6x Gel-Loading buffer to the 1x final concentration and loaded into the wells. Molecular weight marker (1 kb or 100 bp, 500 µg/ml, NEB) was diluted 10 fold with 1x NEB3 buffer, mixed with the Gel-Loading buffer and loaded on the gel (3-5 µl per well). The gels were run at 5-10 V/cm of the distance between the electrodes.

Resolved DNA fragments were visualised by exposing the gel to the UV light in Gel Doc™ XR+ Imager (BioRad).

2.9.7. Analysis of the replication intermediates using 2D-gel electrophoresis

Materials

- Sodium azide, 10% solution in water
- 0.5 M EDTA pH 8.0
- Nuclei isolation buffer (NIB): 17% glycerol, 50 mM MOPS buffer, 150 mM potassium acetate, 2mM magnesium chloride, 0.5 mM spermidine, and 0.15 mM spermine; pH 7.2
- TEN: 50 mM Tris pH 7.5, 50 mM EDTA, 100 mM NaCl
- N-Lauroylsarcosine sodium salt (Sarkosyl, Sigma, L5125)
- Proteinase K (recombinant, PCR grade, Roche) 20 mg/ml stock concentration in water
- Ribonuclease A (RNase A) from bovine pancreas (Sigma, R4875**)**
- Phenol/chlorophorm/isoamyl alcohol solution (24:24:1, Acros organics)
- 3 M potassium acetate stock solution in water
- 96% ethanol (-20°C)
- 70% (v/v) ethanol (4°C)
- 10x TBE: 0.89 M Tris, 0.89 M boric acid, 20 mM EDTA
- 6x Gel-Loading buffer: 0.25% (w/v) bromophenol blue, 0.25% (w/v) xylene cyanol FF, 15% (w/v) Ficoll-400
- Agarose, molecular biology grade (Melford, MB1200)

- Ethidium bromide solution, 10 mg/ml (Fisher Scientific, E/P800/03)
- 1 kb DNA ladder, 500 µg/ml (NEB, N3232L)

Cells from patches grown o/n on YPD plates were inoculated into YPD liquid medium at $OD_{600} \approx 0.1$ and grown at 30 degrees until a mid-log phase ($OD_{600} \approx 0.4$ - 0.6) with an appropriate aeration. Just before the cell harvesting, sodium azide was added to the culture to 0.01% final concentration and EDTA to 60 mM final concentration. 240-300 OD of cells were harvested by centrifugation at 5000 rpm 10 min in Sorvall RC-5B centrifuge at 4^{o}C. The cell pellets were washed with 50 ml of cold Milli-Q water and pelleted again using Eppendorf refrigerated centrifuge 5810R at 3,000 rpm for 3 min at 4^{o}C. The cells were re-suspended in 1.5 ml of NIB buffer, moved to the 15 ml conical tubes and frozen at -80 ^{o}C for storage.

The cell suspensions in NIB were thawed by submerging into water for 1 min at room temperature. 2 ml of glass beads were added to the samples and cells were lysed by vortexing (14 cycles – 30 sec vortexing, 3 min on ice). After the cell lysis, the cell suspensions were moved into 2 ml Eppendorph tubes and centrifuged at 14,000 rpm for 30 min in the Eppendorf refrigerated minicentrifuge 5417R at 4^{o}C.

The supernatant was removed and cells were re-suspended in 0.6 ml of TEN buffer. 1 µl of RNase A was added to each tube and the suspensions were incubated 5 min on ice. 24 µl of 25% Sarkosyl was added to the mixtures to lyse nuclei, the samples were gently inverted several times and 2 µl of Proteinase K were added to each cell lysate. The mixtures were incubated 30 min at 37 ^{o}C.

The lysed nuclei were centrifuged at 14,000 rpm for 5 min in the Eppendorf refrigerated minicentrifuge 5417R at 4^{o}C (from now on the centrifugation conditions are kept the same). The supernatant was moved into the fresh tubes and mixed with 0.6 ml of Phenol/chlorophorm/isoamyl alcohol solution (24:24:1). The mixtures were inverted dozen times, left for 2 min on ice and inverted dozen times again following by 5 min centrifugation.

The top aqueous phase of the solution was moved into the fresh tubes with wide opening tips and mixed with potassium acetate to 0.5 M final concentration and 1 ml of 96% ethanol by inverting tubes gently. The precipitated DNA was pelleted by 5 min centrifugation, washed with 1 ml of 70% ethanol and pelleted again. The ethanol was removed and DNA was dissolved in 70 µl of 1x TE o/n in the fridge.

The dissolved DNA was digested with 50 units of *Bgl*II o/n at 37°C in 150 µl total volume and purified from the restriction enzyme. Potassium acetate was added to 0.3 M final concentration followed by 320 µl of 96% ethanol and the samples were incubated 1 h at -20°C before pelleting DNA with 30 min centrifugation.

To resolve the replication intermediates from the linear DNA, the samples were loaded (with 1 kb molecular weight marker loaded in the side well) on 0.4% agarose gel and run at 0.6V/cm for 30 h in 1x TBE.

After the end of the first dimension, the gel was incubated with 400 ml of 1x TBE with 0.3 µg/ml ethidium bromide for 30 min at room temperature with gentle agitation. The side lane, which contains the molecular weight marker was excised and photographed with a ruler using the Gel Doc^{TM} XR^{+} Imager (BioRad) to evaluate the distance between the comb and the fragment of the relevant molecular weight.

The lanes containing the analysed DNA were excised, transferred into the clean gel casting box and rotated 90° (with the wells always facing left). 0.9% agarose with 0.3 µg/ml ethidium bromide was casted into the casting box, forming the second dimension gel around the lanes excised from the first dimension gel. DNA fragments were further resolved in the second dimension at 10 V/cm for 12 h at 4°C in 1x TBE with 0.3 µg/ml ethidium bromide (with a pump circulating the running buffer from cathode to anode to counteract ethidium bromide migration during the run). After the end of the second dimension, the gel was photographed with a ruler using the Gel Doc^{TM} XR^{+} Imager (BioRad) and used for Southern blotting using the standard protocol (section 2.9.8).

2.9.8. Southern blotting

Materials

- Depurination solution: 0.25 M HCl
- Denaturing solution: 0.5 M NaOH, 1.5 M NaCl
- Neutralizing solution: 1.5 M NaCl, 0.5 M Tris HCl, 1 mM EDTA, pH 7.2
- 20x SSC: 3 M NaCl, 0.3 M tri-Na citrate, pH 7.0
- 20x SSPE: 3 M NaCl, 0.2 M NaH_2PO_4, 20 mM EDTA, pH 7.4
- 100x Denhardt's solution: 2% (w/v) bovine serum albumin (BSA), 2% (w/v) polyvinylpyrrolidone (PVP), 2% (w/v) Ficoll-400.
- Hybridization buffer: 6x SSPE, 0.5% (w/v) SDS, 5x Denhardt's solution
- High-stringency wash buffer: 0.1x SSPE, 0.1% (w/v) SDS
- Low-stringency wash buffer: 1x SSPE, 0.1% (w/v) SDS
- Stripping buffer: 50% (v/v) formamide, 5x SSPE
- Positively charged nylon transfer membrane Amersham Hybond^{TM}-N^{+} (GE Healthcare, RPN303B)

The DNA samples were digested with the chosen restriction enzymes and resolved on an agarose gel. The gel was photographed with a ruler using the Gel Doc^{TM} XR^{+} Imager (BioRad). Before the Sothern transfer, the gel was incubated in the following solutions: Depurination solution (30 min), Denaturing solution (30 min) and Neutralising solution (45 min), all incubations were at room temperature with gentle agitation. Tap water was used to rinse the gel between the incubations.

After the incubation in the Neutralisation buffer, the gel was transferred straight onto the wick in the setup for capillary transfer (with 20x SSC buffer) in the up side down orientation. The gel was covered with a positively charged nylon membrane (Amersham Hybond-N^{+}, GE Healthcare), pre-soaked in 20x SSC buffer, and then with tree pieces of Whatman paper followed by a stack of dry

hand towels. The transfer setup was left o/n at room temperature. Next morning, the membranes were air-dried and the DNA was cross-linked to the membrane by UV exposure (1,200 J/m^2) using the Stratalinker 1800 UV cross-linker (Stratagene).

The DNA hybridization to a radioactively-labelled probe was set up in the glass bottles. First, the membranes were incubated with 15 ml of pre-warmed Hybridization buffer for 1 h at 60^{o}C on a rotation wheel. 10 min before the end of the incubation, 5 µl of α-^{32}P-dATP-labelled probe was mixed with 95 µl of water and boiled to denature. The hybridisation buffer was replaced with 7.5 ml of fresh pre-warmed Hybridization buffer and the denatured probe was added to the membranes. The membranes were incubated at 60^{o}C o/n on a rotation wheel.

Next day, the membranes were rinsed three times with 30 ml of the pre-warmed Wash buffer, incubated 40 min with 30 ml of the Wash buffer at 60^{o}C and rinsed three times once again. The washed membrane was wrapped with a plastic film and left exposing a phosphor screen, which was subsequently scanned with Typhoon FLA 7000 IP^2 imager (GE Healthcare).

To strip the probe, membranes were incubated with 25 ml of Stripping buffer at 65^{o}C for 1 h. After the incubation, the Stripping buffer was removed and the membranes were washed with a wash buffer at 65^{o}C for 15 min as described above.

2.9.9. Labelling DNA probes with ^{32}P

Materials

- QIAquick Gel Extraction Kit (Qiagen)
- Prime-it II Random Primer Labelling Kit (Agilent Technologies, 300385)
- α-^{32}P-dATP 6,000 Ci/mmol (Perkin Elmer, BLU012Z)
- Illustra MicroSpin G-25 columns (GE Healthcare, 27-5325-01)

^{32}P- labelled DNA probes were made using Prime-it II Random Primer Labelling Kit and α-^{32}P-dATP (6,000 Ci/mmol). PCR fragments used to make the

probe were gel-purified using QIAquick Gel Extraction Kit according to the manufacturer's recommendations. The mixture containing 2.5 µl of 2.5 ng/ml of PCR fragments, 2.5 µl of random oligonucleotides (9-mers) and 2 µl of Milli-Q H_2O was incubated at 99°C for 5 minutes and slowly cooled down to room temperature. The contents of the tube were mixed with 2.5 µl of 5x reaction buffer containing all the nucleotides except dATP, 2.5 µl of α-^{32}P-dATP and 0.5 µl of the Exo$^-$ Klenow polymerase (5 Units/ml). The mixture was incubated for 1 h at 37°C, mixed with 60 µl of Milli-Q H_2O and purified from unincorporated nucleotides with Illustra MicroSpin G-25 column following the manufacturer's protocol.

2.9.10. Quantitative analysis of DNA synthesis during BIR using Southern blotting.

Yeast genomic DNA was purified from the cells harvested during the repair time-course experiments (described in Chapter 3, section 3.2). 5 - 10 µl of DNA was digested with *Bam*HI and *Eco*RI enzymes (10 Units/µl) at 37°C o/n. Digested DNA was resolved on 0.7 % agarose gel (with 0.5 µg/ml of ethidium bromide) at 1.3 V/cm. until the dye front reached 20 cm from the wells. The fragments were visualised with a set of probes against donor (BIR6, BIR36, BIR77), recipient (RS2.6, RS6.8, RS15.2) and reference chromosomes.

2.9.11. Analysis of telomere length by Southern blotting

To equilibrate telomere length, cells were passaged on YPD plates at 30°C for 100-140 generations (5-7 passages). Yeast genomic DNA was purified from the last passage. 5-10 µl of DNA was digested with 0.5 µl of *Kpn*I (NEB, 10 Units/µl) in 20 µl total volume at 37°C o/n. Digested DNA was resolved on 0.85% agarose gel (with 0.5 µg/ml of ethidium bromide) at 1.5 V/cm until the dye front reached 20 cm from the wells. The terminal restriction fragments were visualised with the KL1 probe (Makovets et al., 2004) specific to the telomere proximal part of the Y'-repeat sequence and therefore only allows detection of the Y'-telomeres.

2.9.12. Analysis of DNTA by Southern blotting

Yeast genomic DNA was purified from the cells isolated from the $G418^S$ Ura^- colonies formed on YPGal plates after plating strains for BIR/DNTA assay (section 2.8). 5 - 10 µl of DNA was digested with *Eco*RV enzyme (10 Units/µl) at 37°C o/n. Digested DNA was resolved on 0.85 % agarose gel (with 0.5 µg/ml of ethidium bromide) at 1.3 V/cm. until the dye front reached 20 cm from the wells. The fragments were visualised with a probe against *MNT2* locus.

2.9.13. Chromatin immunoprecipitation

Materials

- 37% formaldehyde solution
- HBS buffer: 50 mM HEPES pH7.5, 140 mM NaCl, 1 mM EDTA pH 8.0
- ChIP cell lysis buffer: HBS with 1mM phenylmethylsulfonyl fluoride (PMSF) and 1 tablet of cOmplete™ Protease Inhibitor Cocktail per 10 ml of total volume.
- 2.5 M glycine
- 10% IGEPAL in HBS: 10% (v/v) IGEPAL CA-630, 50 mM HEPES pH7.5, 140 mM NaCl, 1mM EDTA pH8.0
- Chromatin sonication buffer: 50 mM HEPES pH7.5, 140 mM NaCl, 1mM EDTA pH8.0, 10% (v/v) glycerol, 1% (v/v) IGEPAL CA-630, 1 mM PMSF, 1 tablet of cOmplete™ Protease Inhibitor Cocktail per 10 ml of total volume
- High Salt buffer: 50 mM HEPES pH7.5, 0.5 M NaCl, 1 mM EDTA pH8.0
- TL wash buffer: 20mM Tris-HCl pH7.5, 250 mM LiCl, 1mM EDTA pH8.0, 0.5% IGEPAL CA-630, 0.5% Na-deoxycholate
- TE wash buffer: 20 mM Tris-HCl pH7.5, 0.1 mM EDTA pH8.0
- 10xTE: 100mM Tris-HCl pH8.0, 10 mM EDTA pH8.0
- QIAquick™ PCR Purification Kit (QIAGEN, 28106)

50 ml aliquots of yeast cell cultures (OD_{600}≈0.5) were moved into 250 ml Erlenmeyer flasks and placed into a 30^{o}C water bath with shaking to maintain aeration. 1.6 ml of 37% formaldehyde was added to each flask with 20 sec intervals between them. In 10 min, 2.5 ml of 2.5 M glycine was added (to quench formaldehyde) to the flasks while maintaining the 20 sec intervals as in the previous step. 5 min after glycine addition, the cultures were moved to pre-cooled conical tubes and centrifuged at 3,000 rpm for 3 min at 4^{o}C using a refrigerated Eppendorf centrifuge 5810R. Cell pellets were re-suspended in 30 ml of ice-cold HBS buffer and pelleted again at the same conditions. Finally, cells were re-suspended in 500 µl of ChIP cell lysis buffer and frozen at -80^{o}C until needed.

The cell suspensions in ChIP lysis buffer were thawed by submerging into water for 1 min at room temperature. 750 µl of glass beads were added to the samples and cells were lysed by vortexing (12 cycles – 30 sec vortexing, 3 min on ice). The cell lysates were moved into a fresh 1.7 ml Eppendorph tube and 50 µl of IGEPAL in HBS was added to each tube, the samples were mixed by vortexing and incubated for 10 min on ice. After the incubation with IGEPAL CA-630, samples were vortexed again and centrifuged at 14,000 rpm for 30 min in the Eppendorf refrigerated minicentrifuge 5417R at 4^{o}C. The supernatants were removed and the chromatin pellets were re-suspended in 500 µl of Chromatin sonication buffer. At this step the samples were split in halves – 250 µl were frozen at -80^{o}C and 250 µl were sonicated with Bioruptor Plus to break DNA into 0.25 – 0.5 kbp fragments (20 cycles, 30 sec sonication and 30 seconds cool down, 4^{o}C).

After the sonication was complete, the samples were centrifuged at 10,000g (9,700 rpm in the Eppendorf refrigerated microcentrifuge 5417R) for 5 min at 4^{o}C. The supernatants were moved to fresh tubes and centrifuged for 15 min using the same conditions. The supernatants were moved into fresh tubes again and mixed well. 10 µl of sonicated chromatin (input) were moved to another set of tubes and kept on ice until the end of the ChIP. 200 µl aliquots of sonicated chromatin (IP) were mixed with primary antibodies (1:500 dilution) and incubated for 1 h at 4^{o}C with gentle rotation. 50 µl aliquots of magnetic Protein G beads slurry (Dynabeads 10004D, Invitrogen) were aliquoted into the fresh tubes. The beads

were pelleted using DynaMag™-2 Magnet and re-suspended in 200 µl of HBS buffer (see 2.7.4). In an hour, the IP samples were added to the beads while replacing HBS and incubated 2 h at 4°C with gentle rotation.

After the incubation, the ChIP samples were removed from the beads and the beads were rinsed with 200 µl of cold Chromatin sonication buffer and washed sequentially with: 1.5 ml of Chromatin sonication buffer, 1.5 ml of High Salt buffer and 1.5 ml of TL wash buffer (all washes are 5 min at room temperature on a nutator). Finally, the beads were rinsed twice with 0.75 ml of the TE wash buffer and re-suspended in 125 µl of 1x TE with 1% SDS and left at 65°C o/n to reverse protein-DNA crosslinks. The inputs were mixed with 110 µl of 1x TE with 1% SDS and left at 65°C o/n as well.

Next day, immunoprecipitated DNA was purified using QIAquick™ PCR Purification Kit according to the manufacturer's recommendations and dissolved in Elution Buffer diluted 1:5 in water.

2.10. Manipulation of proteins

2.10.1. Rapid yeast protein extraction

Materials

- Cell lysis solution: 1.85 M NaOH, 7.4% (v/v) β-mercaptoethanol
- 50% (v/v) trichloroacetic acid (TCA) (4°C)
- Acetone (-20°C)
- 4x Laemmli Sample Loading buffer: 200 mM Tris-HCl, pH6.8, 400 mM DTT, 10% SDS, 40% (v/v) glycerol, 0.1% (w/v) bromophenol blue
- TCA Sample buffer: 1x Laemmli Sample Loading buffer, 50mM DTT, 30mM Tris (pH is not adjusted)

Cells were patched on YPD plates and grown o/n at 30°C. Next day, the cells were inoculated into 20 ml YPD cultures in 125 ml Erlemeyer flasks at OD_{600} ~ 0.1 and grown until mid-log phase (OD_{600} ≈ 0.5 - 0.6) at 30°C with vigorous

aeration. 3 ODs of cells were pelleted in 15 ml conical tubes at 3,000 rpm for 3 min in Eppendorf refrigerated centrifuge 5810R at 4^{o}C. Cell pellets were washed with 1 ml of ice-cold Milli-Q H_2O and either frozen at -80^{o}C or processed all the way to the end of this protocol.

The washed cell pellets were thoroughly re-suspended in 150 µl of Lysis solution by vortexing and incubated on ice for 10 min. Following the cell lysis, 150 µl of cold 50% (v/v) TCA was added to each tube to precipitate the proteins. The suspensions were mixed well by vortexing and left on ice for 10 min. Precipitated proteins were centrifuged at 14,000 rpm for 2 min, the supernatants were carefully removed and pellets were washed with 1 ml of acetone (-20^{o}C) and spun down again with same centrifugation conditions. After the spin, acetone was removed, the pellets were re-suspended in 100 - 200 µl of the TCA Sample buffer and boiled for 7 min before loading on an SDS polyacrylamide gel or freezing (-80^{o}C for the long term storage).

2.10.2. SDS polyacrylamide gel electrophoresis

Materials

- 30% acrylamide/bis-acrylamide solution (37.5:1)
- 1.5 M Tris-HCl, pH 8.8
- 0.5 M Tris-HCl, pH 6.8
- 10% (w/v) SDS
- Resolving gel solution: acrylamide (the final concentration is experimentally defined based on the protein molecular weight and mobility), 375 mM Tris-HCl, pH 8.8, 0.1% (w/v) SDS
- Stacking gel solution 5% (v/v) acrylamide, 125 mM Tris-HCl, pH 6.8, 0.1% (w/v) SDS
- 10% (w/v) ammonium persulfate (APS)
- Tetramethylethylenediamine (TEMED)

- 4x Laemmli Sample Loading buffer: 200 mM Tris-HCl, pH6.8, 400 mM DTT, 10% SDS, 40% (v/v) glycerol, 0.1% (w/v) bromophenol blue
- 10x SDS-PAGE Running Buffer: 250 mM Tris-HCl, pH8.3, 1.92 M glycine, 1% (w/v) SDS
- Amersham ECL Full Range Rainbow Molecular Weight Protein Marler (GE Healthcare, RPN800E)

To initiate acrylamide polymerisation, 100 µl of 10% (w/v) APS and 10 µl of TEMED were added per 10 ml of Resolving gel solution in a conical tube. Gel was mixed by inverting the tube several times and immediately poured between the glass plates in the assembled casting form, leaving 2 - 2.5 cm for the stacking gel at the top. The resolving gel was covered with 1 ml of 100% ethanol and left for 20 min to polymerase. 5 ml of Stacking Gel solution was prepared in a conical tube and mixed with 62.5 µl of APS and 6.5 µl of TEMED. The ethanol was carefully removed and replaced with the Stacking Gel. A comb was inserted and the gel was left to polymerase for 20 min. After the acrylamide polymerisation was complete, the SDS-PAGE running apparatus was assembled and the chambers were filled with 1x SDS-PAGE running buffer.

Protein samples were boiled for 2 min before loading on the gel. Rainbow Molecular Weight Protein Marker was loaded into one of the wells and used to monitor the progression of the SDS-PAGE and identify the approximate molecular weight of the proteins and the progress of SDS-PAGE and Western Blotting transfer if desired. The gel was run at 100 V until the dye front reached the border between the stacking and resolving gels after which the voltage was increased to 150 – 200 V. After the dye front exited the resolving gel, the gel electrophoresis was stopped and the apparatus was disassembled.

2.10.3. Western blotting

Materials

- 1x Western Blotting Transfer buffer: 25 mM Tris, 192 mM glycine
- Methanol
- 10x TBST: 0.5 M Tris-HCl, pH 7.6, 1.5 M NaCl, 1% (v/v) Tween 20
- Blocking solution: 5% (w/v) non-fat dry milk in 1x TBST
- Immobilon®-FL Transfer Membrane with 0.45 µm pores (Merck Millipore Ltd.)

After the SDS-PAGE apparatus was disassembled, the stacking gel was removed, the resolving gel was rinsed with the Transfer buffer and placed on the three Whatman paper pieces of an appropriate size. The membrane was activated by incubation in methanol for 30 sec and placed onto the gel followed by the additional layer of three Whatman paper pieces. The resulted "sandwich" was placed between two sponges, soaked in the Transfer buffer into the mini-gel transfer apparatus (BioRad) and the transfer was performed at 250 mA for 1 h at room temperature.

After the transfer, the membrane was incubated with 10 ml of the Blocking solution, with gentle rocking for an hour at room temperature. The incubation with primary antibodies was set up in a 50 ml conical tube with 4 ml of TBST and α – myc (9E10 monoclonal antibody 1:1,000 dilution) or α-Act1 (1:200,000 dilution) antibodies on a rotating wheel either for 1 h at room temperature or o/n at 4^{o}C.

Following the incubation with the primary antibodies, the membrane was washed 3 times with TBST for 10 minutes and incubated with 7.5 ml of TBST with 0.6 µl of P680 α-mouse secondary antibodies (1:12,500 dilution). After the incubation with the secondary antibodies, the membrane was washed with TBST two times – for 20 minutes first and then 10 min. The detection of the proteins was performed using Odyssey® CLx fluorescent scanner (LI-COR®) according to the manufacturer's instructions. Image Studio™ Lite software was used for the image analysis and protein quantifications.

2.11 Bioinformatic analysis

The protein sequences were obtained from the Saccharomyces Genome Database (SGD, https://www.yeastgenome.org/). The multiple sequence alignment was performed using the T-Coffee software (https://www.ebi.ac.uk/Tools/msa/tcoffee/). The data were presented using the BOXSHADE software (https://embnet.vital-it.ch/software/BOX_form.html).

Chapter III. Pif1 family of helicases require PCNA-interacting elements to promote DNA replication through the natural replication barriers

3.1. Introduction

As described in sections 1.4.1-3, the members of the Pif1 family helicases are involved in many different aspects of DNA metabolism, which include but not limited to: facilitating DNA replication through certain obstacles (G-4 motifs, R-loops, DNA binding proteins, etc.), alternative Okazaki fragment processing, telomerase inhibition at telomeres and DSBs, promoting DNA damage bypass and BIR.

The recently published data suggest that Pif1 interacts with PCNA (encoded by *POL30* gene in *S. cerevisiae*) both *in vitro* and *in vivo* (Wilson et al. 2013; Buzovetsky et al. 2017; Dahan et al. 2018). The interaction between PCNA and its partners normally occurs via the PIP motif (see section 1.1.4) with the consensus Q x x ψ x x φ φ, where x is any amino acid, ψ is a hydrophobic amino acid and φ is an aromatic amino acid (Figure 3.1 A). Notably, the first PIP identified in the C-terminus of Pif1 did not match the consensus (Figure 3.1 A, compare Pif1-PIP1 to the PIP) and was named a non-canonical PIP (referred to as PIP1 in this work) (Buzovetsky et al. 2017). Pif1 with the mutations in PIP1 (*pif1-pip1,* Figure 3.1 B) had a decreased interaction with PCNA *in vitro*, was partially deficient in promoting Pol δ-mediated DNA synthesis *in vitro*, as well as BIR *in vivo* (Buzovetsky et al. 2017).

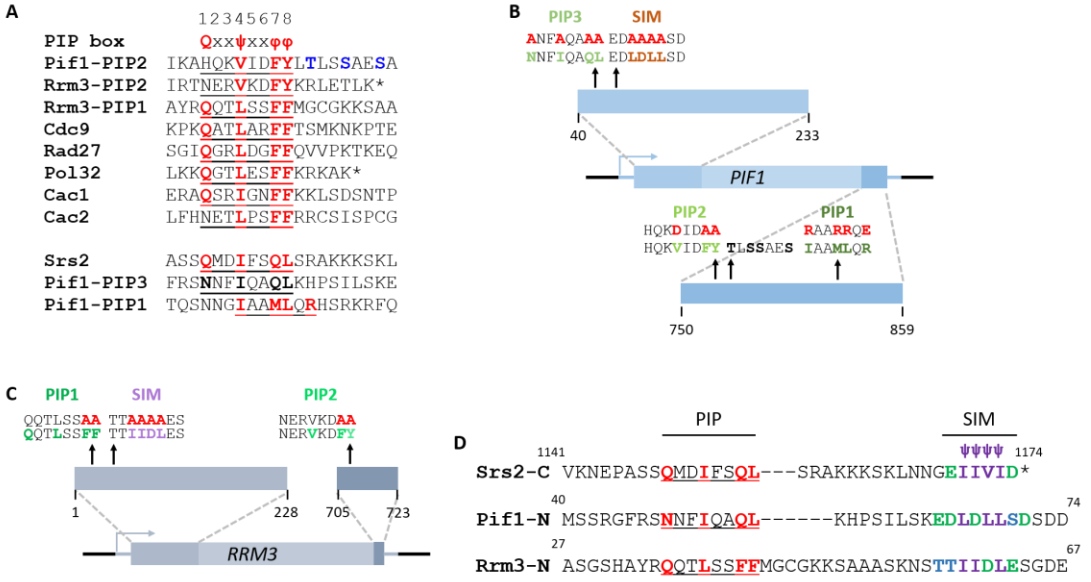

Figure 3.1. PCNA-interacting motifs of Pif1 and Rrm3.

A. Comparison of the PCNA-interacting motifs in different proteins. Top part shows the alignment of the PIPs from Pif1 and Rrm3 to the canonical PIPs from other proteins, the amino acids in red match the canonical PIP consensus (shown at the top). The numbers indicate the amino acid positions within the consensus. Blue font shows the amino acids that are phosphorylated in a DNA damage dependent manner (Makovets and Blackburn 2009). At the bottom – the non-canonical PIP motifs from Pif1 are aligned with the non-canonical PIP motif from Srs2. Amino acids in red were shown to interact with PCNA (Armstrong, Mohideen, and Lima 2012; Buzovetsky et al. 2017). Amino acids in bold black from Pif1-PIP3 are similar to the PIP in Srs2 and are hypothesised to form PIP3 in Pif1. **B.** Schematic of *PIF1* and the N- and C-terminal parts of Pif1. The shades of blue in the schematic illustrate the N- terminal, middle and the C-terminal parts of *PIF1*. Numbers below the N- and C-termini indicate the amino acid coordinates. Black arrows indicate the relative position of the PCNA-interacting motifs and the Rad53/Dun1-dependent phosphosite in Pif1. The sequences of the corresponding motifs are shown above the arrows, with the most important amino acids coloured into the corresponding shade of green (for the PIP motifs), orange (for the SIM motif) or bold black (for the phosphosite). The changed amino acids in the corresponding mutations are indicated in red above the wild type sequence. **C.** Schematic of *RRM3* and the N- and C-terminal parts of Rrm3. The shades of grey in the schematic illustrate the N- terminal, middle and the C-terminal parts of *RRM3*. Black arrows indicate the relative position of the PCNA-interacting motifs in Rrm3. The sequences of the corresponding motifs are shown above the arrows, with the most important amino acids coloured into the corresponding shade of green (for the PIP motifs) or purple (for the SIM motif). The changed amino acids in the corresponding mutations are indicated in red above the wild type sequence. **D.** Alignment of the putative PIP3-SIM to the PIP-SIM at the C-terminus of Srs2. The amino acids in red constitute the interacting surface with PCNA in the non-canonical PIP of Srs2 (Armstrong, Mohideen, and Lima 2012). Hydrophobic amino acids (in purple) and acidic amino acids (in green) form the SIM in Srs2 (Armstrong, Mohideen, and Lima 2012). The amino acids shown in blue could be phosphorylated and provide the negative charge required for the interaction with SUMO. The amino acid position in the context of the corresponding proteins is shown above the sequences in black.

The second PIP (PIP2) in the C-terminus of Pif1 was identified later by Aharoni and colleagues (Dahan et al. 2018). Except for the histidine in the position 1, it fits the requirements of the canonical PIP (Figure 3.1 A). The interaction between Pif1 and PCNA via PIP2 is important for the replication through G4 motifs and this function of Pif1 does not require PIP1 (Dahan et al. 2018). Based on the juxtaposition of PIP2 with the Rad53/Dun1-dependent phosphosite (Figure 3.1. A), the phosphorylation may affect the interaction between Pif1 and PCNA via PIP2.

Certain proteins require additional elements to ensure a strong interaction with PCNA. Srs2 contains a PIP and a SUMO-interacting motif (SIM) in its C-terminus, both of which are required for interaction with SUMOylated-PCNA and recruit Srs2 to the replication forks (see section 3.2) (Armstrong, Mohideen, and Lima 2012). The SIM consensus contains a hydrophobic core composed of four amino acids (Figure 3.1 D), sometimes interrupted by one random amino acid, and a nearby located negatively charged patch which defines the orientation of how the hydrophobic core binds SUMO. The stretch of amino acids in the N-terminus of Pif1 has a substantial similarity to the combination of PIP and SIM of Srs2 (Figure 3.1 D) and may serve as another interaction site between Pif1 and PCNA (S. Makovets, personal observation).

The physical interaction between Rrm3 and PCNA has been shown *in vitro* and *in vivo* (Schmidt, Derry, and Kolodner 2002). The canonical PIP motif was mapped to the N-terminal part of the protein (Figure 3.1 A, Rrm3-PIP1). Interestingly, the N-terminally truncated version of Rrm3 that was missing the PIP1 motif completely was still interacting with PCNA, albeit with the reduced strength, suggesting that Rrm3 could have additional PCNA-interacting elements (Schmidt, Derry, and Kolodner 2002).

The N-terminus of Rrm3 contains a putative SIM (S. Makovets, personal observation). The negative charge is concentrated on the C-terminal side of the hydrophobic core of the SIM in Rrm3, although the two threonine residues located N-terminally may be phosphorylated and provide the required negative charge for the interaction with SUMO (Figure 3.1 D).

A possible candidate for a second PIP motif is located in the C-terminus of Rrm3 (Figure 3.1 A, C, Rrm3-PIP2) because Rrm3 contains a sequence highly homologous to what has been claimed a PIP in Pif1. Just as PIP2 in Pif1, PIP2 in Rrm3 is missing the glutamine at the position 1 of the PIP-box consensus (Figure 3.1. A), but the amino acids at the positions 4, 6 and 7 match the consensus. Overall, the C-terminal regions located between the last helicase motif and PIP2 have a high degree of conservation between S.c.Pif1, S.c.Rrm3 and other Pif1 family helicases from different species (Snow et al. 2007, also disscussed in more details in Chapter VI), suggesting that they may contain important functional elements. The role of the Rrm3-PCNA interaction has not been addressed directly.

As described above, the interactions between the Pif1 family helicases and PCNA might occur via different motifs in Pif1 and Rrm3. This chapter is aimed to address if the PCNA-interacting motifs (reported and hypothetical) are required for the functions of Pif1 and Rrm3 in DNA replication.

3.2. PIP3-SIM from Pif1 can functionally substitute for the C-terminal PIP-SIM in Srs2

The DNA damage, which arises during DNA replication and causes replication forks to stall, triggers Rad6-Rad18 dependent mono-ubiquitination of K164 in PCNA. This allows error-prone translesion DNA synthesis executed by the specialised DNA polymerases (such as Pol η and Pol ζ) to take place (Hoege et al. 2002; Stelter and Ulrich 2003). Subsequent poly-ubiquitination of K164 in Ubc13-Mms2 and Rad5-dependent manner allows the error-free DNA damage bypass.

The ubiquitination of K164 is mutually exclusive with the Ubc9-Siz1-dependent SUMOylation of this residue (Parker et al. 2008). The C-terminus of Srs2 contains a PIP and a SIM motifs (Figure 3.1 D), both of which are required for the Srs2 interaction with the SUMOylated PCNA in order to inhibit recombination at stalled forks: Rad51 presynaptic filaments are dismantled by Srs2 recruited by SUMOylated PCNA (Pfander et al. 2005; Armstrong, Mohideen, and Lima 2012; Andriuskevicius, Kotenko, and Makovets 2018). The interaction

between Srs2 and SUMO-PCNA is well understood and a crystal structure of the involved components has been solved (Armstrong, Mohideen, and Lima 2012).

In *rad18Δ* cells, K164 in PCNA is constitutively SUMOylated in the S phase and therefore both error-prone and error-free branches of the DNA damage bypass are inhibited. *rad18Δ* cells are sensitive to the DNA damaging drugs, such as MMS (Figure 3.2). This phenotype can be suppressed by a mutation in either PIP or SIM in Srs2, as both are required to maintain the interaction with the SUMOylated PCNA (Armstrong, Mohideen, and Lima 2012).

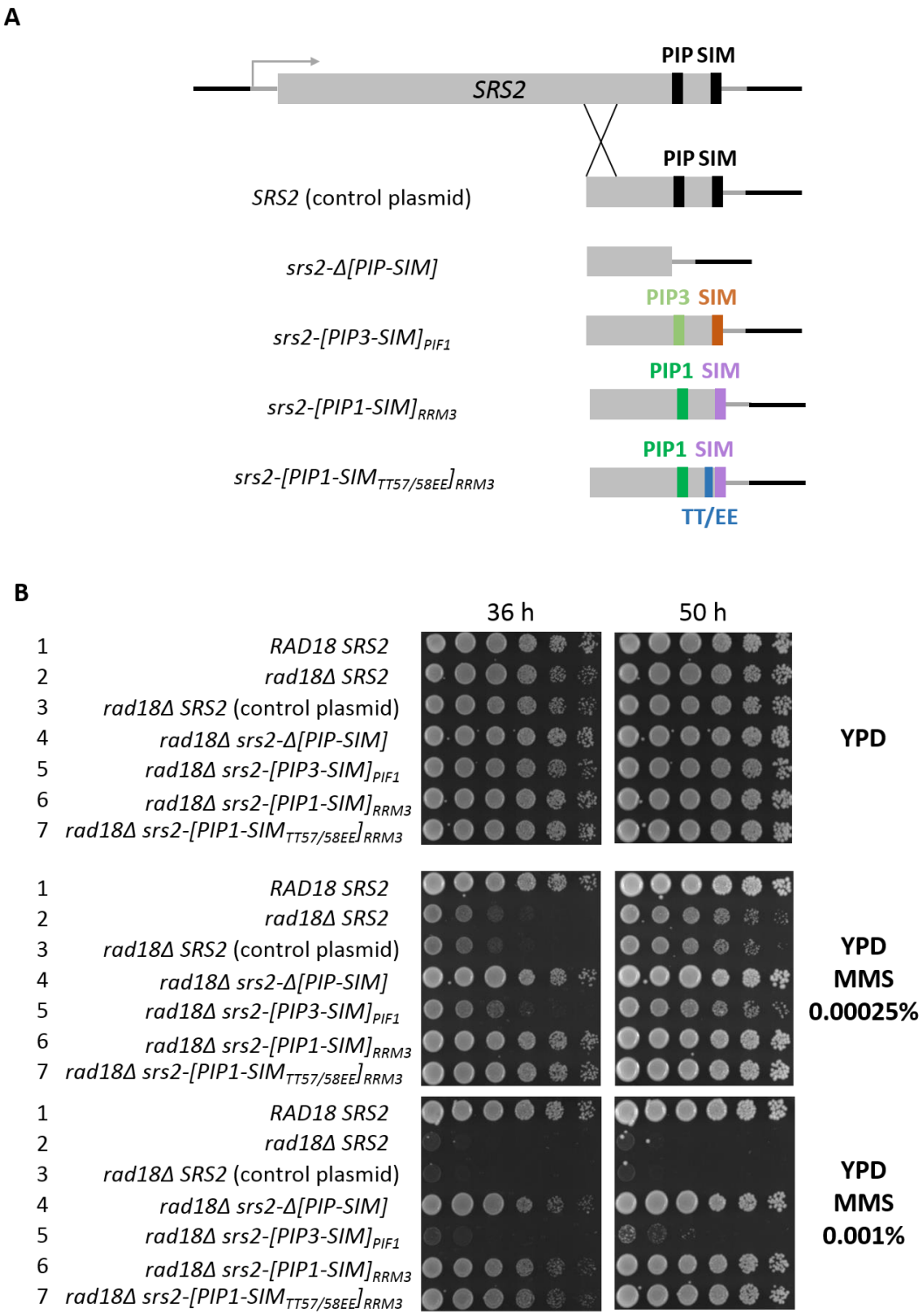

Figure 3.2. The putative PIP3-SIM locus of Pif1 can functionally substitute for the PIP-SIM of Srs2.

A. Schematic of the yeast strains construction. The strains were constructed by integrating the plasmids containing the 3' part of *SRS2* (control plasmid), or *srs2-Δ1149* (*srs2-Δ[PIP-SIM]*), or the sequences to make the chimeric Srs2 proteins with the PIP3-SIM from Pif1 (*srs2-[PIP3-SIM]*$_{PIF1}$), PIP1-SIM from Rrm3 (*srs2-[PIP1-SIM]*$_{RRM3}$) or PIP1-SIM from Rrm3 with TT57/58EE

mutation (*srs2-[PIP1-SIM$_{TT57/58EE}$]$_{RRM3}$*). All the plasmids contained *TRP1* marker and were integrated into the *SRS2* locus as shown on the schematic. **B**. The chimeric Srs2 protein with the PIP-SIM replaced by the PIP3-SIM from Pif1 (*srs2-[PIP3-SIM]$_{PIF1}$*, lane 5) maintains the sensitivity of the *rad18Δ* strain to DNA damage. Five-fold serial dilutions of cells were spotted on YPD with the indicated concentrations of MMS (on the right). The pictures present the results of the one out of the two biological repeats. Strains used: NK1, NK7674, NK7676, NK7682, NK7684, NK7686, NK7688, NK7690, NK7692, NK7694, NK7696.

To test if the putative PIP3 and SIM in the N-terminus of Pif1 can functionally substitute for the PIP and SIM in the C-terminus of Srs2, a chimeric *srs2-[PIP3-SIM]$_{PIF1}$* allele was created by replacing the sequence that encodes amino acids 1149-1174 from *SRS2* with the sequence for amino acids 48-74 from *PIF1* and introduced into the *rad18Δ* cells (Figure 3.1 D, Figure 3.2 lane 5). The putative PIP1-SIM combination from Rrm3 (amino acids 35-67) was also used to substitute the PIP-SIM in Srs2 either in the native state (*srs2-[PIP1-SIM]$_{RRM3}$*) or with the TT57/58EE substitution (*srs2-[PIP1-SIM$_{TT57/58EE}$]$_{RRM3}$*) to mimic a hypothetical phosphorylation of the indicated threonines (described in section 3.1). An isogenic *SRS2* strain with the control plasmid integrated (Figure 3.2, lane 3) and a strain with the C-terminal truncation that removed the PIP-SIM region in *SRS2* (*srs2-Δ[PIP-SIM]*, Figure 3.2 lane 4) were used as a positive and a negative controls respectively.

The *rad18Δ* strain with the wild-type *SRS2* alleles (Figure 3.2 lanes 2 and 3) showed a noticeable MMS sensitivity in comparison with the *RAD18 SRS2* strain. As expected, the MMS-sensitivity of *rad18Δ* was supressed by the removal of PIP-SIM from Srs2 (compare lanes 1, 3 and 4 in Figure 3.2). The PIP3-SIM from the N-terminus of Pif1 was able to functionally substitute for the PIP-SIM of Srs2 (compare lanes 1, 3 and 5 in Figure 3.2), which demonstrates that this locus in Pif1 can provide interaction with SUMOylated PCNA. In contrast, neither of the chimeric proteins containing the PIP1-SIM combinations from Rrm3 could substitute for the Srs2 activity, suggesting that the Rrm3 sequences used do not allow to maintain a sufficient Srs2-PCNA interaction.

The experiment presented here allows to formulate a hypothesis that Pif1 may form a complex with the SUMOylated PCNA and therefore these motives (along with the PIP1 and PIP2 motifs) will be referred to as the PCNA-interacting motifs of Pif1. However, the alternative hypothesis could be that the SIM motif in Pif1 is

used to interact with another SUMOylated component of the replication forks, which coincidentally allows to bypass the requirement of PCNA-dependent recruitment of the Srs2-[PIP3-SIM]$_{PIF1}$ fusion to the stalled replication forks. Therefore, additional experiments are required to test if the PIP3 and SIM motifs can indeed support the physical interaction between Pif1 and PCNA. Another interesting question of how Pif1-PCNA interaction occurs in the context of multiple PIP motifs in Pif1 is also a matter of current investigation in the Makovets lab.

3.3. Pif1 requires PCNA-interacting motifs to promote replication through the tRNA genes

To test if the PCNA-interacting elements in Pif1 are required for its role in DNA replication, fork progression through the *tA(AGC)F* (*tDNA$_{Ala}$*) locus on chromosome VI was assayed by 2D gel electrophoresis in combination with Southern blotting (Friedman and Brewer 1995) (Figure 3.3 A). Replication forks pause at *tDNA$_{Ala}$* in wild type cells (Deshpande and Newlon 1996), however this pausing is greatly elevated in *rrm3Δ* (Ivessa et al. 2003). Although *pif1Δ* cells replicate *tDNA$_{Ala}$* similarly to the wild type cells, *rrm3Δ pif1Δ* have greater replication fork pausing than *rrm3Δ* cells (Osmundson et al. 2017; Tran et al. 2017), suggesting that Pif1 acts as a back-up helicase promoting replication through this region in the absence of Rrm3.

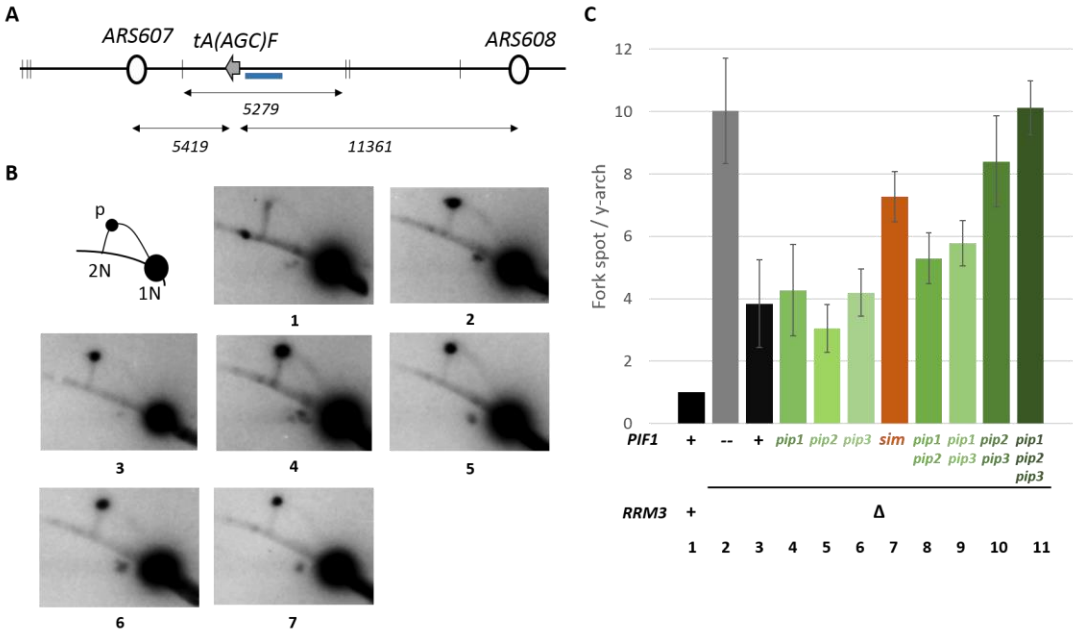

Figure 3.3. PCNA-interacting elements in Pif1 are required for promoting DNA replication through *tDNA$_{Ala}$* locus in *rrm3Δ* cells.

A. Schematic of the *tDNA$_{Ala}$* locus indicating the distance between the *Bgl*II sites surrounding the gene (vertical bars) and the distances from the gene to the closest replication origins on either side (*ARS607* and *ARS608*). Blue bar indicates region homologous to the DNA probe used for Southern blotting. **B.** Representative images of neutral-neutral 2D gel electrophoretic analysis of replication through *tDNA$_{Ala}$* by Southern blotting. Schematic illustrates the expected migration of the linear dsDNA molecules (bottom arch) and branched dsDNA molecules (top arch) generated by the forks passing through the *Bgl*II fragment analysed. The black circle depicts the location of the branched DNA molecules accumulating due to the fork pausing site (P). The numbers under each image indicate the genotypes shown in the legend to the plot in panel C. **C.** Quantitative analysis of replication fork pausing at *tDNA$_{Ala}$* in the indicated strains normalised to the Y-arch and to the corresponding value of the wild type strain (genotype 1). The bars show average ± SD (n≥3). Strains used: NK1, NK7511-7513, NK7614-7628, NK8173-8187

To test if the PCNA-interacting elements in Pif1 are required for the Pif1 role in replication through $tDNA_{Ala}$ the corresponding *pif1* alleles were introduced into the *pif1-m2 rrm3Δ* strain. All of the *pif1-m1-pip* alleles were able to completely suppress the increased fork pausing in *rrm3Δ pif1-m2* cells to the *rrm3Δ* levels (Figure 3.3 C, compare bars 4, 5 and 6 to 3) suggesting that none of the PIP motifs was essential for the replication associated function of Pif1. In contrast, *pif1-m1-sim* showed only partial suppression (Figure 3.3 C, compare 7 to 2 and 3), suggesting that the SIM in Pif1 is required for the DNA replication through $tDNA_{Ala}$ in *rrm3Δ* cells.

It is possible that the single *pip* mutations in Pif1 do not compromise the replication-associated function of the helicase because the PIP motifs are redundant. To test this hypothesis, the *rrm3Δ* cells expressing *pif1* alleles with the double and triple combinations of the *pip* mutations were created. *pif1-m1-pip1-pip2* and *pif1-m1-pip1-pip3* alleles suppressed the increased fork pausing of *rrm3Δ pif1-m2* cells to the levels similar to *rrm3Δ* (Figure 3.3 B, compare 8 and 9 to 3). However, neither *pif1-m1-pip2-pip3 rrm3Δ*, nor *pif1-m1-pip1,pip2,pip3 rrm3Δ* cells were showing a statistically significant decrease in the replication fork pausing compared to the *pif1-m2 rrm3Δ* cells, suggesting that PIP2 and PIP3 are important for promoting replication through the $tDNA_{Ala}$ locus (Figure 3.3 B, compare 10 and 11 to 2 and 3). The requirement for PIP1 is not clear, because the small differences in the relative signal from the stalled forks, observed between *pif1-m1-pip2-pip3 rrm3Δ* and *pif1-m1-pip1,pip2,pip3 rrm3Δ* cells may be within the experimental error. Importantly, the effect of the *pip1,pip2,pip3* mutation in Pif1 was greater than *sim* suggesting that the helicase may contain additional SIM motifs.

3.4. Pif1 localisation to stalled replication forks requires its PCNA-interacting motifs and is promoted by PCNA modifications

Since PCNA is implicated in protein recruitment to the DNA substrates, I explored the possibility that the replication defects of *pif1-m1-pip* mutants are due to the compromised Pif1 recruitment to stalled replication forks. The *pif1-m2* cells

expressing 4myc-tagged *pif1-m1* alleles were synchronised in G1 and released into the S-phase in the presence of high concentration of hydroxyurea (HU) which leads to fast deoxyribonucleotide depletion and replication fork arrest in the close proximity to the origins of replication. The recruitment of Pif1 to an early replicated locus (*ARS601*) was analysed by ChIP-qPCR in a short time-course experiment (Figure 3.4 A).

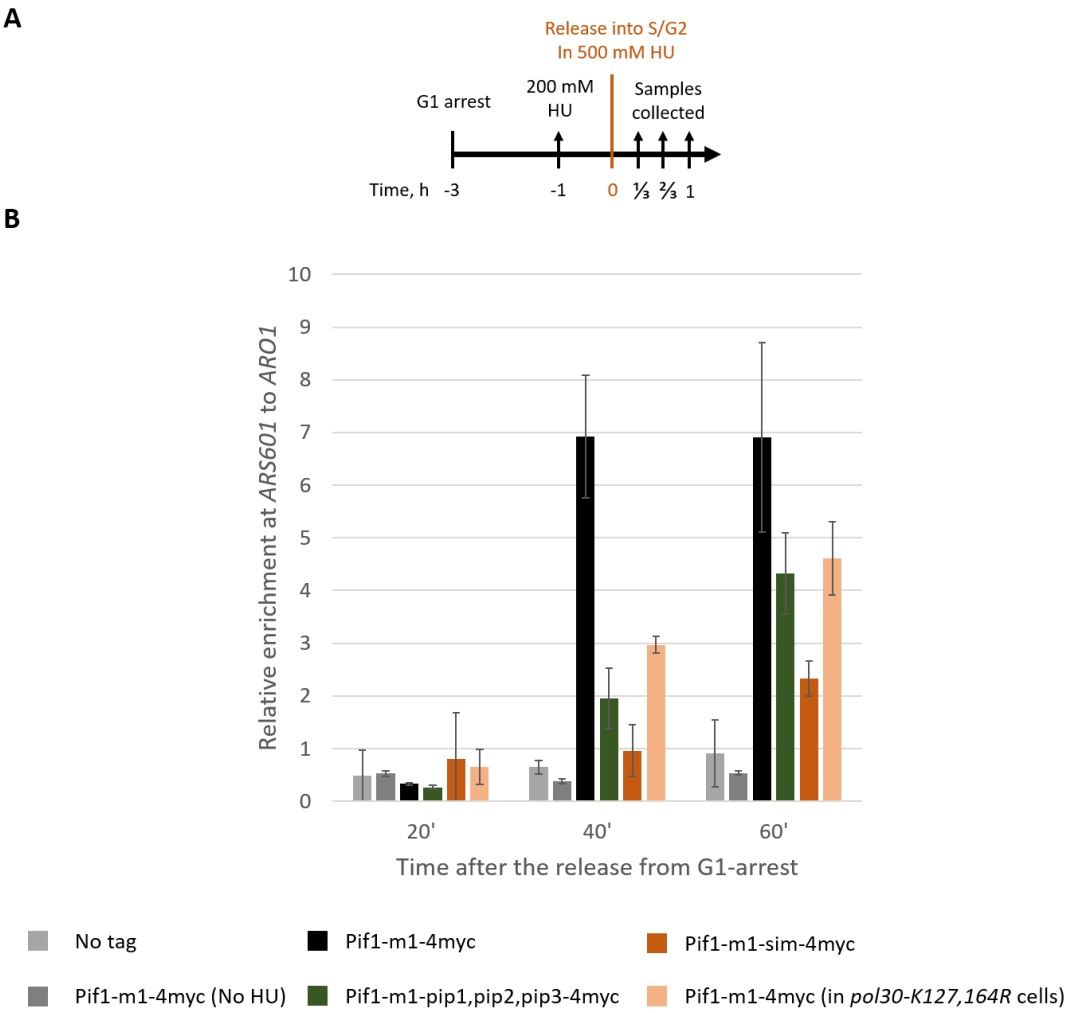

Figure 3.4. PCNA-interacting motifs in Pif1 and posttranslational modifications of PCNA are required for Pif1 localisation to stalled replication forks.

A. Schematic of the experimental design. The logarithmically growing cell cultures were synchronised in G1 by addition of α-factor for 2 h and pre-treated with 200 mM HU for another hour before the α-factor was washed away and the cells were released into the fresh medium with 500 mM HU. The aliquots were taken at 20, 40 and 60 minutes after the release. **B**. Localisation of Pif1-m1-4myc and the specified *pip* and *sim* mutants to the early replicating *ARS601* locus relative to the late replicating control locus (*ARO1*). The bars show average ± SD based on the data from two biological repeats. Strains used: NK1325, NK1335, NK7650, NK7652, NK7894, NK7895, NK8188, NK8189.

Pif1-m1-4myc enrichment above the background was evident at the 40 and 60 min time-points after the release from the G1 arrest, indicating that Pif1 localised to the replication forks stalled in a close proximity to the origin (Figure 3.4 B). Since the PIP motifs might be redundant for the replication-associated function of Pif1, I have tested if Pif1-m1-pip1,pip2,pip3-4myc would localise to stalled replication forks. As evident from the Figure 3.4, Pif1-m1-pip1,pip2,pip3-4myc showed decreased localisation to the forks at both 40 and 60 min time-points in comparison with the wild type equivalent, suggesting that Pif1 recruitment to stalled replication forks is PCNA-dependent.

Pif1-m1-sim-4myc localisation was not detected at 20 and 40 min time-points and only slight increase above the background level was detected at 60 min timepoint (Figure 3.4, B), suggesting that the SIM is also required for Pif1 localisation to the stalled forks. I have tested if Pif1 localisation to the stalled replication forks requires PCNA post-translational modifications by using the *pol30-KK127,164RR* allele, which eliminates the known PCNA SUMOylation sites. Pif1 localisation to the stalled replication forks was reduced in *pol30-KK127,164RR* cells, supporting the hypothesis that Pif1 localisation is PCNA-dependent. However, K164 is also used for mono- and poly-ubiquitination of PCNA which complicates the investigation of which posttranslational modification is responsible for this effect.

Considering that *pif1-m1-pip1,pip2,pip3* allele had a stronger defect in DNA replication through $tDNA_{Ala}$ in *rrm3Δ* cells than *pif1-m1-sim* (Figure 3.3, C), but the *sim* mutation had a bigger effect on the localisation of Pif1 to stalled forks than *pip1,pip2,pip3* (Figure 3.4, B), compromised localisation cannot completely explain the replication-associated phenotype. It is possible that apart from localising Pif1 to its substrates, PCNA also promotes its catalytic activity in a manner requiring some or all of the PIP motifs in Pif1. Addressing this important question would require biochemical characterisation of PCNA-dependent activity of different Pif1 mutants and will not be attempted in this work.

3.5. The C-terminal PIP in Rrm3 is required for DNA replication through the natural replication barriers

Since the PCNA-interacting elements in Pif1 appeared to be required for its replication-associated function (addressed in section 3.3), it was interesting to test if Rrm3 also requires the reported PIP1 or hypothetical SIM and PIP2 for promoting DNA replication through the “hard-to-replicate” loci. To address this question, DNA replication through *rDNA* locus on chromosome XII and $tDNA_{Ala}$ locus on chromosome VI was assayed by the 2D gel electrophoresis in the corresponding mutants (Figure 3.5).

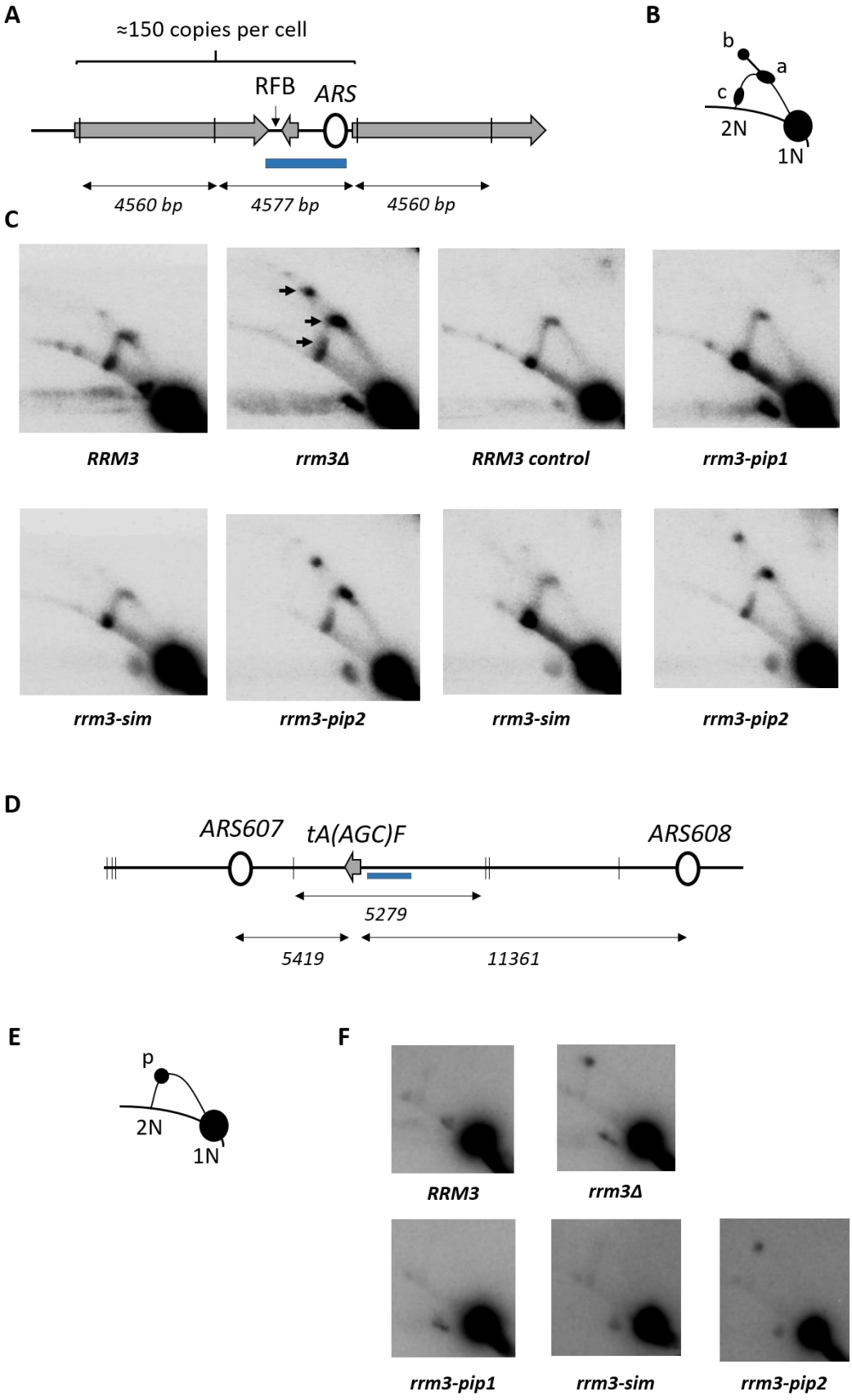
A
≈150 copies per cell
RFB
ARS
4560 bp
4577 bp
4560 bp
B
b
a
c
2N
1N
C
RRM3
rrm3Δ
RRM3 control
rrm3-pip1
rrm3-sim
rrm3-pip2
rrm3-sim
rrm3-pip2
D
ARS607
tA(AGC)F
ARS608
5279
5419
11361
E
p
2N
1N
F
RRM3
rrm3Δ
rrm3-pip1
rrm3-sim
rrm3-pip2

Figure 3.5. Rrm3 requires PIP2 motif to promote DNA replication through the natural replication obstacles.

A. Schematic of *RDN1* monomer, indicating the 35S *rDNA* gene (big right-facing arrows), 5S *rDNA* gene (small left-facing arrow), replication fork barrier (RFB), origin of replication (ARS), the region homologous to the DNA probe used for the Southern blotting (blue bar) and the positions of the relevant *Bgl*II sites (vertical lines). **B.** A schematic illustrating the expected migration of the linear molecules (bottom arch) and branched molecules (top arch) generated by the forks passing through the *Bgl*II fragment analysed. The extension of the fork arch emanating from the top illustrates the expected mobility of the fragments containing two converging replication forks. The regions of the branched molecules trajectory which show increased signal in *rrm3Δ* are depicted with the black circles and ellipsoids and represent the forks paused at RFB (a), converging forks (b) and the forks pausing at the ARS (c) (Ivessa, Zhou, and Zakian 2000). **C.** Representative images of neutral-neutral 2D gel electrophoretic analysis of DNA replication through *rDNA* locus. For each genotype a minimum of two biological repeats analysed. **D.** Schematic of the $tDNA_{Ala}$ locus indicating the distance between the *Bgl*II sites surrounding the gene (vertical bars) and the distances from the gene to the closest replication origins on either side (*ARS607* and *ARS608*). Blue bar indicates region homologous to the DNA probe used for Southern blotting. **E**. A schematic illustrating the expected migration of linear molecules (bottom arch) and branched molecules (top arch) generated by the forks passing through the *Bgl*II fragment analysed. The black circle depicts the location of the expected fork pausing site (P). **F**. Representative images of neutral-neutral 2D gel electrophoretic analysis of replication through $tDNA_{Ala}$. For each genotype a minimum of two biological repeats analysed. Strains used: NK1, NK7760, NK7761, NK7922-7934

The *rDNA* locus consists of 100-200 copies of tandemly repeated *RDN1* repeats, which are 9.1 kb long sequences containing 35S rRNA gene (which encodes 25S, 5.8S and 18S rRNAs), 5S rRNA gene, an origin of replication and a polar replication fork barrier (RFB) located between 35S and 5S rRNA genes (Figure 3.5 A). Not all of the replication origins in the *RDN1* repeats are active in every given S-phase (only 15% on average). Once an origin has been fired it generates leftward and rightward moving forks. The leftward moving fork replicates the adjacent 5S rRNA gene and pauses at the RFB until the rightward moving fork from the adjacent origin converges with it. Thus, most of the *RDN1* are replicated passively by the rightward moving replication forks.

Rrm3 is required for the normal replication of the *rDNA* locus and in its absence the cells have increased persistence of the forks paused at RFB (RFB impedes progression of the rightward moving forks), increased persistence of the converging forks (the resolution of converged forks is compromised) and the forks pausing at the inactive replication origins. This results in the increased Southern blot hybridisation signals corresponding to the branched replication intermediates resolved by 2D electrophoresis.

As expected, the *rrm3Δ* strains showed increased hybridisation signal at RFBs, converging forks and ARSes (Figure 3.5 C, indicated by the arrows). The control strain with the *RRM3* gene expressed from an integration vector had a wild-type-like pattern of replication through the *rDNA* locus, indicating a complete suppression of the *rrm3Δ* defect (Figure 3.5 C, compare *RRM3* control to *RRM3*). The *RRM3* alleles with either *pip* or *sim* mutations (Figure 3.1 C) were integrated into the *rrm3Δ* strains similarly to the *RRM3* allele in the control strain. Neither *rrm3-pip1* nor *rrm3-sim* strain have shown the replication defect in the *rDNA* locus indicating that the corresponding alleles are able to suppress the *rrm3Δ* phenotype (Figure 3.5 C). In contrast, *rrm3-pip2* resembled to *rrm3Δ*, suggesting that the PIP2 motif is required for the replication associated function of Rrm3.

To extend the replication analysis beyond *rDNA*, DNA replication through $tDNA_{Ala}$ locus was analysed in the same strains (Figure 3.5 D). Consistent with the data for the *rDNA* locus, replication through $tDNA_{Ala}$ was normal in the *rrm3-pip1* and *rrm3-sim* strains. However, *rrm3-pip2* was similar to the *rrm3Δ* control

and had a higher frequency of the stalled forks, supporting the finding that Rrm3 requires PIP2 for promoting DNA replication through the “hard-to-replicate” loci.

3.6. Discussion

The results described in this chapter provide new molecular insights into the DNA replication through the natural replication barriers based on the characterisation of the previously reported and new *pif1* and *rrm3* alleles.

The PIP3-SIM region from the N-terminus of Pif1 can functionally substitute for the endogenous PIP-SIM locus of Srs2 (Figure 3.2) and therefore may be able to serve as PCNA-interacting elements in Pif1. In addition to the putative N-terminally located PCNA-interacting elements, the C-terminus of Pif1 contains the two previously reported PIP motifs, called PIP1 and PIP2 in this study. Pif1 is not a unique example of the proteins containing multiple PCNA-interacting elements. Another example is the Y-family polymerase Pol η that has three reported PIPs and a ubiquitin binding domain (Haracska et al. 2001; Masuda et al. 2015). The mutations in these PIP motifs showed that some of them are redundant, but some are functionally distinct, which allowed the authors to hypothesise that there are different types of interactions between PCNA and Pol η (Masuda et al. 2015). In this work, I have tested the functional requirements for the PCNA-interacting motifs in the replication-associated functions of Pif1.

The PIP2 and PIP3 motifs in Pif1 were required for DNA replication through the $tDNA_{Ala}$ locus, but acted redundantly as only the *pif1-m1-pip2,pip3* allele which contained both mutations was not able to completely suppress the increased fork pausing in *pif1-m2 rrm3Δ* cells. The involvement of PIP1 motif in the replication associated function of Pif1 remained unclear due to the small differences in the forks pausing observed between cells with *pif1-m1-pip2,pip3* and *pif1-m1-pip1,pip2,pip3* alleles. SIM in Pif1 was also required for promoting DNA replication, but the cells expressing Pif1-m1-sim had only moderately increased replication fork pausing at $tDNA_{Ala}$, suggesting that Pif1 may contain additional SIM motifs that are also required for the replication-associated function.

The replication phenotype of the cells expressing Pif1-m1-pip1,pip2,pip3 and Pif1-m1-sim could be partially explained by the compromised localisation of the corresponding proteins to the stalled replication forks (Figure 3.4). However, the fact that the *sim* mutation has a bigger effect on the relative enrichment of Pif1 at stalled replication forks than *pip1,pip2,pip3*, but lesser on the replication through $tDNA_{Ala}$ suggests that Pif1-pip1,pip2,pip3 may also be catalytically less active.

DNA replication through the sites which require Rrm3 does not depend on the previously characterised PIP1 or a putative SIM motif in the N-terminus of this helicase (Figure 3.5). In contrast, Rrm3 functions in DNA replication seem to require its C-terminal motif PIP2. Although PIP2 in Rrm3 is very similar to the previously reported PIP2 motif in Pif1, more detailed molecular investigation is required to test if the interaction between PCNA and Rrm3 indeed occurs via this motif.

Thus PCNA-interacting motifs in Pif1 and the putative PIP2 in Rrm3 are required for DNA replication associated functions of these helicases. As described in chapter I, Pif1 is involved in a subset of processes that do not require Rrm3 (including telomerase inhibition at telomeres and at DSB and promoting BIR). The next chapter considers the genetic requirements of the PIP and SIM motifs of Pif1 for these Pif1-specific functions.

Chapter IV. PCNA-interacting motifs in Pif1 are required for its recruitment to DSBs, telomerase inhibition and BIR

4.1. Introduction

As described in section 1.4.1, Pif1 has several distinct functions, which are not shared with Rrm3. These include telomerase inhibition at telomeres and at DSBs and promoting BIR.

Apart from the catalytic activity of Pif1, telomerase inhibition at DSBs and BIR require Rad53/Dun1-dependent phosphorylation of the TLSSAES motif in the C-terminus of Pif1 (Makovets and Blackburn 2009; Vasianovich, Harrington, and Makovets 2014).

Additionally, BIR requires the PIP1 motif previously identified in the C-terminus of Pif1 (Buzovetsky et al. 2017). PIP1 is also required for the Pif1 role in promoting template switching during DNA damage bypass (Garcia-Rodriguez, Wong, and Ulrich 2018). The localisation of Pif1 to the MMS-induced DNA damage loci was significantly impaired in *pif1-pip1* cells suggesting that the interaction between Pif1 and PCNA may be required for the recruitment of the helicase to the DNA repair sites. The requirements for the C-terminally located PIP2 motif for telomerase inhibition or promoting BIR were not addressed.

Based on the published data, it is possible to hypothesise that the unique functions of Pif1 in response to DSB require the C-terminal sequence of Pif1, which is absent in Rrm3. This could be connected with the functional specialisation of the Pif1 family helicases. To test this hypothesis, I am going to address the requirements for the C-terminal sequences in Pif1 for telomerase inhibition at telomeres and at DSB and promoting BIR, using the C-terminal truncations and mutations in the C-terminal PIP motifs.

The N-terminal PCNA-interacting motifs of Pif1 (PIP3 and SIM) were required for the replication associated functions of Pif1 (Figure 3.3 C). The N-terminus of Rrm3 also contains a PIP (PIP1) and a putative SIM. In contrast to PIP3-SIM from Pif1 the PIP1-SIM from Rrm3 could not substitute for the PIP-SIM in the C-terminus of Srs2 (Figure 3.2, B). Moreover, the N-terminally located PIP1 in Rrm3

was not required for the replication-associated functions (Figure 3.5 C, D). Based on this data, the presence of PIP3-SIM in Pif1 could also contribute to the functional divergence from Rrm3. The requirements for the N-terminal PCNA-interacting motifs in Pif1 for BIR and telomerase inhibition at telomeres and at DSBs were addressed in this chapter.

Finally, the defect in the replication associated functions of Pif1 caused by the mutations in the PCNA-interacting motifs could be explained by reduced localisation of Pif1 to stalled replication forks. Similarly, it is interesting to test if Pif1 localisation to DSBs requires PCNA-interacting motifs.

This chapter addresses the requirements of the C-terminus of Pif1 and the PCNA-interacting motifs for BIR, for telomerase inhibition at telomeres and DSBs, and for the Pif1 recruitment to DSBs.

4.2. The C-terminus of Pif1 contains distinct regions required for BIR and telomerase inhibition.

A series of the C-terminal truncations was introduced in *PIF1* in the strains with the inducible DSB and 500 bp of homology between chromosomes VII and II (described in section 2.8) (Vasianovich, Harrington, and Makovets 2014) to test if the C-terminus of Pif1 is required for Pif1 functions in BIR and telomerase inhibition. The full length nuclear Pif1 contains amino acids 40 – 859 expressed from the *PIF1* gene (described in section 1.4.1). The Pif1-Δ805 generated in this work is missing the C-terminal part containing the PIP1 motif (Figure 4.1 A). *pif1-Δ775* is a larger truncation which also removes the positively charged amino acid stretch between PIP1 and PIP2. Finally, Pif1-Δ750 is missing both the C-terminal PIPs and the Rad53/Dun1-dependent phosphosite.

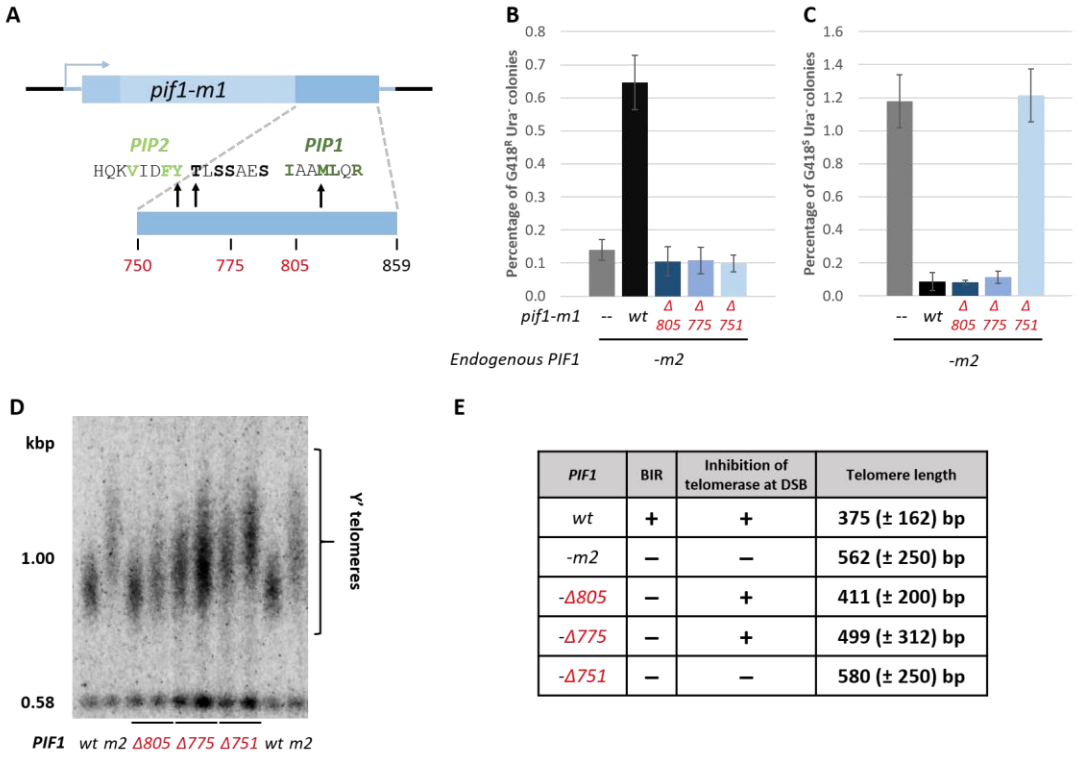

PIF1	BIR	Inhibition of telomerase at DSB	Telomere length
wt	+	+	375 (± 162) bp
-m2	–	–	562 (± 250) bp
-Δ805	–	+	411 (± 200) bp
-Δ775	–	+	499 (± 312) bp
-Δ751	–	–	580 (± 250) bp

Figure 4.1. The C-terminus of Pif1 contains distinct regions required for BIR and telomerase inhibition.

A. Schematic of *pif1-m1*. The shades of blue illustrate the regions that encode the N-terminal, middle and C-terminal parts of Pif1 (not to scale). The blue box at the bottom illustrates the C-terminal part of Pif1 with the position and the amino acid sequence of the reported PIPs (light green for PIP2 and dark green for PIP1) and the Rad53/Dun1-dependent phosphosite (phosphorylatable amino acids in bold) indicated. Black bars below depict the position of the introduced STOP codons to make the C-terminally truncated versions, with the numbers indicating the length of the corresponding proteins in amino acids. **B-C.** The effect of the *pif1-ΔC* mutations on BIR (B) and DNTA (C). Frequency of BIR was estimated as a percentage of $G418^R$ Ura^- colonies on YPGal plates from the total cell titre. Average ± SD (n≥3) is shown for each bar. DNTA was estimated as a percentage of $G418^S$ Ura^- colonies on YPGal plates from the total cell titre. Average ± SD (n≥3) is shown for each bar. Note that most of $G418^S$ Ura^- colonies in *PIF1* strains do not add telomeres to the broken chromosome and the low frequency of G418S Ura^- colonies emerges due to the recombination mediated repair of the lesion (Makovets and Blackburn 2009). **D.** Telomere length analysis in the *pif1-ΔC* strains. **E.** A summary of the data from **B-D.** Strains used: NK3725, NK3726, NK3728, NK3729, NK6351, NK6352, NK6355, NK 6356, NK6359, NK6360, NK7448-NK7450.

Consistent with the previously published data, 0.14% of *pif1-m2* cells produced $G418^R$ Ura^- colonies. (Figure 4.1 B) (Vasianovich, Harrington, and Makovets 2014). Integration of the full length *pif1-m1* allele into *pif1-m2* strain led to the increase in the frequency of BIR to 0.63%, which is less than in the cells with *PIF1* gene (0.89%) (Vasianovich, Harrington, and Makovets 2014). None of the truncated alleles increased the BIR frequency upon integration into *pif1-m2*

cells, suggesting that the C-terminal fragment 805-859 (or its part) is required for the ability of Pif1 to promote BIR, which could be explained by the previously reported requirement for PIP1 motif in Pif1 during BIR (Buzovetsky et al. 2017) (Figure 4.2 B, E).

The frequency of $G418^S$ Ura^- colonies generated on YPGal allows semi-quantitatively address the ability of *pif1* alleles to inhibit telomerase at DSB. Almost 1.2% of *pif1-m2* cells produced $G418^S$ Ura^- colonies on YPGal (Figure 4.1 C), consistent with the high frequency of DNTA in this genetic background (Makovets and Blackburn 2009). Upon introduction of the full length *pif1-m1* allele, the frequency of the $G418^S$ Ura^- colonies decreased to 0.11% and these colonies did not represent the DNTA events anymore (described below in section 4.5), but most likely emerged due to an infrequent homology-mediated repair (Makovets and Blackburn 2009). The *pif1-m2 pif1-m1-Δ805* and *pif1-m2 pif1-m1-Δ775* cells showed frequencies of $G418^S$ Ura^- colonies similar to *pif1-m2 pif1-m1,* which suggests that the truncated isoforms may be competent to inhibit telomerase at the break (Figure 4.1 C, E). In contrast, *pif1-m2 pif1-m1-Δ751* cells produced a frequency of $G418^S$ Ura^- colonies similar to *pif1-m2,* indicating that the fragment of Pif1 C-terminus (751-805) may be completely or partially required for telomerase inhibition at DSBs.

To test the Pif1-ΔC truncations for the ability to inhibit telomerase at telomeres, a telomere length analysis was performed (Figure 4.1 D). As expected, mean telomere length increased in *pif1-m2* cells in comparison to *PIF1* cells (Schulz and Zakian 1994). Introduction of the *pif1-m1-Δ805* and *pif1-m1-Δ775* alleles into *pif1-m2* cells partially suppressed the long telomere phenotype, but to a different degree: the average telomere length in *pif1-m1-Δ805* cells was closer to *PIF1* but the distribution of telomere length was wider. *pif1-m2 pif1-m1-Δ775* cells had an intermediate phenotype and a very wide distribution of telomere length between *PIF1* and *pif1-m2* (Figure 4.1 C, E). This suggests that removing the internal region (775-805) of the C-terminus of Pif1 affects Pif1 functionality at telomeres (the protein levels were not affected, data not shown). Finally, *pif1-m2 pif1-m1-Δ751* cells had similar telomere length to *pif1-m2,* meaning that the C-terminal fragment 751-859 is required for telomerase inhibition at telomeres.

4.3. The C-terminal PCNA interacting motives of Pif1 are required for BIR and telomerase inhibition.

To test if the effect of the C-terminal truncations could be explained by the loss of the interaction between Pif1 and PCNA via the C-terminal PIPs, the *pip1* and *pip2* mutations were introduced into the strains for the BIR/DNTA assay (Figure 4.2 A).

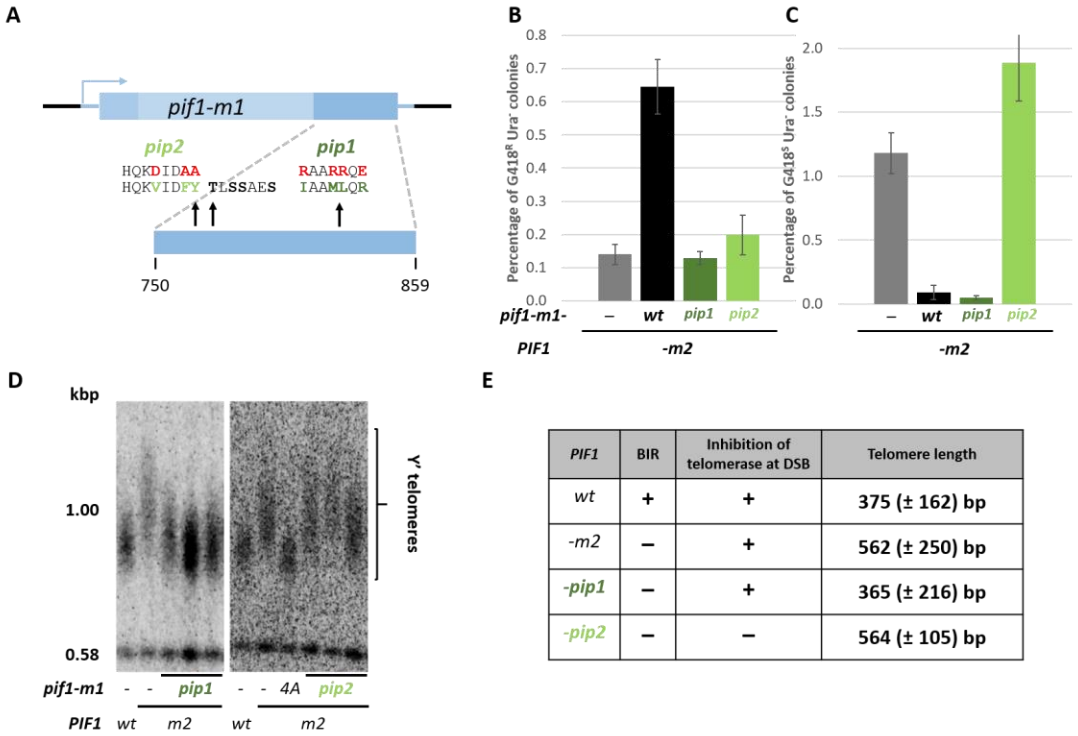

PIF1	BIR	Inhibition of telomerase at DSB	Telomere length
wt	+	+	375 (± 162) bp
-m2	–	+	562 (± 250) bp
-pip1	–	+	365 (± 216) bp
-pip2	–	–	564 (± 105) bp

Figure 4.2. Pif1 requires both PIP1 and PIP2 for its role in BIR and PIP2 only for telomerase inhibition at telomeres and at DSBs.

A. Schematic of *pif1-m1*. The shades of blue illustrate the regions that encode the N-terminal, middle and C-terminal parts of Pif1 (not to scale). The blue box at the bottom represents the C-terminus of Pif1 with the amino acid substitutions in Pif1-pip1 and Pif1-pip2 shown in red above the natural sequence (light green for PIP2 and dark green for PIP1). **B-C.** The effect of the *pif1-pip* mutations on BIR (B) and DNTA (C). Frequency of BIR was estimated as a percentage of $G418^R$ Ura^- colonies on YPGal plates from the total cell titre. Average ± SD (n≥3) is shown for each bar. DNTA was estimated as a percentage of $G418^S$ Ura^- colonies on YPGal plates from the total cell titre. Average ± SD (n≥3) is shown for each bar. **D.** Telomere length analysis in *pif1-pip1* and *pif1-pip2* strains. **E.** A summary of the data from **B-D.** Strains used: NK3725, NK3726, NK3728, NK3729, NK3731, NK7380-NK7383, NK7448-NK7450, NK7458-NK7460.

The frequencies of BIR in *pif1-m2 pif1-m1-pip1* and *pif1-m2 pif1-m1-pip2* cells were similar to *pif1-m2* (Figure 4.2 B, E), suggesting that both PIP1 and PIP2 are required for BIR.

In contrast to BIR, the mutations in the C-terminal PIPs of Pif1 had a different effect on the ability of the helicase to inhibit telomerase at DSB. Integration of the *pif1-m1-pip1* allele into *pif1-m2* cells reduced the frequency of $G418^S$ Ura^- colonies to the *PIF1* levels, whereas *pif1-m2 pif1-m1-pip2* cells had a high

frequency of G418^{S} Ura^{-} colonies, suggesting that PIP2 may be required to prevent DNTA (Figure 4.2 C, E).

pif1-m2 pif1-m1-pip1 cells had normal telomere length, while *pif1-m2 pif1-m1-pip2* cells had long telomeres similarly to *pif1-m2* cells (Figure 4.2 D, E). Thus, in contrast to the requirement for the Rad53/Dun1-dependent phosphorylation of Pif1 that differentiates between telomerase inhibition at telomeres and DSBs, the PIP2 motif is required for telomerase inhibition both at telomeres and at DSBs, which may suggest that the interaction between Pif1 and PCNA via PIP2 occurs under normal conditions, rather than in response to DSBs.

4.4. The N-terminal PCNA interacting motives of Pif1 are required for BIR and telomerase inhibition

To test the requirement in the N-terminal PIP3 and SIM for Pif1 function in BIR and telomerase inhibition, the *pip3* and *sim* mutations were introduced into the strains for BIR/DNTA assay (Figure 4.3 A).

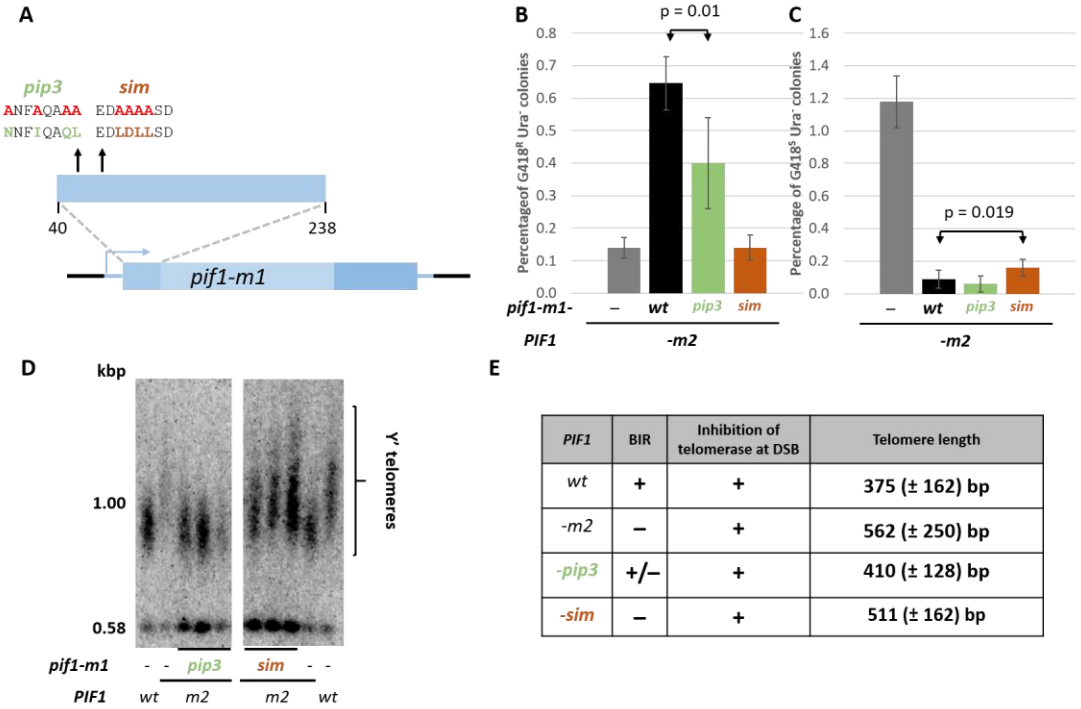

PIF1	BIR	Inhibition of telomerase at DSB	Telomere length
wt	+	+	375 (± 162) bp
-m2	–	+	562 (± 250) bp
-pip3	+/–	+	410 (± 128) bp
-sim	–	+	511 (± 162) bp

Figure 4.3. Pif1 requires both PIP3 and SIM motifs for its role in BIR and SIM only for telomerase inhibition at telomeres and DSBs.

A. Schematic of *pif1-m1*. The shades of blue illustrate the regions that encode the N-terminal, middle and C-terminal parts of Pif1 (not to scale).The blue box at the top represents the N-terminal part of Pif1 with the amino acid substitutions in Pif1-pip3 and Pif1-sim indicated in red above the natural sequence (green for PIP3 and orange for SIM). **B-C.** The effect of the *pif1-pip* mutations on BIR (B) and DNTA (C). Frequency of BIR was estimated as a percentage of $G418^R$ Ura^- colonies on YPGal plates from the total cell titre. Average ± SD (n≥3) is shown for each bar. DNTA was estimated as a percentage of $G418^S$ Ura^- colonies on YPGal plates from the total cell titre. Average ± SD (n≥3) is shown for each bar. p value was calculated with the two-tailed t-test. **D.** Telomere length analysis in *pif1-pip3* and *pif1-sim* strains. **E.** A summary of the data from **B-D.** Strains used: NK3725, NK3726, NK3728, NK3729, NK7448-NK7450, NK7635-NK7640.

pif1-m2 pif1-m1-pip3 cells had a slight but significant (p=0.01) decrease in the frequency of BIR after DSB induction compared to *pif1-m2 pif1-m1* (Figure 4.4 B). In contrast, the *pif1-m1-sim* allele failed to compensate for the BIR defect in *pif1-m2* cells. This suggests that, while both PIP3 and SIM are required for BIR, SIM is more important.

Both *pif1-m1-pip3* and *pif1-m1-sim* significantly reduced the frequency of $G418^S$ Ura^- colonies formed on YPGal in comparison to the *pif1-m2* strains, although the suppression may be incomplete in *pif1-m2 pif1-m1-sim* cells, based

on the higher frequency of G418^S Ura$^-$ colonies compared to the *pif1-m2 pif1-m1* cells (Figure 4.4 C).

The telomere length in *pif1-m2 pif1-m1-pip3* cells was comparable to the telomere length in *PIF1* cells (Figure 4.3 C). However, the *pif1-m2 pif1-m1-sim* cells had long telomeres, which suggests that SIM is important for telomerase inhibition at telomeres. Given that both *pif1-m1-sim* and *pif1-m1-pip2* alleles result in a long telomere phenotype, it is possible that the interaction between Pif1 and SUMOylated PCNA occurs mainly via PIP2 and SIM. This hypothesis is consistent with the different effects that *pip3* and *sim* mutations had on the ability of Pif1 to promote BIR.

4.5. Pif1 function in inhibiting telomerase at DSB requires PCNA interacting motives

To confirm the involvement of the PCNA interacting motifs of Pif1 in inhibition of telomerase activity at DSBs the *MNT2* region was analysed by Southern blotting in the cells from the G418^S Ura$^-$ colonies emerged after break induction in the corresponding strains (Figure 4.4).

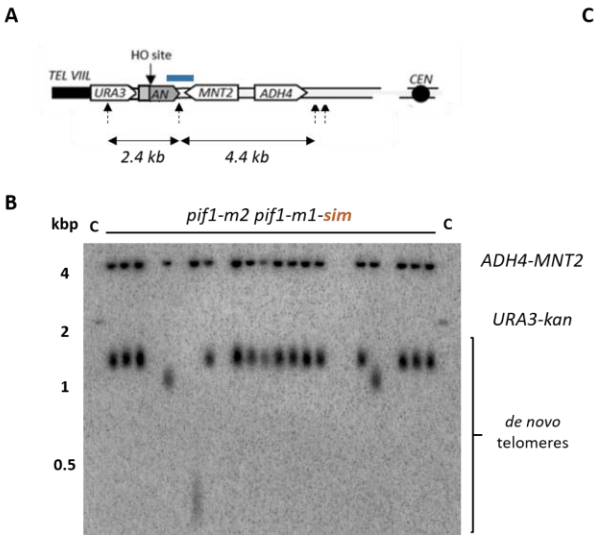

C

Genotype	DNTA	G418^S Ura$^-$ analysed	Frequency
pif1-m2	13	14	0.93
pif1-m2 pif1-m1	0	67	0.00
pif1-m2 pif1-m1-pip1	10	56	0.18
pif1-m2 pif1-m1-pip2	20	25	0.80
pif1-m2 pif1-m1-pip3	2	40	0.05
pif1-m2 pif1-m1-sim	27	27	1.00

Figure 4.4. Most of G418^S Ura$^-$ colonies formed after break induction in the *pif1-m2 pif1-m1-pip2 and pif1-m2 pif1-m1-sim* strains repaired the lesion by DNTA.

A. Schematic of the *MNT2* region in the strains for the BIR/DNTA assay (Vasianovich, Harrington, and Makovets 2014). The dashed arrows indicate positions of the relevant *Eco*RV sites. The blue bar indicates the region homologous to the probe used for Southern blotting.

B. DNTA at *MNT2* locus. DNA isolated from the cells from the G418^S Ura$^-$ colonies formed on YPGal plates was digested with *Eco*RV and used for Southern bloting with the *MNT2* probe. The control samples (C) contain DNA isolated from the cells before break induction and produce two restriction fragments detected with *MNT2* probe – *ADH4-MNT2* and *URA3-kan* (see schematic in A). Smeary bands are formed by the *kan* fragments with the new telomeres added during the repair. **C**. Summary of DNTA analysis in the strains indicated. G418^S Ura$^-$ colonies formed after break induction in at least two different strains analysed for each genotype. Strains used: NK3728, NK3729, NK7448, NK7449, NK7380-NK7383, NK7458-NK7460, NK7635-NK7640.

The conclusion about telomere addition to the break was made if the 2.4 kb *URA3-kan* fragment (present in the control samples with no DSB induction) was replaced with the smeary band of a higher electrophoretic mobility, characteristic of the restriction fragments with heterogeneous telomeric repeats (Figure 4.4 B).

As expected, the majority of *pif1-m2* colonies formed after break induction had restriction pattern characteristic of DNTA, while no such colonies were detected in *PIF1* background (Figure 4.4 C).

Similar to the *pif1-m2* cells, G418^S Ura$^-$ colonies generated by the *pif1-m2 pif1-m1-pip2* and *pif1-m2 pif1-m1-sim* strains were formed after telomere addition to the break (Figure 4.4 B, C). This suggests that the PIP2 and SIM motifs in Pif1 are required for telomerase inhibition at DSBs, although partial DNTA suppression by the *pif1-m1-sim* allele suggests that PIP2 alone may be sufficient in most of the cases. In contrast, DNTA was confirmed in only a small fraction of G418^S Ura$^-$ colonies isolated after plating *pif1-m2 pif1-m1-pip1* and *pif1-m2 pif1-m1-pip3* strains, suggesting that the corresponding PIP motifs are much less involved in this function of Pif1. This points toward the hierarchy of the PIP motifs in Pif1 function at DSB, with PIP2 being the most important while PIP1 and PIP3 playing secondary role.

4.6. Pif1 recruitment to DSB requires PIP2 and SIM

To test the requirements for the PCNA-interacting motifs in Pif1 recruitment to a DSB, *pif1-m1-4myc* alleles with the corresponding mutations were introduced into the strain with an HO-inducible DSB at the *HEM13* locus (Makovets and Blackburn 2009). After the DSB induction, the predominant fraction (about 99%)

of the cells are expected to initiate the resection and permanently arrest due to the DNA damage checkpoint activation.

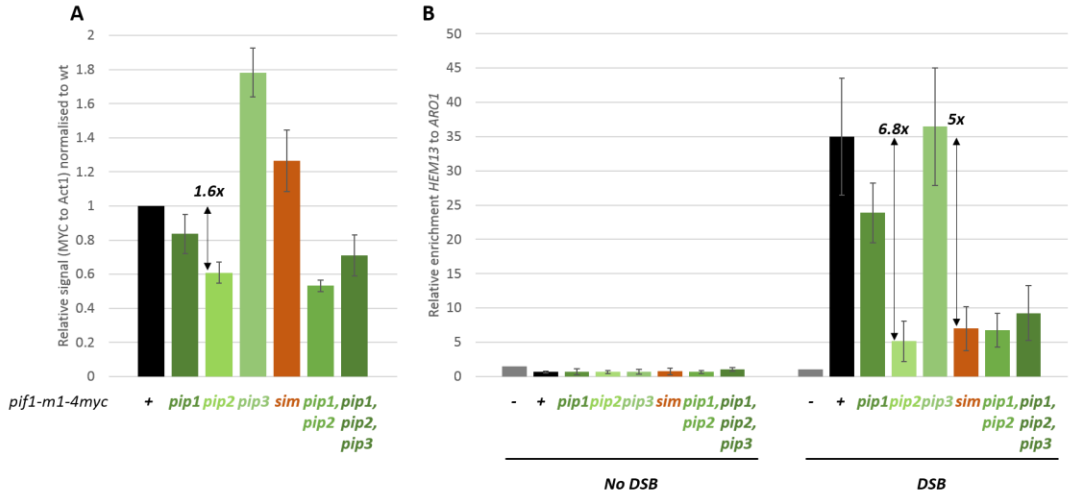

Figure 4.5. Pif1 requires both SIM and PIP2 motifs for the localisation to DSBs.

A. Relative protein levels (steady-state) with the mutations indicated. Protein levels were measured in logarithmically growing cultures relative to Act1 and the wt equivalent (Pif1-m1-4myc). Western blotting was done using α-myc (9E10) and αi-Act1 antibodies and Odyssey® Fc Imaging System (Li-Cor®) as described in section 2.10.3. **B.** Localisation of Pif1-m1-4myc with the indicated mutations to the DSB induced at *HEM13*. Cultures were grown to the mid-log phase in YPRaf (no DSB). DSB was induced by adding galactose to the log-phase cultures for three hours prior to harvesting aliquots for the cross-linking. Normalisation was made to the signal from the reference locus (*ARO1*), not affected by the DSB (described in 2.9.3). Strains used: NK7462-NK7464, NK7468-NK7470, NK7477-7479, NK7647-NK7652, NK7894-NK7896.

Prior to testing the localisation to DSBs, relative protein levels of Pif1-m1-4myc were compared between the strains constructed (Figure 4.5 A). Mutations in the C-terminal PIP motifs reduced the relative protein levels compared to the wild type equivalent to a different degree (16% decline in Pif1-pip1-4myc and 39% in Pif1-pip2-4myc). Combination of *pip1* and *pip2* mutations in one gene had a mild additive effect on the reduction of the protein levels compared to *pip2* single mutation. In contrast, mutations in PIP3 and SIM led to the increased protein levels (78% and 27% respectively) in comparison to the wild type equivalent. The combination of the *pip1*, *pip2* and *pip3* mutations resulted in a moderate increase of the protein levels in comparison with Pif1-pip1,pip2-4myc, but Pif1-pip1,pip2,pip3-4myc protein was less abundant than the wild type equivalent. Based on the published data, Pif1 levels are regulated in a cell-cycle-dependent manner (Vega et al. 2007), therefore it is possible that the mutations in the PCNA-interacting motives may affect either the turnover of the protein or the cell cycle

distribution in the populations. However it is also possible that some of the mutations interfere with the protein folding or lead to the aggregation, the effect observed earlier for the recombinant Pif1 protein (Buzovetsky et al. 2017).

As expected, Pif1-m1-4myc was enriched at *HEM13* relative to the reference locus (*ARO1)* at 3 hours after the break induction (Figure 4.5 B) (Makovets and Blackburn 2009). Pif1-pip1-4myc had a mild reduction in the localisation to DSB consistent with the small numbers of the DNTA events detected in the strains with *pif1-m1-pip1* (Figure 4.4 C), however this mild phenotype could also be explained by the slightly lower protein levels compared to the wild type equivalent (Figure 4.5 A). Pif1-pip2-4myc had a substantial defect in the recruitment to the DSB (6.8x, Figure 4.5 B), much bigger than the effect of the *pip2* mutation on the relative Pif1 protein level (1.6x, Figure 4.5 A). The relative enrichment of Pif1-pip1,pip2-4myc at *HEM13* was comparable to Pif1-pip2-4myc suggesting that PIP1 is not essential for the recruitment of Pif1 to DSBs.

The relative enrichment of Pif1-pip3-4myc at *HEM13* was similar to the wild type equivalent, despite the 80% increase in the protein levels of the mutated isoform (Figure 4.5 A, B). This suggested that the localisation of the Pif1-pip3-4myc may occur with a lower efficiency than the wild type equivalent, however Pif1-pip1,pip2,pip3-4myc did not have an additional defect in the localisation compared to Pif1-pip2-4myc. In contrast, *pif1-sim* cells showed a substantial defect in Pif1 recruitment close to the one observed in *pif1-pip2* cells, suggesting that SIM is also required for the localisation to DSBs.

4.7. Discussion

The experiments presented in this chapter were aimed to address the requirements for the C-terminus of Pif1 and the PCNA-interacting motifs in BIR, telomerase inhibition at telomeres and DSBs, and for Pif1 recruitment to DSBs.

The strains expressing the C-terminally truncated Pif1 isoforms were constructed to test the requirements for the C-terminus of Pif1 (Figure 4.1 A). The analysis has shown that the C-terminal fragment 805-859 was required for BIR (Figure 4.1 B), consistent with the previously reported requirement for PIP1

(Buzovetsky et al. 2017). However, the C-terminal fragment 805-859 was not essential for telomerase inhibition at DSBs and the cells expressing Pif1-Δ805 had only slightly longer telomeres than the *PIF1* cells (Figure 4.1 C, D). In contrast, the C-terminal fragment 751-805 was required for telomerase inhibition both at telomeres and DSBs (Figure 4.1 C, D). Thus, the C-terminal sequence of Pif1 is required for the Pif1-specific functions in BIR and telomerase inhibition both at telomeres and DSBs.

Next, the requirements for PCNA-interacting motifs in Pif1 were tested for BIR, telomerase inhibition at telomeres and DSBs and Pif1 recruitment to DSBs (summarised in Table 6).

Table 6. Summary of the genetic requirements for the PCNA-interacting motifs and the Rad53/Dun1-regulated phosphosite TLSSAES in Pif1 for BIR, telomerase inhibition at telomeres and DSBs and Pif1 recruitment to DSBs.

	PIF1	***pif1-m2***	***pif1-pip1***	***pif1-pip2***	***pif1-pip3***	***pif1-sim***	***pif1-4A****
BIR	+	-	-	-	+/--	-	-
Telomerase inhibition at telomeres	+	-	+	-	+	-	+
Telomerase inhibition at DSBs	+	-	+/-	-	+/-	+/--	-
Recruitment to DSBs	+	-	+/-	+/--	+	+/--	+

*Note: The requirements for the TLSSAES phosphorylation have been published previously (Makovets and Blackburn 2009; Vasianovich, Harrington, and Makovets 2014) Table legend: "+" - proficient, "-" – deficient, "+/- " – mild partial defect, "+/--" – severe partial defect.

In contrast to the replication associated function of Pif1, telomerase inhibition at telomeres and at DSBs required PIP2 and SIM motifs and relied much less on the PIP1 and PIP3 motifs (Table 6).

Pif1 recruitment to DSBs required PIP2 and SIM motifs, which could explain the defect in inhibiting telomerase at the breaks. However, the recruitment of Pif1-m1 was not completely abolished by *pip2* or *sim* mutations. Consistent with this,

pif1-m1-sim allele partially supressed the high DNTA in *pif1-m2* cells (Figure 4.3 C; Figure 4.4 B, C), but *pif1-m1-pip2* did not show any suppression (Figure 4.2 C) indicating that, in addition to the localisation defect, Pif1-m1-pip2 may be catalytically less active. Small frequency of DNTA detected in *pif1-m1-pip1* and *pif1-m1-pip3* cell may be explained either by the mild localisation defect not detected by CHIP-qPCR (Figure 4.5 B) or compromised catalytic activity of the corresponding Pif1 variants. Overall, this experiment suggests that Pif1 recruitment to DSBs is PCNA-dependent, similarly to the recruitment to stalled forks.

Based on the previously published data, Rad53/Dun1-dependent phosphorylation of the TLSSAES motif in the C-terminus of Pif1 is required for inhibiting telomerase at DSBs, but is not required for Pif1 localisation to the breaks (Makovets and Blackburn 2009) (Table 6). This suggests that despite the close location of the phosphosite to the PIP2 motif (Figure 4.2 A), the Rad53/Dun1-dependent phosphorylation is not required for the interaction between Pif1 and PCNA via PIP2. However, it is possible that the phosphorylation is required for disrupting the interaction between Pif1 and PCNA via PIP2 motif, which could be required to vacate the site on PCNA for another factor involved in telomerase inhibition, or to switch the PIP motif in Pif1 used for interacting with PCNA. Thus, addressing the effect of Rad53/Dun1-dependent phosphorylation on the interaction between Pif1 and PCNA may be important for understanding the molecular mechanism of damage-dependent regulation of Pif1 at DSBs.

Rrm3 has a C-terminally located PIP motif (PIP2, Figure 3.1 C), which is homologous to the PIP2 motif in Pif1. It could be interesting to test if the chimeric gene encoding Rrm3 helicase with the additional N- and C-terminal sequences from Pif1, containing SIM and TLSSAES motifs respectively, could suppress the telomerase inhibition defect in *pif1-m2* cells. This could potentially provide the experimental evidences supporting the hypothesis that the functional specialisation between the Pif1 family helicases in the budding yeast is imposed by the unique C- and N-terminal sequences.

The experiments presented in this chapter show that BIR requires PIP3, PIP2 and SIM motifs in addition to the previously reported requirements for the

Rad53/Dun1-dependent phosphorylation (Vasianovich, Harrington, and Makovets 2014) and the PIP1 motif (Buzovetsky et al. 2017). This may be explained by the complexity of BIR, which could involve Pif1 recruitment to the resected DSB prior to the invasion and to the displaced strand of the donor chromosome after D-loop formation (discussed in more details in Chapter VI).

As described in section 1.2.2, Pif1 role during BIR could be underestimated. The next chapter considers the involvement of Pif1 and its Rad53/Dun1-dependent phosphorylation in other aspects of BIR, such as the D-loop formation, initiation of the DNA synthesis and DNA re-synthesis of the resected recipient strand.

Chapter V. The requirements for Pif1 during BIR

5.1. Introduction.

As described in section 1.2.2, Pif1 is required for BIR. The major advances in understanding the molecular role of Pif1 during BIR have been reported in the recent publications (Saini et al. 2013; Wilson et al. 2013; Vasianovich, Harrington, and Makovets 2014; Buzovetsky et al. 2017; Chung et al. 2010). It has been shown that the *pif1-m2* cells have lower frequency of BIR than the *PIF1* cells (Chung et al. 2010). Although the D-loops are formed in these cells, the DNA synthesis during BIR occurs with lower processivity and often leads to the formation of half-crossovers and loss of the donor chromosome (Wilson et al. 2013). Pif1 localises to the sites of BIR-associated DNA synthesis (Wilson et al. 2013). Pif1 has been shown to promote Pol δ-dependent DNA synthesis *in vitro*, and the recruitment of Pol δ to the BIR sites is decreased in *pif1-m2* cells *in vivo* (Wilson et al. 2013). The physical interaction between Pif1 and PCNA was reported *in vivo* (Buzovetsky et al. 2017; Dahan et al. 2018) and the PCNA-interacting motifs in the C- and N-termini of Pif1 are required for BIR (Table 6).

The generally accepted view postulates that Pif1 is required for promoting Pol δ-dependent DNA synthesis during BIR, however the involvement of Pif1 into the other stages of this repair pathway has not been conclusively addressed. In order to address this general question, I tested if Pif1 was involved in the three specific stages of BIR: a) break processing and invasion into the donor chromosome; b) initiation of DNA synthesis; c) long-range DNA synthesis and re-synthesis of the resected strand. The experiments addressing the requirements of Pif1 in each of these stages are described in this chapter.

The genetic system used to test the effect of Pif1 on the dynamics of DNA synthesis and re-synthesis during BIR, has been previously developed in the Makovets lab (Vasianovich et al. 2017). Briefly, HO nuclease expressed from the conditional *GAL1* promotor introduces a single DSB in the subtelomeric region of chromosome VII, between the *URA3* marker and an extensive sequence (6,272 bp) homologous to chromosome II (Figure 5.1 A, part 1). After the resection machinery exposes the homology, the latter can be used to form a D-loop and

trigger the conservative DNA synthesis passing through the 94 kb long arm of chromosome II, thereby duplicating it to chromosome VII (Figure 5.1 A, parts 2 and 3). The frequency of repair is estimated as a fraction of Ura^- colonies formed on YPGal plates to the total cell titre (colonies on YPD) and constitutes about 57% in *PIF1* cells (Figure 5.1 B). This frequency is dramatically decreased in *pif1-m2*, *pol32Δ* and *rad51Δ* cells suggesting that most of the repair events are BIR. As expected, *pol32Δ* and *rad51Δ* mutations were epistatic with *pif1-m2* suggesting that Pif1 is only required for BIR associated repair of this lesion.

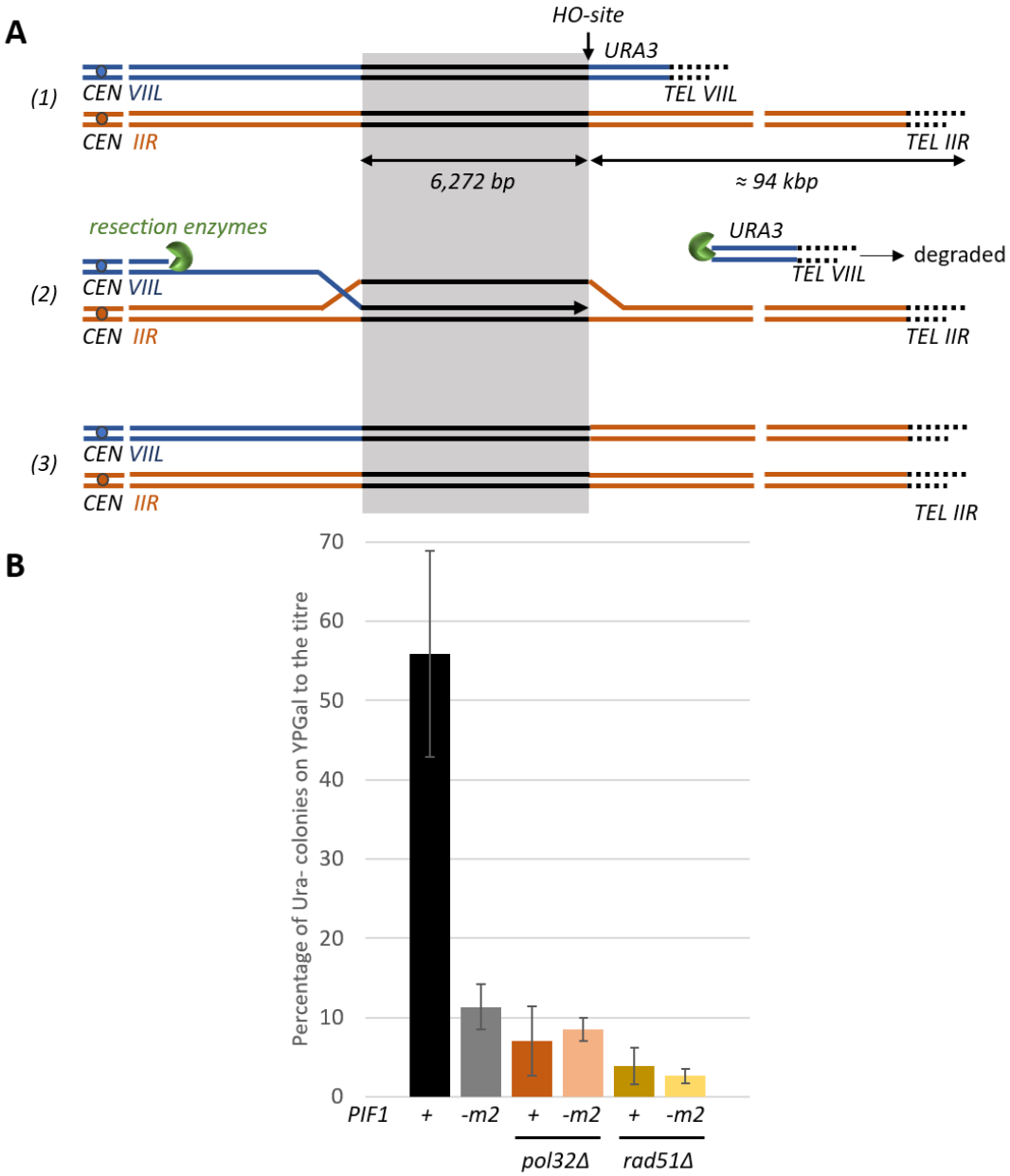

Figure 5.1. The experimental system for analysing the repair dynamics during BIR.

A. Schematic of the break induction (1), D-loop formation (2) and repair product generated as a result of BIR (3). Blue lines indicate the recipient chromosome, orange – the donor chromosome. Grey box shows the location of the homology between the two chromosomes. **B.** The frequency of BIR in the strains with the indicated mutations. Frequency of BIR was estimated as a percentage of Ura$^-$ colonies formed on YPGal plates relative to the plating titre (colonies on YPD plates). Average ± SD (n≥3) is shown for each bar. Strains used: NK4070, NK4072, NK4079, NK4080, NK6025-NK6028, NK6974-6979.

5.2. Pif1 is required for DNA synthesis during BIR and completion of the repair.

High frequency of BIR in the experimental system described above (Figure 5.1) allows to study the dynamics of repair using Southern blotting (Vasianovich et al. 2017). DSBs were induced in the cells synchronised in G1 by alpha-factor and released into S/G2 to allow resection and BIR to occur. Samples were collected every 2 h for subsequent analysis of DNA synthesis and reconstitution of the resected 5'-strand of the recipient chromosome (DNA re-synthesis) (Figure 5.2 A, B). The following sets of probes were used to detect the DNA fragments on the donor (BIR6, BIR36 and BIR77), recipient (RS2.6, RS6.8 and RS15.2) and the reference (*ARS522*) chromosomes (Figure 5.2 A, C). Considering that 57% of *PIF1* cells repair the lesion (Figure 5.1), the expected amount of the signal from the probes against the donor chromosome should increase up to 1.57 of the reference locus signal as the cells duplicate the donor chromosome arm. The signal from the recipient chromosome probes is expected to decrease as the DNA at the break is resected and the restriction sites become resistant to the endonuclease treatment. In later timepoints, the signal from the recipient chromosome probes is expected to re-appear when the DNA re-synthesis occurs recovering to 0.57 of the initial signal before the break induction.

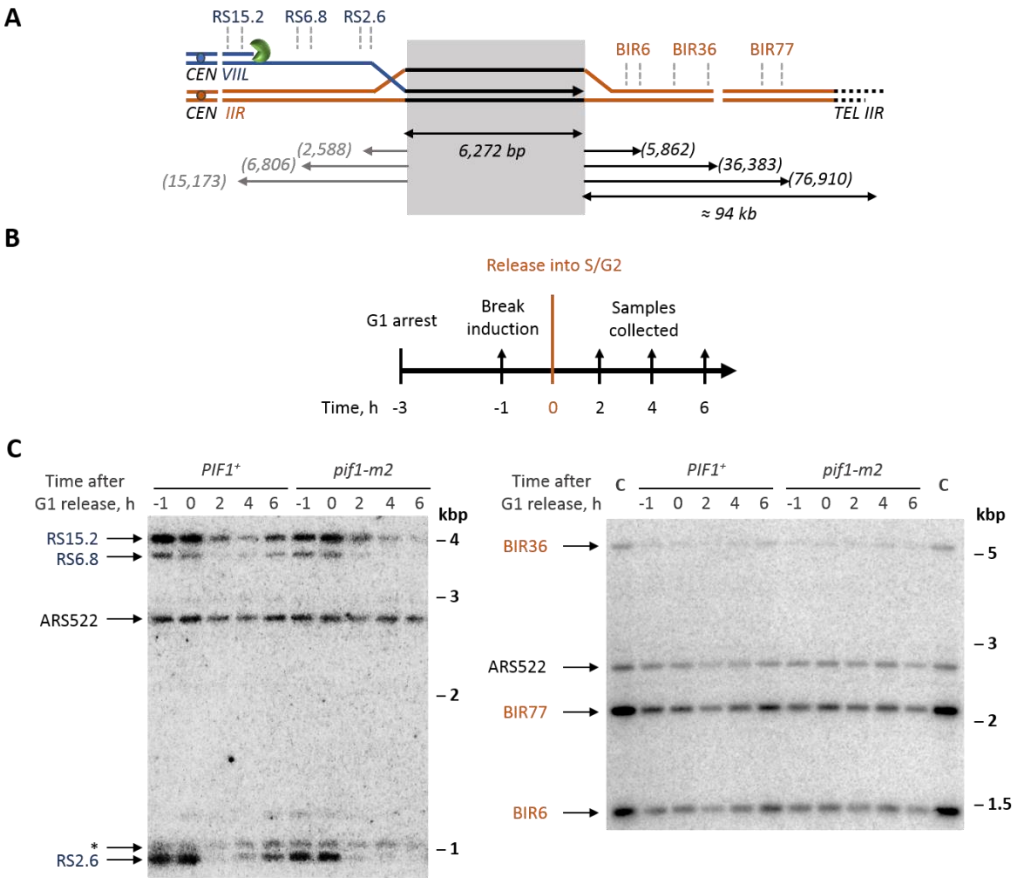
A
RS15.2
RS6.8
RS2.6
CEN VIIL
CEN IIR
BIR6
BIR36
BIR77
TEL IIR
6,272 bp
(2,588)
(6,806)
(15,173)
(5,862)
(36,383)
(76,910)
≈ 94 kb
B
Release into S/G2
G1 arrest
Break induction
Samples collected
Time, h -3 -1 0 2 4 6
C
Time after G1 release, h
PIF1+
pif1-m2
-1 0 2 4 6 -1 0 2 4 6
kbp
RS15.2
RS6.8
ARS522
*
RS2.6
4
3
2
1
C
BIR36
ARS522
BIR77
BIR6
5
3
2
1.5

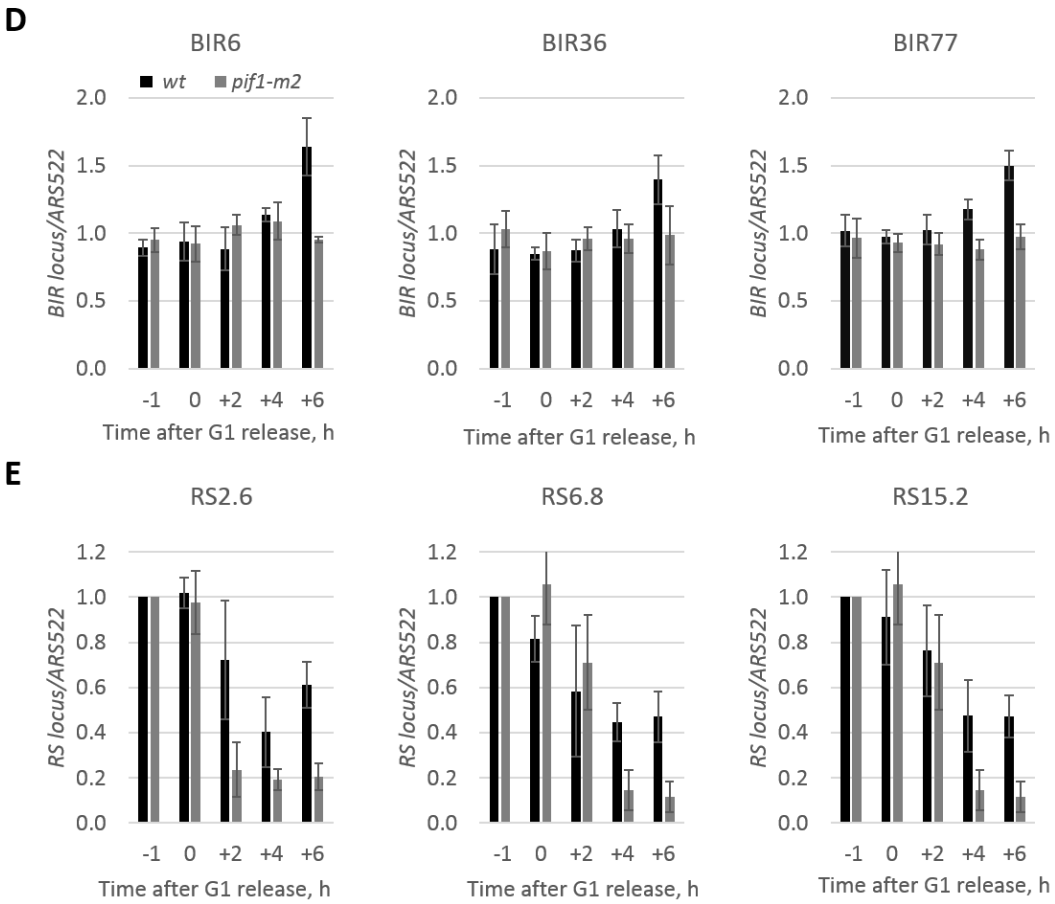

Figure 5.2. Pif1 is required for DNA synthesis and DNA re-synthesis during BIR.

A. Schematic of the assay allowing to monitor DNA synthesis and re-synthesis during BIR. Labels on the top indicate the position and name of the probes against the donor chromosome loci (orange) and the recipient chromosome loci (blue). Grey dashed lines illustrate the position of the relevant restriction sites (*Eco*RI and *Bam*HI). Numbers at the bottom show the length of the homology and the distances between the homology and the fragments analysed by Southern blotting. **B.** Schematic illustrating the timecourse of cells synchronisation, break induction and the samples harvested for Southern blotting. **C.** Southern blot analysis of DNA re-synthesis (on the left) and BIR-dependent DNA synthesis (on the right). The arrows refer to the corresponding fragments from panel **A**, ARS522 is the reference locus on chromosome V, not involved in the repair. The asterisk indicates a fragment detected by the alternative reference probe, which was excluded from the analysis due to the poor signal. The representative images show one of the three biological repeats analysed. **D.** Quantitative analysis of BIR-dependent DNA synthesis. *PIF1* strains plotted in black and *pif1-m2* ─ in grey. Average from the three biological repeats in at least two experimental repeats ± SD is shown for each bar. **E.** Quantitative analysis of DNA re-synthesis. *PIF1* strains plotted in black and *pif1-m2* ─ in grey. Average from the three biological repeats in at least two experimental repeats ± SD is shown for each bar. Strains used: NK4070, NK4072, NK4079, NK4080.

Consistent with the published data (Donnianni and Symington 2013; Malkova et al. 2005), the relative amount of donor DNA signal in *PIF1* cells remained close to 1 within the first 2 h after the release into S/G2 and only slight increase was observed at 4 h, indicating the late initiation of DNA synthesis during BIR. By the 6 h time-point the relative signal from all donor chromosome probes reached 1.5, suggesting that the majority of cells expected to repair have finished duplication of donor chromosome arm up to 77 kb from the beginning of homology. In contrast, *pif1-m2* cells did not have any detectable increase in the signal from the donor chromosome probes within the time analysed, suggesting that they have a defect in the long-range DNA synthesis during BIR and that Pif1 is required during D-loop migration through the first 6 kb of the donor chromosome sequence.

The signal from the recipient chromosome probes decreased throughout the first 4 h after the release into S/G2 in *PIF1* cells and recovered at around 0.5 by the end of the timecourse. Noticeably, there was an increase in the relative signal from RS2.6 between the timepoints 4 h and 6 h, and it was much less pronounced for RS6.8 and RS15.2. One possible explanation to this could be that the peak of resection occurred between the timepoints 4 h and 6 h and was not detected in this experiment. Alternatively, most of the repairing cells have initiated DNA re-synthesis earlier than 4 h and resection was stopped before reaching the RS6.8 fragment.

The *pif1-m2* cells had faster rates of the decrease in signal from the recipient chromosome probes consistent with the absence of BIR DNA synthesis. The signals from the probes RS6.8 and RS15.2 decreased to below 20% by 4 h which is consistent with a small fraction of BIR-independent survivors detected after plating on YPGal (Figure 5.1 B).

The most logical interpretation of the observed correlation between the defects in DNA synthesis and DNA re-synthesis during BIR in *pif1-m2* cells is that DNA re-synthesis during BIR is coupled with DNA synthesis. Perhaps, the priming of the new 5'-strand occurs at the migrating D-loop during certain stage of the long-range DNA synthesis. In *pif1-m2* cells the long-range DNA synthesis is compromised and therefore the priming event may not occur.

Alternatively, DNA synthesis and DNA re-synthesis steps of BIR could be independent processes. In this scenario, the interpretation of the observed data could be that Pif1 is required for DNA re-synthesis, however this question should be addressed in a simpler system, such as the one based on the DSB repair via the single strand annealing (Vasianovich et al. 2017).

5.3. Pif1 is not required for the recipient strand invasion

The invasion of the broken chromosome end into the homologous sequence of the donor chromosome is a critical step during BIR. Pif1 could use its reported strand re-annealing activity (Ramanagoudr-Bhojappa et al. 2013) to promote D-loop formation and therefore be required for the invasion.

To test if Pif1 is required for the invasion, *pol32Δ* derivatives of *PIF1* and *pif1-m2* strains with the genetic construct described in section 5.1 were created. *pol32Δ* cells have a substantial defect in DNA synthesis during BIR (Figure 5.1 B), and therefore BIR is expected to pause at the stage of D-loop formation. Rad51 ChIP-qPCR at the region of chromosome II adjacent to, but not part of the homology (Figure 5.3 A), was performed after the break induction (Figure 5.3 B, C). The relative enrichment of Rad51 next to the homology should be proportional to the frequency of the D-loops formed in the cell populations. *rad51Δ* strains and the strains lacking the homology were used as negative controls in this experiment. The *PIF1* strains showed a clear enrichment of Rad51 at the invasion site. Similarly, *pif1-m2* strains had the Rad51 signal at the invasion site and it was comparable to the enrichment observed in *PIF1* cells, suggesting that the lack of Pif1 does not affect the formation or the stability of the D-loops.

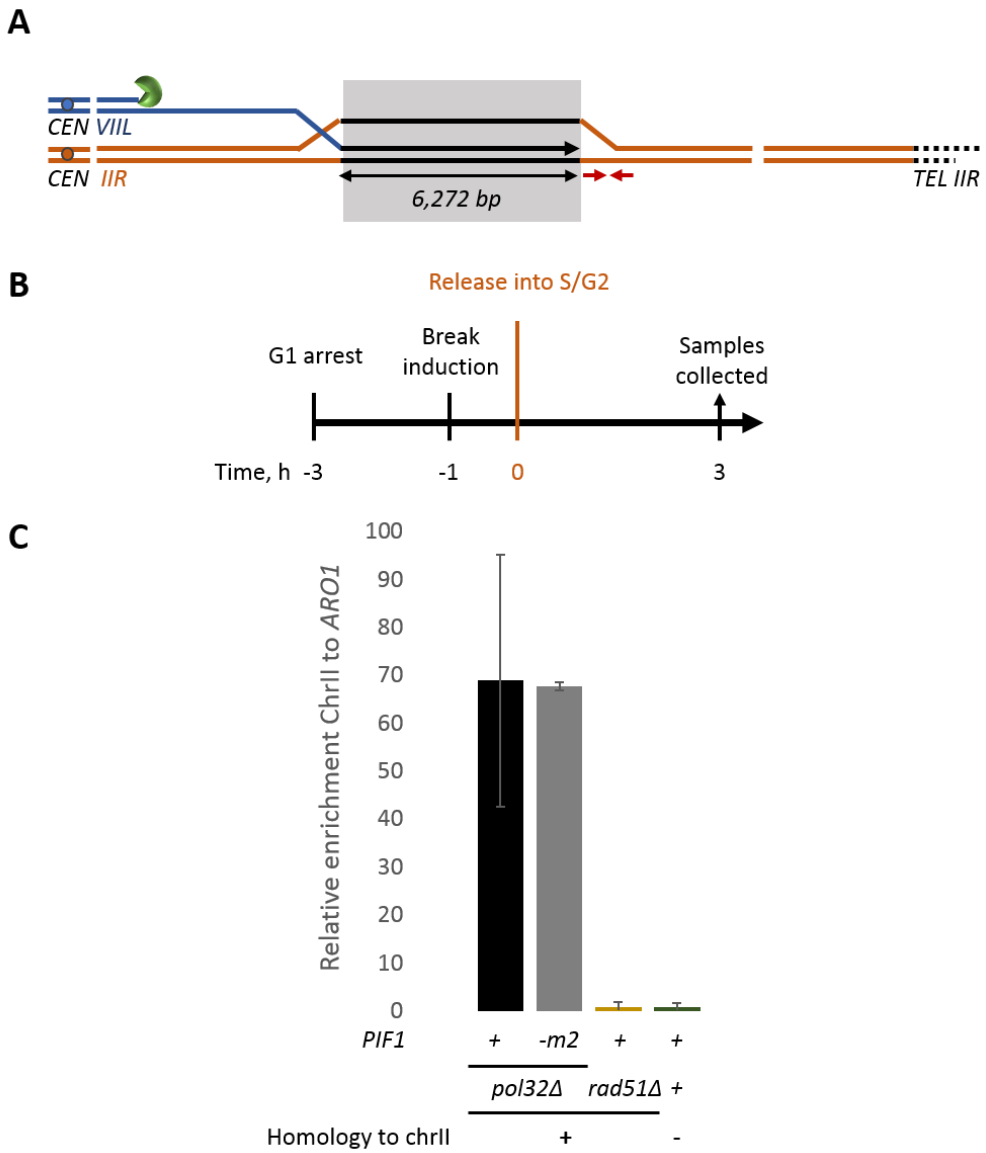

Figure 5.3. Pif1 is not required for the invasion of the broken chromosome end into the donor chromosome.

A. Schematic of the D-loop formed after the break induction and strand invasion using 6.2 kb homology. The red arrows indicate the qPCR oligos to test the enrichment of Rad51 at the invasion site (ChIP qPCR). **B.** Schematic illustrating the experimental timeline including cell-cycle synchronisation, break induction and samples taken for ChIP. **C.** Relative enrichment of Rad51 at the invasion site normalised to *ARO1* reference locus in the strains with indicated genotypes. Strains used: NK4232, NK6025, NK6974-NK6979.

5.4. Initiation of DNA synthesis during BIR occurs independently of Pif1.

The experiments described in the previous sections allowed to conclude that Pif1 is not required for the recipient chromosome invasion but is required for the DNA synthesis of the first 6 kb of the donor DNA from homology. One of the possible explanations for this could be that Pif1 is required for initiation of DNA synthesis during BIR.

To address this question, I used the cells with a similar genetic construct to the one described in section 2.8, with the HO-inducible DSB on chromosome VII and 500 bp homology between the chromosomes VII and XIV (the regions of chromosomes VII and XIV chosen for introducing the homology are expected to replicate late in S phase), which can be used for BIR. Short homology between the donor and recipient chromosomes allowed to perform qPCR with a pair of oligos where one was complementary to the unique recipient chromosome sequence adjacent to the homology and the other one – to the unique donor chromosome sequence adjacent to the homology (Figure 5.4 A). The PCR product can only be formed after the recipient chromosome gains the donor chromosome sequence homologous to the reverse oligo (the crossover template), which is expected during BIR DNA synthesis. Thus, this analysis allows to detect the initiation of BIR DNA synthesis.

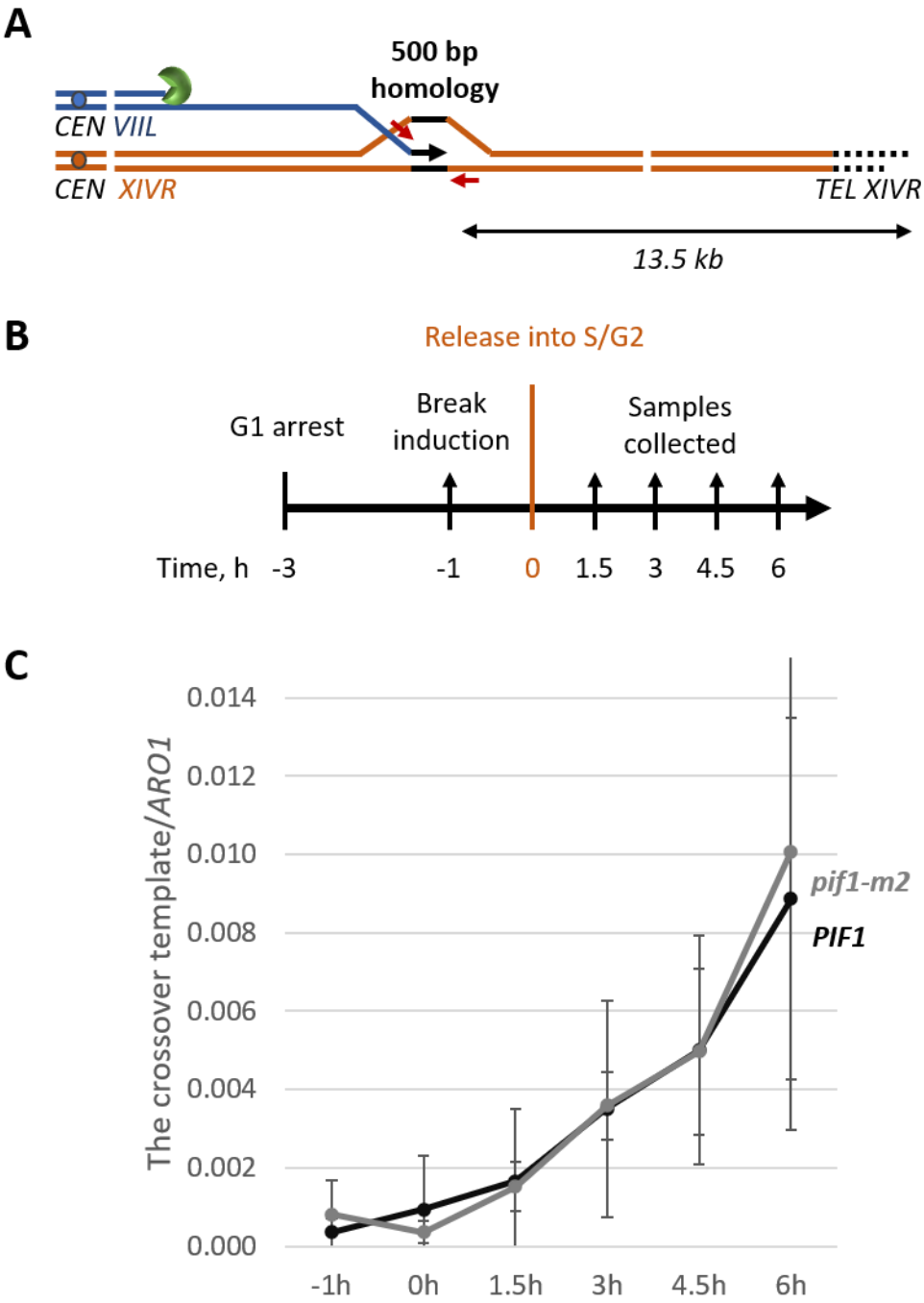

Figure 5.4. Pif1 is not required for the initiation of DNA synthesis during BIR.

A. Schematic of the D-loop formed after break induction and invasion using 500 bp homology. The red arrows indicate the oligos used to detect the initiation of DNA synthesis. **B.** Schematic illustrating the experimental timeline including cell-cycle synchronisation, break induction and the samples harvested for qPCRs. **C.** BIR DNA synthesis initiation. The chart shows relative amount of the extended recipient chromosome (initiated DNA synthesis) normalised to the reference locus (*ARO1*). The error bars represent the standard deviation from at least three repeats. Strains used: NK4626-NK4629.

The cultures were arrested in G1 for synchronous break induction and subsequently released into S/G2 to allow DNA resection and BIR to occur (Figure 5.4 B). Samples were taken every 1.5 h after the release. The relative amount of the crossover template (normalised to the late replicating reference locus *ARO1*) increased in *PIF1* cells throughout the timecourse starting from the 3 h time-point and peaking at about 0.01 at 6 h, consistent with the expected frequency of BIR in this genetic background (1.3%, unpublished data from the Makovets lab). The *pif1-m2* cells have shown a similar pattern of the crossover template generation, suggesting that the initiation of DNA synthesis occurs independently of Pif1, although these strains have a substantial defect in BIR (0.17% repair via BIR, unpublished data from the Makovets lab). The wide variability of the data obtained in different repeats of this experiment, however, makes impossible to detect any small differences in the dynamics of the recipient chromosome extension. Therefore, it cannot be excluded that *pif1-m2* cells have slower dynamics of the initiation of DNA synthesis.

5.5. Rad53/Dun1-dependent phosphorylation of Pif1 is required for DNA synthesis during BIR.

Rad53/Dun1-dependent phosphorylation of Pif1 is required for BIR (Vasianovich, Harrington, and Makovets 2014). To understand if this phosphorylation is required for promoting the long-range DNA synthesis, strains with a non-phosphorylatable *pif1-m1-4A* allele integrated into *pif1-m2* locus were generated. Since the strains have two *pif1* alleles, the internal positive control in this experiment were *pif1-m2 pif1-m1* strains. The experimental conditions and the timepoints were the same as in Figure 5.2 B.

The data for the *PIF1* and *pif1-m2* strains are described in the section 5.2 and presented in the Figure 5.5 for the comparison. The *pif1-m2 pif1-m1* cells repaired the DSB with a similar frequency to the *PIF1* strain, indicating that *pif1-m1* allele supressed BIR deficiency of the *pif1-m2* cells (Figure 5.5 A). In contrast, *pif1-m2 pif1-m1-4A* cells behaved similar to *pif1-m2* suggesting that the Rad53/Dun1-dependent phosphorylation of Pif1 is required for BIR in this genetic

assay, which was expected from the previously published data (Vasianovich, Harrington, and Makovets 2014).

The BIR-associated DNA synthesis in *pif1-m2 pif1-m1* cells was overall similar to *PIF1* (Figure 5.5 B). Consistent with the defect in the DSB repair, *pif1-m2 pif1-m1-4A* cells did not show a detectable BIR-associated DNA synthesis.

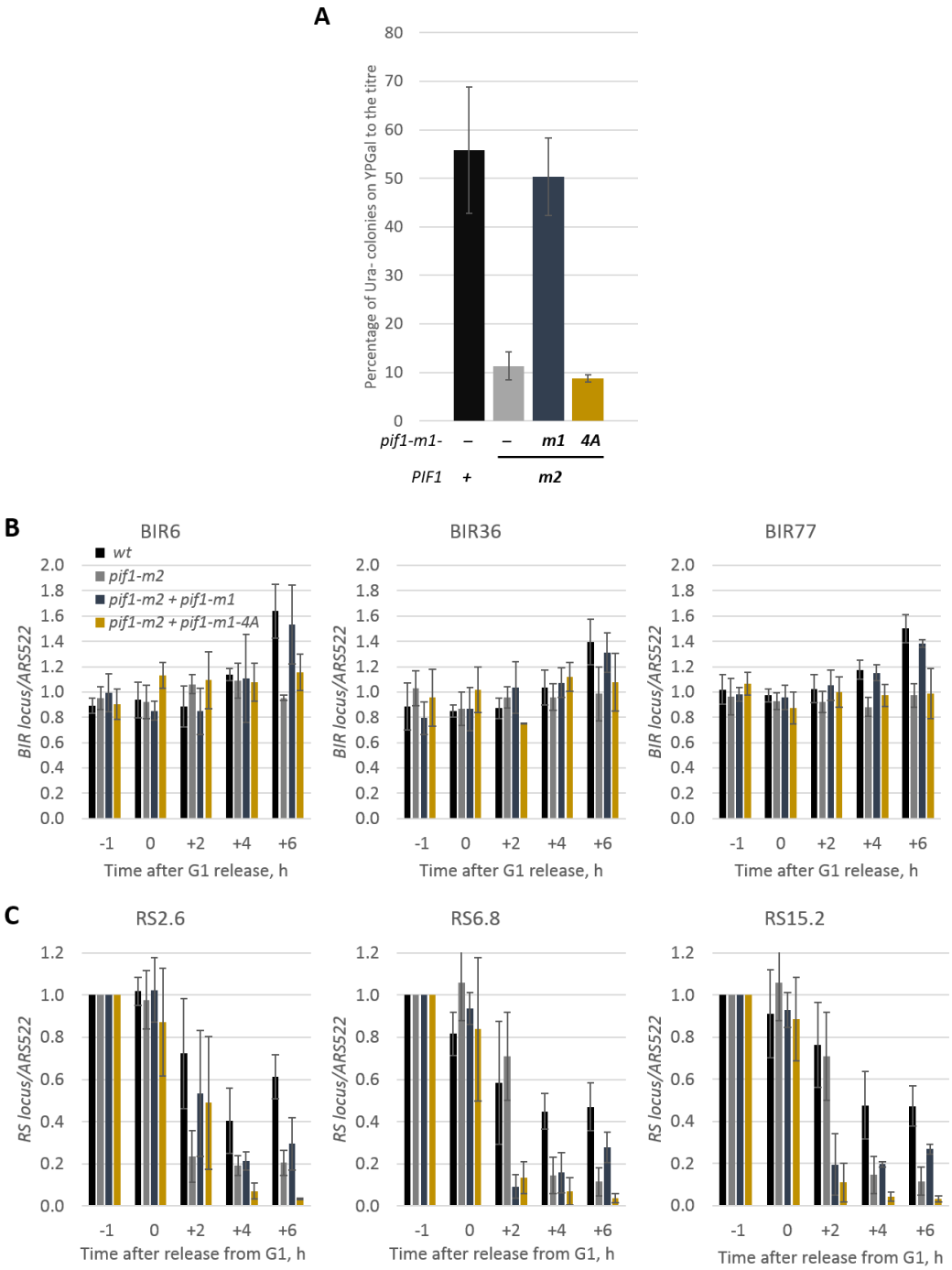

Figure 5.5. The Rad53/Dun1-dependent phosphorylation of Pif1 is required for DNA synthesis and DNA re-synthesis during BIR.

A. The frequency of BIR in the strains with the indicated mutations. Frequency of BIR was estimated as a percentage of Ura$^-$ colonies formed on YPGal plates relative to the plating titre (colonies on YPD plates). Average ± SD (n≥3) is shown for each bar. **B.** Quantitative analysis of BIR-dependent DNA synthesis. Average from the three biological repeats in at least two experimental repeats ± SD is shown for each bar. **C.** Quantitative analysis of DNA re-synthesis. Average from the three biological repeats in at least two experimental repeats ± SD is shown for each bar. Strains used: NK4070, NK4072, NK4079, NK4080, NK5474-NK5481.

The signal from the recipient chromosome declined until the 4 h timepoint in *pif1-m2 pif1-m1* cells indicating the loss of dsDNA due to DNA resection. Surprisingly, the signal from RS15.2 declined to 20% by the 2 h timepoint in *pif1-m2 pif1-m1* cells, which is faster than the experimentally determined average speed of resection (4 kb/hour) (Zhu et al. 2008). The signal from RS probes have recovered to about 0.3 of the initial amount before break induction by the last timepoint, which suggests that the repair is not finished by the end of a timecourse as the fraction of the cells that finish DNA repair appears underestimated (Figure 5.5 A). Differences in the signal from the RS probes after the release from the G1-arrest in *pif1-m2 pif1-m1* cells relative to the *PIF1* cells suggest that the initiation of the DNA re-synthesis in the former may be delayed, which is another indication of the slower DNA repair kinetics in these cells. This phenomenon could be a consequence of a mild overexpression of the nuclear Pif1 when expressed from *pif1-m1* gene (as 100% of the produced protein is imported into the nucleus in comparison to the *PIF1* gene that produces a mixture of the nuclear and mitochondrial Pif1) which could have some negative implications on the kinetics of the repair. In support of this, Pif1 overexpression from the *GAL1* promotor is toxic and leads to the accumulation of RPA and Mre11 foci in the logarithmically growing cells (Chang et al. 2009)

Consistent with the lack of the BIR-associated DNA synthesis*, pif1-m2 pif1-m1-4A* cells showed a greater decline in the signal from the RS fragments compared to the corresponding control strain (*pif1-m2 pif1-m1*). Additionally, no recovery was detected at the later timepoints in the *pif1-m2 pif1-m1-4A* strains indicating the defect in DNA re-synthesis in these strains.

5.6. Discussion.

The experiments described in this chapter were aimed to address the requirements for Pif1 in the different stages of BIR.

Consistent with the previously published data (Wilson et al. 2013), the analysis of BIR repair in the timecourse experiments showed that *pif1-m2* cells

have a defect in the DNA synthesis during BIR. The requirement in Pif1 occurs within the first 6 kb of DNA synthesis during BIR (Figure 5.2 D). Additionally, *pif1-m2* cells had a defect in the re-synthesis of the resected strand on the recipient chromosome. This is likely to be a consequence of the coordination between the DNA synthesis and DNA re-synthesis during BIR. As the genetic requirements of BIR include most of the DNA replication machinery, it is logical to assume that the replisome complex may be assembled at the certain point of the repair. This may involve recruitment of the Pol α/primase complex to prime the re-synthesis of the resected strand. Perhaps this event occurs efficiently only in the BIR competent *PIF1* cells. Notably, a small fraction of *pif1-m2* cells managed to escape resection of the sites analysed, which is consistent with cells surviving the lesion in a BIR-independent way (Figure 5.1 B).

Importantly, Pif1 is not required for the invasion of the recipient chromosome end into the homologous region of the donor chromosome, as evidenced by Rad51 ChIP (Figure 5.3 C). The initiation of DNA synthesis occurs similarly in the *PIF1* and *pif1-m2* cells, suggesting that this step of BIR does not require Pif1 (Figure 5.4 C). These results point towards the DNA synthesis step of BIR being the only step that requires Pif1, supporting the model proposed earlier (Wilson et al. 2013; Saini et al. 2013; Buzovetsky et al. 2017).

The BIR defect of *pif1-m2* cells was completely suppressed by *pif1-m1* allele, but not *pif1-m1-4A,* suggesting that this suppression requires the previously reported Rad53/Dun1-dependent phosphorylation of Pif1 (Figure 5.5 A) (Vasianovich, Harrington, and Makovets 2014). In accordance with the genetic data, Pif1-4A failed to promote DNA synthesis and DNA re-synthesis during BIR (Figure 5.5 B, C).

Chapter VI. Summary and general discussion

As described in Chapter I, Pif1 is a multifunctional helicase involved in DNA replication, DSB repair and regulation of telomere length. In response to DNA damage, Pif1 is phosphorylated by Rad53/Dun1 and this phosphorylation is required for BIR (Vasianovich, Harrington, and Makovets 2014) and inhibition of telomerase at DSB, but not at telomeres (Makovets and Blackburn 2009). The molecular mechanism of this DNA damage-dependent regulation of Pif1 activity is currently not understood.

The recently published data indicate that Pif1 can physically interact with PCNA via the C-terminal PIP1 and PIP2 motifs (Wilson et al. 2013; Buzovetsky et al. 2017; Dahan et al. 2018). In addition to the C-terminal PIP motifs, Pif1 contains a putative PIP3 and SIM motifs in its N-terminal domain. The experiments presented in this work show that PIP3 and SIM from Pif1 can functionally substitute for the well characterised PIP and SIM motifs in the C-terminus of Srs2. This suggests that Pif1 might use PIP3 and SIM to interact with SUMOylated PCNA in a manner similar to Srs2 (Armstrong, Mohideen, and Lima 2012).

The reported PIP motifs in the C-terminus of Pif1 were required for DNA replication through the G4 structures (PIP2, Dahan et al., 2018) and BIR (PIP1, Buzovetsky et al., 2017). However, to better understand the functions of the published and the newly described PCNA-interacting motifs in Pif1, the requirements of these elements in replication and repair were addressed systematically in this work using the functional assays summarised in Table 7. Based on the obtained results I would like to propose a hypothetical model aimed to explain the complicated genetic data by assuming that several different complexes between Pif1 and PCNA exist depending on which PCNA-interacting motifs in Pif1 are involved in the interaction (Figure 6.1).

Table 7. The genetic requirements of the PCNA-interacting motifs and the Rad53/Dun1-regulated phosphosite TLSSAES for different functions of Pif1

	PIF1	*pif1-m2*	*pif1-pip1*	*pif1-pip2*	*pif1-pip3*	*pif1-sim*	*pif1-4A*
Replication through the barriers	+	-	+	+*	+*	+/--	N/A
Recruitment to stalled replication forks	+	-	N/A	N/A	N/A	+/--	N/A
Telomerase inhibition at telomeres	+	-	+	-	+	-	+
Recruitment to DSBs	+	-	+/-	+/--	+	+/--	-
Telomerase inhibition at DSBs	+	-	+/-	-	+/-	+/--	-
BIR	+	-	-	-	+/--	-	-

Table legend: "+" - proficient, "-" – deficient, "+/- " – mild partial defect, "+/--" – severe partial defect. "N/A" – not assayed. * although the single mutations in PIP2 or PIP3 motifs did not affect the replication-associated function of Pif1, the requirements for the either one of the two motifs became evident after testing the effect of the *pif1-m1-pip2-pip3* mutation (see section 3.3). The requirements for the TLSSAES phosphorylation have been published previously (Makovets and Blackburn 2009, Vasianovich et al., 2014).

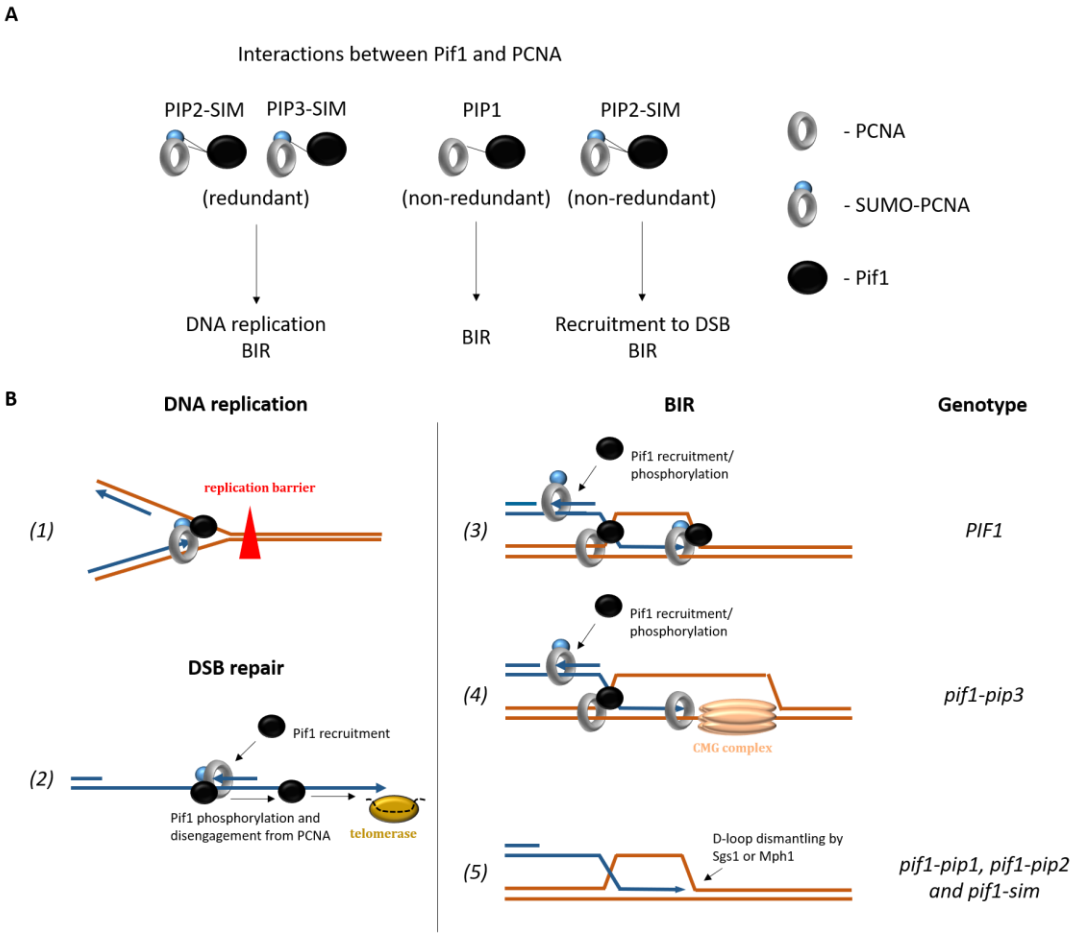

Figure 6.1. Hypothetical model of the possible interactions between Pif1 and PCNA and their implications in the context of Pif1 functions analysed

A. Schematic represents Pif1 and PCNA (or SUMO-PCNA) interacting via the different PCNA-interacting motifs in Pif1. **B.** Hypothetical model suggesting different functions of Pif1-PCNA complex in DNA-replication (1), DSB repair (2) and BIR (3-6).

Ability of Pif1 to promote DNA replication through the $tDNA_{Ala}$ in *rrm3Δ* cells required SIM, and either one of the PIP2 and PIP3 motifs which acted redundantly (Table 7). The requirement for the PIP1 motif in promoting DNA replication was not conclusively established, as minor differences in the replication fork pausing between the *rrm3Δ* cells expressing Pif1-m1-pip2,pip3 and Pif1-m1-pip1,pip2,pip3 may be within the experimental error. In contrast, mutations in the SIM motif led to significant defect in the replication-associated function of Pif1. This may suggest that Pif1 interaction with PCNA is induced by PCNA SUMOylation and requires a combination of SIM with either PIP2 or PIP3 motifs (Figure 6.1 A).

PCNA-dependent Pif1 localisation to stalled replication forks could explain the observed requirement for the PCNA-interacting motifs in Pif1. Indeed, both Pif1-pip1,pip2,pip3 and Pif1-sim proteins showed compromised recruitment to stalled replication forks in comparison to the wild type Pif1 (Table 7). In concert with this observation, *pol30-KK127,164RR* cells, which lack the two known SUMOylation sites in PCNA had lower Pif1 recruitment to stalled replication forks relative to the *POL30* cells. Therefore, Pif1 could be recruited to stalled replication forks by SUMO-PCNA via the SIM and the partially redundant PIP2 and PIP3 motifs during replication stress, where it may be required to promote replication fork progression through certain replication barriers (Fig. 6.1 A, B).

The PIP2 and SIM motifs were required for Pif1 localisation to DSBs and DNTA inhibition, while the involvement of the PIP1 and PIP3 motifs in this was much lower (Table 7, Figure 6.1 A). This suggests that Pif1 recruitment to DSBs may require interaction with SUMOylated PCNA through the PIP2 and SIM motifs in the manner that does not allow the redundancy between the PIP motifs.

Due to the ring-shaped structure of PCNA trimer, its loading onto DNA is an ATP-dependent process which requires RFC complex. RFC itself has distinct substrate preference towards the ssDNA-dsDNA junctions which are brunched or contain a free 3'-end (Gomes and Burgers 2001). At DSBs such substrate could appear due to the DNA re-synthesis initiation by Pol α (Figure 6.1 B, part 2). In turn, this could lead to PCNA loading and recruitment of Pif1, although the orientation of PCNA in such scenario would be away from the broken chromosome end, where Pif1 activity is required to inhibit telomerase. The previously reported Rad53/Dun1-dependent phosphorylation of Pif1 is required for telomerase inhibition at DSB, but not for the Pif1 recruitment to DSBs (Makovets and Blackburn 2009). Pif1 phosphorylation could decrease PIP2 affinity to PCNA and release Pif1 from the complex, allowing it to migrate towards the DNA end where telomerase adds telomeric repeats (Figure 6.1 B, part 2).

Telomere length regulation also requires PIP2 and SIM motives in Pif1, which may suggest that Pif1 recruitment to telomeres requires interaction with PCNA. In contrast to DSBs, the Rad53/Dun1-dependent phosphorylation of Pif1 is not required for telomerase inhibition at telomeres, which is expected as DNA damage

checkpoint is inhibited at telomeres. Therefore, Pif1 release from the complex with PCNA could be achieved through a different mechanism, e.g. Elg1-dependent PCNA unloading from DNA. Consistent with this hypothesis, ***elg1Δ*** cells have long telomere phenotype (Johnson et al., 2016).

Pif1 has been previously reported to promote DNA synthesis during BIR (Wilson et al. 2013). Experiments described in this work show that Pif1 was not required neither for the D-loop formation nor for the initiation of DNA synthesis during BIR, but efficient DNA synthesis of the first 6 kb was strongly dependent on Pif1 and its Rad53/Dun1-dependent phosphorylation. In addition to the compromised DNA synthesis, the reconstitution of the resected recipient strand during BIR was deficient in the *pif1-m2 and pif1-m2 pif1-m1-4A* strains, suggesting that these processes may be coordinated or inter-dependent.

The genetic requirements for BIR involved all of the analysed PCNA-interacting motifs in Pif1, resembling the requirements for the replication-associated function of Pif1 (Table 7, Figure 6.1 A). The key difference between these two roles is the lack of the functional redundancy between the PIP motifs in Pif1 for its role in BIR. From all tested *pip* mutations in *PIF1, pip3* had the mildest BIR defect – reducing the frequency of the repair approximately two-fold. Similar BIR defect was previously observed in the *pol30-KK127,164RR* cells, which may suggest that the complex between Pif1 and SUMO-PCNA is required during BIR (Lydeard et al. 2010, Makovets lab unpublished data). Moderate BIR defect of *pif1-pip3* cells could be explained by the partial redundancy between Pif1 and the replicative helicase (Figure 6.1 B, parts 3 and 4), which was previously reported to be required for BIR (Lydeard et al. 2010).

In contrast to the mild BIR defect observed in *pif1-pip3* cells, the strains lacking the nuclear Pif1 or expressing Pif1 variants with either PIP1, PIP2 or SIM motifs mutated had a severe BIR defect. This could suggest that apart from the redundant role during BIR, Pif1 has a second role which is essential for this DNA repair pathway. Such role could be the recipient chromosome strand ejection from the donor template, suggested earlier by Ira and colleagues (Wilson et al., 2013). In analogy to DSBs, Pif1 could be recruited to the DNA re-synthesis initiation sites on the recipient chromosome in SUMO-PCNA dependent manner (Figure 6.1 B,

part 3). After initial recruitment to the recipient chromosome, Pif1 could be phosphorylated and released from the complex with PCNA and translocate to the base of the D-loop along the recipient strand. Finally, the PIP1 motif could be required for the strand displacement activity, assuming it also involves the formation of the complex between Pif1 and PCNA (Figure 6.1 B). Therefore, in the cells lacking one of the three key PCNA-interacting motives for BIR, D-loop migration would be non-efficient, and the structure would be more susceptible for the inhibitory activity of the recombination execution checkpoint proteins Sgs1 and Mph1 (Figure 6.1 B, part 5).

Based on the combined data, I propose that Pif1 uses PIP2 and SIM as the primary PCNA interacting motifs, since *pip2* and *sim* mutations affected all the tested functions of Pif1 (Table 7). PIP3 is likely to be a replication-associated motif, as the *pip3* mutation affects primarily Pif1 roles in facilitating DNA synthesis during DNA replication and BIR. Finally, PIP1 may be a BIR-specific motif with a possible minor role during DNA replication and DNTA inhibition.

The middle part of Pif1-family proteins is highly conserved from the budding yeast to humans, while the N- and the C-terminal parts are much more diverse (Figure 6.2). PIP2 motif, located in the end of the conserved part of Pif1 is very conserved between Pif1 and Rrm3. Mutations in the PIP2 motif of Rrm3 led to a severe replication defect similar to the one observed in *rrm3Δ* cells, suggesting that this motif is essential for the replication-associated functions. Importantly, conservation of the PIP2 motif extends to the Pif1 homologues in *S. pombe*, *M. musculus* and *H. sapiens* (Figure 6.2), which suggests that the role of Pif1-PCNA interaction may be also evolutionarily conserved.

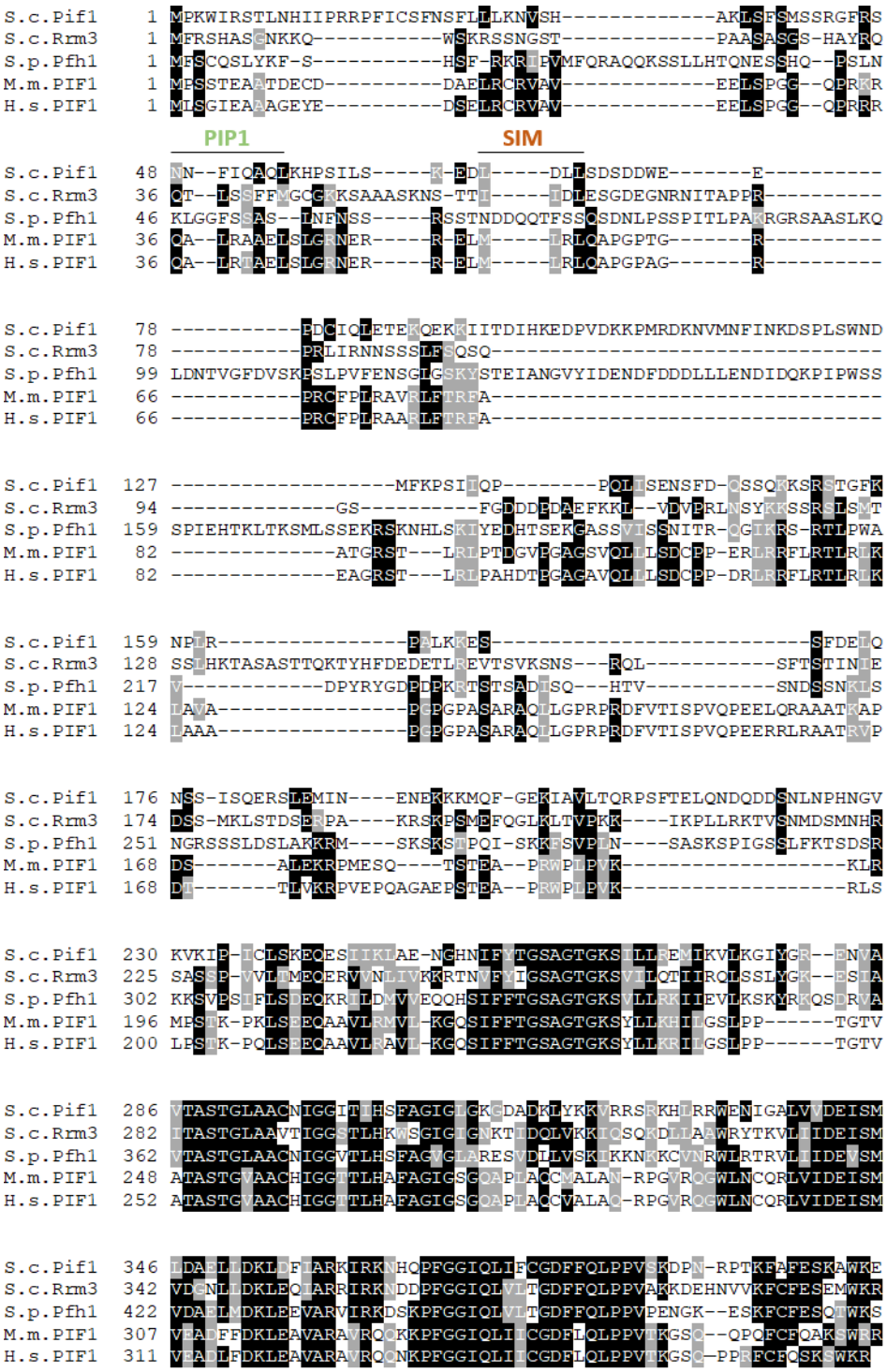
PIP1
SIM

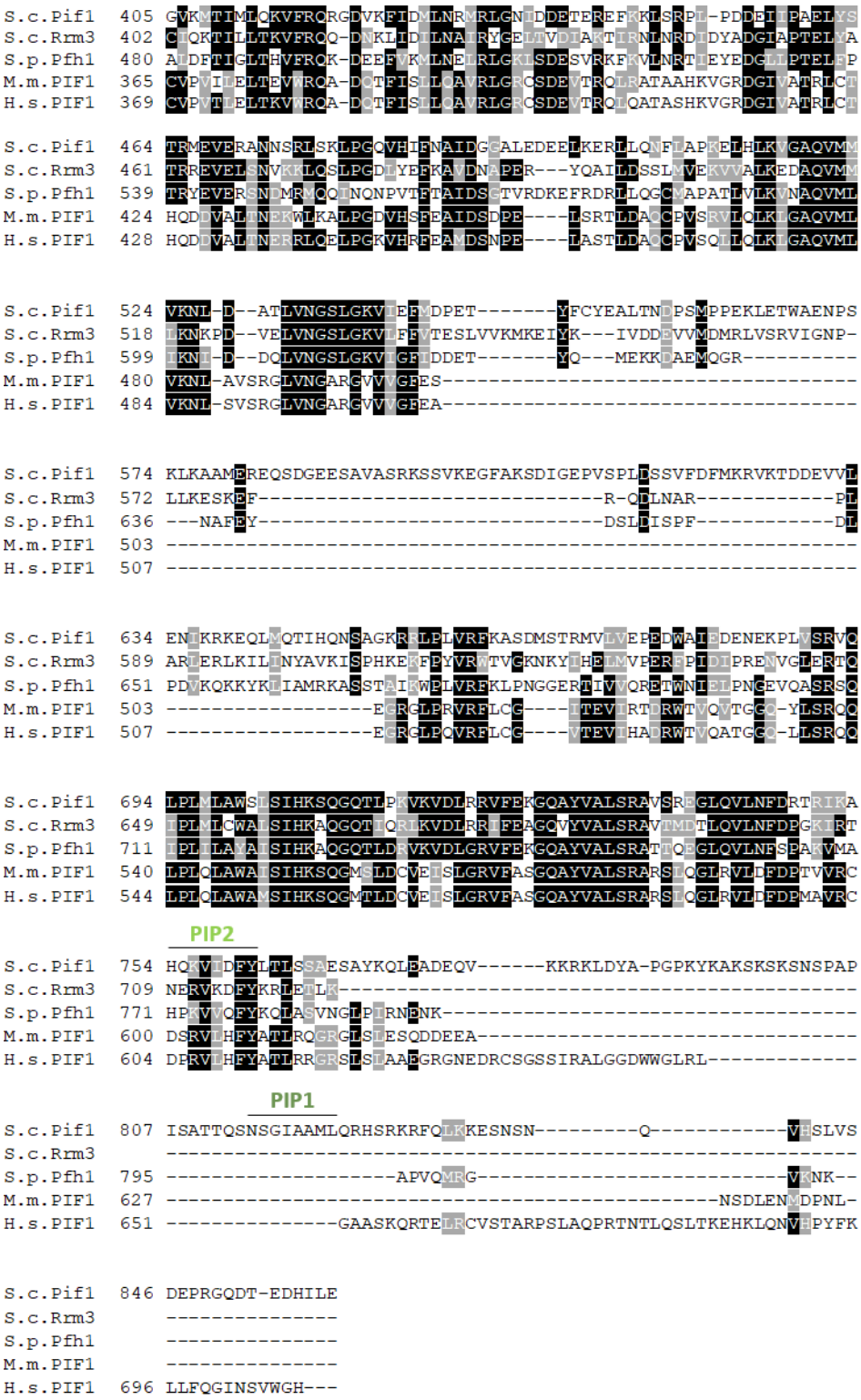

Figure 6.2. Sequence alignment of Pif1 homologues.

S.c.Pif1 – *S. cerevisiae* Pif1, S.c.Rrm3 – *S. cerevisiae* Rrm3, S.p.Pfh1 – *S. pombe* Pfh1, M.m.PIF1 – *M. musculus* PIF1, H.s.PIF1 – *H. sapiens* PIF1. Identical amino acids are

highlighted in black, similar amino acids – in gray. The positions of the PCNA-interacting motifs of Pif1 are indicated above the alignments.

PIP3 and SIM motifs of are located in the N-terminal region of Pif1 which is quite diverse between the Pif1-family helicases (Figure 6.2). The physical interaction between Rrm3 and PCNA via the N-terminal PIP (PIP1 in Rrm3) has been previously reported (Schmidt, Derry, and Kolodner 2002). Additionally, the N-terminus of Rrm3 contains the sequence which reminds the SIM motif in Pif1 (Figure 6.2), although the chimeric Srs2-[PIP-SIM]$_{RRM3}$ fusion failed to confer MMS sensitivity of the *rad18Δ* cells, suggesting that the defined motif does not allow sufficient interaction with SUMO-PCNA. Neither PIP1, nor SIM motifs in Rrm3 were required for promoting DNA replication through the Rrm3-sensitive loci. This may suggest that, in contrast to Pif1, Rrm3 interacts with PCNA via the PIP2 motif only and does not require PCNA SUMOylation.

Finally, the PIP1 motif of Pif1 is located in the very C-terminal region of the protein that has unique sequence, suggesting that the essential Pif1 function in BIR is not conserved in other species.

A hypothetical mechanism of the differentiation between the Pif1 family helicases could be based on the mutually exclusive interaction between PCNA and Pif1 or Rrm3. Association of Rrm3 with the replication forks was reported earlier (Azvolinsky et al. 2006; Paeschke, Capra, and Zakian 2011). Perhaps, under normal conditions, Rrm3 has higher affinity to PCNA than Pif1. However, replication forks may stall after encountering the replication barriers resistant to Rrm3, which would cause posttranslational modification of PCNA, such as SUMOylation. This could increase the affinity of Pif1 to PCNA and lead to a switch from Rrm3 to Pif1 to restore the replication fork progression. Such a mechanism is likely to be further complicated by the presence of different PCNA-interacting motifs and posttranslational modifications in Pif1 and Rrm3, which could also affect the interactions between the corresponding helicases and PCNA. These posttranslational modifications include the phosphorylations at the N-termini of Rrm3 and Pif1 by Rad53 in response to replication stress (Rossi et al. 2015), the phosphorylation of the C-terminal TLLSSAES motif in Pif1 in a Rad53/Dun1

dependent manner (Makovets and Blackburn 2009) and SUMOylation of Pif1 (Hang et al. 2011).

RecQ helicases are another example of the multifunctional helicases that went through the functional diversification. In contrast to the budding yeast, which have one RecQ family helicase Sgs1, human cells have five reported RecQ helicases (RECQ1, BLM, WRN, RECQ4, RECQ5) that have non-redundant functions (Urban, Dobrovolna, and Janscak 2017). Mutations in BLM, WRN and RECQ4 were associated with severe hereditary diseases (Croteau et al. 2014), while defects in RECQ1 and RECQ5 were connected to cancer development (Cybulski et al. 2015; Sun, Wang, et al. 2015; Zhi et al. 2014; Qi and Zhou 2014; He et al. 2014). However, the underlying mechanisms which lead to the diverse functions of RecQ helicases are not understood. It is possible that the helicases of the Pif1 and RecQ families have adapted to their specific roles via a similar mechanism. Understanding how Pif1 family helicases achieve their functional specificity in *S. cerevisiae* might help to reveal some of the underlying principles of the helicase functional diversification. Thus, further genetic and biochemical analysis of the interactions between PCNA and Pif1 family helicases may help solving the mysteries of the functional divergence of closely related multifunctional helicases.

Overall, this work provides a systematic characterisation of the newly identified and previously reported *pif1* and *rrm3* alleles and shows that different functions of Pif1 can be distinguished by the genetic requirements for its PCNA-interacting elements.

References

Acharya, S., Z. Kaul, A. S. Gocha, A. R. Martinez, J. Harris, J. D. Parvin, and J. Groden. 2014. 'Association of BLM and BRCA1 during Telomere Maintenance in ALT Cells', *PLoS One*, 9: e103819.

Addinall, S. G., E. M. Holstein, C. Lawless, M. Yu, K. Chapman, A. P. Banks, H. P. Ngo, L. Maringele, M. Taschuk, A. Young, A. Ciesiolka, A. L. Lister, A. Wipat, D. J. Wilkinson, and D. Lydall. 2011. 'Quantitative fitness analysis shows that NMD proteins and many other protein complexes suppress or enhance distinct telomere cap defects', *PLoS Genet*, 7: e1001362.

Anbalagan, S., D. Bonetti, G. Lucchini, and M. P. Longhese. 2011. 'Rif1 supports the function of the CST complex in yeast telomere capping', *PLoS Genet*, 7: e1002024.

Andriuskevicius, T., O. Kotenko, and S. Makovets. 2018. 'Putting together and taking apart: assembly and disassembly of the Rad51 nucleoprotein filament in DNA repair and genome stability', *Cell Stress*, 2: 96-112.

Araki, H., S. H. Leem, A. Phongdara, and A. Sugino. 1995. 'Dpb11, which interacts with DNA polymerase II(epsilon) in Saccharomyces cerevisiae, has a dual role in S-phase progression and at a cell cycle checkpoint', *Proc Natl Acad Sci U S A*, 92: 11791-5.

Armstrong, A. A., F. Mohideen, and C. D. Lima. 2012. 'Recognition of SUMO-modified PCNA requires tandem receptor motifs in Srs2', *Nature*, 483: 59-63.

AS, I. Jpma, and C. W. Greider. 2003. 'Short telomeres induce a DNA damage response in Saccharomyces cerevisiae', *Mol Biol Cell*, 14: 987-1001.

Azvolinsky, A., S. Dunaway, J. Z. Torres, J. B. Bessler, and V. A. Zakian. 2006. 'The S. cerevisiae Rrm3p DNA helicase moves with the replication fork and affects replication of all yeast chromosomes', *Genes Dev*, 20: 3104-16.

Bae, S. H., K. H. Bae, J. A. Kim, and Y. S. Seo. 2001. 'RPA governs endonuclease switching during processing of Okazaki fragments in eukaryotes', *Nature*, 412: 456-61.

Bairwa, N. K., S. Zzaman, B. K. Mohanty, and D. Bastia. 2010. 'Replication fork arrest and rDNA silencing are two independent and separable functions of the replication terminator protein Fob1 of Saccharomyces cerevisiae', *J Biol Chem*, 285: 12612-9.

Baranovskiy, A. G., N. D. Babayeva, Y. Zhang, J. Gu, Y. Suwa, Y. I. Pavlov, and T. H. Tahirov. 2016. 'Mechanism of Concerted RNA-DNA Primer Synthesis by the Human Primosome', *J Biol Chem*, 291: 10006-20.

Baroni, E., V. Viscardi, H. Cartagena-Lirola, G. Lucchini, and M. P. Longhese. 2004. 'The functions of budding yeast Sae2 in the DNA damage response require Mec1- and Tel1-dependent phosphorylation', *Mol Cell Biol*, 24: 4151-65.

Bell, S. P., R. Kobayashi, and B. Stillman. 1993. 'Yeast origin recognition complex functions in transcription silencing and DNA replication', *Science*, 262: 1844-9.

Bell, S. P., and B. Stillman. 1992. 'ATP-dependent recognition of eukaryotic origins of DNA replication by a multiprotein complex', *Nature*, 357: 128-34.

Bertuch, A. A., and V. Lundblad. 2003. 'The Ku heterodimer performs separable activities at double-strand breaks and chromosome termini', *Mol Cell Biol*, 23: 8202-15.

Bhowmick, R., S. Minocherhomji, and I. D. Hickson. 2016. 'RAD52 Facilitates Mitotic DNA Synthesis Following Replication Stress', *Mol Cell*, 64: 1117-26.

Bianchi, A., S. Negrini, and D. Shore. 2004. 'Delivery of yeast telomerase to a DNA break depends on the recruitment functions of Cdc13 and Est1', *Mol Cell*, 16: 139-46.

Biessmann, H., J. M. Mason, K. Ferry, M. d'Hulst, K. Valgeirsdottir, K. L. Traverse, and M. L. Pardue. 1990. 'Addition of telomere-associated HeT DNA sequences "heals" broken chromosome ends in Drosophila', *Cell*, 61: 663-73.

Biggins, S. 2013. 'The composition, functions, and regulation of the budding yeast kinetochore', *Genetics*, 194: 817-46.
Billon, P., J. Li, J. P. Lambert, Y. Chen, V. Tremblay, J. S. Brunzelle, A. C. Gingras, A. Verreault, T. Sugiyama, J. F. Couture, and J. Cote. 2017. 'Acetylation of PCNA Sliding Surface by Eco1 Promotes Genome Stability through Homologous Recombination', *Mol Cell*, 65: 78-90.
Bochman, M. L., C. P. Judge, and V. A. Zakian. 2011. 'The Pif1 family in prokaryotes: what are our helicases doing in your bacteria?', *Mol Biol Cell*, 22: 1955-9.
Bochman, M. L., N. Sabouri, and V. A. Zakian. 2010. 'Unwinding the functions of the Pif1 family helicases', *DNA Repair (Amst)*, 9: 237-49.
Boehm, E. M., and M. T. Washington. 2016. 'R.I.P. to the PIP: PCNA-binding motif no longer considered specific: PIP motifs and other related sequences are not distinct entities and can bind multiple proteins involved in genome maintenance', *Bioessays*, 38: 1117-22.
Bonetti, D., M. Clerici, S. Anbalagan, M. Martina, G. Lucchini, and M. P. Longhese. 2010. 'Shelterin-like proteins and Yku inhibit nucleolytic processing of Saccharomyces cerevisiae telomeres', *PLoS Genet*, 6: e1000966.
Bonetti, D., M. Clerici, N. Manfrini, G. Lucchini, and M. P. Longhese. 2010. 'The MRX complex plays multiple functions in resection of Yku- and Rif2-protected DNA ends', *PLoS One*, 5: e14142.
Bosco, G., and J. E. Haber. 1998. 'Chromosome break-induced DNA replication leads to nonreciprocal translocations and telomere capture', *Genetics*, 150: 1037-47.
Boule, J. B., L. R. Vega, and V. A. Zakian. 2005. 'The yeast Pif1p helicase removes telomerase from telomeric DNA', *Nature*, 438: 57-61.
Boule, J. B., and V. A. Zakian. 2007. 'The yeast Pif1p DNA helicase preferentially unwinds RNA DNA substrates', *Nucleic Acids Res*, 35: 5809-18.
Brewer, B. J., and W. L. Fangman. 1987. 'The localization of replication origins on ARS plasmids in S. cerevisiae', *Cell*, 51: 463-71.
———. 1988. 'A replication fork barrier at the 3' end of yeast ribosomal RNA genes', *Cell*, 55: 637-43.
Bruning, J. B., and Y. Shamoo. 2004. 'Structural and thermodynamic analysis of human PCNA with peptides derived from DNA polymerase-delta p66 subunit and flap endonuclease-1', *Structure*, 12: 2209-19.
Brush, G. S., D. M. Morrow, P. Hieter, and T. J. Kelly. 1996. 'The ATM homologue MEC1 is required for phosphorylation of replication protein A in yeast', *Proc Natl Acad Sci U S A*, 93: 15075-80.
Budd, M. E., I. A. Antoshechkin, C. Reis, B. J. Wold, and J. L. Campbell. 2011. 'Inviability of a DNA2 deletion mutant is due to the DNA damage checkpoint', *Cell Cycle*, 10: 1690-8.
Budd, M. E., and J. L. Campbell. 2000. 'The pattern of sensitivity of yeast dna2 mutants to DNA damaging agents suggests a role in DSB and postreplication repair pathways', *Mutat Res*, 459: 173-86.
Budd, M. E., C. C. Reis, S. Smith, K. Myung, and J. L. Campbell. 2006. 'Evidence suggesting that Pif1 helicase functions in DNA replication with the Dna2 helicase/nuclease and DNA polymerase delta', *Mol Cell Biol*, 26: 2490-500.
Bupp, J. M., A. E. Martin, E. S. Stensrud, and S. L. Jaspersen. 2007. 'Telomere anchoring at the nuclear periphery requires the budding yeast Sad1-UNC-84 domain protein Mps3', *J Cell Biol*, 179: 845-54.
Burgers, P. M. J., and T. A. Kunkel. 2017. 'Eukaryotic DNA Replication Fork', *Annu Rev Biochem*, 86: 417-38.

Buzovetsky, O., Y. Kwon, N. T. Pham, C. Kim, G. Ira, P. Sung, and Y. Xiong. 2017. 'Role of the Pif1-PCNA Complex in Pol delta-Dependent Strand Displacement DNA Synthesis and Break-Induced Replication', *Cell Rep*, 21: 1707-14.

Byrd, A. K., and K. D. Raney. 2015. 'A parallel quadruplex DNA is bound tightly but unfolded slowly by pif1 helicase', *J Biol Chem*, 290: 6482-94.

Capra, J. A., K. Paeschke, M. Singh, and V. A. Zakian. 2010. 'G-quadruplex DNA sequences are evolutionarily conserved and associated with distinct genomic features in Saccharomyces cerevisiae', *PLoS Comput Biol*, 6: e1000861.

Cazzalini, O., S. Sommatis, M. Tillhon, I. Dutto, A. Bachi, A. Rapp, T. Nardo, A. I. Scovassi, D. Necchi, M. C. Cardoso, L. A. Stivala, and E. Prosperi. 2014. 'CBP and p300 acetylate PCNA to link its degradation with nucleotide excision repair synthesis', *Nucleic Acids Res*, 42: 8433-48.

Cejka, P., E. Cannavo, P. Polaczek, T. Masuda-Sasa, S. Pokharel, J. L. Campbell, and S. C. Kowalczykowski. 2010. 'DNA end resection by Dna2-Sgs1-RPA and its stimulation by Top3-Rmi1 and Mre11-Rad50-Xrs2', *Nature*, 467: 112-6.

Cesare, A. J., and R. R. Reddel. 2010. 'Alternative lengthening of telomeres: models, mechanisms and implications', *Nat Rev Genet*, 11: 319-30.

Chabes, A., B. Georgieva, V. Domkin, X. Zhao, R. Rothstein, and L. Thelander. 2003. 'Survival of DNA damage in yeast directly depends on increased dNTP levels allowed by relaxed feedback inhibition of ribonucleotide reductase', *Cell*, 112: 391-401.

Chan, C. S., and B. K. Tye. 1983. 'Organization of DNA sequences and replication origins at yeast telomeres', *Cell*, 33: 563-73.

Chang, M., B. Luke, C. Kraft, Z. Li, M. Peter, J. Linger, and R. Rothstein. 2009. 'Telomerase is essential to alleviate pif1-induced replication stress at telomeres', Genetics, 183(3):779-91.

Chandra, A., T. R. Hughes, C. I. Nugent, and V. Lundblad. 2001. 'Cdc13 both positively and negatively regulates telomere replication', *Genes Dev*, 15: 404-14.

Chapman, J. R., P. Barral, J. B. Vannier, V. Borel, M. Steger, A. Tomas-Loba, A. A. Sartori, I. R. Adams, F. D. Batista, and S. J. Boulton. 2013. 'RIF1 is essential for 53BP1-dependent nonhomologous end joining and suppression of DNA double-strand break resection', *Mol Cell*, 49: 858-71.

Chen, C. F., T. J. Pohl, S. Pott, and V. A. Zakian. 2019. 'Two Pif1 Family DNA Helicases Cooperate in Centromere Replication and Segregation in Saccharomyces cerevisiae', *Genetics*, 211: 105-19.

Chen, C., L. Zhang, N. J. Huang, B. Huang, and S. Kornbluth. 2013. 'Suppression of DNA-damage checkpoint signaling by Rsk-mediated phosphorylation of Mre11', *Proc Natl Acad Sci U S A*, 110: 20605-10.

Chen, H., J. Xue, D. Churikov, E. P. Hass, S. Shi, L. D. Lemon, P. Luciano, A. A. Bertuch, D. C. Zappulla, V. Geli, J. Wu, and M. Lei. 2018. 'Structural Insights into Yeast Telomerase Recruitment to Telomeres', *Cell*, 172: 331-43 e13.

Chen, X., D. Cui, A. Papusha, X. Zhang, C. D. Chu, J. Tang, K. Chen, X. Pan, and G. Ira. 2012. 'The Fun30 nucleosome remodeller promotes resection of DNA double-strand break ends', *Nature*, 489: 576-80.

Chen, X., H. Niu, W. H. Chung, Z. Zhu, A. Papusha, E. Y. Shim, S. E. Lee, P. Sung, and G. Ira. 2011. 'Cell cycle regulation of DNA double-strand break end resection by Cdk1-dependent Dna2 phosphorylation', *Nat Struct Mol Biol*, 18: 1015-9.

Chilkova, O., P. Stenlund, I. Isoz, C. M. Stith, P. Grabowski, E. B. Lundstrom, P. M. Burgers, and E. Johansson. 2007. 'The eukaryotic leading and lagging strand DNA polymerases are loaded onto primer-ends via separate mechanisms but have comparable processivity in the presence of PCNA', *Nucleic Acids Res*, 35: 6588-97.

Choe, K. N., and G. L. Moldovan. 2017. 'Forging Ahead through Darkness: PCNA, Still the Principal Conductor at the Replication Fork', *Mol Cell*, 65: 380-92.
Chung, W. H., Z. Zhu, A. Papusha, A. Malkova, and G. Ira. 2010. 'Defective resection at DNA double-strand breaks leads to de novo telomere formation and enhances gene targeting', *PLoS Genet*, 6: e1000948.
Ciccia, A., and S. J. Elledge. 2010. 'The DNA damage response: making it safe to play with knives', *Mol Cell*, 40: 179-204.
Ciccia, A., A. V. Nimonkar, Y. Hu, I. Hajdu, Y. J. Achar, L. Izhar, S. A. Petit, B. Adamson, J. C. Yoon, S. C. Kowalczykowski, D. M. Livingston, L. Haracska, and S. J. Elledge. 2012. 'Polyubiquitinated PCNA recruits the ZRANB3 translocase to maintain genomic integrity after replication stress', *Mol Cell*, 47: 396-409.
Claussin, C., D. Porubsky, D. C. Spierings, N. Halsema, S. Rentas, V. Guryev, P. M. Lansdorp, and M. Chang. 2017. 'Genome-wide mapping of sister chromatid exchange events in single yeast cells using Strand-seq', *Elife*, 6.
Cohen, H., and D. A. Sinclair. 2001. 'Recombination-mediated lengthening of terminal telomeric repeats requires the Sgs1 DNA helicase', *Proc Natl Acad Sci U S A*, 98: 3174-9.
Coic, E., T. Feldman, A. S. Landman, and J. E. Haber. 2008. 'Mechanisms of Rad52-independent spontaneous and UV-induced mitotic recombination in Saccharomyces cerevisiae', *Genetics*, 179: 199-211.
Costantino, L., S. K. Sotiriou, J. K. Rantala, S. Magin, E. Mladenov, T. Helleday, J. E. Haber, G. Iliakis, O. P. Kallioniemi, and T. D. Halazonetis. 2014. 'Break-induced replication repair of damaged forks induces genomic duplications in human cells', *Science*, 343: 88-91.
Croteau, D. L., V. Popuri, P. L. Opresko, and V. A. Bohr. 2014. 'Human RecQ helicases in DNA repair, recombination, and replication', *Annu Rev Biochem*, 83: 519-52.
Cubizolles, F., F. Martino, S. Perrod, and S. M. Gasser. 2006. 'A homotrimer-heterotrimer switch in Sir2 structure differentiates rDNA and telomeric silencing', *Mol Cell*, 21: 825-36.
Cybulski, C., J. Carrot-Zhang, W. Kluzniak, B. Rivera, A. Kashyap, D. Wokolorczyk, S. Giroux, J. Nadaf, N. Hamel, S. Zhang, T. Huzarski, J. Gronwald, T. Byrski, M. Szwiec, A. Jakubowska, H. Rudnicka, M. Lener, B. Masojc, P. N. Tonin, F. Rousseau, B. Gorski, T. Debniak, J. Majewski, J. Lubinski, W. D. Foulkes, S. A. Narod, and M. R. Akbari. 2015. 'Germline RECQL mutations are associated with breast cancer susceptibility', *Nat Genet*, 47: 643-6.
Dahan, D., I. Tsirkas, D. Dovrat, M. A. Sparks, S. P. Singh, R. Galletto, and A. Aharoni. 2018. 'Pif1 is essential for efficient replisome progression through lagging strand G-quadruplex DNA secondary structures', *Nucleic Acids Res*, 46: 11847-57.
Dandjinou, A. T., N. Levesque, S. Larose, J. F. Lucier, S. Abou Elela, and R. J. Wellinger. 2004. 'A phylogenetically based secondary structure for the yeast telomerase RNA', *Curr Biol*, 14: 1148-58.
de Lange, T. 2018. 'Shelterin-Mediated Telomere Protection', *Annu Rev Genet*, 52: 223-47.
De March, M., N. Merino, S. Barrera-Vilarmau, R. Crehuet, S. Onesti, F. J. Blanco, and A. De Biasio. 2017. 'Structural basis of human PCNA sliding on DNA', *Nat Commun*, 8: 13935.
Deegan, T. D., J. Baxter, M. A. Ortiz Bazan, J. T. P. Yeeles, and K. P. M. Labib. 2019. 'Pif1-Family Helicases Support Fork Convergence during DNA Replication Termination in Eukaryotes', *Mol Cell*, 74: 231-44 e9.

Deem, A., A. Keszthelyi, T. Blackgrove, A. Vayl, B. Coffey, R. Mathur, A. Chabes, and A. Malkova. 2011. 'Break-induced replication is highly inaccurate', *PLoS Biol*, 9: e1000594.

Degrassi, F., M. Fiore, and F. Palitti. 2004. 'Chromosomal aberrations and genomic instability induced by topoisomerase-targeted antitumour drugs', *Curr Med Chem Anticancer Agents*, 4: 317-25.

Deshpande, A. M., and C. S. Newlon. 1996. 'DNA replication fork pause sites dependent on transcription', *Science*, 272: 1030-3.

Di Virgilio, M., E. Callen, A. Yamane, W. Zhang, M. Jankovic, A. D. Gitlin, N. Feldhahn, W. Resch, T. Y. Oliveira, B. T. Chait, A. Nussenzweig, R. Casellas, D. F. Robbiani, and M. C. Nussenzweig. 2013. 'Rif1 prevents resection of DNA breaks and promotes immunoglobulin class switching', *Science*, 339: 711-5.

Dilley, R. L., and R. A. Greenberg. 2015. 'ALTernative Telomere Maintenance and Cancer', *Trends Cancer*, 1: 145-56.

Dilley, R. L., P. Verma, N. W. Cho, H. D. Winters, A. R. Wondisford, and R. A. Greenberg. 2016. 'Break-induced telomere synthesis underlies alternative telomere maintenance', *Nature*, 539: 54-58.

Donnianni, R. A., and L. S. Symington. 2013. 'Break-induced replication occurs by conservative DNA synthesis', *Proc Natl Acad Sci U S A*, 110: 13475-80.

Dovrat, D., J. L. Stodola, P. M. Burgers, and A. Aharoni. 2014. 'Sequential switching of binding partners on PCNA during in vitro Okazaki fragment maturation', *Proc Natl Acad Sci U S A*, 111: 14118-23.

Dua, R., D. L. Levy, and J. L. Campbell. 1999. 'Analysis of the essential functions of the C-terminal protein/protein interaction domain of Saccharomyces cerevisiae pol epsilon and its unexpected ability to support growth in the absence of the DNA polymerase domain', *J Biol Chem*, 274: 22283-8.

Duan, X. L., N. N. Liu, Y. T. Yang, H. H. Li, M. Li, S. X. Dou, and X. G. Xi. 2015. 'G-quadruplexes significantly stimulate Pif1 helicase-catalyzed duplex DNA unwinding', *J Biol Chem*, 290: 7722-35.

Enomoto, S., L. Glowczewski, and J. Berman. 2002. 'MEC3, MEC1, and DDC2 are essential components of a telomere checkpoint pathway required for cell cycle arrest during senescence in Saccharomyces cerevisiae', *Mol Biol Cell*, 13: 2626-38.

Evans, S. K., and V. Lundblad. 1999. 'Est1 and Cdc13 as comediators of telomerase access', *Science*, 286: 117-20.

Feng, W., and G. D'Urso. 2001. 'Schizosaccharomyces pombe cells lacking the amino-terminal catalytic domains of DNA polymerase epsilon are viable but require the DNA damage checkpoint control', *Mol Cell Biol*, 21: 4495-504.

Fisher, T. S., A. K. Taggart, and V. A. Zakian. 2004. 'Cell cycle-dependent regulation of yeast telomerase by Ku', *Nat Struct Mol Biol*, 11: 1198-205.

Fouladi, B., L. Sabatier, D. Miller, G. Pottier, and J. P. Murnane. 2000. 'The relationship between spontaneous telomere loss and chromosome instability in a human tumor cell line', *Neoplasia*, 2: 540-54.

Foury, F., and J. Kolodynski. 1983. 'pif mutation blocks recombination between mitochondrial rho+ and rho- genomes having tandemly arrayed repeat units in Saccharomyces cerevisiae', *Proc Natl Acad Sci U S A*, 80: 5345-9.

Friedberg, E. C., A. Aguilera, M. Gellert, P. C. Hanawalt, J. B. Hays, A. R. Lehmann, T. Lindahl, N. Lowndes, A. Sarasin, and R. D. Wood. 2006. 'DNA repair: from molecular mechanism to human disease', *DNA Repair (Amst)*, 5: 986-96.

Friedman, K. L., and B. J. Brewer. 1995. 'Analysis of replication intermediates by two-dimensional agarose gel electrophoresis', *Methods Enzymol*, 262: 613-27.

Friedman, K. L., and T. R. Cech. 1999. 'Essential functions of amino-terminal domains in the yeast telomerase catalytic subunit revealed by selection for viable mutants', *Genes Dev*, 13: 2863-74.
Friedman, K. L., J. J. Heit, D. M. Long, and T. R. Cech. 2003. 'N-terminal domain of yeast telomerase reverse transcriptase: recruitment of Est3p to the telomerase complex', *Mol Biol Cell*, 14: 1-13.
Futami, K., A. Shimamoto, and Y. Furuichi. 2007. 'Mitochondrial and nuclear localization of human Pif1 helicase', *Biol Pharm Bull*, 30: 1685-92.
Gallardo, F., C. Olivier, A. T. Dandjinou, R. J. Wellinger, and P. Chartrand. 2008. 'TLC1 RNA nucleo-cytoplasmic trafficking links telomerase biogenesis to its recruitment to telomeres', *EMBO J*, 27: 748-57.
Garcia-Rodriguez, N., R. P. Wong, and H. D. Ulrich. 2018. 'The helicase Pif1 functions in the template switching pathway of DNA damage bypass', *Nucleic Acids Res*, 46: 8347-56.
Garcia, V., S. E. Phelps, S. Gray, and M. J. Neale. 2011. 'Bidirectional resection of DNA double-strand breaks by Mre11 and Exo1', *Nature*, 479: 241-4.
Garvik, B., M. Carson, and L. Hartwell. 1995. 'Single-stranded DNA arising at telomeres in cdc13 mutants may constitute a specific signal for the RAD9 checkpoint', *Mol Cell Biol*, 15: 6128-38.
George, T., Q. Wen, R. Griffiths, A. Ganesh, M. Meuth, and C. M. Sanders. 2009. 'Human Pif1 helicase unwinds synthetic DNA structures resembling stalled DNA replication forks', *Nucleic Acids Res*, 37: 6491-502.
Gerik, K. J., X. Li, A. Pautz, and P. M. Burgers. 1998. 'Characterization of the two small subunits of Saccharomyces cerevisiae DNA polymerase delta', *J Biol Chem*, 273: 19747-55.
Geronimo, C. L., S. P. Singh, R. Galletto, and V. A. Zakian. 2018. 'The signature motif of the Saccharomyces cerevisiae Pif1 DNA helicase is essential in vivo for mitochondrial and nuclear functions and in vitro for ATPase activity', *Nucleic Acids Res*, 46: 8357-70.
Gibb, B., L. F. Ye, Y. Kwon, H. Niu, P. Sung, and E. C. Greene. 2014. 'Protein dynamics during presynaptic-complex assembly on individual single-stranded DNA molecules', *Nat Struct Mol Biol*, 21: 893-900.
Gobbini, E., D. Cesena, A. Galbiati, A. Lockhart, and M. P. Longhese. 2013. 'Interplays between ATM/Tel1 and ATR/Mec1 in sensing and signaling DNA double-strand breaks', *DNA Repair (Amst)*, 12: 791-9.
Goldstein, A. L., and J. H. McCusker. 1999. 'Three new dominant drug resistance cassettes for gene disruption in Saccharomyces cerevisiae', *Yeast*, 15: 1541-53.
Gomes, X.V. and P. M. Burgers. 2001 ' ATP utilization by yeast replication factor C. I. ATP-mediated interaction with DNA and with proliferating cell nuclear antigen', J Biol Chem, 276(37):34768-75.
Gotta, M., and S. M. Gasser. 1996. 'Nuclear organization and transcriptional silencing in yeast', *Experientia*, 52: 1136-47.
Goudsouzian, L. K., C. T. Tuzon, and V. A. Zakian. 2006. 'S. cerevisiae Tel1p and Mre11p are required for normal levels of Est1p and Est2p telomere association', *Mol Cell*, 24: 603-10.
Graham, I. R., R. A. Haw, K. G. Spink, K. A. Halden, and A. Chambers. 1999. 'In vivo analysis of functional regions within yeast Rap1p', *Mol Cell Biol*, 19: 7481-90.
Grandin, N., and M. Charbonneau. 2013. 'RPA provides checkpoint-independent cell cycle arrest and prevents recombination at uncapped telomeres of Saccharomyces cerevisiae', *DNA Repair (Amst)*, 12: 212-26.

Greenfeder, S. A., and C. S. Newlon. 1992. 'Replication forks pause at yeast centromeres', *Mol Cell Biol*, 12: 4056-66.
Gregan, J., K. Lindner, L. Brimage, R. Franklin, M. Namdar, E. A. Hart, S. J. Aves, and S. E. Kearsey. 2003. 'Fission yeast Cdc23/Mcm10 functions after pre-replicative complex formation to promote Cdc45 chromatin binding', *Mol Biol Cell*, 14: 3876-87.
Grossi, S., A. Puglisi, P. V. Dmitriev, M. Lopes, and D. Shore. 2004. 'Pol12, the B subunit of DNA polymerase alpha, functions in both telomere capping and length regulation', *Genes Dev*, 18: 992-1006.
Gu, Y., Y. Masuda, and K. Kamiya. 2008. 'Biochemical analysis of human PIF1 helicase and functions of its N-terminal domain', *Nucleic Acids Res*, 36: 6295-308.
Hang, L. E., X. Liu, I. Cheung, Y. Yang, and X. Zhao. 2011. 'SUMOylation regulates telomere length homeostasis by targeting Cdc13', *Nat Struct Mol Biol*, 18: 920-6.
Haracska, L., C. M. Kondratick, I. Unk, S. Prakash, and L. Prakash. 2001. 'Interaction with PCNA is essential for yeast DNA polymerase eta function', *Mol Cell*, 8: 407-15.
Hardy, C. F., D. Balderes, and D. Shore. 1992. 'Dissection of a carboxy-terminal region of the yeast regulatory protein RAP1 with effects on both transcriptional activation and silencing', *Mol Cell Biol*, 12: 1209-17.
Hardy, C. F., L. Sussel, and D. Shore. 1992. 'A RAP1-interacting protein involved in transcriptional silencing and telomere length regulation', *Genes Dev*, 6: 801-14.
Hass, E. P., and D. C. Zappulla. 2015. 'The Ku subunit of telomerase binds Sir4 to recruit telomerase to lengthen telomeres in S. cerevisiae', *Elife*, 4.
Hastings, P. J., G. Ira, and J. R. Lupski. 2009. 'A microhomology-mediated break-induced replication model for the origin of human copy number variation', *PLoS Genet*, 5: e1000327.
Havens, C. G., and J. C. Walter. 2011. 'Mechanism of CRL4(Cdt2), a PCNA-dependent E3 ubiquitin ligase', *Genes Dev*, 25: 1568-82.
Hays, S. L., A. A. Firmenich, and P. Berg. 1995. 'Complex formation in yeast double-strand break repair: participation of Rad51, Rad52, Rad55, and Rad57 proteins', *Proc Natl Acad Sci U S A*, 92: 6925-9.
He, Y. J., Z. Y. Qiao, B. Gao, X. H. Zhang, and Y. Y. Wen. 2014. 'Association between RECQL5 genetic polymorphisms and susceptibility to breast cancer', *Tumour Biol*, 35: 12201-4.
Heaphy, C. M., A. P. Subhawong, S. M. Hong, M. G. Goggins, E. A. Montgomery, E. Gabrielson, G. J. Netto, J. I. Epstein, T. L. Lotan, W. H. Westra, M. Shih Ie, C. A. Iacobuzio-Donahue, A. Maitra, Q. K. Li, C. G. Eberhart, J. M. Taube, D. Rakheja, R. J. Kurman, T. C. Wu, R. B. Roden, P. Argani, A. M. De Marzo, L. Terracciano, M. Torbenson, and A. K. Meeker. 2011. 'Prevalence of the alternative lengthening of telomeres telomere maintenance mechanism in human cancer subtypes', *Am J Pathol*, 179: 1608-15.
Heller, R. C., S. Kang, W. M. Lam, S. Chen, C. S. Chan, and S. P. Bell. 2011. 'Eukaryotic origin-dependent DNA replication in vitro reveals sequential action of DDK and S-CDK kinases', *Cell*, 146: 80-91.
Hershman, S. G., Q. Chen, J. Y. Lee, M. L. Kozak, P. Yue, L. S. Wang, and F. B. Johnson. 2008. 'Genomic distribution and functional analyses of potential G-quadruplex-forming sequences in Saccharomyces cerevisiae', *Nucleic Acids Res*, 36: 144-56.
Hirano, Y., K. Fukunaga, and K. Sugimoto. 2009. 'Rif1 and rif2 inhibit localization of tel1 to DNA ends', *Mol Cell*, 33: 312-22.
Hishiki, A., H. Hashimoto, T. Hanafusa, K. Kamei, E. Ohashi, T. Shimizu, H. Ohmori, and M. Sato. 2009. 'Structural basis for novel interactions between human translesion

synthesis polymerases and proliferating cell nuclear antigen', *J Biol Chem*, 284: 10552-60.
Hodgson, B., A. Calzada, and K. Labib. 2007. 'Mrc1 and Tof1 regulate DNA replication forks in different ways during normal S phase', *Mol Biol Cell*, 18: 3894-902.
Hoege, C., B. Pfander, G. L. Moldovan, G. Pyrowolakis, and S. Jentsch. 2002. 'RAD6-dependent DNA repair is linked to modification of PCNA by ubiquitin and SUMO', *Nature*, 419: 135-41.
Hogg, M., and E. Johansson. 2012. 'DNA polymerase epsilon', *Subcell Biochem*, 62: 237-57.
Hogg, M., P. Osterman, G. O. Bylund, R. A. Ganai, E. B. Lundstrom, A. E. Sauer-Eriksson, and E. Johansson. 2014. 'Structural basis for processive DNA synthesis by yeast DNA polymerase varepsilon', *Nat Struct Mol Biol*, 21: 49-55.
Hoggard, T., E. Shor, C. A. Muller, C. A. Nieduszynski, and C. A. Fox. 2013. 'A Link between ORC-origin binding mechanisms and origin activation time revealed in budding yeast', *PLoS Genet*, 9: e1003798.
Hu, J., L. Sun, F. Shen, Y. Chen, Y. Hua, Y. Liu, M. Zhang, Y. Hu, Q. Wang, W. Xu, F. Sun, J. Ji, J. M. Murray, A. M. Carr, and D. Kong. 2012. 'The intra-S phase checkpoint targets Dna2 to prevent stalled replication forks from reversing', *Cell*, 149: 1221-32.
Hu, Y., H. B. Tang, N. N. Liu, X. J. Tong, W. Dang, Y. M. Duan, X. H. Fu, Y. Zhang, J. Peng, F. L. Meng, and J. Q. Zhou. 2013. 'Telomerase-null survivor screening identifies novel telomere recombination regulators', *PLoS Genet*, 9: e1003208.
Huang, P., F. E. Pryde, D. Lester, R. L. Maddison, R. H. Borts, I. D. Hickson, and E. J. Louis. 2001. 'SGS1 is required for telomere elongation in the absence of telomerase', *Curr Biol*, 11: 125-9.
Huang, Q., Y. Mat-Arip, and P. Guo. 1997. 'Sequencing of a 5.5-kb DNA fragment and identification of a gene coding for a subunit of the helicase/primase complex of avian laryngotracheitis virus (ILTV)', *Virus Genes*, 15: 119-21.
Huberman, J. A., L. D. Spotila, K. A. Nawotka, S. M. el-Assouli, and L. R. Davis. 1987. 'The in vivo replication origin of the yeast 2 microns plasmid', *Cell*, 51: 473-81.
Huberman, J. A., J. G. Zhu, L. R. Davis, and C. S. Newlon. 1988. 'Close association of a DNA replication origin and an ARS element on chromosome III of the yeast, Saccharomyces cerevisiae', *Nucleic Acids Res*, 16: 6373-84.
Ivessa, A. S., B. A. Lenzmeier, J. B. Bessler, L. K. Goudsouzian, S. L. Schnakenberg, and V. A. Zakian. 2003. 'The Saccharomyces cerevisiae helicase Rrm3p facilitates replication past nonhistone protein-DNA complexes', *Mol Cell*, 12: 1525-36.
Ivessa, A. S., J. Q. Zhou, V. P. Schulz, E. K. Monson, and V. A. Zakian. 2002. 'Saccharomyces Rrm3p, a 5' to 3' DNA helicase that promotes replication fork progression through telomeric and subtelomeric DNA', *Genes Dev*, 16: 1383-96.
Ivessa, A. S., J. Q. Zhou, and V. A. Zakian. 2000. 'The Saccharomyces Pif1p DNA helicase and the highly related Rrm3p have opposite effects on replication fork progression in ribosomal DNA', *Cell*, 100: 479-89.
Jain, S., N. Sugawara, J. Lydeard, M. Vaze, N. Tanguy Le Gac, and J. E. Haber. 2009. 'A recombination execution checkpoint regulates the choice of homologous recombination pathway during DNA double-strand break repair', *Genes Dev*, 23: 291-303.
Jain, S., N. Sugawara, A. Mehta, T. Ryu, and J. E. Haber. 2016. 'Sgs1 and Mph1 Helicases Enforce the Recombination Execution Checkpoint During DNA Double-Strand Break Repair in Saccharomyces cerevisiae', *Genetics*, 203: 667-75.
Jimeno, S., R. Camarillo, F. Mejias-Navarro, M. J. Fernandez-Avila, I. Soria-Bretones, R. Prados-Carvajal, and P. Huertas. 2018. 'The Helicase PIF1 Facilitates Resection over Sequences Prone to Forming G4 Structures', *Cell Rep*, 25: 3543.

Jin, Y. H., R. Ayyagari, M. A. Resnick, D. A. Gordenin, and P. M. Burgers. 2003. 'Okazaki fragment maturation in yeast. II. Cooperation between the polymerase and 3'-5'-exonuclease activities of Pol delta in the creation of a ligatable nick', *J Biol Chem*, 278: 1626-33.

Jin, Y. H., R. Obert, P. M. Burgers, T. A. Kunkel, M. A. Resnick, and D. A. Gordenin. 2001. 'The 3'-->5' exonuclease of DNA polymerase delta can substitute for the 5' flap endonuclease Rad27/Fen1 in processing Okazaki fragments and preventing genome instability', *Proc Natl Acad Sci U S A*, 98: 5122-7.

Johansson, E., P. Garg, and P. M. Burgers. 2004. 'The Pol32 subunit of DNA polymerase delta contains separable domains for processive replication and proliferating cell nuclear antigen (PCNA) binding', *J Biol Chem*, 279: 1907-15.

Johnson C., V. K. Gali, T. S. Takahashi, and T. Kubota. 2016. ' PCNA Retention on DNA into G2/M Phase Causes Genome Instability in Cells Lacking Elg1', Cell Rep, 16(3):684-95.

Kamimura, Y., H. Masumoto, A. Sugino, and H. Araki. 1998. 'Sld2, which interacts with Dpb11 in Saccharomyces cerevisiae, is required for chromosomal DNA replication', *Mol Cell Biol*, 18: 6102-9.

Kamimura, Y., Y. S. Tak, A. Sugino, and H. Araki. 2001. 'Sld3, which interacts with Cdc45 (Sld4), functions for chromosomal DNA replication in Saccharomyces cerevisiae', *EMBO J*, 20: 2097-107.

Kanke, M., Y. Kodama, T. S. Takahashi, T. Nakagawa, and H. Masukata. 2012. 'Mcm10 plays an essential role in origin DNA unwinding after loading of the CMG components', *EMBO J*, 31: 2182-94.

Kannouche, P. L., J. Wing, and A. R. Lehmann. 2004. 'Interaction of human DNA polymerase eta with monoubiquitinated PCNA: a possible mechanism for the polymerase switch in response to DNA damage', *Mol Cell*, 14: 491-500.

Kesti, T., K. Flick, S. Keranen, J. E. Syvaoja, and C. Wittenberg. 1999. 'DNA polymerase epsilon catalytic domains are dispensable for DNA replication, DNA repair, and cell viability', *Mol Cell*, 3: 679-85.

Kobayashi, T. 2003. 'The replication fork barrier site forms a unique structure with Fob1p and inhibits the replication fork', *Mol Cell Biol*, 23: 9178-88.

Kramer, K. M., and J. E. Haber. 1993. 'New telomeres in yeast are initiated with a highly selected subset of TG1-3 repeats', *Genes Dev*, 7: 2345-56.

Kyrion, G., K. A. Boakye, and A. J. Lustig. 1992. 'C-terminal truncation of RAP1 results in the deregulation of telomere size, stability, and function in Saccharomyces cerevisiae', *Mol Cell Biol*, 12: 5159-73.

Kyrion, G., K. Liu, C. Liu, and A. J. Lustig. 1993. 'RAP1 and telomere structure regulate telomere position effects in Saccharomyces cerevisiae', *Genes Dev*, 7: 1146-59.

Lahaye, A., S. Leterme, and F. Foury. 1993. 'PIF1 DNA helicase from Saccharomyces cerevisiae. Biochemical characterization of the enzyme', *J Biol Chem*, 268: 26155-61.

Lahaye, A., H. Stahl, D. Thines-Sempoux, and F. Foury. 1991. 'PIF1: a DNA helicase in yeast mitochondria', *EMBO J*, 10: 997-1007.

Laroche, T., S. G. Martin, M. Gotta, H. C. Gorham, F. E. Pryde, E. J. Louis, and S. M. Gasser. 1998. 'Mutation of yeast Ku genes disrupts the subnuclear organization of telomeres', *Curr Biol*, 8: 653-6.

Larrivee, M., C. LeBel, and R. J. Wellinger. 2004. 'The generation of proper constitutive G-tails on yeast telomeres is dependent on the MRX complex', *Genes Dev*, 18: 1391-6.

Larrivee, M., and R. J. Wellinger. 2006. 'Telomerase- and capping-independent yeast survivors with alternate telomere states', *Nat Cell Biol*, 8: 741-7.

Lazzaro, F., V. Sapountzi, M. Granata, A. Pellicioli, M. Vaze, J. E. Haber, P. Plevani, D. Lydall, and M. Muzi-Falconi. 2008. 'Histone methyltransferase Dot1 and Rad9 inhibit single-stranded DNA accumulation at DSBs and uncapped telomeres', *EMBO J*, 27: 1502-12.

Le, S., J. K. Moore, J. E. Haber, and C. W. Greider. 1999. 'RAD50 and RAD51 define two pathways that collaborate to maintain telomeres in the absence of telomerase', *Genetics*, 152: 143-52.

Lendvay, T. S., D. K. Morris, J. Sah, B. Balasubramanian, and V. Lundblad. 1996. 'Senescence mutants of Saccharomyces cerevisiae with a defect in telomere replication identify three additional EST genes', *Genetics*, 144: 1399-412.

Leonard, A. C., and M. Mechali. 2013. 'DNA replication origins', *Cold Spring Harb Perspect Biol*, 5: a010116.

Levikova, M., and P. Cejka. 2015. 'The Saccharomyces cerevisiae Dna2 can function as a sole nuclease in the processing of Okazaki fragments in DNA replication', *Nucleic Acids Res*, 43: 7888-97.

Li, S., S. Makovets, T. Matsuguchi, J. D. Blethrow, K. M. Shokat, and E. H. Blackburn. 2009. 'Cdk1-dependent phosphorylation of Cdc13 coordinates telomere elongation during cell-cycle progression', *Cell*, 136: 50-61.

Li, X., and W. D. Heyer. 2009. 'RAD54 controls access to the invading 3'-OH end after RAD51-mediated DNA strand invasion in homologous recombination in Saccharomyces cerevisiae', *Nucleic Acids Res*, 37: 638-46.

Lillard-Wetherell, K., A. Machwe, G. T. Langland, K. A. Combs, G. K. Behbehani, S. A. Schonberg, J. German, J. J. Turchi, D. K. Orren, and J. Groden. 2004. 'Association and regulation of the BLM helicase by the telomere proteins TRF1 and TRF2', *Hum Mol Genet*, 13: 1919-32.

Lim, D. S., and P. Hasty. 1996. 'A mutation in mouse rad51 results in an early embryonic lethal that is suppressed by a mutation in p53', *Mol Cell Biol*, 16: 7133-43.

Lin, C. Y., H. H. Chang, K. J. Wu, S. F. Tseng, C. C. Lin, C. P. Lin, and S. C. Teng. 2005. 'Extrachromosomal telomeric circles contribute to Rad52-, Rad50-, and polymerase delta-mediated telomere-telomere recombination in Saccharomyces cerevisiae', *Eukaryot Cell*, 4: 327-36.

Lin, J., H. Ly, A. Hussain, M. Abraham, S. Pearl, Y. Tzfati, T. G. Parslow, and E. H. Blackburn. 2004. 'A universal telomerase RNA core structure includes structured motifs required for binding the telomerase reverse transcriptase protein', *Proc Natl Acad Sci U S A*, 101: 14713-8.

Lingner, J., T. R. Cech, T. R. Hughes, and V. Lundblad. 1997. 'Three Ever Shorter Telomere (EST) genes are dispensable for in vitro yeast telomerase activity', *Proc Natl Acad Sci U S A*, 94: 11190-5.

Linskens, M. H., and J. A. Huberman. 1988. 'Organization of replication of ribosomal DNA in Saccharomyces cerevisiae', *Mol Cell Biol*, 8: 4927-35.

Liu, B., J. Hu, J. Wang, and D. Kong. 2017. 'Direct Visualization of RNA-DNA Primer Removal from Okazaki Fragments Provides Support for Flap Cleavage and Exonucleolytic Pathways in Eukaryotic Cells', *J Biol Chem*, 292: 4777-88.

Liu, B., J. Wang, N. Yaffe, M. E. Lindsay, Z. Zhao, A. Zick, J. Shlomai, and P. T. Englund. 2009. 'Trypanosomes have six mitochondrial DNA helicases with one controlling kinetoplast maxicircle replication', *Mol Cell*, 35: 490-501.

Liu, B., J. Wang, G. Yildirir, and P. T. Englund. 2009. 'TbPIF5 is a Trypanosoma brucei mitochondrial DNA helicase involved in processing of minicircle Okazaki fragments', *PLoS Pathog*, 5: e1000589.

Liu, B., G. Yildirir, J. Wang, G. Tolun, J. D. Griffith, and P. T. Englund. 2010. 'TbPIF1, a Trypanosoma brucei mitochondrial DNA helicase, is essential for kinetoplast minicircle replication', *J Biol Chem*, 285: 7056-66.

Livengood, A. J., A. J. Zaug, and T. R. Cech. 2002. 'Essential regions of Saccharomyces cerevisiae telomerase RNA: separate elements for Est1p and Est2p interaction', *Mol Cell Biol*, 22: 2366-74.

Llorente, B., and L. S. Symington. 2004. 'The Mre11 nuclease is not required for 5' to 3' resection at multiple HO-induced double-strand breaks', *Mol Cell Biol*, 24: 9682-94.

Longhese, M. P. 2008. 'DNA damage response at functional and dysfunctional telomeres', *Genes Dev*, 22: 125-40.

Lopes, J., A. Piazza, R. Bermejo, B. Kriegsman, A. Colosio, M. P. Teulade-Fichou, M. Foiani, and A. Nicolas. 2011. 'G-quadruplex-induced instability during leading-strand replication', *EMBO J*, 30: 4033-46.

Lou, H., M. Komata, Y. Katou, Z. Guan, C. C. Reis, M. Budd, K. Shirahige, and J. L. Campbell. 2008. 'Mrc1 and DNA polymerase epsilon function together in linking DNA replication and the S phase checkpoint', *Mol Cell*, 32: 106-17.

Luciano, P., S. Coulon, V. Faure, Y. Corda, J. Bos, S. J. Brill, E. Gilson, M. N. Simon, and V. Geli. 2012. 'RPA facilitates telomerase activity at chromosome ends in budding and fission yeasts', *EMBO J*, 31: 2034-46.

Lue, N. F., J. Chan, W. E. Wright, and J. Hurwitz. 2014. 'The CDC13-STN1-TEN1 complex stimulates Pol alpha activity by promoting RNA priming and primase-to-polymerase switch', *Nat Commun*, 5: 5762.

Lundblad, V., and E. H. Blackburn. 1993. 'An alternative pathway for yeast telomere maintenance rescues est1- senescence', *Cell*, 73: 347-60.

Lundblad, V., and J. W. Szostak. 1989. 'A mutant with a defect in telomere elongation leads to senescence in yeast', *Cell*, 57: 633-43.

Lydeard, J. R., S. Jain, M. Yamaguchi, and J. E. Haber. 2007. 'Break-induced replication and telomerase-independent telomere maintenance require Pol32', *Nature*, 448: 820-3.

Lydeard, J. R., Z. Lipkin-Moore, S. Jain, V. V. Eapen, and J. E. Haber. 2010. 'Sgs1 and exo1 redundantly inhibit break-induced replication and de novo telomere addition at broken chromosome ends', *PLoS Genet*, 6: e1000973.

Lydeard, J. R., Z. Lipkin-Moore, Y. J. Sheu, B. Stillman, P. M. Burgers, and J. E. Haber. 2010. 'Break-induced replication requires all essential DNA replication factors except those specific for pre-RC assembly', *Genes Dev*, 24: 1133-44.

Mailand, N., I. Gibbs-Seymour, and S. Bekker-Jensen. 2013. 'Regulation of PCNA-protein interactions for genome stability', *Nat Rev Mol Cell Biol*, 14: 269-82.

Makovets, S., and E. H. Blackburn. 2009. 'DNA damage signalling prevents deleterious telomere addition at DNA breaks', *Nat Cell Biol*, 11: 1383-6.

Makovets, S., I. Herskowitz, and E. H. Blackburn. 2004. 'Anatomy and dynamics of DNA replication fork movement in yeast telomeric regions', *Mol Cell Biol*, 24: 4019-31.

Malkova, A., M. L. Naylor, M. Yamaguchi, G. Ira, and J. E. Haber. 2005. 'RAD51-dependent break-induced replication differs in kinetics and checkpoint responses from RAD51-mediated gene conversion', *Mol Cell Biol*, 25: 933-44.

Mangahas, J. L., M. K. Alexander, L. L. Sandell, and V. A. Zakian. 2001. 'Repair of chromosome ends after telomere loss in Saccharomyces', *Mol Biol Cell*, 12: 4078-89.

Marcand, S., B. Pardo, A. Gratias, S. Cahun, and I. Callebaut. 2008. 'Multiple pathways inhibit NHEJ at telomeres', *Genes Dev*, 22: 1153-8.

Maringele, L., and D. Lydall. 2004a. 'EXO1 plays a role in generating type I and type II survivors in budding yeast', *Genetics*, 166: 1641-9.

———. 2004b. 'Telomerase- and recombination-independent immortalization of budding yeast', *Genes Dev*, 18: 2663-75.
Masai, H., C. Taniyama, K. Ogino, E. Matsui, N. Kakusho, S. Matsumoto, J. M. Kim, A. Ishii, T. Tanaka, T. Kobayashi, K. Tamai, K. Ohtani, and K. Arai. 2006. 'Phosphorylation of MCM4 by Cdc7 kinase facilitates its interaction with Cdc45 on the chromatin', *J Biol Chem*, 281: 39249-61.
Masuda, Y., R. Kanao, K. Kaji, H. Ohmori, F. Hanaoka, and C. Masutani. 2015. 'Different types of interaction between PCNA and PIP boxes contribute to distinct cellular functions of Y-family DNA polymerases', *Nucleic Acids Res*, 43: 7898-910.
Masumoto, H., S. Muramatsu, Y. Kamimura, and H. Araki. 2002. 'S-Cdk-dependent phosphorylation of Sld2 essential for chromosomal DNA replication in budding yeast', *Nature*, 415: 651-5.
Mateyak, M. K., and V. A. Zakian. 2006. 'Human PIF helicase is cell cycle regulated and associates with telomerase', *Cell Cycle*, 5: 2796-804.
Matsuda, K., M. Makise, Y. Sueyasu, M. Takehara, T. Asano, and T. Mizushima. 2007. 'Yeast two-hybrid analysis of the origin recognition complex of Saccharomyces cerevisiae: interaction between subunits and identification of binding proteins', *FEMS Yeast Res*, 7: 1263-9.
Matsuo, Y., I. Sakane, Y. Takizawa, M. Takahashi, and H. Kurumizaka. 2006. 'Roles of the human Rad51 L1 and L2 loops in DNA binding', *FEBS J*, 273: 3148-59.
Mayle, R., I. M. Campbell, C. R. Beck, Y. Yu, M. Wilson, C. A. Shaw, L. Bjergbaek, J. R. Lupski, and G. Ira. 2015. 'DNA REPAIR. Mus81 and converging forks limit the mutagenicity of replication fork breakage', *Science*, 349: 742-7.
McClintock, B. 1939. 'The Behavior in Successive Nuclear Divisions of a Chromosome Broken at Meiosis', *Proc Natl Acad Sci U S A*, 25: 405-16.
McDonald, K. R., N. Sabouri, C. J. Webb, and V. A. Zakian. 2014. 'The Pif1 family helicase Pfh1 facilitates telomere replication and has an RPA-dependent role during telomere lengthening', *DNA Repair (Amst)*, 24: 80-86.
McEachern, M. J., and E. H. Blackburn. 1994. 'A conserved sequence motif within the exceptionally diverse telomeric sequences of budding yeasts', *Proc Natl Acad Sci U S A*, 91: 3453-7.
McEachern, M. J., and J. E. Haber. 2006. 'Break-induced replication and recombinational telomere elongation in yeast', *Annu Rev Biochem*, 75: 111-35.
Mellor, J., W. Jiang, M. Funk, J. Rathjen, C. A. Barnes, T. Hinz, J. H. Hegemann, and P. Philippsen. 1990. 'CPF1, a yeast protein which functions in centromeres and promoters', *EMBO J*, 9: 4017-26.
Mendoza, O., N. M. Gueddouda, J. B. Boule, A. Bourdoncle, and J. L. Mergny. 2015. 'A fluorescence-based helicase assay: application to the screening of G-quadruplex ligands', *Nucleic Acids Res*, 43: e71.
Mimitou, E. P., and L. S. Symington. 2009. 'DNA end resection: many nucleases make light work', *DNA Repair (Amst)*, 8: 983-95.
———. 2010. 'Ku prevents Exo1 and Sgs1-dependent resection of DNA ends in the absence of a functional MRX complex or Sae2', *EMBO J*, 29: 3358-69.
Min, J., W. E. Wright, and J. W. Shay. 2017. 'Alternative Lengthening of Telomeres Mediated by Mitotic DNA Synthesis Engages Break-Induced Replication Processes', *Mol Cell Biol*, 37.
Mitchell, M. T., J. S. Smith, M. Mason, S. Harper, D. W. Speicher, F. B. Johnson, and E. Skordalakes. 2010. 'Cdc13 N-terminal dimerization, DNA binding, and telomere length regulation', *Mol Cell Biol*, 30: 5325-34.

Mohammad, J. B., M. Wallgren, and N. Sabouri. 2018. 'The Pif1 signature motif of Pfh1 is necessary for both protein displacement and helicase unwinding activities, but is dispensable for strand-annealing activity', *Nucleic Acids Res*, 46: 8516-31.
Mohanty, B. K., N. K. Bairwa, and D. Bastia. 2006. 'The Tof1p-Csm3p protein complex counteracts the Rrm3p helicase to control replication termination of Saccharomyces cerevisiae', *Proc Natl Acad Sci U S A*, 103: 897-902.
Moldovan, G. L., B. Pfander, and S. Jentsch. 2007. 'PCNA, the maestro of the replication fork', *Cell*, 129: 665-79.
Mozdy, A. D., and T. R. Cech. 2006. 'Low abundance of telomerase in yeast: implications for telomerase haploinsufficiency', *RNA*, 12: 1721-37.
Muller, H. J. 1938. 'The remaking of chromosomes. ', *The Collecting Net.*: 181–95, 98.
Muramatsu, S., K. Hirai, Y. S. Tak, Y. Kamimura, and H. Araki. 2010. 'CDK-dependent complex formation between replication proteins Dpb11, Sld2, Pol (epsilon}, and GINS in budding yeast', *Genes Dev*, 24: 602-12.
Murnane, J. P. 2012. 'Telomere dysfunction and chromosome instability', *Mutat Res*, 730: 28-36.
Myler, L. R., I. F. Gallardo, Y. Zhou, F. Gong, S. H. Yang, M. S. Wold, K. M. Miller, T. T. Paull, and I. J. Finkelstein. 2016. 'Single-molecule imaging reveals the mechanism of Exo1 regulation by single-stranded DNA binding proteins', *Proc Natl Acad Sci U S A*, 113: E1170-9.
Myung, K., C. Chen, and R. D. Kolodner. 2001. 'Multiple pathways cooperate in the suppression of genome instability in Saccharomyces cerevisiae', *Nature*, 411: 1073-6.
Nabetani, A., O. Yokoyama, and F. Ishikawa. 2004. 'Localization of hRad9, hHus1, hRad1, and hRad17 and caffeine-sensitive DNA replication at the alternative lengthening of telomeres-associated promyelocytic leukemia body', *J Biol Chem*, 279: 25849-57.
Navas, T. A., Z. Zhou, and S. J. Elledge. 1995. 'DNA polymerase epsilon links the DNA replication machinery to the S phase checkpoint', *Cell*, 80: 29-39.
Neale, M. J., J. Pan, and S. Keeney. 2005. 'Endonucleolytic processing of covalent protein-linked DNA double-strand breaks', *Nature*, 436: 1053-7.
Negrini, S., V. Ribaud, A. Bianchi, and D. Shore. 2007. 'DNA breaks are masked by multiple Rap1 binding in yeast: implications for telomere capping and telomerase regulation', *Genes Dev*, 21: 292-302.
New, J. H., and S. C. Kowalczykowski. 2002. 'Rad52 protein has a second stimulatory role in DNA strand exchange that complements replication protein-A function', *J Biol Chem*, 277: 26171-6.
New, J. H., T. Sugiyama, E. Zaitseva, and S. C. Kowalczykowski. 1998. 'Rad52 protein stimulates DNA strand exchange by Rad51 and replication protein A', *Nature*, 391: 407-10.
Ngo, G. H., and D. Lydall. 2015. 'The 9-1-1 checkpoint clamp coordinates resection at DNA double strand breaks', *Nucleic Acids Res*, 43: 5017-32.
Nimonkar, A. V., J. Genschel, E. Kinoshita, P. Polaczek, J. L. Campbell, C. Wyman, P. Modrich, and S. C. Kowalczykowski. 2011. 'BLM-DNA2-RPA-MRN and EXO1-BLM-RPA-MRN constitute two DNA end resection machineries for human DNA break repair', *Genes Dev*, 25: 350-62.
Niu, H., W. H. Chung, Z. Zhu, Y. Kwon, W. Zhao, P. Chi, R. Prakash, C. Seong, D. Liu, L. Lu, G. Ira, and P. Sung. 2010. 'Mechanism of the ATP-dependent DNA end-resection machinery from Saccharomyces cerevisiae', *Nature*, 467: 108-11.
O'Sullivan, R. J., N. Arnoult, D. H. Lackner, L. Oganesian, C. Haggblom, A. Corpet, G. Almouzni, and J. Karlseder. 2014. 'Rapid induction of alternative lengthening of

telomeres by depletion of the histone chaperone ASF1', *Nat Struct Mol Biol*, 21: 167-74.
Obodo, U. C., E. A. Epum, M. H. Platts, J. Seloff, N. A. Dahlson, S. M. Velkovsky, S. R. Paul, and K. L. Friedman. 2016. 'Endogenous Hot Spots of De Novo Telomere Addition in the Yeast Genome Contain Proximal Enhancers That Bind Cdc13', *Mol Cell Biol*, 36: 1750-63.
Ohya, T., Y. Kawasaki, S. Hiraga, S. Kanbara, K. Nakajo, N. Nakashima, A. Suzuki, and A. Sugino. 2002. 'The DNA polymerase domain of pol(epsilon) is required for rapid, efficient, and highly accurate chromosomal DNA replication, telomere length maintenance, and normal cell senescence in Saccharomyces cerevisiae', *J Biol Chem*, 277: 28099-108.
Olovnikov, A. M. 1971. '[Principle of marginotomy in template synthesis of polynucleotides]', *Dokl Akad Nauk SSSR*, 201: 1496-9.
Ortega, J., J. Y. Li, S. Lee, D. Tong, L. Gu, and G. M. Li. 2015. 'Phosphorylation of PCNA by EGFR inhibits mismatch repair and promotes misincorporation during DNA synthesis', *Proc Natl Acad Sci U S A*, 112: 5667-72.
Osmundson, J. S., J. Kumar, R. Yeung, and D. J. Smith. 2017. 'Pif1-family helicases cooperatively suppress widespread replication-fork arrest at tRNA genes', *Nat Struct Mol Biol*, 24: 162-70.
Osterhage, J. L., J. M. Talley, and K. L. Friedman. 2006. 'Proteasome-dependent degradation of Est1p regulates the cell cycle-restricted assembly of telomerase in Saccharomyces cerevisiae', *Nat Struct Mol Biol*, 13: 720-8.
Ouenzar, F., M. Lalonde, H. Laprade, G. Morin, F. Gallardo, S. Tremblay-Belzile, and P. Chartrand. 2017. 'Cell cycle-dependent spatial segregation of telomerase from sites of DNA damage', *J Cell Biol*, 216: 2355-71.
Ozer, O., R. Bhowmick, Y. Liu, and I. D. Hickson. 2018. 'Human cancer cells utilize mitotic DNA synthesis to resist replication stress at telomeres regardless of their telomere maintenance mechanism', *Oncotarget*, 9: 15836-46.
Paeschke, K., M. L. Bochman, P. D. Garcia, P. Cejka, K. L. Friedman, S. C. Kowalczykowski, and V. A. Zakian. 2013. 'Pif1 family helicases suppress genome instability at G-quadruplex motifs', *Nature*, 497: 458-62.
Paeschke, K., J. A. Capra, and V. A. Zakian. 2011. 'DNA replication through G-quadruplex motifs is promoted by the Saccharomyces cerevisiae Pif1 DNA helicase', *Cell*, 145: 678-91.
Palladino, F., T. Laroche, E. Gilson, A. Axelrod, L. Pillus, and S. M. Gasser. 1993. 'SIR3 and SIR4 proteins are required for the positioning and integrity of yeast telomeres', *Cell*, 75: 543-55.
Papouli, E., S. Chen, A. A. Davies, D. Huttner, L. Krejci, P. Sung, and H. D. Ulrich. 2005. 'Crosstalk between SUMO and ubiquitin on PCNA is mediated by recruitment of the helicase Srs2p', *Mol Cell*, 19: 123-33.
Pardo, B., and S. Marcand. 2005. 'Rap1 prevents telomere fusions by nonhomologous end joining', *EMBO J*, 24: 3117-27.
Parker, J. L., A. Bucceri, A. A. Davies, K. Heidrich, H. Windecker, and H. D. Ulrich. 2008. 'SUMO modification of PCNA is controlled by DNA', *EMBO J*, 27: 2422-31.
Pavlov, Y. I., P. V. Shcherbakova, and T. A. Kunkel. 2001. 'In vivo consequences of putative active site mutations in yeast DNA polymerases alpha, epsilon, delta, and zeta', *Genetics*, 159: 47-64.
Pennock, E., K. Buckley, and V. Lundblad. 2001. 'Cdc13 delivers separate complexes to the telomere for end protection and replication', *Cell*, 104: 387-96.

Perera, R. L., R. Torella, S. Klinge, M. L. Kilkenny, J. D. Maman, and L. Pellegrini. 2013. 'Mechanism for priming DNA synthesis by yeast DNA polymerase alpha', *Elife*, 2: e00482.

Perez-Arnaiz, P., I. Bruck, and D. L. Kaplan. 2016. 'Mcm10 coordinates the timely assembly and activation of the replication fork helicase', *Nucleic Acids Res*, 44: 315-29.

Peterson, S. E., A. E. Stellwagen, S. J. Diede, M. S. Singer, Z. W. Haimberger, C. O. Johnson, M. Tzoneva, and D. E. Gottschling. 2001. 'The function of a stem-loop in telomerase RNA is linked to the DNA repair protein Ku', *Nat Genet*, 27: 64-7.

Pfander, B., and J. F. Diffley. 2011. 'Dpb11 coordinates Mec1 kinase activation with cell cycle-regulated Rad9 recruitment', *EMBO J*, 30: 4897-907.

Pfander, B., G. L. Moldovan, M. Sacher, C. Hoege, and S. Jentsch. 2005. 'SUMO-modified PCNA recruits Srs2 to prevent recombination during S phase', *Nature*, 436: 428-33.

Pfingsten, J. S., K. J. Goodrich, C. Taabazuing, F. Ouenzar, P. Chartrand, and T. R. Cech. 2012. 'Mutually exclusive binding of telomerase RNA and DNA by Ku alters telomerase recruitment model', *Cell*, 148: 922-32.

Phillips, J. A., A. Chan, K. Paeschke, and V. A. Zakian. 2015. 'The pif1 helicase, a negative regulator of telomerase, acts preferentially at long telomeres', *PLoS Genet*, 11: e1005186.

Pickett, H. A., and R. R. Reddel. 2015. 'Molecular mechanisms of activity and derepression of alternative lengthening of telomeres', *Nat Struct Mol Biol*, 22: 875-80.

Pike, J. E., P. M. Burgers, J. L. Campbell, and R. A. Bambara. 2009. 'Pif1 helicase lengthens some Okazaki fragment flaps necessitating Dna2 nuclease/helicase action in the two-nuclease processing pathway', *J Biol Chem*, 284: 25170-80.

Pinter, S. F., S. D. Aubert, and V. A. Zakian. 2008. 'The Schizosaccharomyces pombe Pfh1p DNA helicase is essential for the maintenance of nuclear and mitochondrial DNA', *Mol Cell Biol*, 28: 6594-608.

Porter, S. E., P. W. Greenwell, K. B. Ritchie, and T. D. Petes. 1996. 'The DNA-binding protein Hdf1p (a putative Ku homologue) is required for maintaining normal telomere length in Saccharomyces cerevisiae', *Nucleic Acids Res*, 24: 582-5.

Potts, P. R., and H. Yu. 2007. 'The SMC5/6 complex maintains telomere length in ALT cancer cells through SUMOylation of telomere-binding proteins', *Nat Struct Mol Biol*, 14: 581-90.

Prasad, T. K., C. C. Yeykal, and E. C. Greene. 2006. 'Visualizing the assembly of human Rad51 filaments on double-stranded DNA', *J Mol Biol*, 363: 713-28.

Prestel, A., N. Wichmann, J. M. Martins, R. Marabini, N. Kassem, S. S. Broendum, M. Otterlei, O. Nielsen, M. Willemoes, M. Ploug, W. Boomsma, and B. B. Kragelund. 2019. 'The PCNA interaction motifs revisited: thinking outside the PIP-box', *Cell Mol Life Sci*.

Puglisi, A., A. Bianchi, L. Lemmens, P. Damay, and D. Shore. 2008. 'Distinct roles for yeast Stn1 in telomere capping and telomerase inhibition', *EMBO J*, 27: 2328-39.

Putnam, C. D., V. Pennaneach, and R. D. Kolodner. 2004. 'Chromosome healing through terminal deletions generated by de novo telomere additions in Saccharomyces cerevisiae', *Proc Natl Acad Sci U S A*, 101: 13262-7.

Qi, H., and V. A. Zakian. 2000. 'The Saccharomyces telomere-binding protein Cdc13p interacts with both the catalytic subunit of DNA polymerase alpha and the telomerase-associated est1 protein', *Genes Dev*, 14: 1777-88.

Qi, Y., and X. Zhou. 2014. 'Haplotype analysis of RECQL5 gene and laryngeal cancer', *Tumour Biol*, 35: 2669-73.

Qiao, F., and T. R. Cech. 2008. 'Triple-helix structure in telomerase RNA contributes to catalysis', *Nat Struct Mol Biol*, 15: 634-40.

Qiu, J., Y. Qian, P. Frank, U. Wintersberger, and B. Shen. 1999. 'Saccharomyces cerevisiae RNase H(35) functions in RNA primer removal during lagging-strand DNA synthesis, most efficiently in cooperation with Rad27 nuclease', *Mol Cell Biol*, 19: 8361-71.

Quan, Y., Y. Xia, L. Liu, J. Cui, Z. Li, Q. Cao, X. S. Chen, J. L. Campbell, and H. Lou. 2015. 'Cell-Cycle-Regulated Interaction between Mcm10 and Double Hexameric Mcm2-7 Is Required for Helicase Splitting and Activation during S Phase', *Cell Rep*, 13: 2576-86.

Ramanagoudr-Bhojappa, R., S. Chib, A. K. Byrd, S. Aarattuthodiyil, M. Pandey, S. S. Patel, and K. D. Raney. 2013. 'Yeast Pif1 helicase exhibits a one-base-pair stepping mechanism for unwinding duplex DNA', *J Biol Chem*, 288: 16185-95.

Ramer, M. D., E. S. Suman, H. Richter, K. Stanger, M. Spranger, N. Bieberstein, and B. P. Duncker. 2013. 'Dbf4 and Cdc7 proteins promote DNA replication through interactions with distinct Mcm2-7 protein subunits', *J Biol Chem*, 288: 14926-35.

Rathmell, W. K., and G. Chu. 1994. 'Involvement of the Ku autoantigen in the cellular response to DNA double-strand breaks', *Proc Natl Acad Sci U S A*, 91: 7623-7.

Reddel, R. R. 2014. 'Telomere maintenance mechanisms in cancer: clinical implications', *Curr Pharm Des*, 20: 6361-74.

Resnick, M. A., and P. Martin. 1976. 'The repair of double-strand breaks in the nuclear DNA of Saccharomyces cerevisiae and its genetic control', *Mol Gen Genet*, 143: 119-29.

Ribeyre, C., J. Lopes, J. B. Boule, A. Piazza, A. Guedin, V. A. Zakian, J. L. Mergny, and A. Nicolas. 2009. 'The yeast Pif1 helicase prevents genomic instability caused by G-quadruplex-forming CEB1 sequences in vivo', *PLoS Genet*, 5: e1000475.

Ricke, R. M., and A. K. Bielinsky. 2004. 'Mcm10 regulates the stability and chromatin association of DNA polymerase-alpha', *Mol Cell*, 16: 173-85.

Rossi, S. E., A. Ajazi, W. Carotenuto, M. Foiani, and M. Giannattasio. 2015. 'Rad53-Mediated Regulation of Rrm3 and Pif1 DNA Helicases Contributes to Prevention of Aberrant Fork Transitions under Replication Stress', *Cell Rep*, 13: 80-92.

Rossi, S. E., M. Foiani, and M. Giannattasio. 2018. 'Dna2 processes behind the fork long ssDNA flaps generated by Pif1 and replication-dependent strand displacement', *Nat Commun*, 9: 4830.

Roumelioti, F. M., S. K. Sotiriou, V. Katsini, M. Chiourea, T. D. Halazonetis, and S. Gagos. 2016. 'Alternative lengthening of human telomeres is a conservative DNA replication process with features of break-induced replication', *EMBO Rep*, 17: 1731-37.

Ryu, G. H., H. Tanaka, D. H. Kim, J. H. Kim, S. H. Bae, Y. N. Kwon, J. S. Rhee, S. A. MacNeill, and Y. S. Seo. 2004. 'Genetic and biochemical analyses of Pfh1 DNA helicase function in fission yeast', *Nucleic Acids Res*, 32: 4205-16.

Sabouri, N., K. R. McDonald, C. J. Webb, I. M. Cristea, and V. A. Zakian. 2012. 'DNA replication through hard-to-replicate sites, including both highly transcribed RNA Pol II and Pol III genes, requires the S. pombe Pfh1 helicase', *Genes Dev*, 26: 581-93.

Sabouri, N., J. Viberg, D. K. Goyal, E. Johansson, and A. Chabes. 2008. 'Evidence for lesion bypass by yeast replicative DNA polymerases during DNA damage', *Nucleic Acids Res*, 36: 5660-7.

Saini, N., S. Ramakrishnan, R. Elango, S. Ayyar, Y. Zhang, A. Deem, G. Ira, J. E. Haber, K. S. Lobachev, and A. Malkova. 2013. 'Migrating bubble during break-induced replication drives conservative DNA synthesis', *Nature*, 502: 389-92.

Sakofsky, C. J., S. A. Roberts, E. Malc, P. A. Mieczkowski, M. A. Resnick, D. A. Gordenin, and A. Malkova. 2014. 'Break-induced replication is a source of mutation clusters underlying kataegis', *Cell Rep*, 7: 1640-48.

Sanchez, Y., J. Bachant, H. Wang, F. Hu, D. Liu, M. Tetzlaff, and S. J. Elledge. 1999. 'Control of the DNA damage checkpoint by chk1 and rad53 protein kinases through distinct mechanisms', *Science*, 286: 1166-71.
Sandell, L. L., and V. A. Zakian. 1993. 'Loss of a yeast telomere: arrest, recovery, and chromosome loss', *Cell*, 75: 729-39.
Sanders, C. M. 2010. 'Human Pif1 helicase is a G-quadruplex DNA-binding protein with G-quadruplex DNA-unwinding activity', *Biochem J*, 430: 119-28.
Schmidt, K. H., K. L. Derry, and R. D. Kolodner. 2002. 'Saccharomyces cerevisiae RRM3, a 5' to 3' DNA helicase, physically interacts with proliferating cell nuclear antigen', *J Biol Chem*, 277: 45331-7.
Schmidt, K. H., and R. D. Kolodner. 2006. 'Suppression of spontaneous genome rearrangements in yeast DNA helicase mutants', *Proc Natl Acad Sci U S A*, 103: 18196-201.
Schramke, V., P. Luciano, V. Brevet, S. Guillot, Y. Corda, M. P. Longhese, E. Gilson, and V. Geli. 2004. 'RPA regulates telomerase action by providing Est1p access to chromosome ends', *Nat Genet*, 36: 46-54.
Schulz, V. P., and V. A. Zakian. 1994. 'The saccharomyces PIF1 DNA helicase inhibits telomere elongation and de novo telomere formation', *Cell*, 76: 145-55.
Sengupta, S., F. van Deursen, G. de Piccoli, and K. Labib. 2013. 'Dpb2 integrates the leading-strand DNA polymerase into the eukaryotic replisome', *Curr Biol*, 23: 543-52.
Seto, A. G., A. J. Livengood, Y. Tzfati, E. H. Blackburn, and T. R. Cech. 2002. 'A bulged stem tethers Est1p to telomerase RNA in budding yeast', *Genes Dev*, 16: 2800-12.
Shampay, J., J. W. Szostak, and E. H. Blackburn. 1984. 'DNA sequences of telomeres maintained in yeast', *Nature*, 310: 154-7.
Sheu, Y. J., and B. Stillman. 2006. 'Cdc7-Dbf4 phosphorylates MCM proteins via a docking site-mediated mechanism to promote S phase progression', *Mol Cell*, 24: 101-13.
———. 2010. 'The Dbf4-Cdc7 kinase promotes S phase by alleviating an inhibitory activity in Mcm4', *Nature*, 463: 113-7.
Shi, T., R. D. Bunker, S. Mattarocci, C. Ribeyre, M. Faty, H. Gut, A. Scrima, U. Rass, S. M. Rubin, D. Shore, and N. H. Thoma. 2013. 'Rif1 and Rif2 shape telomere function and architecture through multivalent Rap1 interactions', *Cell*, 153: 1340-53.
Shinohara, A., and T. Ogawa. 1998. 'Stimulation by Rad52 of yeast Rad51-mediated recombination', *Nature*, 391: 404-7.
Simon, A. C., J. C. Zhou, R. L. Perera, F. van Deursen, C. Evrin, M. E. Ivanova, M. L. Kilkenny, L. Renault, S. Kjaer, D. Matak-Vinkovic, K. Labib, A. Costa, and L. Pellegrini. 2014. 'A Ctf4 trimer couples the CMG helicase to DNA polymerase alpha in the eukaryotic replisome', *Nature*, 510: 293-97.
Singer, M. S., and D. E. Gottschling. 1994. 'TLC1: template RNA component of Saccharomyces cerevisiae telomerase', *Science*, 266: 404-9.
Slade, D. 2018. 'Maneuvers on PCNA Rings during DNA Replication and Repair', *Genes (Basel)*, 9.
Smith, C. E., B. Llorente, and L. S. Symington. 2007. 'Template switching during break-induced replication', *Nature*, 447: 102-5.
Snow, B. E., M. Mateyak, J. Paderova, A. Wakeham, C. Iorio, V. Zakian, J. Squire, and L. Harrington. 2007. 'Murine Pif1 interacts with telomerase and is dispensable for telomere function in vivo', *Mol Cell Biol*, 27: 1017-26.
Sobinoff, A. P., J. A. Allen, A. A. Neumann, S. F. Yang, M. E. Walsh, J. D. Henson, R. R. Reddel, and H. A. Pickett. 2017. 'BLM and SLX4 play opposing roles in recombination-dependent replication at human telomeres', *EMBO J*, 36: 2907-19.

Song, B., and P. Sung. 2000. 'Functional interactions among yeast Rad51 recombinase, Rad52 mediator, and replication protein A in DNA strand exchange', *J Biol Chem*, 275: 15895-904.

Sotiriou, S. K., I. Kamileri, N. Lugli, K. Evangelou, C. Da-Re, F. Huber, L. Padayachy, S. Tardy, N. L. Nicati, S. Barriot, F. Ochs, C. Lukas, J. Lukas, V. G. Gorgoulis, L. Scapozza, and T. D. Halazonetis. 2016. 'Mammalian RAD52 Functions in Break-Induced Replication Repair of Collapsed DNA Replication Forks', *Mol Cell*, 64: 1127-34.

Speck, C., Z. Chen, H. Li, and B. Stillman. 2005. 'ATPase-dependent cooperative binding of ORC and Cdc6 to origin DNA', *Nat Struct Mol Biol*, 12: 965-71.

Stauffer, M. E., and W. J. Chazin. 2004. 'Physical interaction between replication protein A and Rad51 promotes exchange on single-stranded DNA', *J Biol Chem*, 279: 25638-45.

Stavropoulos, D. J., P. S. Bradshaw, X. Li, I. Pasic, K. Truong, M. Ikura, M. Ungrin, and M. S. Meyn. 2002. 'The Bloom syndrome helicase BLM interacts with TRF2 in ALT cells and promotes telomeric DNA synthesis', *Hum Mol Genet*, 11: 3135-44.

Steinacher, R., F. Osman, J. Z. Dalgaard, A. Lorenz, and M. C. Whitby. 2012. 'The DNA helicase Pfh1 promotes fork merging at replication termination sites to ensure genome stability', *Genes Dev*, 26: 594-602.

Stellwagen, A. E., Z. W. Haimberger, J. R. Veatch, and D. E. Gottschling. 2003. 'Ku interacts with telomerase RNA to promote telomere addition at native and broken chromosome ends', *Genes Dev*, 17: 2384-95.

Stelter, P., and H. D. Ulrich. 2003. 'Control of spontaneous and damage-induced mutagenesis by SUMO and ubiquitin conjugation', *Nature*, 425: 188-91.

Strecker, J., S. Stinus, M. P. Caballero, R. K. Szilard, M. Chang, and D. Durocher. 2017. 'A sharp Pif1-dependent threshold separates DNA double-strand breaks from critically short telomeres', *Elife*, 6.

Sugawara, N., X. Wang, and J. E. Haber. 2003. 'In vivo roles of Rad52, Rad54, and Rad55 proteins in Rad51-mediated recombination', *Mol Cell*, 12: 209-19.

Sun, J., C. Evrin, S. A. Samel, A. Fernandez-Cid, A. Riera, H. Kawakami, B. Stillman, C. Speck, and H. Li. 2013. 'Cryo-EM structure of a helicase loading intermediate containing ORC-Cdc6-Cdt1-MCM2-7 bound to DNA', *Nat Struct Mol Biol*, 20: 944-51.

Sun, J., Y. Shi, R. E. Georgescu, Z. Yuan, B. T. Chait, H. Li, and M. E. O'Donnell. 2015. 'The architecture of a eukaryotic replisome', *Nat Struct Mol Biol*, 22: 976-82.

Sun, J., Y. Wang, Y. Xia, Y. Xu, T. Ouyang, J. Li, T. Wang, Z. Fan, T. Fan, B. Lin, H. Lou, and Y. Xie. 2015. 'Mutations in RECQL Gene Are Associated with Predisposition to Breast Cancer', *PLoS Genet*, 11: e1005228.

Sung, P. 1997. 'Function of yeast Rad52 protein as a mediator between replication protein A and the Rad51 recombinase', *J Biol Chem*, 272: 28194-7.

Syed, S., C. Desler, L. J. Rasmussen, and K. H. Schmidt. 2016. 'A Novel Rrm3 Function in Restricting DNA Replication via an Orc5-Binding Domain Is Genetically Separable from Rrm3 Function as an ATPase/Helicase in Facilitating Fork Progression', *PLoS Genet*, 12: e1006451.

Szostak, J. W., and E. H. Blackburn. 1982. 'Cloning yeast telomeres on linear plasmid vectors', *Cell*, 29: 245-55.

Taggart, A. K., S. C. Teng, and V. A. Zakian. 2002. 'Est1p as a cell cycle-regulated activator of telomere-bound telomerase', *Science*, 297: 1023-6.

Takawa, M., H. S. Cho, S. Hayami, G. Toyokawa, M. Kogure, Y. Yamane, Y. Iwai, K. Maejima, K. Ueda, A. Masuda, N. Dohmae, H. I. Field, T. Tsunoda, T. Kobayashi, T. Akasu, M. Sugiyama, S. Ohnuma, Y. Atomi, B. A. Ponder, Y. Nakamura, and R. Hamamoto.

2012. 'Histone lysine methyltransferase SETD8 promotes carcinogenesis by deregulating PCNA expression', *Cancer Res*, 72: 3217-27.

Takayama, Y., Y. Kamimura, M. Okawa, S. Muramatsu, A. Sugino, and H. Araki. 2003. 'GINS, a novel multiprotein complex required for chromosomal DNA replication in budding yeast', *Genes Dev*, 17: 1153-65.

Takeda, D. Y., Y. Shibata, J. D. Parvin, and A. Dutta. 2005. 'Recruitment of ORC or CDC6 to DNA is sufficient to create an artificial origin of replication in mammalian cells', *Genes Dev*, 19: 2827-36.

Talley, J. M., D. C. DeZwaan, L. D. Maness, B. C. Freeman, and K. L. Friedman. 2011. 'Stimulation of yeast telomerase activity by the ever shorter telomere 3 (Est3) subunit is dependent on direct interaction with the catalytic protein Est2', *J Biol Chem*, 286: 26431-9.

Tanaka, H., G. H. Ryu, Y. S. Seo, K. Tanaka, H. Okayama, S. A. MacNeill, and Y. Yuasa. 2002. 'The fission yeast pfh1(+) gene encodes an essential 5' to 3' DNA helicase required for the completion of S-phase', *Nucleic Acids Res*, 30: 4728-39.

Tanaka, S., Y. Komeda, T. Umemori, Y. Kubota, H. Takisawa, and H. Araki. 2013. 'Efficient initiation of DNA replication in eukaryotes requires Dpb11/TopBP1-GINS interaction', *Mol Cell Biol*, 33: 2614-22.

Tanaka, S., R. Nakato, Y. Katou, K. Shirahige, and H. Araki. 2011. 'Origin association of Sld3, Sld7, and Cdc45 proteins is a key step for determination of origin-firing timing', *Curr Biol*, 21: 2055-63.

Tanaka, S., T. Umemori, K. Hirai, S. Muramatsu, Y. Kamimura, and H. Araki. 2007. 'CDK-dependent phosphorylation of Sld2 and Sld3 initiates DNA replication in budding yeast', *Nature*, 445: 328-32.

Teng, S. C., J. Chang, B. McCowan, and V. A. Zakian. 2000. 'Telomerase-independent lengthening of yeast telomeres occurs by an abrupt Rad50p-dependent, Rif-inhibited recombinational process', *Mol Cell*, 6: 947-52.

Teng, S. C., and V. A. Zakian. 1999. 'Telomere-telomere recombination is an efficient bypass pathway for telomere maintenance in Saccharomyces cerevisiae', *Mol Cell Biol*, 19: 8083-93.

Torres, J. Z., S. L. Schnakenberg, and V. A. Zakian. 2004. 'Saccharomyces cerevisiae Rrm3p DNA helicase promotes genome integrity by preventing replication fork stalling: viability of rrm3 cells requires the intra-S-phase checkpoint and fork restart activities', *Mol Cell Biol*, 24: 3198-212.

Tran, P. L. T., T. J. Pohl, C. F. Chen, A. Chan, S. Pott, and V. A. Zakian. 2017. 'PIF1 family DNA helicases suppress R-loop mediated genome instability at tRNA genes', *Nat Commun*, 8: 15025.

Tseng, S. F., J. J. Lin, and S. C. Teng. 2006. 'The telomerase-recruitment domain of the telomere binding protein Cdc13 is regulated by Mec1p/Tel1p-dependent phosphorylation', *Nucleic Acids Res*, 34: 6327-36.

Tsurimoto, T., and B. Stillman. 1991. 'Replication factors required for SV40 DNA replication in vitro. II. Switching of DNA polymerase alpha and delta during initiation of leading and lagging strand synthesis', *J Biol Chem*, 266: 1961-8.

Tuzon, C. T., Y. Wu, A. Chan, and V. A. Zakian. 2011. 'The Saccharomyces cerevisiae telomerase subunit Est3 binds telomeres in a cell cycle- and Est1-dependent manner and interacts directly with Est1 in vitro', *PLoS Genet*, 7: e1002060.

Urban, V., J. Dobrovolna, and P. Janscak. 2017. 'Distinct functions of human RecQ helicases during DNA replication', *Biophys Chem*, 225: 20-26.

van Deursen, F., S. Sengupta, G. De Piccoli, A. Sanchez-Diaz, and K. Labib. 2012. 'Mcm10 associates with the loaded DNA helicase at replication origins and defines a novel step in its activation', *EMBO J*, 31: 2195-206.

Vasianovich, Y., V. Altmannova, O. Kotenko, M. D. Newton, L. Krejci, and S. Makovets. 2017. 'Unloading of homologous recombination factors is required for restoring double-stranded DNA at damage repair loci', *EMBO J*, 36: 213-31.

Vasianovich, Y., L. A. Harrington, and S. Makovets. 2014. 'Break-induced replication requires DNA damage-induced phosphorylation of Pif1 and leads to telomere lengthening', *PLoS Genet*, 10: e1004679.

Vega, L. R., J. A. Phillips, B. R. Thornton, J. A. Benanti, M. T. Onigbanjo, D. P. Toczyski, and V. A. Zakian. 2007. 'Sensitivity of yeast strains with long G-tails to levels of telomere-bound telomerase', *PLoS Genet*, 3: e105.

Verma, P., and R. A. Greenberg. 2016. 'Noncanonical views of homology-directed DNA repair', *Genes Dev*, 30: 1138-54.

Vilenchik, M. M., and A. G. Knudson. 2003. 'Endogenous DNA double-strand breaks: production, fidelity of repair, and induction of cancer', *Proc Natl Acad Sci U S A*, 100: 12871-6.

Villa, F., A. C. Simon, M. A. Ortiz Bazan, M. L. Kilkenny, D. Wirthensohn, M. Wightman, D. Matak-Vinkovic, L. Pellegrini, and K. Labib. 2016. 'Ctf4 Is a Hub in the Eukaryotic Replisome that Links Multiple CIP-Box Proteins to the CMG Helicase', *Mol Cell*, 63: 385-96.

Vodenicharov, M. D., N. Laterreur, and R. J. Wellinger. 2010. 'Telomere capping in non-dividing yeast cells requires Yku and Rap1', *EMBO J*, 29: 3007-19.

Vodenicharov, M. D., and R. J. Wellinger. 2006. 'DNA degradation at unprotected telomeres in yeast is regulated by the CDK1 (Cdc28/Clb) cell-cycle kinase', *Mol Cell*, 24: 127-37.

Vujanovic, M., J. Krietsch, M. C. Raso, N. Terraneo, R. Zellweger, J. A. Schmid, A. Taglialatela, J. W. Huang, C. L. Holland, K. Zwicky, R. Herrador, H. Jacobs, D. Cortez, A. Ciccia, L. Penengo, and M. Lopes. 2017. 'Replication Fork Slowing and Reversal upon DNA Damage Require PCNA Polyubiquitination and ZRANB3 DNA Translocase Activity', *Mol Cell*, 67: 882-90 e5.

Wach, A., A. Brachat, R. Pohlmann, and P. Philippsen. 1994. 'New heterologous modules for classical or PCR-based gene disruptions in Saccharomyces cerevisiae', *Yeast*, 10: 1793-808.

Walmsley, R. W., C. S. Chan, B. K. Tye, and T. D. Petes. 1984. 'Unusual DNA sequences associated with the ends of yeast chromosomes', *Nature*, 310: 157-60.

Wang, H., D. Liu, Y. Wang, J. Qin, and S. J. Elledge. 2001. 'Pds1 phosphorylation in response to DNA damage is essential for its DNA damage checkpoint function', *Genes Dev*, 15: 1361-72.

Wang, J., P. T. Englund, and R. E. Jensen. 2012. 'TbPIF8, a Trypanosoma brucei protein related to the yeast Pif1 helicase, is essential for cell viability and mitochondrial genome maintenance', *Mol Microbiol*, 83: 471-85.

Wang, S. C., Y. Nakajima, Y. L. Yu, W. Xia, C. T. Chen, C. C. Yang, E. W. McIntush, L. Y. Li, D. H. Hawke, R. Kobayashi, and M. C. Hung. 2006. 'Tyrosine phosphorylation controls PCNA function through protein stability', *Nat Cell Biol*, 8: 1359-68.

Waraky, A., Y. Lin, D. Warsito, F. Haglund, E. Aleem, and O. Larsson. 2017. 'Nuclear insulin-like growth factor 1 receptor phosphorylates proliferating cell nuclear antigen and rescues stalled replication forks after DNA damage', *J Biol Chem*, 292: 18227-39.

Ward, J. 1998. 'The nature of lesions formed by ionizing radiation.': 65-84.

Watson, J. D. 1972. 'Origin of concatemeric T7 DNA', *Nat New Biol*, 239: 197-201.

Watson, J. D., and F. H. Crick. 1953. 'Genetical implications of the structure of deoxyribonucleic acid', *Nature*, 171: 964-7.
Weinert, T. A., and L. H. Hartwell. 1988. 'The RAD9 gene controls the cell cycle response to DNA damage in Saccharomyces cerevisiae', *Science*, 241: 317-22.
Weitao, T., M. Budd, and J. L. Campbell. 2003. 'Evidence that yeast SGS1, DNA2, SRS2, and FOB1 interact to maintain rDNA stability', *Mutat Res*, 532: 157-72.
Weston, R., H. Peeters, and D. Ahel. 2012. 'ZRANB3 is a structure-specific ATP-dependent endonuclease involved in replication stress response', *Genes Dev*, 26: 1558-72.
Wilson, M. A., Y. Kwon, Y. Xu, W. H. Chung, P. Chi, H. Niu, R. Mayle, X. Chen, A. Malkova, P. Sung, and G. Ira. 2013. 'Pif1 helicase and Poldelta promote recombination-coupled DNA synthesis via bubble migration', *Nature*, 502: 393-6.
Wotton, D., and D. Shore. 1997. 'A novel Rap1p-interacting factor, Rif2p, cooperates with Rif1p to regulate telomere length in Saccharomyces cerevisiae', *Genes Dev*, 11: 748-60.
Wu, G., W. H. Lee, and P. L. Chen. 2000. 'NBS1 and TRF1 colocalize at promyelocytic leukemia bodies during late S/G2 phases in immortalized telomerase-negative cells. Implication of NBS1 in alternative lengthening of telomeres', *J Biol Chem*, 275: 30618-22.
Wu, Y., and V. A. Zakian. 2011. 'The telomeric Cdc13 protein interacts directly with the telomerase subunit Est1 to bring it to telomeric DNA ends in vitro', *Proc Natl Acad Sci U S A*, 108: 20362-9.
Yabuuchi, H., Y. Yamada, T. Uchida, T. Sunathvanichkul, T. Nakagawa, and H. Masukata. 2006. 'Ordered assembly of Sld3, GINS and Cdc45 is distinctly regulated by DDK and CDK for activation of replication origins', *EMBO J*, 25: 4663-74.
Yeager, T. R., A. A. Neumann, A. Englezou, L. I. Huschtscha, J. R. Noble, and R. R. Reddel. 1999. 'Telomerase-negative immortalized human cells contain a novel type of promyelocytic leukemia (PML) body', *Cancer Res*, 59: 4175-9.
Yeeles, J. T., T. D. Deegan, A. Janska, A. Early, and J. F. Diffley. 2015. 'Regulated eukaryotic DNA replication origin firing with purified proteins', *Nature*, 519: 431-5.
Yu, E. Y., J. Perez-Martin, W. K. Holloman, and N. F. Lue. 2015. 'Mre11 and Blm-Dependent Formation of ALT-Like Telomeres in Ku-Deficient Ustilago maydis', *PLoS Genet*, 11: e1005570.
Yuzhakov, A., Z. Kelman, and M. O'Donnell. 1999. 'Trading places on DNA--a three-point switch underlies primer handoff from primase to the replicative DNA polymerase', *Cell*, 96: 153-63.
Zakharyevich, K., Y. Ma, S. Tang, P. Y. Hwang, S. Boiteux, and N. Hunter. 2010. 'Temporally and biochemically distinct activities of Exo1 during meiosis: double-strand break resection and resolution of double Holliday junctions', *Mol Cell*, 40: 1001-15.
Zappulla, D. C., and T. R. Cech. 2004. 'Yeast telomerase RNA: a flexible scaffold for protein subunits', *Proc Natl Acad Sci U S A*, 101: 10024-9.
Zegerman, P., and J. F. Diffley. 2007. 'Phosphorylation of Sld2 and Sld3 by cyclin-dependent kinases promotes DNA replication in budding yeast', *Nature*, 445: 281-5.
Zhang, D. H., B. Zhou, Y. Huang, L. X. Xu, and J. Q. Zhou. 2006. 'The human Pif1 helicase, a potential Escherichia coli RecD homologue, inhibits telomerase activity', *Nucleic Acids Res*, 34: 1393-404.
Zhang, J. M., T. Yadav, J. Ouyang, L. Lan, and L. Zou. 2019. 'Alternative Lengthening of Telomeres through Two Distinct Break-Induced Replication Pathways', *Cell Rep*, 26: 955-68 e3.

Zhang, W., and D. Durocher. 2010. 'De novo telomere formation is suppressed by the Mec1-dependent inhibition of Cdc13 accumulation at DNA breaks', *Genes Dev*, 24: 502-15.

Zhang, X. P., V. E. Galkin, X. Yu, E. H. Egelman, and W. D. Heyer. 2009. 'Loop 2 in Saccharomyces cerevisiae Rad51 protein regulates filament formation and ATPase activity', *Nucleic Acids Res*, 37: 158-71.

Zhi, L. Q., W. Ma, H. Zhang, S. X. Zeng, and B. Chen. 2014. 'Association of RECQL5 gene polymorphisms and osteosarcoma in a Chinese Han population', *Tumour Biol*, 35: 3255-9.

Zhou, J., E. K. Monson, S. C. Teng, V. P. Schulz, and V. A. Zakian. 2000. 'Pif1p helicase, a catalytic inhibitor of telomerase in yeast', *Science*, 289: 771-4.

Zhou, J. Q., H. Qi, V. P. Schulz, M. K. Mateyak, E. K. Monson, and V. A. Zakian. 2002. 'Schizosaccharomyces pombe pfh1+ encodes an essential 5' to 3' DNA helicase that is a member of the PIF1 subfamily of DNA helicases', *Mol Biol Cell*, 13: 2180-91.

Zhou, R., J. Zhang, M. L. Bochman, V. A. Zakian, and T. Ha. 2014. 'Periodic DNA patrolling underlies diverse functions of Pif1 on R-loops and G-rich DNA', *Elife*, 3: e02190.

Zhu, Z., W. H. Chung, E. Y. Shim, S. E. Lee, and G. Ira. 2008. 'Sgs1 helicase and two nucleases Dna2 and Exo1 resect DNA double-strand break ends', *Cell*, 134: 981-94.

Zou, L., and S. J. Elledge. 2003. 'Sensing DNA damage through ATRIP recognition of RPA-ssDNA complexes', *Science*, 300: 1542-8.